1993

The behaviour of laterally loaded masonry panels with openings

Chong , Vun Leong

THE BEHAVIOUR OF LATERALLY LOADED MASONRY PANELS WITH OPENINGS

By

VUN LEONG CHONG

The thesis is submitted to the University of Plymouth in partial fulfilment of the requirements for the Degree of Doctor of Philosophy.

SCHOOL OF CIVIL AND STRUCTURAL ENGINEERING

UNIVERSITY OF PLYMOUTH

JANUARY 1993

THE BEHAVIOUR OF LATERALLY LOADED MASONRY PANELS WITH OPENINGS

V.L. CHONG

PH.D. THESIS

SCHOOL OF CIVIL AND STRUCTURAL ENGINEERING

UNIVERSITY OF PLYMOUTH

ACKNOWLEDGEMENTS

The Author acknowledges with thanks the financial support given by the Science and Engineering Research Council for the study of lateral loaded masonry panels with openings.

The Author also would like to mention the following people for their contributions during the course of the research:

Colin Southcombe and Ian May for their constant supervision, encouragement and assistance.

The Technical Staff of the School of Civil and Structural Engineering, University of Plymouth, particularly Antony Tapp, Brian Worley and Gregory Regan for their help with the laboratory testing.

Brian the bricklayer.

Westbrick PLC and Armitage Brick who provided the bricks used in the tests.

DECLARATION

This thesis does not contain any material which has been preciously submitted for any other degree or diploma in any University, and published or written by another person, except where due reference is made in the text.

In collaboration with others the author has published two articles relating to the aspects of the work reported. All the experimental and theoretical work was carried out under the supervision of Mr. C.Southcombe and Prof. I.M.May. The publications were as follows:

(1) CHONG, V.L, MAY, I.M, SOUTHCOMBE, C. and MA, S.Y.A. "An Investigation of the Behaviour of Laterally Loaded Masonry Panels using Non-Linear Finite Element Program ". Computer Methods in Structural Masonry, Eds. Middleton, J. and Pander, G.N, Books and journals Int. Ldt., pp. 49-63., 1991.

(2) CHONG, V.L, SOUTHCOMBE, C. and MAY I.M. "The Behaviour of Laterally Loaded Masonry Panels with Openings". The British Masonry Society, 3rd Int. Masonry Conference, London, Oct. 1992.

THE BEHAVIOUR OF LATERALLY LOADED MASONRY PANELS WITH OPENINGS

VUN LEONG CHONG

ABSTRACT

In recent years the use of masonry as a structural material has increased in advance of the necessary theoretical and corroborative experimental investigations. One aspect of structural masonry where particular problems have been encountered is the design of masonry panels subjected to lateral loadings. Research undertaken, principally in the United Kingdom and Australia, has led to the development of empirical methods of analysis applicable to solid rectangular panels. However, the effects of the presence of openings on the behaviour of a masonry panel has received scant attention. The aim of the research is to rectify this situation. The principal objective of the research is to put the design of this form of panel subjected to lateral load, on a more rational footing. To do this it has been necessary to investigate the behaviour of masonry panels with openings.

The research can be divided in four stages. Firstly, an extensive literature survey has raised questions concerning the suitability of the current British Standard Code of Practice ,BS5628, and other design methods such as elastic plate theory, and empirical strip method, for the design of laterally load masonry panels. Secondly, a non-linear finite element analysis has been developed. The analysis is capable of analysing panels under lateral loading up to and beyond the peak load. The results obtained using the computer program were initially validated with the existing results from two previous laboratory investigations [1,2]. Initial analysis of the results from the experimental and theoretical studies highlighted areas where further investigation was required.

In conjunction with the development of the computer program, the investigation involved the laboratory testing of 18 full scale panels.

One of the major problems encountered was the determination of material parameters. In this work wallettes have been used to obtain flexural strength values, however the strength of the specimen is influenced by the size of specimens and the number of bed and perpend joints [3,4].

In order to clarify the position, a computer based statistics analysis similar to that reported by Lawrence [4], was employed to investigate the format of the specimens. Estimations of the single joint strengths from the wallette results were obtained from the analysis.

Single joint strengths obtained from the statistics analysis were then used in the finite element analysis and comparisons with the experimental load-displacement relationships and the failure patterns made. A Monte-carlo simulation of the finite element analysis was also carried out to investigate the effect of material variability on the failure strength of masonry panels. Good correlation has been obtained.

Lastly, parameter studies using the finite element analysis and the experimental results have indicated that yield line method consistently over estimates the failure strength of masonry panels. However, the reduction of strength due to the inclusion of openings predicted by yield line is in a reasonable good agreement with the experimental results obtained. A simple formula for the design of laterally loaded masonry panels with openings is proposed based on the present studies.

TABLE OF CONTENTS

NOTATION

σ_x, σ_y	Stresses in the x and y directions
σ_n, σ_p	Stresses normal and parallel to the crack direction
τ_{xy}, τ_{np}	Shear stresses
ϵ_x, ϵ_y	Strains in the x and y directions
ϵ_n, ϵ_p	Stresses normal and parallel to the crack direction
γ_{xy}, γ_{np}	Shear strains
E_b	Elastic modulus of brickwork
ν	Poisson's ratio
F_v, F_h	Extreme fibre stresses in Biaxial bending
F'_v, F'_h	Moduli of rupture in one-way bending
α	Angle between the maximum prescribed stress and the bed joints
σ_1, σ_2	Principal stresses
$\sigma_{1\alpha}$, $\sigma_{2\alpha}$	Principal stresses at an angle α
θ	Rotation
x, y, z	Coordinate axes
f_1, f_2	Principal stresses
f_c	Compressive strength of brickwork
f_t, f_b	Uniaxial tensile and compressive strengths
ϵ_t, ϵ_b	Uniaxial tensile and compressive strains
TOD, TOR	Convergence tolerances for iterations
M_x, M_y	Local moment in the x and y axis
μ, σ	Mean and standard deviation of a distribution
m_n	Yield moment
m_{ns},M_{xy}	Twisting moment
m_1, m_2	Moment of resistance in the x and y axis
ϕ	Angle from m_1 to the yield line
m_s	Tangential moment
M_1 and M_2	Principal moments
F_{kx}, F_{ky}	Flexural strengths normal and parallel to bed joints
μ	Orthogonal ratio

1.0 INTRODUCTION AND LITERATURE REVIEW

1.1 Introduction

Despite the long history and associated research into the use of masonry in non-loadbearing walls, there is still disagreement over the suitability of the methods for predicting the resistance of panels to wind and other lateral forces, especially for panels with openings. Masonry panels subject to wind loading, perpendicular to the panel face, were traditionally designed by rule-of-thumb methods. Such methods have always been found to be inappropriate to determine the ultimate strength of panels made with a material such as masonry, which is fundamentally brittle and is not homogenous.

Design rules for loadbearing walls in Great Britain were introduced in the 1948 British Standards Institution Code of Practice, CP 111 [5], which was based on experimental work carried out at the Building Research Station. The design rules were subsequently improved in the 1964 revision [6]. Until comparatively recently masonry buildings have been designed exploiting only the compressive strength of the material. Prior to 1970 there was very little sound advice available regarding the tensile strength of masonry. The publication of CP 111; part 1 in 1970 [7] gave some guidance and suggested values for the tensile strength, but discouraged its use.

Extensive research at the British Ceramic Research Association led to two design methods for laterally loaded walls being introduced in the 1978 British Standard Code of Practice for Structural use of Masonry, BS5628: Part 1 [8]. The first method is based on yield line theory, assuming constant moments of resistance along yield lines, although there appears

to be no justification for the use of such a theory because of the lack of ductility of masonry. The second method employs arching theory which allows a masonry panel to act as an arch between suitable rigid supports; however in practice it is often difficult to provide such support. Following publication of the Code further research has been carried out which has shown that, particularly for walls with large height to length ratios, the yield line method overestimates the failure pressure [2,9,10]. This is to be expected from an upper-bound theory which was developed for plastic materials. The use of yield line theory for a brittle material like masonry is doubtful, without further justification.

BS5628: Part 3 [11], published in 1985, also contains a section dealing with walls subjected to imposed lateral load; this gives guidance on panel sizes and is based on the same work as BS5628: Part 1. Some limited guidance is also given on walls with openings. However, the Code fails to give proper advice on the design of such panels. A publication [12] by the Property Services Agency (PSA) in 1986 suggests that a panel with openings should be divided into sub-panels with these being designed using the design curves provided. The line loads carried over from the opening and as reactions from one panels to the next are also taken into consideration. This method of design which covers all aspects of wall panels with openings is essentially based on yield line theory.

The principal objective of the research is to put the design of masonry panels with openings, subjected to lateral load, on a more rational footing. To do this it is first necessary to determine, by testing, the behaviour of single skin and cavity walls with openings, from the initial application of load through to the ultimate failure.

The full scale laboratory test programme is a continuation of the work carried out by Tapp [1] and incorporates a wider range of panels and materials. A total of 18 full size panels have been tested.

A non-linear finite element analysis, which was initially developed by Tellett [13] ,and May and Ma [10] was further developed and modified was used to assist in the design of the physical tests as well as to provide additional data on the behaviour of lateral loaded masonry panels for the development of an improved design method.

The non-linear finite element analysis is described in Chapter two and an initial correlation made with the existing laboratory results [1,2,14] is presented in Chapter three.

Before evaluating the current available analytical and design methods of laterally masonry walls, a review on the lateral behaviour and flexural strength of masonry walls is given.

1.2 Factors Affecting the Flexural Strength of Laterally Loaded Masonry Walls

1.2.1 Introduction

It is possible to distinguish two categories of wall when considering the lateral strength of the wall. The first category of walls are those found in low-rise buildings and in the upper floors of multi-storey buildings where the lateral resistance depends entirely on the flexural strength of the masonry. This category of walls were also found in framed buildings where the wall is only used for cladding. The second category includes infill panels in framed

structures and walls having a degree of precompression normally found in two or more storeys below roof level in a loadbearing masonry structure. The lateral resistance of these panels is greatly enhanced by the action of in-plane forces or arching, and will almost certainly exceed that required to resist the wind loads encountered.

In order that the two categories of wall described above can be designed, the flexural properties and behaviour of the panel must be established. Many factors are known to influence these properties and behaviour; they can be divided into two groups, namely:

(1) Material factors relating to the flexural strength of the masonry, for example, the constituent components and the method of assembly.

(2) Secondary factors relating to the panels itself, for example, the panel size, shape and edge support conditions, and the different modes of failure.

Masonry is normally a combination of two structural materials, the units and the mortar, each of which can have highly variable properties [15,16]. The masonry units and the mortar are hand assembled by the mason. Thus the variability of the units and mortar, and other secondary factors mentioned above, cause the behaviour of the complete wall to be complex. As most of the material factors have been previously covered in details by Tapp [1], these factors are only briefly summarised below. Before considering these factors, it is useful to discuss the behaviour of masonry panels.

1.2.2 Behaviour of Masonry Walls

Within the range of stresses and strains to which masonry walls are subjected under lateral loading, the behaviour of the units may be considered as sensibly linear elastic. The same is not true of the mortar joints. Anderson [17] and Cajdert [18] have strain gauged the joints and adjacent masonry in flexure and noted marked non-elastic behaviour with a movement of the neutral axis toward the compressive face with increasing load. The strains are much greater in the mortar than in the masonry unit leading to redistribution of stresses through the masonry composite. This is reflected in the marked non-linearity of the load deflection characteristics of certain wall panels. This non-linearity in stiffness has also been noted by Baker [9] during the loading of brick masonry wallettes tested in horizontal flexure.

Such non-linear load deflection behaviour appears to result from the ability of masonry, once a perpend joint has cracked, to maintain a substantial proportion of its moment of resistance over a considerable change in strain because of the torsional resistance of the mortar/unit interface where the masonry units overlap. It is evident [16,17,3] from the lower coefficients of variation obtained for small specimens spanning in the strong direction that this torsional effect overcomes, to a certain extent, the effect of local weaknesses which result in the larger variation found in the orthogonal, weak, direction. Lawrence's finite element analysis [4] extended the understanding of horizontal flexure behaviour by showing that the perpends did not crack progressively but their stiffness dropped to effectively zero once their initial cracking moment was exceeded, and the perpend moments reduced as their stiffness dropped and the brick moments increased to compensate. Because the proportion of joints in brick masonry is larger than in block masonry, it is reasonable to expect a greater degree of non-

linearity in the former.

Flexural failure of masonry panels spanning in the vertical direction generally starts at a horizontal mortar joint. Initial failure is at the tensile face of the panel by splitting of the unit/mortar interface, by fracture within the mortar joint, or by fracture of the masonry unit. A factor influencing the flexural strength across the bed joints is the stiffening effect of the junction of the perpend joints on the bed joints. It has been found [19] in small specimen tests that a bed joint will preferentially crack along the joint interface at which fewer perpend joints terminate and also that horizontal cracks will cross joints between perpend joints.

Lawrence [20] has described three distinct points in the behaviour of masonry wall panels under lateral load. Depending on the nature of the support conditions, two of these, or even all three, might be coincident, but the pattern is always the same for each particular support configuration.

The first of these points is the occurrence of the first crack. For panels supported on four sides the first crack is usually horizontal, through a bed joint near the mid-height of the panel, but in some cases where the length to height ratio is small, it may be a vertical crack near the mid-length. For panels supported on three sides with the top edge free, the first crack is always vertical or steeply inclined, usually near the mid-length, but occasionally, for long panels, nearer to the third points.

The second distinct point is the formation of the full crack pattern. This point occurs in panels with four sides supported, where the formation of diagonal cracks, connecting the

initial horizontal or vertical crack to the corners, is necessary to form a mechanism. The margin of load between first cracking and the formation of the full crack pattern can be quite substantial for short walls with four sides supported, where the first crack is vertical, the margin can be quite small.

The third point in behaviour is the panel failure, defined as being the maximum load that the panel can withstand.

1.2.3 The Interaction of Units and Mortar

Masonry units can be of clay, calcium silicate or concrete brick, concrete block, real or reconstituted stone.

The mortar composition is usually expressed in terms of the volume ratio of binder and sand, the binder element commonly being ordinary portland cement (OPC) and/or hydrated lime. It is normally up to the mason to add the required quantity of water to obtain the desired workability. Five types of mortar mix have been classified by BS5628 [8] based on different volume ratio of binder and sand, i.e. mortar designations (i), (ii), (iii), (iv) and (v).

The water suction of masonry units is perhaps the most important intrinsic factor affecting the fresh mortar, and, consequently the properties of the hardened mortar and the properties of the combination. Water removal or migration affects the mortar bed as a whole and consequently the properties of the interface between the masonry unit and the mortar.

Shrinkage and swelling of the mortar and the masonry units due to moisture changes and thermal movements also affect the quality of the joint.

When a masonry unit and the fresh mortar come into contact with each other, the variation of the suction depends upon many factors connected both with the unit and the mortar. In some cases little or no water may be removed from the mortar, the other extreme being that almost all of the water is absorbed by the masonry unit. The strength and the porosity of the mortar bond, watertightness, etc., are some of the properties which are dependent upon the suction. Indeed the strength of the mortar is not dependent upon its initial water content but on the water present after suction.

A relationship between the flexural bond strength and the initial rate of suction of clay brick units has been established [19,21,22] and adopted in the British Code of Practice [8]. The adjustment of the initial rate of suction by immersing bricks in water or docking them is a well established method which it has been claimed improves the bond of bricks with high suction rate. Adjustment of the initial rate of suction of bricks has been found [23] to be desirable when the unadjusted rate exceeds 2 kg/m^2/min for 1:1/4:3 ordinary portland cement:lime:sand designation (i) mortar, and 3 kg/m^2/min for 1:1/2:4 designation (ii) and 1:2:9 designation (iv) mortars. The laying of bricks with high water absorption and high initial rate of suction dry can lead to a large reduction in flexural strength, Palmer and Parson [24].

De Vekey and West [25] have found that there is no general relationship between the flexural bond strength and the suction rate of concrete blocks, however the flexural bond strength

increases with an increase in suction rate up to a maximum of 2 kg/m^2/min for 1:1:6 designation (iii) mortar and about 2.5 kg/m^2/min for 1:2:9 designation (iv) mortar. The flexural strength then declines to a minimum at about 7.5 kg/m^2/min for both mortars thereafter levelling out or possibly increasing again up to 11 kg/m^2/min. However, the relationship between flexural bond strength and the compressive strength of concrete blocks has been well established [8,25,26].

Docking of concrete blocks has a variable effect on the flexural bond strength of concrete blockwork as found by Gairns, Fried and Anderson [27,28]. Soaking was found to enhance the flexural strength of weak units, autoclaved aerated concrete (AAC) blocks, but weaken that of stronger units, dense concrete (DC) or light-weight aggregate (LWA) blocks. This reduction may be because the blocks tended to float due to the high moisture content of the soaked LWA and DC concrete blocks. This made it difficult for the blocklayer to obtain accurate specimens and uniform joints .

Other characteristics of the units that affect the flexural bond strength beside the type of material [2,28,29], rate of absorption [19,21,22,24] and moisture content [2,21,30,31] are the unit size, shape, and aspect ratio [18,3,32,33], unit flexural [27,34,35,36] and compressive strengths [25,26], perforation or surface indentations [25,28,37], and surface texture [38].

1.2.4 Mortar

The bond between the mortar and the masonry unit is of fundamental importance to the lateral strength of masonry. Bond must be good in both tension and torsion, the latter governing the flexural strength in the stronger direction. Mortar characteristics that influence bond strength are initial water content, water retentivity of the mortar and lime content, and thus consistence retentivity [23,39,40], type of mortar [41,42,43] and cement content [19,21,24,30], use of additive, thickness of mortar bed [2,44], pore structure [45,46,47,48], grading of sand [2,41,49], workmanship [28,30] and age [2,39].

The tensile strength of the mortar itself will also be of consequence.

Polyakov [40] found that for a mortar of given consistency the maximum bond strength was achieved when the brick contained an optimum amount of water. As discussed earlier in section (1.2.3), this occurred when the amount of 'free' water in the mortar matched the initial rate of suction of the brick, which in turn is dependent on the amount of water in the brick at the time of laying.

The use of lime is a way of altering the consistency and thus the workability of mortars. Alternatively the workability can be altered by the introduction of a plasticizer or air entraining agent, or the addition of water. Work by Kamph [23] has shown that for a ratio of binder:sand, increasing the amount of lime or the air content causes the strength to decrease. The effect of an increase of lime or air content is to cause greater water retention and to increase the workability. The mortar strength decreases with the corresponding

increase in water:cement ratio. The effect on bond strength however differs according to the type of brick being used; for a high suction brick the improvement in water retentivity enhances the bond strength whilst the reverse is true for low suction bricks. Similar findings have also been reported by Baker [39], Polyakov [40], Hamid, Yagi and Awad [41], and Palmer and Parson [24] as mentioned in Section (1.2.3).

Studies of the microstructure at the interface between brick and mortar at mortar/brick bond by Lawrence and Cao [47] have brought about a greater understanding by showing that the effect of lime on the interface microstructure is to facilitate the formation of the initial calcium rich film and to increase the amount of calcium hydroxide at the interface. The microstructure at the interface between lime mortar/brick was found to be denser and more continuous than with a plain mortar. The addition of lime improves the extent of bonding, but also increases the water demand of the mortar. The strength of lime mortar tends to be low due to this increase in water content, and the "optimum" cement:lime:sand ratio for bond strength and durability consideration is closer to 1:0.5:4.5 rather than the commonly used 1:1:6 [47].

The interface between brick and mortar mixed with air entraining agent has been found to contain a significant number of voids which can have a detrimental effect on the resulting bond [47]. The general trend is a decrease in unit-mortar bond strength for increasing air content of the mortar has been shown by many workers [45,46,47,48]. However the type of air entraining agent and the air bubble structure have significant influence on bonding, and air content alone does not determine bond strength [46].

1.2.5 Age

The relationship between flexural strength of masonry and age is erratic [50]. The ratio of seven day flexural strength to 28 day was found to range from 0.44 to 1.25 by Baker [39], and from 0.78 to 1.34 by Maltys and Grimm [50].

It is usually assumed that the flexural strength of masonry increases with time, as the hydration of cement becomes more complete. Preliminary results from long-term, 10 years, exposure tests suggest that the flexural strength of clay brickwork built with 1:1:6 designation (iii) mortar or higher tends to increase with age [51,52]. However, tests carried out by Baker and Franken [16] indicated that full strength occurred as early as three to seven days after building.

Apart from the variability of the materials, there are several reasons for this erratic behaviour. Firstly, shrinkage cracking of the outer portions of the joints may reduce the effective section modulus. Secondly, hydration in the outer portion of the mortar may cease after 3 days of drying at warm temperature [53]. As flexural strength is largely determined by the strength of the material in the outer fibre, the drying rate of the outer portion of the mortar joints is most important. Tests by Baker and Franken [16] showed that specimens cured in air for seven days exhibited a marked increase in strength than when water cured. A consideration is that hydrated-lime does not harden in water but requires carbon dioxide in the air for carbonation to occur. This was indicated in tests by Baker [39] in which the specimens made with limed mortar, were placed under water after initial setting in air for 24 hours. When removed from the water after seven days, they had practically zero strength

but then gained strength at the same rate as the specimens that had been air cured from the time of building. Thus, shrinkage cracking, hydration of cement and carbonation of lime, each appear to have effects in the development of flexural-bond strength in masonry that are not well understood.

However, West et al [2] have shown that in general, for flexural strength normal to the bed joints, that 28 days curing gives a slightly higher strength than 14 days curing.

1.2.6 Curing Condition

The effects of curing conditions on the flexural strength of masonry have been investigated by a number of authors, for example, Anderson [54], Held and Anderson [49], Scrivener and Gairns [55] James [56] and Marquis and Borchelt [57].

In 1982 Anderson [54] reported the results of a programme of testing using the BS5628 wallette test method. These tests were mainly with blockwork and covered both specimens cured by sealing and those open to the laboratory air. A small reduction in flexural strength, from 0.256 to 0.226 N/mm^2, for all the sealed specimens was found and it was stated that "The comparisons of the limited number of results where different curing regimes have been adopted shows that there is no consistent relationship for all masonry material...". Later work by Held and Anderson [49] confirmed these findings.

Scrivener and Gairns [55] have reported their work covering flexural strength tests, "beam"

and "joint" tests, of block specimens cured under various environmental conditions. These conditions ranged from warm and humid, 20° c and 70% relative humidity, to very hot and very dry, 38° c and 35% relative humidity. Masonry specimens which had been sprayed with a concrete curing compound and wrapped with polythene were found to have a moderate increase in the flexural bond strength over that obtained from uncovered specimens. However, in the hot and dry condition, fully enclosed specimens with polythene were found to produce dramatic increases in strength under all environmental conditions. Humid conditions also favoured an increase in the flexural strength of concrete masonry under the same temperature.

These four programmes were carried out in the laboratory under environmentally controlled conditions. Two other programmes attempted to obtain information pertinent to site conditions.

James [56] investigated the effect of various workmanship factors including curing, on the flexural bond strength of brickwork. A reduction from 83 Ibf/in^2 was reported with 9-high stack bonded piers, cured in the shade and covered with polythene, to 48 Ibf/in^2 when cured in the sun and not covered. However, there was no difference between outdoor curing and indoor curing for bricks with a low initial rate of suction.

Marquis and Borchelt [57] reported on the use of the bond-wrench to test both laboratory and site constructed 7-high brick piers. The laboratory specimens were air cured and the site piers were reported to have experienced wide variations in temperature and humidity and to have been subjected to wind. The site piers were found to be generally much lower in

flexural strength than the laboratory specimens.

From the above it is clear that, compared with air cured specimens, close covering has a generally unpredictable effect on the vertical flexural strength. As expected, masonry built on site, or representative of that built on site, appears to have a lower strength than masonry built under laboratory conditions.

1.2.7 Workmanship

Very high factors of safety, material and load factors [8], are applied to the design of masonry in comparison with those adopted for designs using other structural materials. While this reflects, in part, inadequacies in the understanding of some aspects of masonry behaviour and the high inherent variability of many masonry properties, especially flexural strength, it also reflects the relatively low level of workmanship and supervision often associated with masonry construction. While the variability of the properties can be catered for in limit state design by use of the characteristic strength values, variations in building control are less easy to cope with. West et al [2] investigated the effect of bad workmanship. The study in part indicated that workmanship was less important than that might be expected, and that the effects were found to be confined to mortar weaker than 1:1/4:3 and to bending across the bed joints, i.e. the weaker direction.

1.2.8 Panel Shape and Edge Conditions

Where masonry walls are subjected to out-of-plane lateral loading, the applied loads are resisted by the vertical flexural strength and/or the horizontal flexural strength of the masonry, depending on the support conditions and wall panel geometry.

Panels that span vertically, i.e. are laterally supported only along their top and bottom edges, rely entire on the tensile bond strength of their bed joints for lateral resistance. This may be enhanced by in-plane forces generated by the self-weight of the masonry, by in-plane restraint provided by the top or bottom supports, or by applied vertical loading [58,59,60]. When one or both of the vertical edges of a panel are also supported, two-way spanning is introduced and the lateral strength of the panel is increased markedly over that of the vertically spanning panel. Continuity across the panel supports [61,62] will further increase the lateral strength of the panel, although the extent of the increase is a matter of some debate; Baker et al [9], and May and Ma [10], for example, questioned the development of the full moment of resistance of masonry over a support, especially a horizontal support because of the brittle behaviour of masonry in vertical flexure.

Panels that are built into rigid supports can develop a substantial amount of in-plane arching action and increase the ultimate failure load of the panels considerably. These effects have been demonstrated by a number of tests [62,63,64,65,66,67]. From the results of tests carried out by Hodgkinson, West and Haseltine [66], it has been established that very high pressures are needed to fail walls which were built between very rigid supports. The arch develops within the wall and failure is due to compression failure of the brick/mortar

combination. The increase in the lateral load capacity was reported to be more than six times of the capacity of walls in pure bending.

For walls which were built between flexible steel frames, an increase of lateral load capacity of more than 40% was reported [62,65,66]. The effect of edge restraint and arching action provided by continuity of wall panels was reported by Moore, Haseltine and Hodgkinson [66], and Anderson [63]. Up to 100% increase in strength was observed.

Extensive research has identified and quantified enhancement of the in-plane flexural strength of masonry due to vertical axial prestress of precompression. Various researchers have also shown an increase in horizontal flexural strength with vertical prestress [68,69,70], and attributed this increase of flexural strength to an increased frictional moment on the bed joints.

Baker [71] proposed a failure criterion for brickwork in biaxial bending and confirmed experimentally both vertical and horizontal flexural strengths of brickwork increased with the application of vertical prestress. However, an increase in the modulus of rupture in vertical bending greater than that of the applied compressive stress of 0.1 N/mm^2 was reported. This indicates that the neutral axis for brickwork in bending may be between the centre of the wall and the compression face. The increase in the horizontal modulus of rupture strength was found such that the orthogonal strength ratio was the same with or without the applied compressive stress. As reported by other researchers [68,69,70], Baker noted that in horizontal bending, where failure occurred in the mortar joints, an increase in the horizontal strength could be expected due to the increased torsional resistance at the bed joints caused

by the applied compressive stress. Where the horizontal strength is determined by brick strength, no increase in the strength of brickwork due to prestress could be expected since a small compressive stress would probably have negligible effect on the bending strength of the brick. No experimental results were published to support this finding.

Baker et al. [72] developed a plastic theory to predict the torsional friction moment of resistance mobilised at failure in the bed joints of overlapping masonry units. Experimental work agreed closely with the plastic theory and the moment of resistance mobilised by friction was found to be proportional to the normal applied load and the coefficient of friction.

Experimental study carried out Garrity and Phipps [73] has shown that vertical prestress increased the horizontal flexural strength of clay brickwork, without arching, up to a maximum value equal to the modulus of rupture of the bricks.

1.2.9 Failure Criteria

In tests of small specimens, for example the 'beam' test , the 'bond wrench' test and the 'wallette' test, the load at initial cracking is always the ultimate load. This is usually recorded as the modulus of rupture or ultimate flexural strength, from which mean or characteristic strengths are obtained as required. Normally, the modulus of rupture in the two directions, normal and parallel to the bed joints, and therefore orthogonal strength ratio [8] are obtained, although some workers [4,71] propose that the orthogonal strength ratio can be obtained from

a single modulus of rupture. The orthogonal strength ratio for masonry is being defined as the ratio of the modulus of rupture in horizontal flexure to the modulus of rupture in vertical flexural strengths.

The inclusion of these moduli of rupture or orthogonal strengths for establishing a failure criterion for full-size wall panels can be difficult. There are a number or reasons for this, e.g. the effect on the measured orthogonal strengths of specimen size, curing regime, loading regime, restraint condition, workmanship, etc.

There are three other difficulties in finding and applying a failure criterion to masonry panels. Firstly, there is the question of which types of small specimen are to be used to obtain modulus of rupture values because the strength of the specimen is influenced by the number of bed and perpend joints in the span. In vertical bending it has been shown [16,74] that the strength of the specimen is influenced by the number of bed joints in the span, the number of bricks in the width of the specimen and the distribution of applied bending moments. There is also the question of over what area the criterion is to apply in the panel. Finally there is the problem of calculating the moments that occur in the panel. Analysis is often based on the assumption that masonry has the same elastic modulus in both vertical and horizontal directions. While this may be true at low stress levels, an accurate analysis should consider the effects of anisotropy and the changes of elastic modulus with stress level. However, it has been shown that [75] the non-linearity caused by the constituent materials is insignificant compared with that resulting from progressive cracking.

Baker [71,76] has proposed a failure criterion represented by an elliptical curve related to

the orthogonal strengths obtained from small specimens. May and Ma [77] have proposed a complete biaxial stress failure criterion covering the compression-compression, compression-tension, and tension-tension regions for use in their non-linear finite element analysis.

1.3 Analytical and Design Methods of Laterally Loaded Masonry Walls

1.3.1 Introduction

Before considering the analysis and design of masonry panels, the behaviour of masonry panels under lateral load is briefly summarised below.

Panels of masonry subjected to lateral loading are orthotropic, i.e. they have different properties in orthogonal directions. In one direction the bed joints form continuous, parallel, planes of weakness, with failure in bending occurring when the bond strength between the masonry unit and mortar in one of the bed joints is exceeded. This may or may not be at the bed joint subjected to the highest moment, depending on the small variations in bond strength from one unit to another and along each bed joint. The failure will occur at the masonry unit/mortar interface where the ratio of applied bending moment, or extreme fibre stress, to bond strength is the greatest [78].

In the orthogonal, stronger direction, failure is a much more complex process, involving some combination of the following:

(a) bond failure in perpend joints

(b) crushing of mortar or masonry at the perpend joints

(c) torsional shear failure in bed joints where masonry units overlap

(d) shear failure of mortar across or within frogs, across perforations or voids, etc.

When masonry spans in two directions, failure may be the result of the interaction of the above processes. Thus, the difficulty of arriving at a rigorous theoretical method of analysis, which takes all these factors into account, as well as variation in materials, unit dimensions, and edge conditions, is significant. Unless the method also makes some allowance for the inherent variability of masonry, its accuracy cannot be confirmed.

The accuracy of any method of analysis depends largely on the values assigned to the material properties used in the calculations. Thus comparison of the methods of analysis is difficult where different methods of obtaining material property values are used.

The available methods for the design and analysis of laterally loaded masonry walls are based on various methods including elastic plate theory [79] assuming isotropic or orthotropic properties and conventional yield line analysis. Other methods developed specially for masonry include the fracture line theory [80], the empirical strip method [81], the British code moment coefficients [8] which are based on yield line theory, and finite element analysis [10,82].

Purely elastic methods are plainly inappropriate for a composite material which exhibits such non-linear behaviour, although they have been used in the past. There may be justification for its use where bending occurs only across the bed joints and/or to determine the cracking

load where first cracking occurs along a bed joint in two-way spanning panels [9].

The application of yield line theory to a brittle material like masonry is obviously doubtful although it may have practical advantages over the elastic plate theory because simple solutions can be obtained for many different shapes of panels and load cases.

The yield line method has been used by many researchers to predict failure strengths of masonry panels with openings. Although the results have been inconclusive, the yield line method is considered to be feasible.

The use of finite element analysis is perhaps the method most likely to bridge the gap between theory and experiment, being able to cope with linear and non-linear behaviour and orthotropic properties, using a variety of elements to model the units, joints, and even wall ties, in a cavity wall construction.

1.3.2 Elastic Plate Analysis

Use of elastic plate analysis is limited to predicting the loads at cracking or failure loads where the panels show no reserve of strength after cracking. Negligible differences in the magnitudes for the moduli of elasticity in the two orthogonal directions have been reported [78,81,83] and hence isotropic plate solutions have been suggested. However, others [84] have reported considerable anisotropy and accordingly proposed orthotropic plate solutions. It should be noted that the modulus of elasticity parallel to the bed joints has been reported

to be both higher and lower than the modulus normal to the bed joints.

In addition to the uncertainty regarding the elastic modulus of masonry, Hendry [85] has identified three other factors as complications in the application of elastic plate theory to masonry panels. These factors are, the non-linear load-displacement relationship of the panels, the lack of knowledge about the failure criterion for masonry in biaxial bending, and the difficulty of dealing with irregularly shaped walls or walls with openings.

Recently, Baker [83] has proposed a principal stress failure criterion and has developed an expression for the determination of the strength at different directions based on available data for off axis bending of masonry assemblages. This failure criterion was incorporated in a finite difference computer simulation, using elastic plate analysis. The analysis included the variation of the strengths, and the load sharing concept for prediction of first cracking load and panel capacity.

Lawrence [78] suggested a Monte Carlo simulation approach to take account of the random variation in flexural strength, combined with isotropic elastic plate analysis to evaluate the bending moment in the panel. Four different failure criteria were applied and their effects studied. The criteria were , no interaction between horizontal and vertical moment, elliptical interaction, simple linear interaction, and principal moment elliptical interaction as proposed by Baker [83].

These two theories have yielded reasonably good correlations for the model and full scale brickwork panels tested by Baker [83] and Lawrence [33].

A similar analysis without the random variation in masonry properties was presented by Seward [84].

1.3.3 Yield Line Theory

Many researchers [18,19,85,86] using the yield line method have reported good agreement with the test results. However, it has been pointed out there is no rational justification for the use of a theory based on ductile behaviour for a brittle material like masonry [19,85]. Lovegrove [87,88] has tried to justify the use of yield line by stating that "The observation that yield line makes correct predictions is in fact a statement that the work equation does. It is possible that the work equation might be correct, even though the theory that has been used to developed it is not". Discussion of the use of the yield line method has also lead to the argument that the good results in some cases were mainly due to favourable loading and support conditions and the selected lower bound characteristic flexural strengths, e.g. the bottom abutment of the test panels was taken as simply supported regardless whether a damp proof course (d.p.c) was introduced [2]. Although, the good prediction of failure pattern by the yield line method is undeniable, this does not justify its use as the basis for design in the current British code [8]. The yield line method has been consistently reported [2,9,10,19] to provide non-conservative predictions.

1.3.4 Fracture Line Theory

The fracture line theory was proposed and verified by Sinha [80] for brickwork panels of different shapes and support conditions. This theory was basically yield line theory but modified to include the anisotropy of the panels.

1.3.5 Empirical Strip Method

The empirical strip method proposed by Baker [81] is without a rational basis, but it gives reasonable agreement with the results of laterally load tests of model and full scale walls built of clay bricks [81]. A horizontal strip at mid-height and a vertical strip at mid-length of the panel, each of unit width are considered. The load capacities of the two strips, considered as simple beams, are added together to give the load capacity of the panel as a whole. Thus the two way acting of the panel is taken into account to some extended. No attempt is made to ensure deflection compatibility for the two orthogonal strips. In the cases of three-sided support where the top of a panel is free and the base simple supported, the strength of the vertical strip is based on a span double the panel height.

1.3.6 Finite Element Analysis

Analyses using the non-linear finite element method were reported by May and Ma [10], and Drysdale and Essawy [82].

May and Ma [10] used a non-linear finite element analysis and correlated the results from their computer analysis with those from full scale tests carried out by a number of researchers. An accurate description of the flexural strength properties of a material is essential if the behaviour of a plate of a material subjected to lateral loading is to be predicted. May and Ma [77] proposed a tri-linear stress-strain relationship and a complete biaxial failure criterion for masonry in flexure.

Drysdale and Essawy [82] proposed a macroscopic biaxial failure criterion to predict the strength and the mode of failure of masonry assemblages. This criterion accounted for the anisotropic and composite nature of masonry and was based on physical interpretations rather than being strictly a phenomenological criterion. In this model, the anisotropic nature of masonry, the non-linearity due to cracking and the effects of the transverse shear deformations due to the presence and the discontinuity of the block webs were taken into consideration.

Although the results obtained from these analyses correlated well with solid panels, none have yet been fully tested for application to panels with openings.

2.0 FINITE ELEMENT ANALYSIS

2.1 Masonry Constitutive Model

One of the fundamental requirements of non-linear structural analysis using the finite element method is a suitable model for the materials. Over the past 20 years, since the finite element method was first applied to the analysis of reinforced concrete beams, the numerical modelling of concrete has received considerable attention. Some of the modelling techniques used in concrete can be applied to masonry [10,13,82],and are used in the analysis described. Any numerical model used should include the following:

(1) A stress-strain relationship to simulate the behaviour of masonry prior to failure.

(2) A failure criterion representing the ultimate strength of masonry under different loading states.

(3) A post failure stress-strain relationship to account for the change of behaviour, if any.

(4) A crack model to define the direction and propagation of cracks.

The following sections describe these requirements and the models used in the program.

Details of the finite elements, the integration rules, and the non-linear solution techniques adopted in the program are given elsewhere [13,89].

2.1.1 Stress-Strain Models

One way of modelling the composite behaviour of a masonry panel described in sections (1.2.2) and (1.3.1) would require, ideally, a number of elements for each brick and mortar in conjunction with failure criteria for brick, mortar, and the interface as used by Page [90,91]. This would be impractical for the present investigation because of the large number of elements required. The strategy adopted in the analysis is therefore to simulate the behaviour of bricks and mortars by a 'smeared' model to reduce the number of elements and hence the complete time required for analysis. This is achieved by obtaining the flexural behaviour of masonry from the flexural strengths and behaviour of one way spanning wall specimens, particularly the vertical and horizontal flexural tensile strengths obtained from the 'wallette' tests. The ultimate strength of masonry is then represented using a principal stress biaxial failure criterion.

In the present analysis masonry is modelled as a tri-linear elastic-plastic material in compression, Figure 2.1. Under uniaxial tension, a linear elastic-brittle behaviour is assumed for bending both parallel and normal to the bed joint, Figure 2.1. It is thought that strain softening behaviour may be included in bending normal to the bed joint to account for the torsional resistance of the mortar/unit interface as described in section (1.2.2). However, both the elastic-brittle and the elastic strain-hardening models need to be fully examined to check the effect of any softening model.

Within the elastic range, masonry can be considered as either isotropic or anisotropic. However, in the present analysis, masonry is treated as an isotropic material as it has been

reported [75] that the non-linearity caused by the constituent materials is insignificant compared with that resulting from progressive cracking. The biaxial stress-strain relationships for isotropic linear elastic material are given by eqn. (2.1).

$$\begin{bmatrix} \sigma_x \\ \sigma_y \\ \tau_{xy} \end{bmatrix} = \frac{E_b}{1-\nu^2} \begin{bmatrix} 1 & \nu & 0 \\ \nu & 1 & 0 \\ 0 & 0 & \frac{1-\nu}{2} \end{bmatrix} \begin{bmatrix} e_x \\ e_y \\ \gamma_{xy} \end{bmatrix} \qquad \ldots(2.1)$$

Where σ_x and σ_y are stresses parallel and normal to the bed joint,

and τ_{xy} is the shear stress.

2.1.2 Biaxial Stress Failure Criterion

In order to use the finite element method to analyse masonry panels from zero load up to collapse accurately a biaxial failure criterion for the flexural stresses, which includes the directional properties of masonry, is required. The flexural stresses in terms of the two principal stresses and their orientation to the bed joints are also required. A biaxial failure criterion for a complete failure criterion should cover the compression-compression, compression-tension, and tension-tension zones. The failure criterion is similar to that proposed by May and Ma [77].

Biaxial constitutive relationships for masonry, have received little attention from researchers although Page [90,91] has examined both the tension-tension range and compressive-compressive range by using a non-linear finite element model. Samarasinghe, Page and

Hendry [75] have studied the tension-compression range in a similar manner. In both investigations the ratio of the principal stresses and their orientation to the bed joint were found to be important.

Few experimental studies of masonry subjected to simultaneous vertical and horizontal bending moments have been carried out because it is difficult to apply moments to masonry specimens. Baker [76] considered that the behaviour of a panel can be approximately reproduced by tests on 'single joint' specimens. A number of joints were tested under various combinations of horizontal and vertical moments. A series of tests were conducted and it was shown that the failure criterion for combined vertical and horizontal moments for range of brickwork could be represented using an elliptical interaction curve, eqn (2.2).

$$\left[\frac{F_v}{F'_v}\right]^2 + \left[\frac{F_h}{F'_h}\right]^2 - 1 \qquad \ldots(2.2)$$

Where F_v, F_h, are extreme fibre stresses in biaxial bending

and F'_v, F'_h, are moduli of rupture in one-way bending or uniaxial flexural strengths.

Baker's tests only covered the cases with bed joint orientation $\theta = 0°$ and $\theta = 90°$. For the present study, a linear relationship between the change of stresses and the change of bed joint orientation is assumed. The failure surface together with the bed joint orientation, θ, can then be related through a 3-dimensional model as shown in Figure 2.2a. The equation governing the surface of the failure criterion is given by eqn (2.3).

$$\left[\frac{\sigma_x}{\sigma_{1\alpha}}\right]^2 + \left[\frac{\sigma_y}{\sigma_{2\alpha}}\right]^2 - 1 \qquad \ldots(2.3)$$

Where $\sigma_{1\alpha} = \sigma_{10} - (\sigma_{10} - \sigma_{1\pi/2})\, 2\alpha/\pi$

$\sigma_{2\alpha} = \sigma_{20} - (\sigma_{20} - \sigma_{2\pi/2})\, 2\alpha/\pi$

σ_x, σ_y, are the failure stresses at a particular θ,

and α is the angle between the direction of the maximum prescribed stress and the bed joints.

In the tension-compression zone, a linear relationship between the tensile strength and the uniaxial compressive strength of masonry is assumed, Figure 2.2b.

In the compression-compression region a square failure criterion is assumed, Figure 2.2c.

The onset of cracks in a laterally loaded masonry panel is caused by the tensile failure of the material. It would therefore appear that, irrespective of the mode of failure described in sections (1.2.2) and (1.3.1), the tensile-tensile zone, Figure 2.2a, in the failure criterion is the most critical region for the determination of the ultimate flexural capacity of a masonry panel.

The biaxial stress failure surfaces in the three zones are shown in Figure 2.2d and 2.3. From Figure 2.3, it can be seen the proposed failure criterion gives a reasonable approximation to the results obtained by Page [90,91] and Samarasinghe and Hendry [75]. In the compressive-compressive region it can be seen to be conservative. In the other regions, which generally

govern the failure of masonry panels subject to bending, it shows good correlation.

2.1.3 Modelling of Cracking and Crushing

In general, failure can be divided into either crushing in compression or cracking in tension. Crushing failure leads to the complete disintegration of the material. Masonry is assumed to crush when the deformation level reaches its ultimate capacity, Figure 2.1. After crushing, the stresses drop abruptly to zero, and the masonry is assumed to completely lose its resistance against further deformation in any direction.

Cracking is assumed to occur when the tensile stress within an element reaches the limiting tensile value given by the biaxial failure envelope, Figure 2.2a. The direction of the crack is fixed normal to the direction of the principal stress violating the failure criterion. After cracking, the masonry abruptly loses its strength normal to the crack direction. However, material parallel to the crack is assumed to carry stress according to the uniaxial conditions prevailing in that direction.

In the tension-compression zone, Figure 2.2b, only tensile failure is assumed to occur initially. Once a crack has formed, the material sustains compressive stress parallel to the direction of the crack according to the uniaxial compressive failure condition, Figure 2.1.

The onset of tensile failure causes highly anisotropic conditions to develop. After cracking occurs, the material property matrix in the cracked zones is given by eqn (2.4).

$$\begin{bmatrix} \sigma_n \\ \sigma_p \\ \tau_{np} \end{bmatrix} = \begin{bmatrix} 0 & 0 & 0 \\ 0 & E_b & 0 \\ 0 & 0 & 0 \end{bmatrix} \begin{bmatrix} e_n \\ e_p \\ \gamma_{np} \end{bmatrix} \quad \ldots(2.4)$$

Where σ_n is the stress normal to the crack direction

and σ_p is the stress parallel to the crack direction.

Equation (2.4) allows no shear stresses thus this converts the biaxial stress system for uncracked masonry into a uniaxial system after cracking.

2.2 Masonry Representation

Masonry is simulated by four noded flat shell elements with offset axes [92]. Each node has six degrees of freedom, three axial displacements u,v and w in the x, y and z directions respectively and three rotations θ_x, θ_y and θ_z.

It is possible to stack elements into layers with different material properties, each element having a common reference surface which may be offset from the mid plane of the element.

For the modelling of a cavity wall, a slip plane is introduced between the two layers of stacked elements with each layer sharing one common axial displacement w and two common rotations θ_x and θ_y. Inplane displacements u and v and rotation θ_z are not restrained since the wall is free to move in the individual layer of elements. Thus, the degrees of freedom in each node is increased from six to nine, five axial displacement u_1, u_2, v_1, v_2, w and four rotations

θ_x, θ_y, θ_{z1} and θ_{z2}, where subscripts 1 and 2 correspond to the two layers of elements. In this case, the tie stiffness is assumed to have an infinite value.

2.3 Integration Rules

In plane a 2x2 point Gauss-quadrature integration scheme is employed. In addition to sampling the strains on the x-y plane, they are sampled at ten stations through the depth of the element (out of plane) to detect non-linear behaviour (cracks) and to determine the moments.

2.4 Non-Linear Algorithms

An incremental iterative approach with a constant stiffness matrix is used in the program. Line search techniques are used to reduce the number of iterations required, and hence accelerate convergence.

2.5 Loading Schemes

Two types of loading schemes are employed in the program.

(a) An incremental loading scheme with the size of the increment specified by the user. If convergence is not achieved after a specified number of iterations, the load

increment is reduced automatically to one quarter of the size. This is continued, when necessary, until the size of the increment is 1/64 of the initial load increment. When convergence is not achieved with this load increment size, the program is terminated. In this approach, the behaviour of a panel up to the maximum load capacity can be found in a single run.

(b) In the arc length incremental scheme [93], the initial increment load factor and the number of iterations within an increment are specified by the user. Subsequent load increments are automatically generated, since both load and displacement are varied in the arc length iteration procedure. The full load-displacement relationship, including that beyond the maximum load capacity of any masonry panel, can be traced.

2.6 Convergence Criteria

In an incremental-iterative solution technique, it is impractical to strictly satisfy equilibrium between the externally applied forces and the internal stresses. Thus a method is used where during the iterative process, the solution is checked against specified convergence criteria. The convergence criteria, usually used for non-linear structural analysis, are based on the out of balance forces, changes in the displacement, or the internal energy.

The convergence criteria adopted in this work are based on a residual displacement norm, eqn. (2.5a) and a residual rotation norm. eqn. (2.5).

$$TOD > \sqrt{\frac{\sum (Change\ In\ Incremental\ Displacement)^2}{\sum (Total\ Displacement)^2}} \qquad \ldots(2.5a)$$

$$TOR > \sqrt{\frac{\sum (Change\ In\ Incremental\ Rotation)^2}{\sum (Total\ Rotation)^2}} \qquad \ldots(2.5b)$$

Where TOD and TOR are pre-selected convergence tolerance. A value of 0.002 was found to be suitable for both TOD and TOR. Both criteria have to be satisfied before convergence is said to be achieved.

2.7 Termination of the Analysis

The analysis is terminated when any of the following criteria is satisfied:-

(a) the number of load increments exceeds a maximum specified number.

(b) convergence is not achieved after the load increment has been reduced three times, each time the new increment being 1/4 of the previous.

(c) convergence is not achieved in 120 iterations.

2.8 Effects of Element Discretisation

It is considered important to examine the performance of the finite element model for analysing laterally loaded masonry panels. The first example chosen is a 4800mm long,

2400mm high and 100 mm thick rectangular masonry wall simply supported on all four edges. A quarter of the panel was analysed with various element densities until convergence occurred. It was established that reasonable convergence of the load-deflection relationship occurred when an element mesh of 6 x 6 (36 elements) was used. However, an element mesh of 8 x 8 (64 elements) was used in the present study as it was found to produce a smoother load-deflection curve and lie much closer to the 10x10 element result, Figure 2.4. For this reason, all of the solid panels analysed in this chapter are of 8 x 8 element discretisation, unless indicated otherwise. The reduction in panel stiffness, Figure 2.4, was caused when the initial horizontal crack at the mid-height of the panel occurred. This transformed the load carrying mechanism of the panel from a two-way bending, four edges simple supported, to a one way bending, three edges simple supported.

The second example is a panel tested by the British Ceramic Research Association [2], which contained an opening. It was fixed at the three sides and had the top edge free. The panel configurations and the element mesh patterns are shown in Figure 2.5a. Mesh pattern 1 produced a much stiffer response with a higher failure capacity. It can be seen from Figure 2.5b that refinement of mesh density produced a lower failure pressure. The finite element mesh has been refined at the vertical support, mesh pattern 4, as the failure was found to be initiated by diagonal cracks generated at the panel's vertical supports. Further mesh refinement at the vertical support, mesh pattern 5, showed no significant differences in the predicted behaviour indicating a converged solution. Thus, mesh 4 was adopted in the present study for the analysis of panels with openings unless stated otherwise.

The third example is chosen in particular to investigate the effect of stress concentration at

the corners of an openings. The panel is 4.0m square with a 1.0m square central opening. The wall thickness is 100mm. The panel is simple supported along all four edges. The material of the panel has the properties: Initial elastic modulas = 9 kN/m^2; Poison's ratio = 0.2; flexural strength normal to the bed joint = 0.9 N/mm^2 and a orthogonal ratio = 0.33. A quarter of the panel is modelled with refining mesh toward the opening corner. The element mesh pattern is shown in Figure 2.6a. It can be seen from Figure 2.6b that the analytical principal stress 1 at the corner of the opening increased as the mesh was refined. This increase in the principal stress was due to the increase of twisting moment M_{xy} while local moments M_x an M_y practically remained unchanged, Figure 2.6d and 2.6e. However, this stress concentration was found to be localised at a very small area at the opening corners and generally did not effect the analytical failure strength of the panel, Figure 2.6f. Unless the element mesh is excessively refined, the effect of this stress concentration on the failure strength is negligible.

Using the heterosis element, Cope and Clark [94] have demonstrated the inaccuracy of a finite element solution based on a classical thin plate theory in modelling a free boundary condition because of the assumption of plane remaining plane, Figure 2.7.

At a free edge, force boundary conditions are not satisfied exactly in a displacement finite element solution. With a sufficient fine mesh of elements close to a free edge, the heterosis element predicts values of normal and twisting moment, and shear force, that tend to zero on the free edge, Figure 2.7. Because shear forces and rates of change of moments are linked by equilibrium, the shear forces on sections intersecting a free edge are also erroneously predicted by solutions based on classical plate theory. Similarly, the principal stresses and

their orientations are also erroneously predicted.

As the failure criterion adopted is a principal stresses biaxial failure criterion, the effect of the presence of twisting moment at an free edge can give rise to erroneous failure predictions with fine mesh of elements close to an edge.

Figure 2.1 Uniaxial Stress-Strain Relationship.

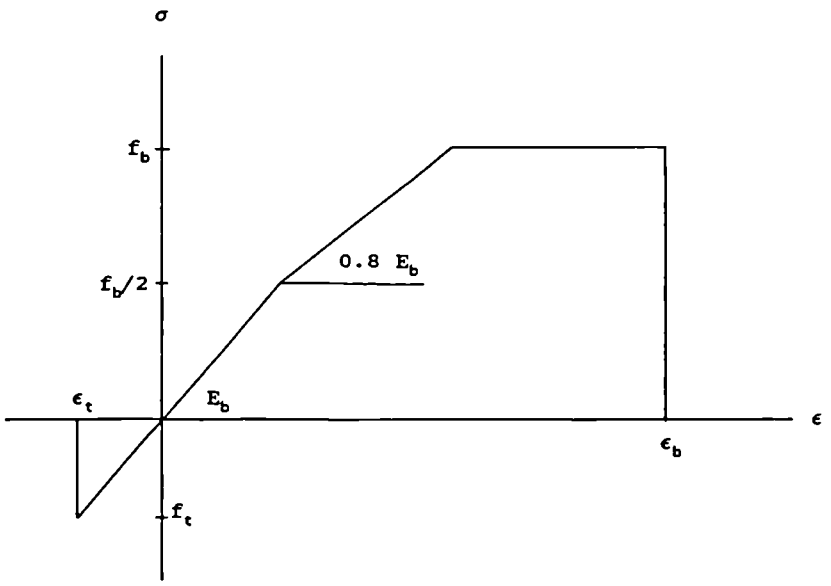

Figure 2.2 Complete Biaxial Failure Criterion.

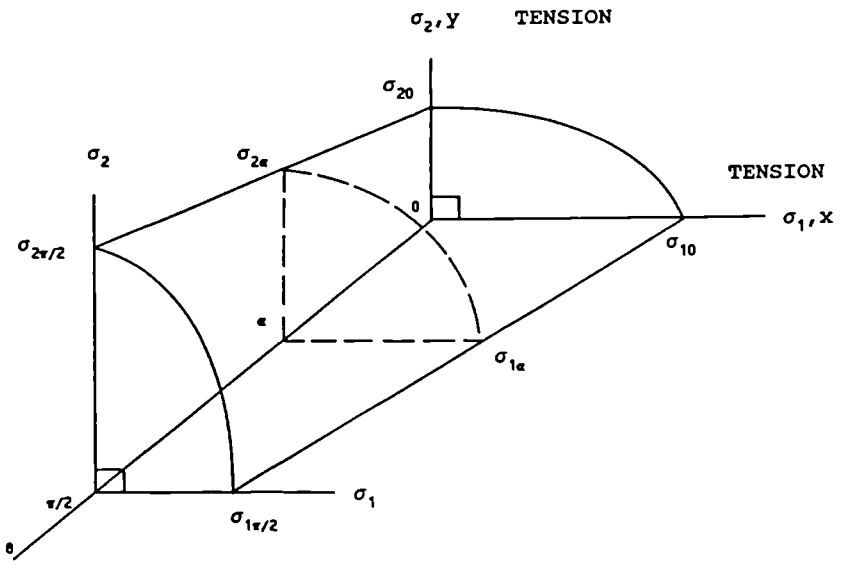

(a) Tension-tension

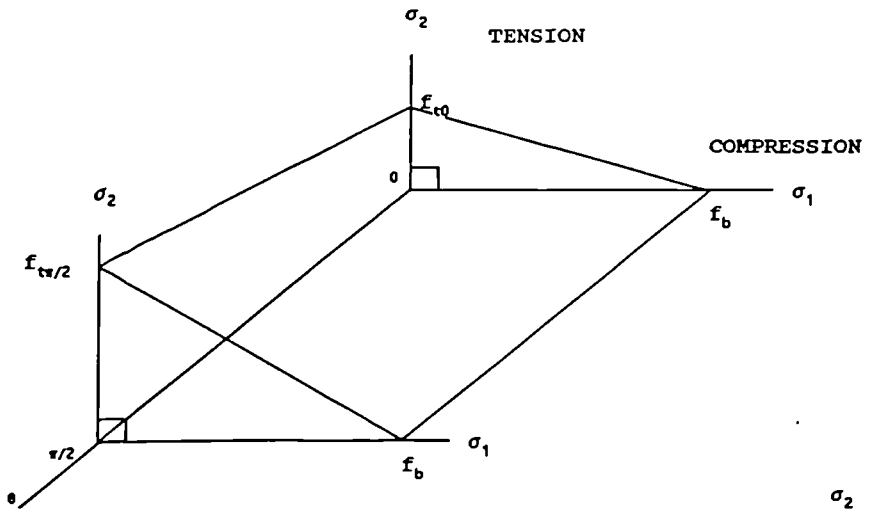

(b) Compression-tension

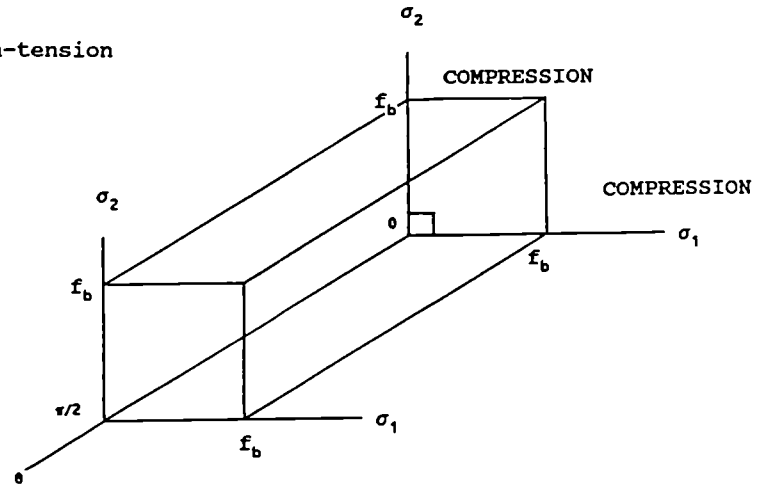

(c) Compression-compression

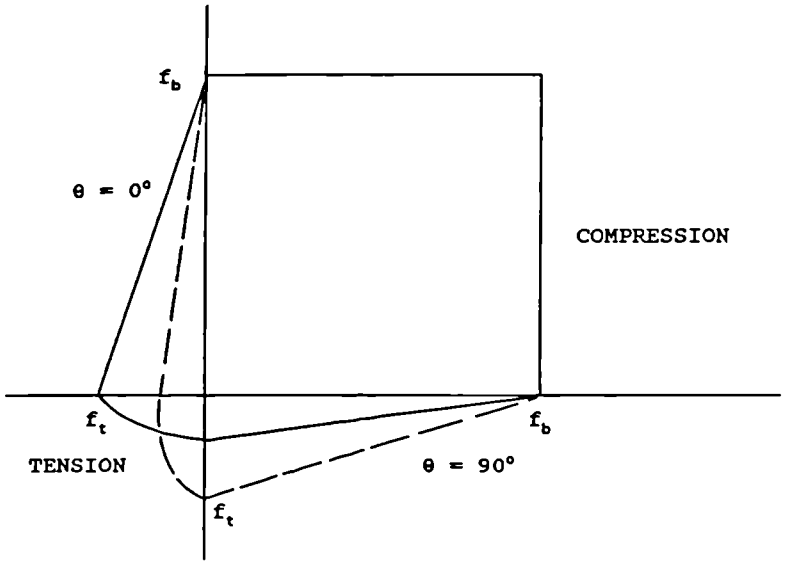

(d) Complete failure criterion.

Figure 2.3 Comparison of the Biaxial Relationship with the Proposed Biaxial Failure Criterion.

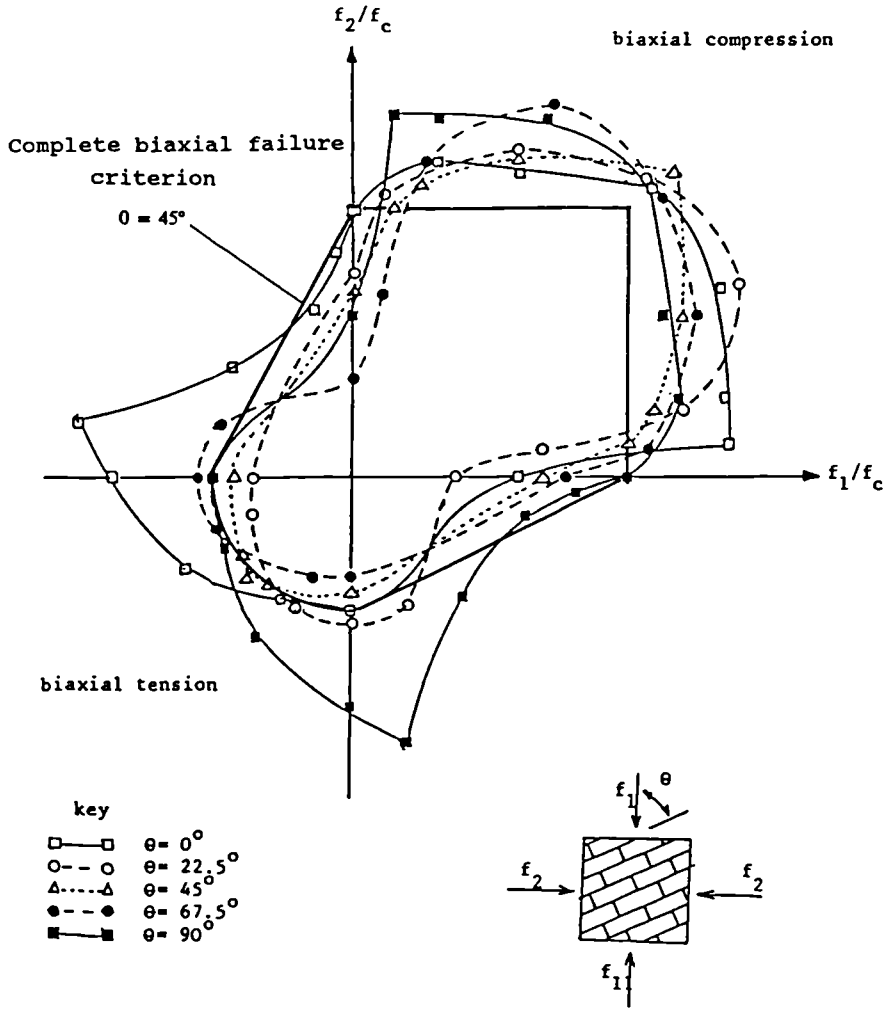

Figure 2.4a Comparison of Load Displacement Relationship, Simply Supported Solid Panel - Load Control.

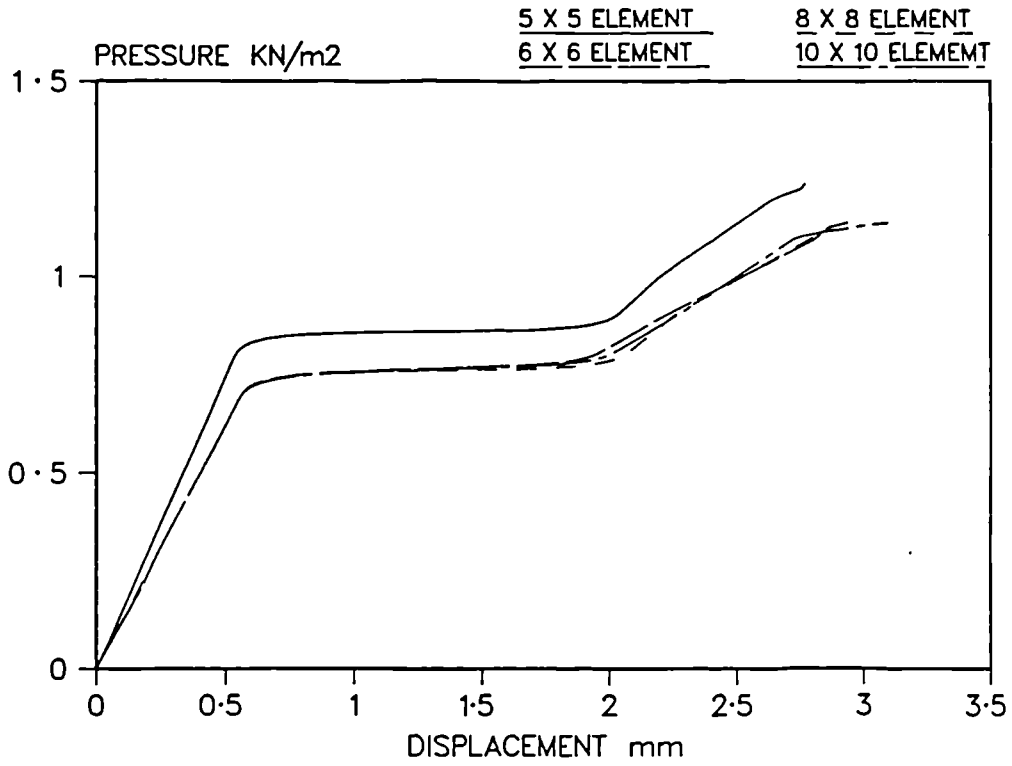

Figure 2.4b Comparison of Load Displacement Relationship, Simply Supported Solid Panel - Arch Length Control.

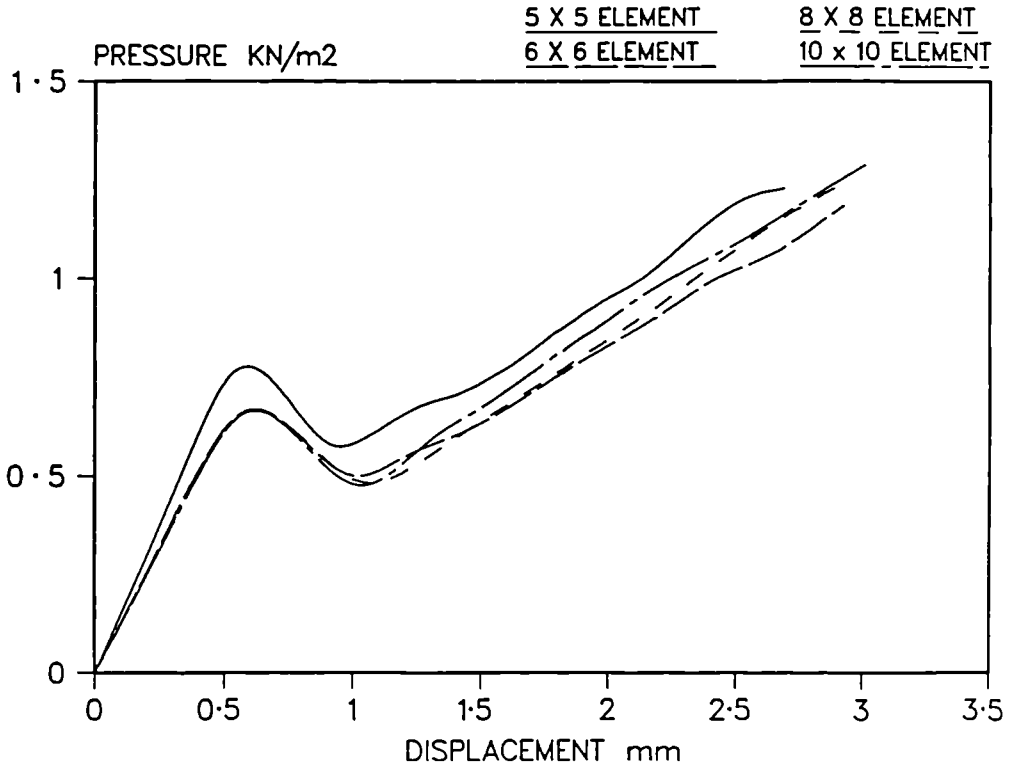

Figure 2.5a Wall 1139 Finite Element Mesh Patterns.

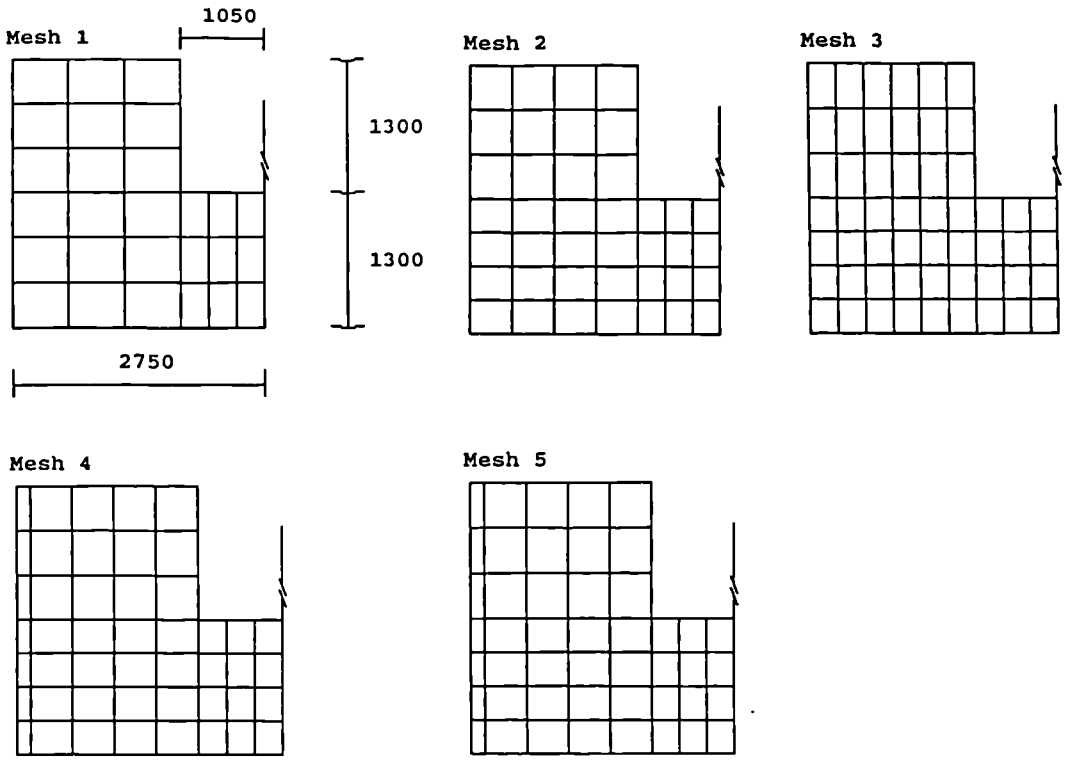

Figure 2.5b Comparison of Load Displacement Relationship of Panel with Opening - Wall 1139.

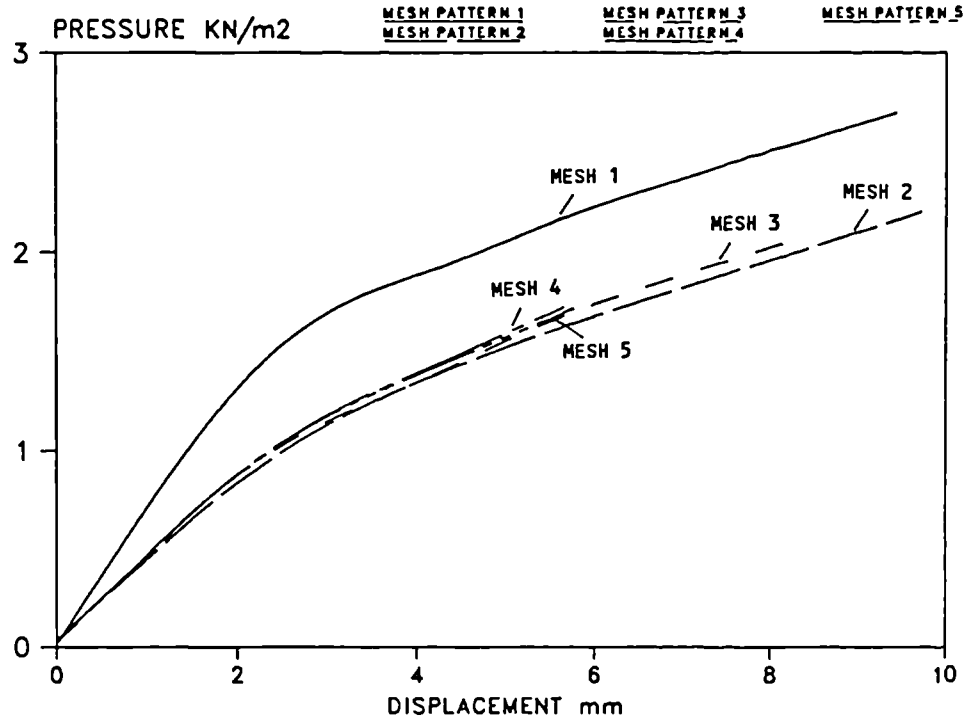

Figure 2.6 Investigation of Stress Concentration at Corner of an Opening.

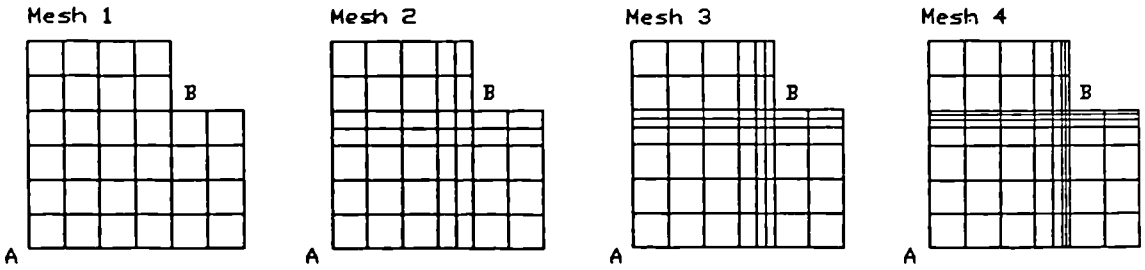

(a) Finite Element Mesh Patterns

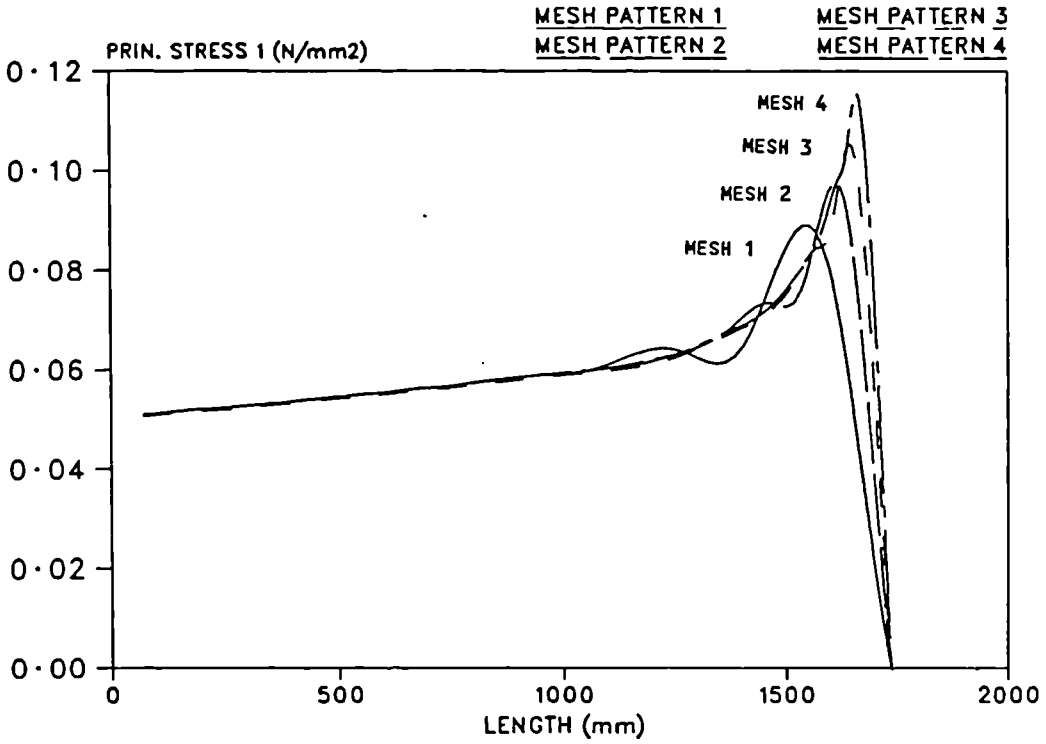

(b) Principal Stress 1 Distributions on Section A-B

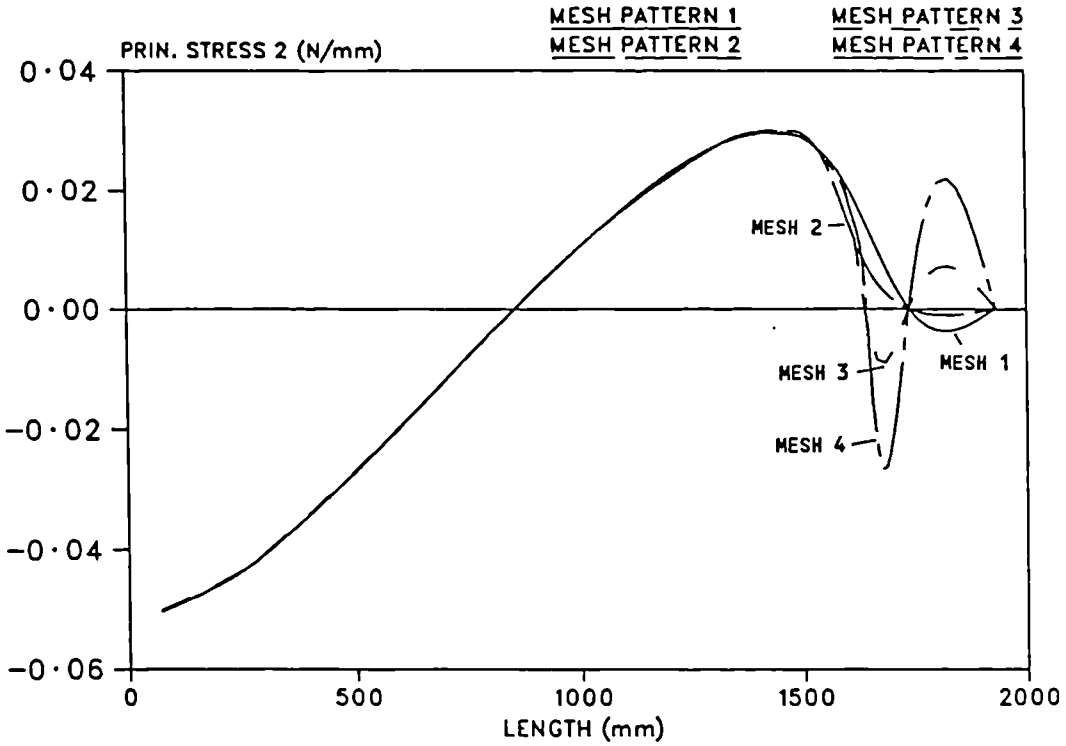

(c) Principal Stress 2 Distributions on Section A-B

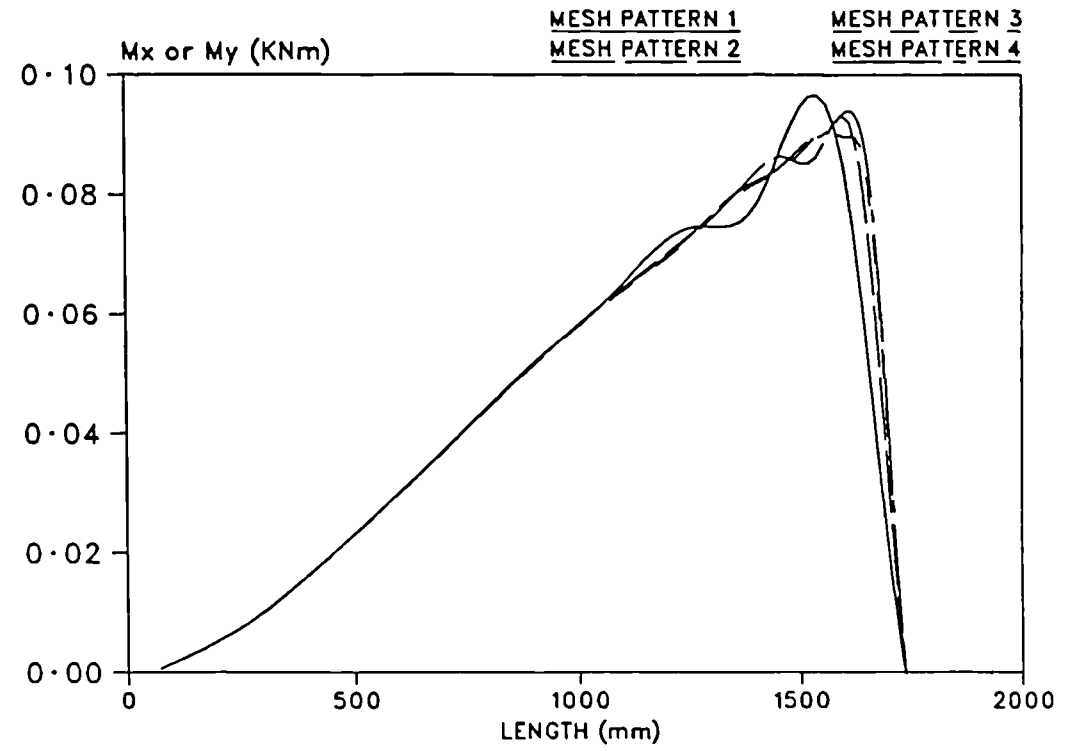

(d) Moment X and Moment Y Distributions on Section A-B

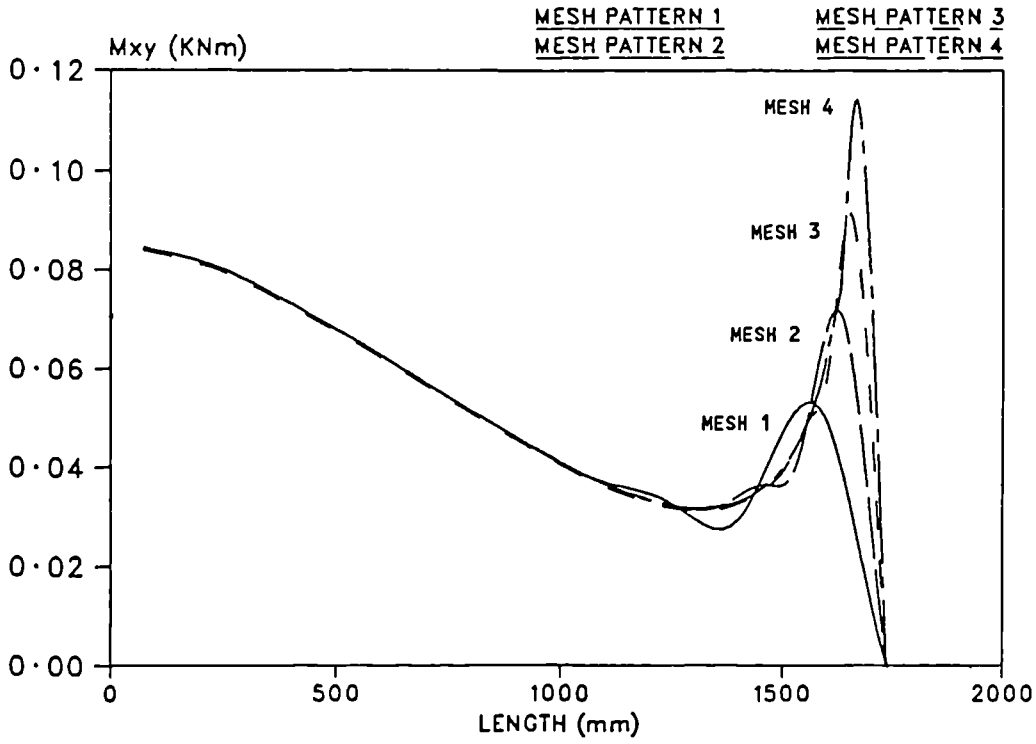

(e) Twisting Moment Distributions on Section A-B

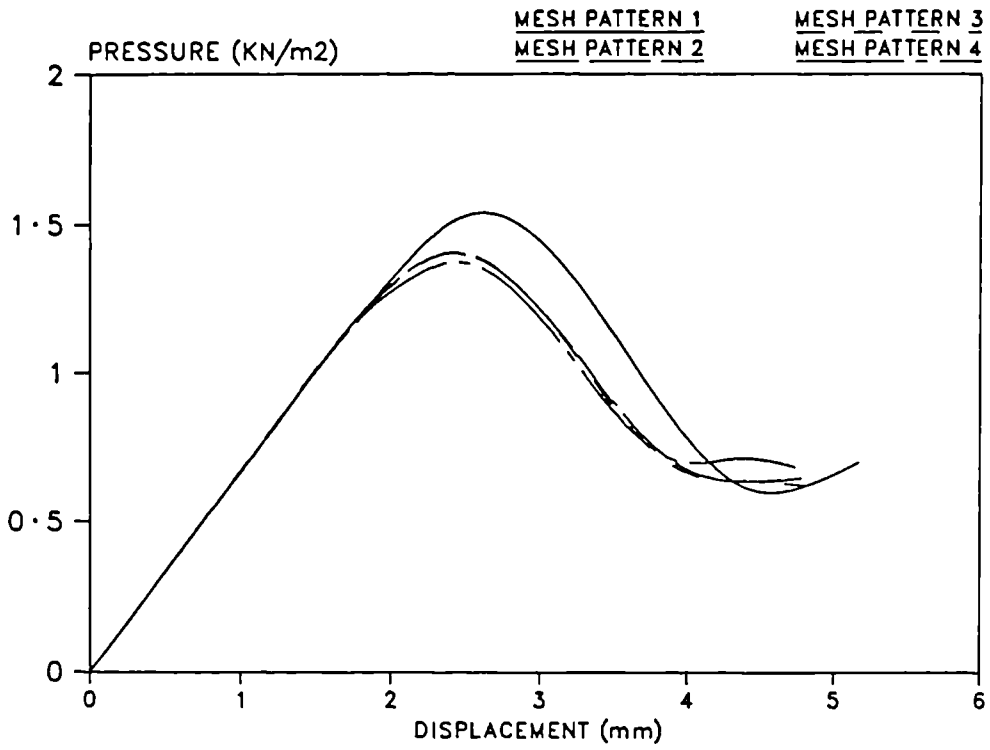

(f) Load Displacement Relationship on Point B.

Figure 2.7a Nine-Panel Building Slab.

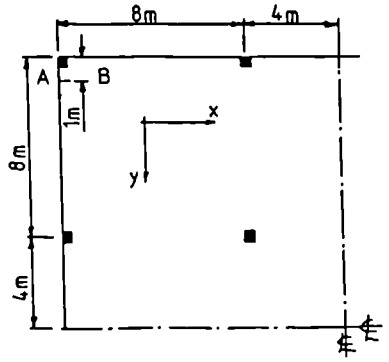

Figure 2.7b Twisting Moment and Shear Force Distributions on Section A-B of Figure 2.7a, with no Moment Transfer to Columns.

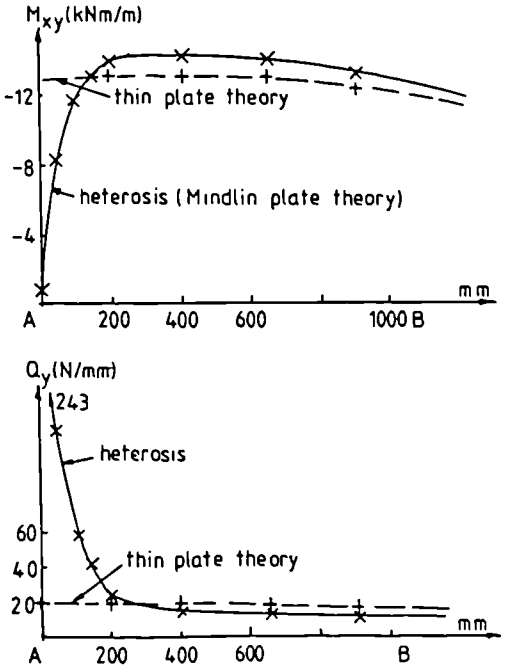

3.0 COMPARISON WITH EXISTING EXPERIMENTAL RESULTS

3.1 Tests Reported by Haseltine Et. Al.

More than 200 tests on large scale brick walls under lateral loads have been carried out at the British Ceramic Research Association since 1977 [2]. In this report, results of several single leaf brick walls from their test program have been analysed. They cover both solid panels and panels with opening. The analytical load-displacement curves have been compared with the experimental results for the following:

(a) Wall 1150 - solid panel,

(b) Wall 1136 - panel with bonded returns at each end,

and (c) Wall 1134, 1139 and 1141 - identical panels with openings.

The predicted failure patterns have also been compared with the experimental failure patterns.

May and Ma [10] analysed these panels using an orthogonal ratio of 1. Crack patterns at failure were not given. However, similar conclusions as those given in this Chapter were drawn.

The material and geometrical properties and edge restraint assumed for the specimens are summarised in Tables 3.1 and 3.2. All walls were built on the laboratory floor within a steel frame and were tied at both vertical edges and had the top edge free. There was a bituminous d.p.c between the first and second brick course. The uniformly distributed loads were applied using air-bags. Wall 1136 was 2.6m high and of overall length 8.2 m supported at either end

by two 1m returns. The central portion of the wall, 2.7m long, was continuous over two stiff steel channels.

In the finite element analysis, all panels except 1136 were analysed with boundaries rotationally restrained, the assumption being that the d.p.c. is of similar strength in flexure to other horizontal mortar joints in the wall. As it was doubtful that the brick ties at the vertical supports would be able to provided full rotational restraint, especially for thick walls, analyses with the vertical edges simple supported were also carried out. The flexural strengths normal and parallel to the bed joints were taken as those reported, Table 3.3. The elastic modulus was taken as 9 kN/m^2 in all analyses.

In general, good agreement was found to exist between the analytical and the experimental ultimate loads for the panels analysed, as shown in Figures 3.1 and 3.2. The experimental results of the 102mm thick walls were found to correlate well with the analytical results assuming the vertical edges rotationally restrained while the results of the 215mm thick walls was in better correlation with that assuming the vertical edges simple supported. The predicted and experimental failure loads are summarised in Table 3.1.

3.1.1 Wall 1150

The analysis employs the arc length method [93] which allows it to follow falling branches in the load-displacement relationship. Figure 3.3 demonstrates the advantage of the method over normal load control. In the analysis, a horizontal crack was first generated at the surface

along the bottom edge of the panel and this caused the panel stiffness to reduce. Further increase of pressure induced a vertical crack at the vertical edge supports. The panel reached an initial peak of 7.3 kN/m^2 and then lost strength after the formation of the initial horizontal and vertical cracks. The panel required a further increase in the pressure to cause further deformation and to generate diagonal cracks near the bottom corners, which joined the initial horizontal and vertical cracks, and further diagonal cracks which ran from the free edge to the bottom corners of the panel, Figure 3.3. The ultimate failure capacity predicted was 8.95 kN/m^2 compared to the experimental value of 10.7 kN/m^2. It is suggested that the decrease of the analysed panel capacity was due to moment re-distribution in the panel during the transition from horizontal cracking to diagonal cracking. Overall, the analytical load-displacement graph shows similar trends to those in the experiment. The crack pattern predicted by the analysis is identical to the experimental failure crack pattern, Figure 3.3.

3.1.2 Wall 1136

The ability of a wall panel within a continuously supported wall, to carry load by arching action [63,66] is demonstrated by reference to Figure 3.4. Despite the occurrence of an initial horizontal crack along the bottom edge of the panel at load about 2 kN/m^2, the internal arching effect enabled the panel to carry further load up to 3.82 kN/m^2, compared to the experimental value of 4.1 kN/m^2. The panel has been reanalysed assuming the rotation restrained on three sides, but with the inplane displacement free, to investigate the amount of arching action generated. The reanalysed panel yielded a much stiffer response initially, and lost strength after the first horizontal crack developed before reaching a much lower

failure capacity of 3.0 kN/m^2 than the previous analysis. The experimental and analytical failure patterns are nominally identical, Figure 3.4.

3.1.3 Walls 1139, 1141

The difference in the load-displacement relationship and the failure loads for the two nominally identical panels indicates the variability [16] associated with masonry panels, Figure 3.5. It can be seen that the analysis shows similar behaviour to that observed in the tests, and that the non-linearity occurred because of the propagation of a horizontal crack along the bottom edge of the panel, and the collapse mechanism was caused by diagonal cracks which formed across the panel. The failure pattern predicted by the analysis is similar to the experimental failure pattern, Figure 3.5.

3.1.4 The Effect of Limited Ductility on Collapse Loads

Before assessing the results of the preliminary parametric survey carried out using the computer program, Figure 3.6, it is of interest to study the behaviour of uniformly loaded beams with materials that exhibit elastic-plastic and elastic-brittle behaviour. May and Ma [10] have shown that the collapse load for a simply supported beam constructed of either material is $8M_c/l^2$ where l is the span of the beam and M_c is the maximum moment carrying capacity of the section. However if the same beam is fully fixed at both ends then for the elastic-plastic material the first hinges will occur at the supports when $W_{cp} = 12M_{cp}/l^2$, where

the subscript p indicates plastic material, the moment at the centre being $M_{cp}/2$. Further load can be carried until a third hinge forms at the centre of the beam when $W_{cp} = 16M_{cp}/l^2$, and collapse will occur.

With the brittle material the first hinges also occur at a load of $12M_{cp}/l^2$. However any further increase in load causes the moment capacity at the support to reduced to zero. In order to preserve equilibrium the moment at the centre would have to increase to $3M_{cp}/2$, which is greater than the maximum moment capacity and therefore the beam will fail. Thus the load capacity of the fixed ended brittle beam is only three-quarters of the ductile beam although the maximum moment capacity for each cross-section is the same. This reinforces the earlier comment of Baker et al [9] in section (1.2.8).

BS5628 does not include one way spanning walls in the panel design clauses. However if the same method as that used in BS5628 were to be used for the two examples above then, assuming the correct value of the ultimate moment capacity is known, the correct value of the collapse load would be obtained for the simply supported one-way spanning member. However for the fixed ended member the code method would estimate the collapse to be $16M_{cp}/l^2$, which is obviously unconservative. The method given in BS5628 is thus likely to overestimate the collapse load by up to 33% and possibly more for panels supported on three or four sides [10]. It can be appreciated from the above that the major problem with yield line analysis because of the lack of ductility of masonry, limits its ability to redistribute the internal moment.

3.1.5 Solid Panels

The experimental failure pressures from some of the tests on solid panels are plotted against the finite element predictions in Figure 3.1. It can be seen that the analysis, when flexural strengths from wallette tests are used, gives a slightly conservative prediction of failure pressures for the range of walls reported.

The ratio of the collapse loads obtained from the finite element analyses, P_{ex} and the loads obtained using the yield line analyses by Haseltine et. al. [2], and as used in BS5628, p_d, are presented on Figures 3.6 and 3.7. It can be seen from Figure 3.6 that as H/L increases to 2 the method of BS5628 produces increasing unconservative results. As H/L becomes larger so the ratio P_{ex}/P_d tends to 0.75 as would be expected for a brittle material since the panel is becoming, effectively, a fixed ended beam. Also plotted on Figures 3.6 and 3.7 are the results of tests reported [2] and, even thought the boundary conditions are not identical, and therefore the results are not strictly comparable, these can be seen to follow a similar trend, indicating the BS5628 design method consistently overestimates the failure strength.

It is also evident from Figures 3.1, 3.6 and 3.7, that the finite element analysis provides consistent predictions of ultimate flexural capacity of masonry panels in comparison with the experimental results. Hence, the assumption of the d.p.c having similar flexural strength to the other horizontal joints appears to be reasonable. This confirms the results of May and Ma [10].

3.1.6 Panels with Openings

The ability of the analysis to account for the inclusion of openings in masonry panels is demonstrated in Figure 3.8 and Table 3.2. Good correlation exists between the analytical and the experimental collapse loads. These again indicate the unconservative assumption made by many researchers when comparing experimental results with yield line theory, that the d.p.c has zero flexural strength. Yield line analysis, however, overestimates the lateral strengths of the shorter panels, those with higher H/L ratio, Table 3.2.

3.2 Tests carried out at Polytechnic South West

Two series of lateral loading tests on 11 full size brick panels with openings have been carried out by Tapp and Southcombe [1,14]. The uniformly distributed pressures were applied using an air bag loading system. Seven panels from the two series have been analysed using the computer program.

The panel configurations are shown in Figures 3.9 and 3.10. The experimental failure pressure for each of the panels, along with the pressure predicted by the program for the panels are given in Table 3.4, and Figure 3.8.

3.2.1 Panel 1-3

Three panels, with various opening sizes, were constructed in a similar manner. Each single leaf panel, 4840mm long by 2417mm high, was built between two abutments of 432 x 102mm R.S.C sections bolted to a strong floor. The vertical edges of each panel were tied to the vertical abutments by vertical twisted ties whilst the bottom course of each panel was built directly onto the floor with a polythene d.p.c in the first bed joint. The top of the panels was unsupported. The panels were constructed using clay bricks of water absorption of 16.8% and a compressive strength of 34.4 N/mm^2, set in 1:1:6 designation (iii) mortar of 10 N/mm^2 cube strength. The panel configurations and finite element meshes used are shown in Figure 3.9.

In the analysis, the panels were analysed with fixed boundaries. The d.p.c was assumed to have a similar flexural strength to the other horizontal joint. The tensile strengths normal and parallel to the bed joints of the brickwork were taken as 1.2 N/mm^2 and 0.4 N/mm^2. The crushing strength of the brickwork was taken as 15 N/mm^2.

It is evident from Table 3.4 that the finite element analysis produces reasonably accurate predictions, and a decrease of lateral capacity with an increase in opening size. The higher experimental failure pressure obtained for panel 3 may be due to the variability of material properties and the edge restraints provided by the abutment ties. As it is expected the lateral capacity of a panel decreases with larger openings.

3.2.2 Panel ART01-ART06

The six wall panels, one solid and five with openings, were each 4715mm long, 2465mm high and 102.5mm thick. All six panels were built directly onto the laboratory floor within two post-tensioned masonry abutments. The vertical edges of the panels were simply supported against two steel angles bolted to the abutments with a 10mm gap left between the panel edges and the abutments. The panel configurations and the finite element mesh patterns are shown in Figure 3.10. Each panel was constructed using perforated class A engineering bricks with a mean compressive of 130 N/mm^2 and a initial rate of suction 0.28 kg/m^2/min. The unit modulus of rupture was 14.1 N/mm^2. The mortar used in panel ART01 was a mortar designation (i) mix with volume proportion 1:1/4:3 OPC:lime:sand and with a mean compressive strength of 35 N/mm^2. Mortar designation (ii) of 1:1/2:4 1/2 OPC:lime:sand by volume mix was used in the other three panels. The mean compressive strength of the mortar was 22 N/mm^2. The sand used was crushed limestone sand and was classified as a zone 2 sand to BS1200 [95]. The fineness modulus was 3.68.

The tensile strengths of the brickwork normal and parallel to the bed joints were taken as 0.32 and 0.12 N/mm^2. The crushing strength of the brickwork, f_{cr}, was assumed to be 66 N/mm^2 for panel ART01 and 40 N/mm^2 for the rest of the panels.

The deflection at the centre of the top edge of the wall obtained from the analysis and the tests have been plotted, Figures 3.11 to 3.15. A summary of the experimental failure pressure for each of the panel, along with the pressure predicted by the computer program is given in Table 3.4.

It can be seen that the analytical results follow the initial loading curve and also lie close to the final loading curve above the initial cracking load. According to the analysis, the non-linearity began after the initial horizontal crack developed along the panel bottom edge. The panel continued to take load as the horizontal crack extended to virtually the whole panel length until collapse when diagonal cracks formed across the panel. The predicted crack patterns, Figures 3.11 to 3.15, are generally in good agreement to the experimental failure modes.

Table 3.1 Experimental and Analytical Failure Pressure - Solid Panels

Panel Ref.	Unit/ Mortar	Panel Dimensions	Failure Pressure kN/m²			
			Expt.	Yield Line[a]	FEA Model[b]	FEA Model[c]
1120	W4X	1.3 x 2.7 x 0.1025	10.9	13.16	9.65	9.19
1135	W4X	2.6 x 2.7 x 0.1025	6.5	9.87	6.85	5.43
1116	W4X	3.6 x 2.7 x 0.1025	7.9	8.88	6.67	4.86
1126	W4X	3.6 x 2.7 x 0.1025	6.4	8.88	6.67	4.86
1190	W4X	5.2 x 2.7 x 0.1025	6.4	8.46	6.65	4.43
1108	W4X	1.3 x 4.5 x 0.1025	5.2	6.66	4.87	4.79
1109	W4X	3.6 x 4.5 x 0.1025	3.2	3.80	2.77	2.09
1187	W4X	5.2 x 4.5 x 0.1025	2.8	3.38	2.33	1.61
1094	W4X	1.3 x 5.5 x 0.1025	3.6	5.04	4.08	4.02
1110	W4X	1.3 X 5.5 x 0.1025	5.0	5.04	4.08	4.02
1095	W4X	3.6 x 5.5 x 0.1025	2.9	2.77	1.95	1.77
1171	W4X	5.2 x 5.5 x 0.1025	2.2	2.41	1.67	1.28
1121	W6Y	1.3 x 2.7 x 0.1025	5.8	6.88	4.69	4.25
1123	W6Y	2.6 x 2.7 x 0.1025	4.4	5.35	3.04	2.31
1117	W6Y	3.6 x 2.7 x 0.1025	4.3	4.98	3.02	2.10
1203	W6Y	5.2 x 2.7 x 0.1025	3.4	4.74	2.97	1.87
1107	W6Y	1.3 x 4.5 x 0.1025	5.0	3.43	2.31	2.19
1111	W6Y	3.6 x 4.5 x 0.1025	2.5	2.06	1.17	0.94
1201	W6Y	5.2 x 4.5 x 0.1025	2.1	1.87	1.01	0.71
1096	W6Y	1.3 x 5.5 x 0.1025	2.8	1.65	1.89	1.84
1097	W6Y	3.6 x 5.5 x 0.1025	1.8	1.50	0.91	0.72
1157	W6Y	5.2 x 5.5 x 0.1025	1.4	1.35	0.73	0.55
1172	W4X	2.6 x 2.7 x 0.215	20.9	31.35	23.75	19.88
1192	W4X	3.6 x 2.7 x 0.215	18.8	28.08	23.60	17.36
1261	W4X	4.5 x 2.7 x 0.215	15.0	27.26	23.59	16.20
1169	W4X	2.6 x 4.5 x 0.215	9.5	14.40	11.66	10.87
1173	W4X	3.6 x 4.5 x 0.215	8.0	12.31	9.49	7.83
1244	W4X	4.5 x 4.5 x 0.215	8.0	11.28	8.63	6.78
1150	W4X	2.6 x 5.5 x 0.215	10.7	11.05	8.83	8.41
1153	W4X	3.6 x 5.5 x 0.215	6.7	9.06	7.04	6.47
1237	W4X	4.5 x 5.5 x 0.215	6.5	8.24	6.20	5.41
1148	W6Y	2.6 x 2.7 x 0.215	15.8	22.09	15.37	12.71
1211	W6Y	3.6 x 2.7 x 0.215	12.8	20.25	14.90	11.19
1246	W6Y	4.5 x 2.7 x 0.215	11.8	19.29	15.09	10.39
1170	W6Y	2.6 x 4.5 x 0.215	8.6	9.96	7.53	6.94
1178	W6Y	3.6 x 4.5 x 0.215	5.2	8.76	5.93	4.98
1224	W6Y	4.5 x 4.5 x 0.215	4.8	8.11	5.49	4.39
1149	W6Y	2.6 x 5.5 x 0.215	6.6	7.7	5.63	5.38
1162	W6Y	3.6 x 5.5 x 0.215	4.3	6.37	4.50	4.15
1231	W6Y	4.5 x 5.5 x 0.215	3.9	5.86	3.92	3.40

(a) Yield Line theory with allowances on edge restraint and self weight.
(b) FEA model assuming fixed boundaries on three sides.
(c) FEA model assuming fixed base and two vertical edges simply supported.

Table 3.2 Experimental and Analytical Failure Pressure - Panels with Openings

Wall no.	Geometry properties	Failure Pressure kN/m²		
		Exptal.	Y.Line	F.E.A.
1128	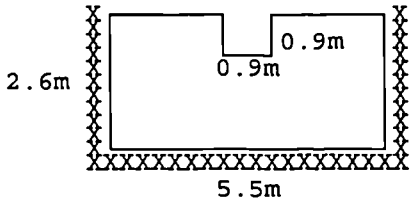	2.3	2.21	1.8
1129		2.6	2.21	1.8
1131		2.3	2.21	1.8
1132		2.4	2.21	1.8
1134	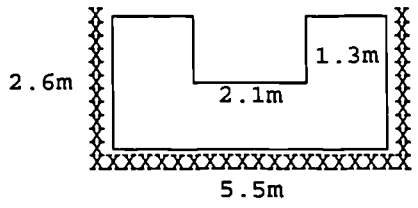	2.3	1.86	1.73
1139		1.6	1.86	1.73
1141		1.9	1.86	1.73
1142	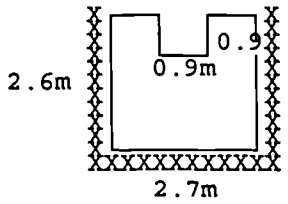	4.4	6.89	5.63
1143		4.9	6.89	5.63
1155	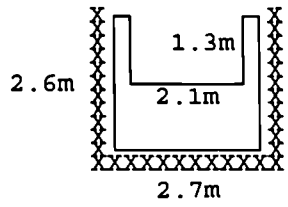	6.3	7.12	5.75
1175		6.4	7.12	5.75

Table 3.3 Wallette Strength

Units/ Mortar	Thickness mm	Wallette strength	
		Normal N/mm^2	Parallel N/mm^2
W4X	102.5	2.44	0.92
W6Y	102.5	1.19	0.32
W4X	215.0	1.78	0.85
W6Y	215.0	1.15	0.53

Table 3.4 Experimental and Analytical Failure Pressure

Panel	Wallette Strength		Failure Pressure	
	Normal N/mm^2	Parallel N/mm^2	Exptal. kN/m^2	FEA kN/m^2
1	1.2	0.4	1.50	1.31
2	1.2	0.4	1.15	1.22
3	1.2	0.4	2.00	1.24
ART01	3.2	1.2	4.40	4.56
ART02	3.2	1.2	2.75	2.39
ART03	3.2	1.2	2.60	2.60
ART04	3.2	1.2	2.50	2.21
ART05	3.2	1.2	2.50	2.39
ART06	3.2	1.2	2.50	2.69

Figure 3.1 Experimental Failure Pressure Vs FEA Predicted Pressure, Base Fixed and Vertical Edge Simply Supported - Solid Panels.

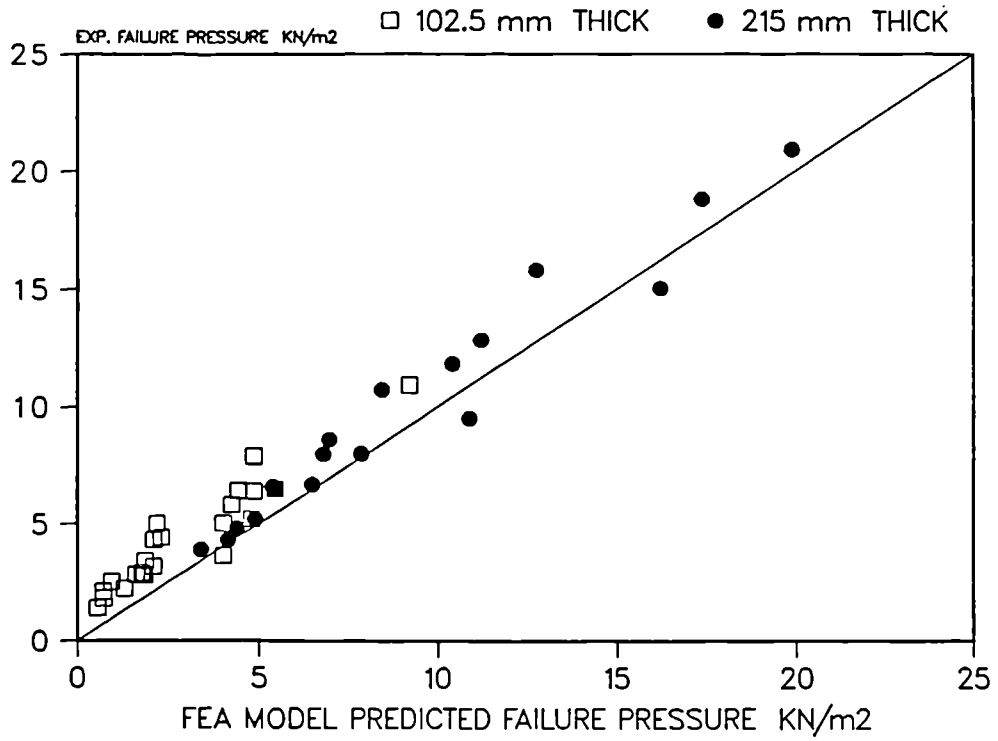

Figure 3.2 Experimental Failure Pressure Vs FEA Predicted Pressure, Fixed on Three Sides - Solid Panels.

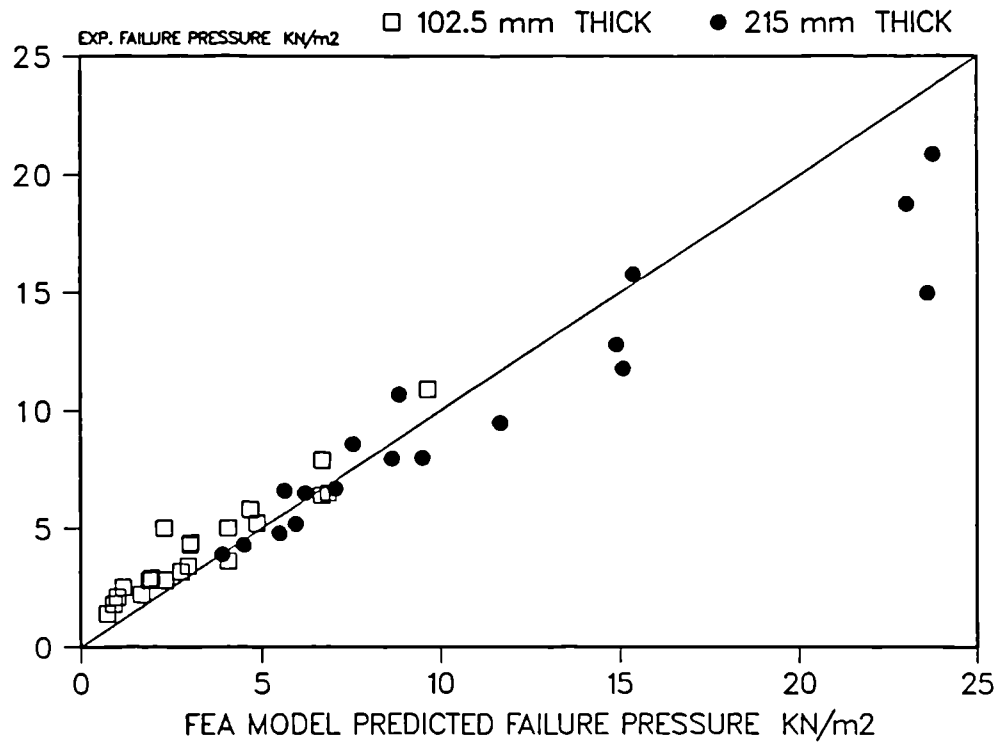

Figure 3.3 Wall 1150 Load-Displacement Relationship.

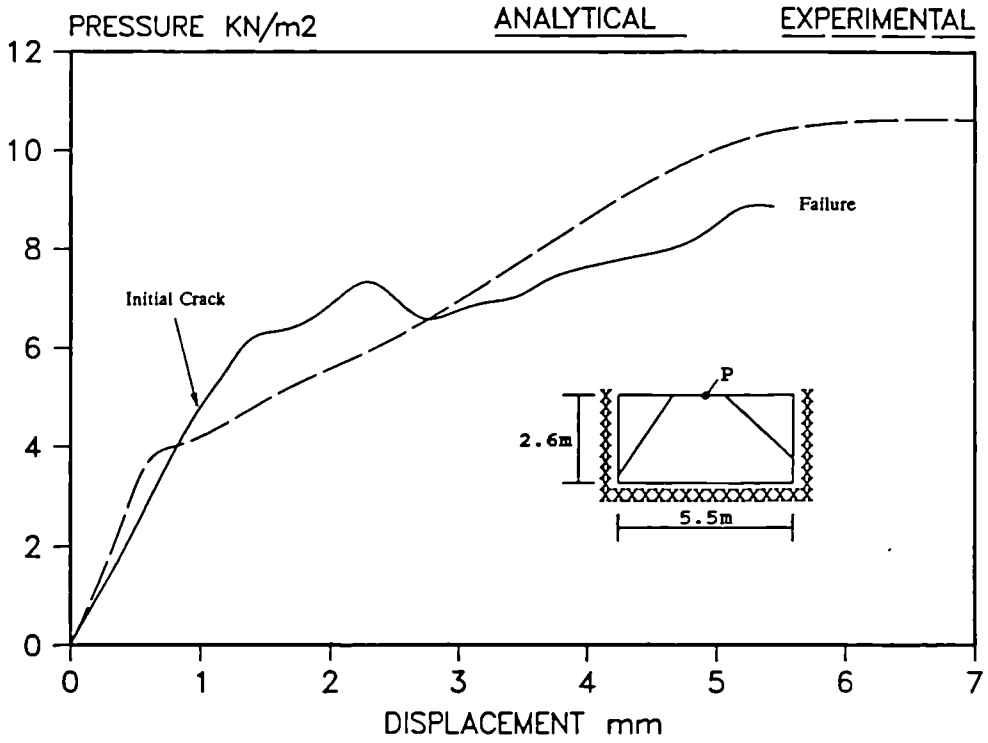

Figure 3.4 Wall 1136 Load-Displacement Relationship.

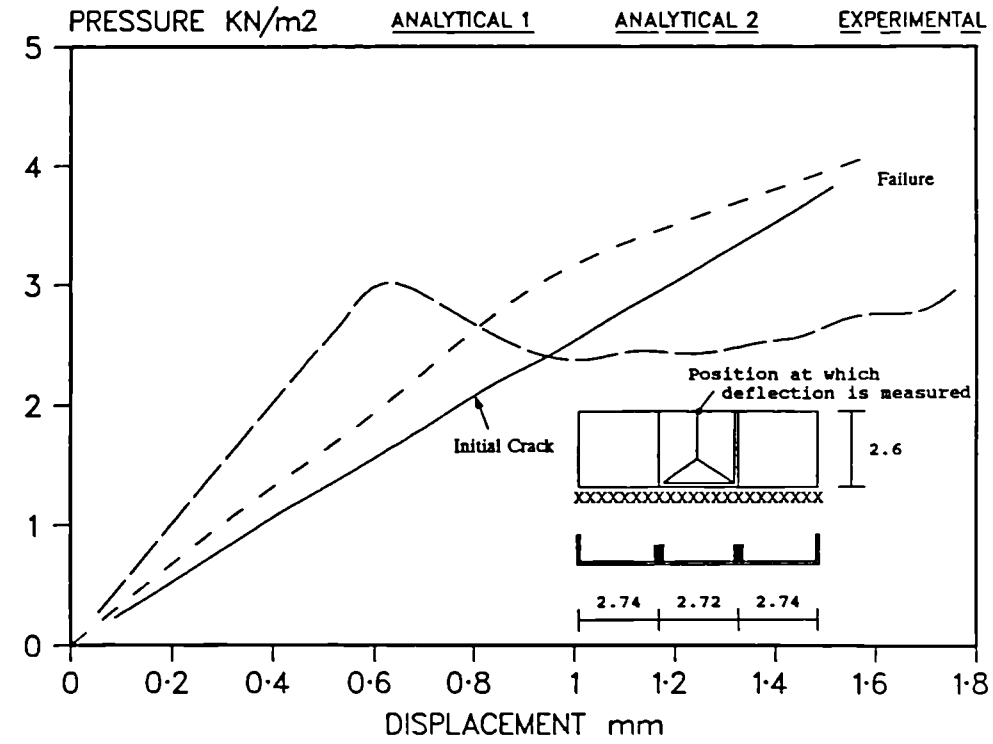

Figure 3.5 Wall 1139 and 1141 Load-Displacement Relationship.

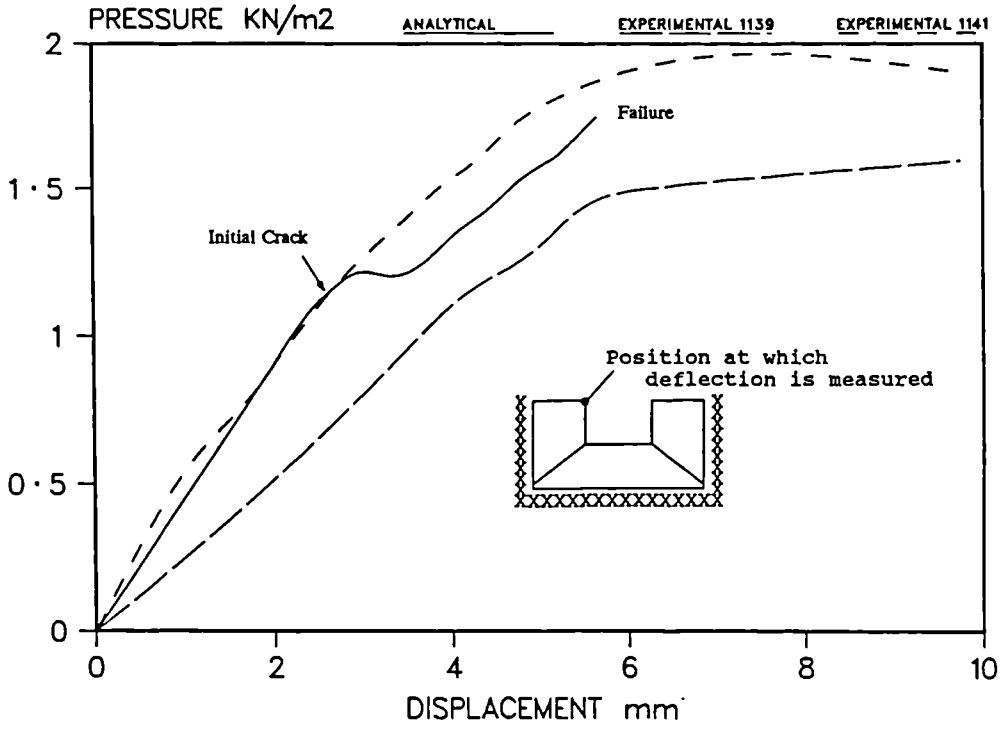

Figure 3.6 Comparison of Lateral Load Capacity of 102.5mm Thick Wall with Yield Line Design Method, 3 Sides Fixed.

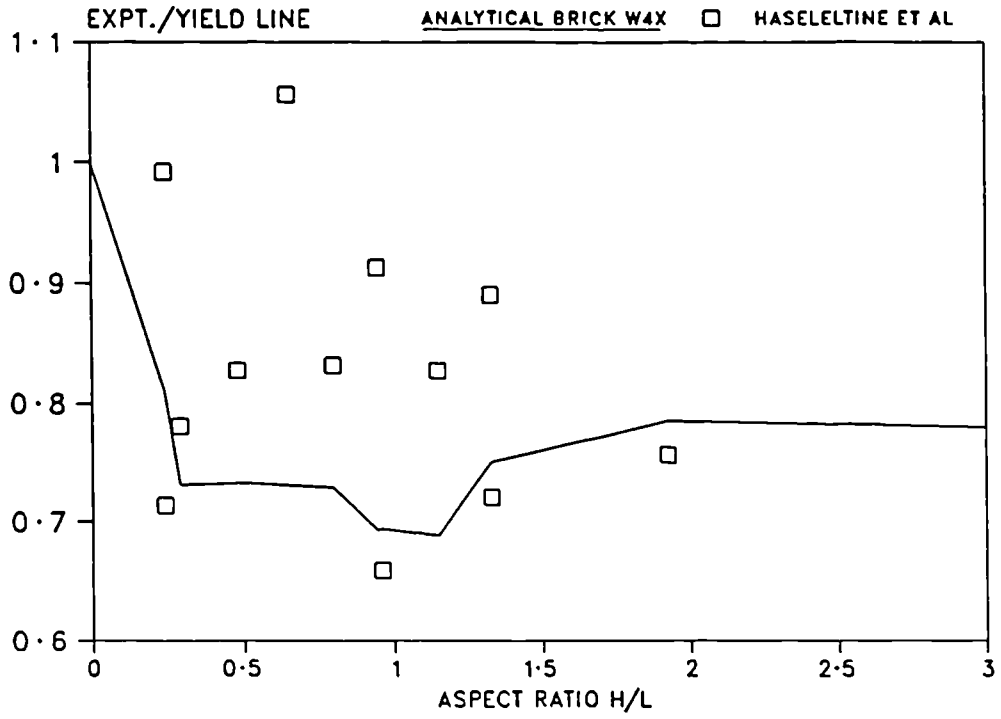

Figure 3.7 Comparison of Lateral Load Capacity of 215mm Thick Wall with Yield Line Design Method, Based Fixed and Vertical Edges Simply Supported.

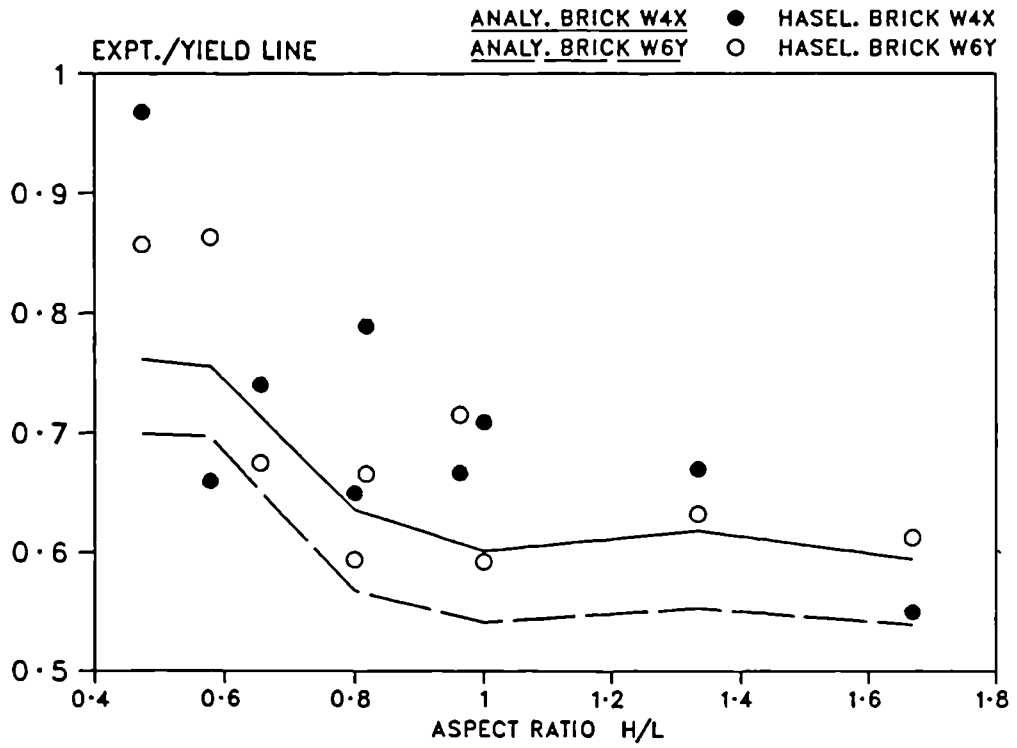

Figure 3.8 Experimental Failure Pressure Vs FEA Predicted Pressure, Walls with Opening.

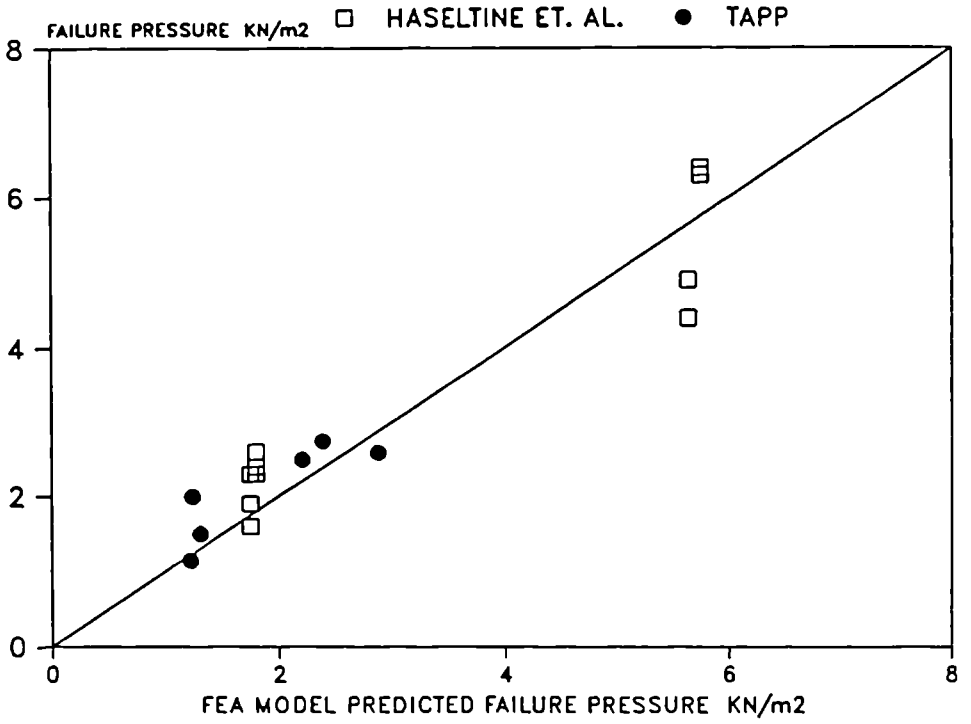

Figure 3.9 Panel Configurations and Finite Element Mesh Patterns.

All Dimensions in mm

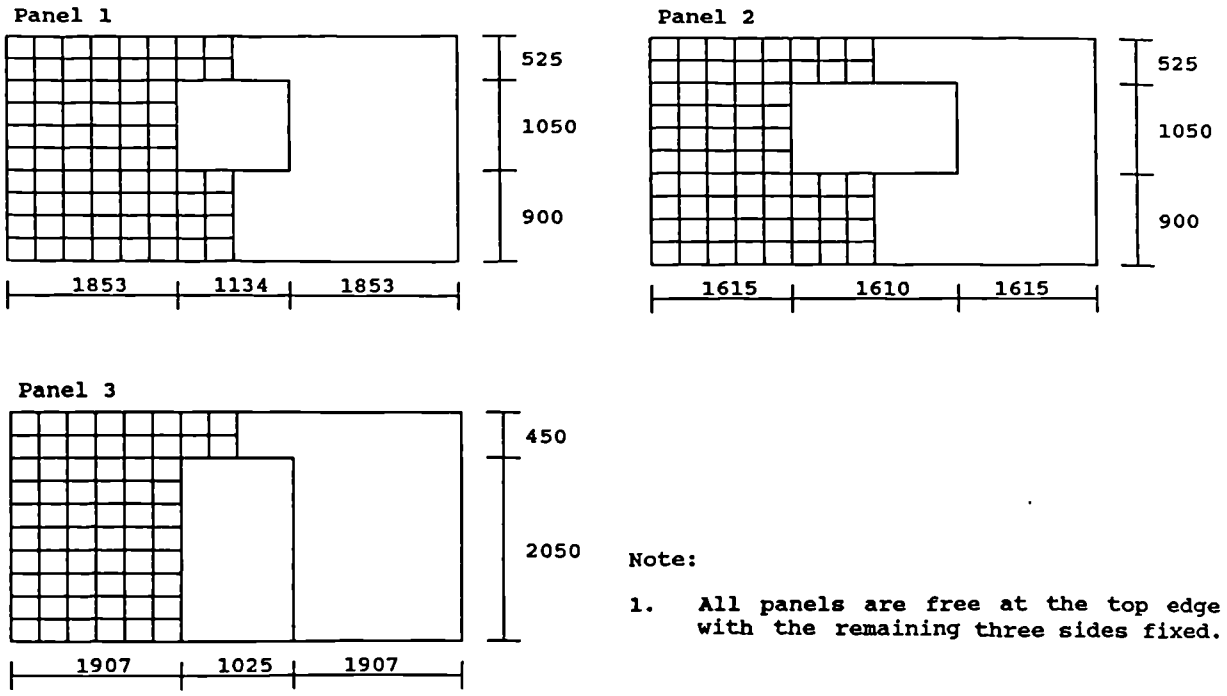

Figure 3.10 Panel Configurations and Finite Element Mesh Patterns.

All Dimensions in mm

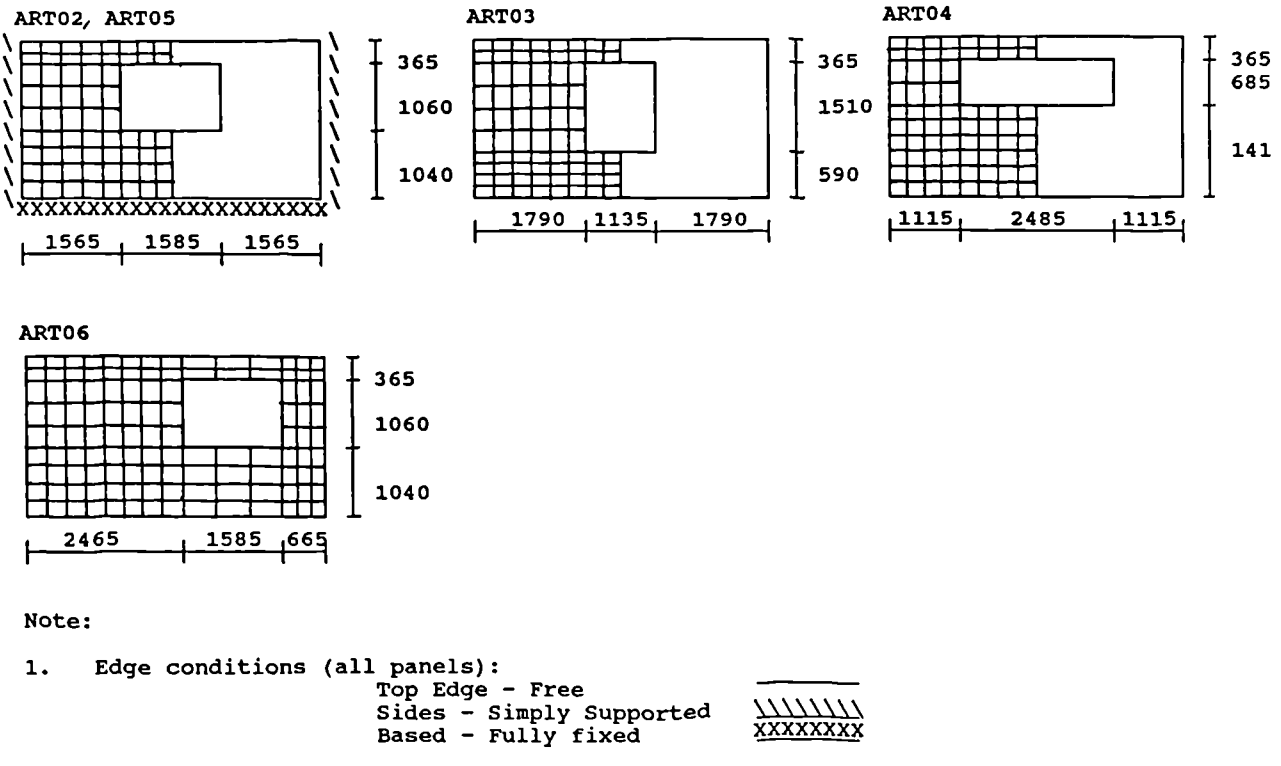

Figure 3.11 Wall ART01 Load-Displacement Relationship.

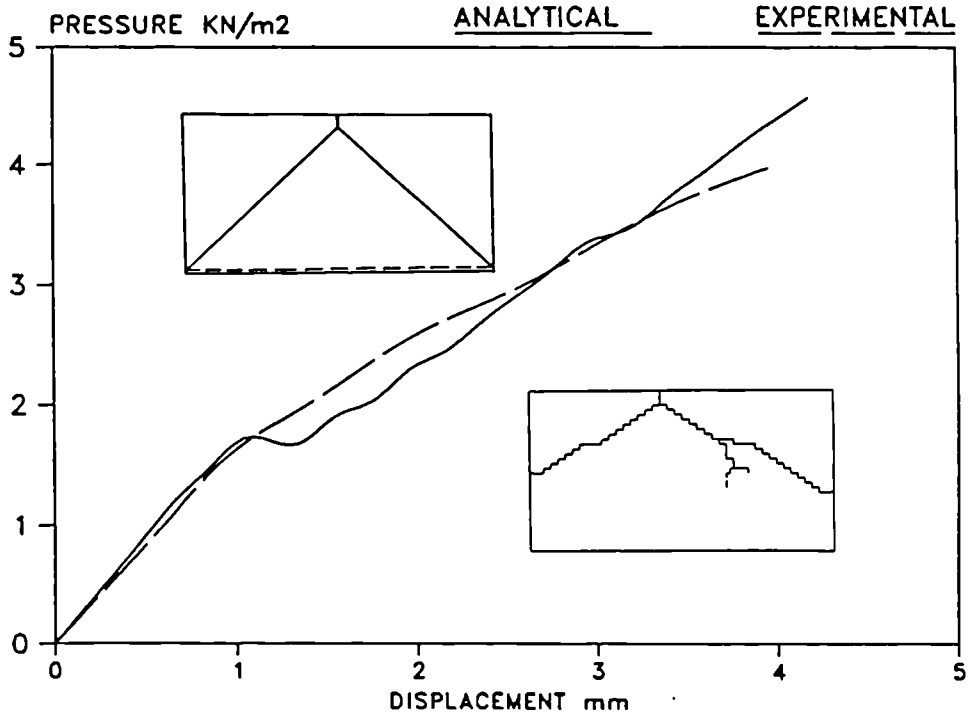

Figure 3.12 Wall ART02 and AR05 Load-Displacement Relationship.

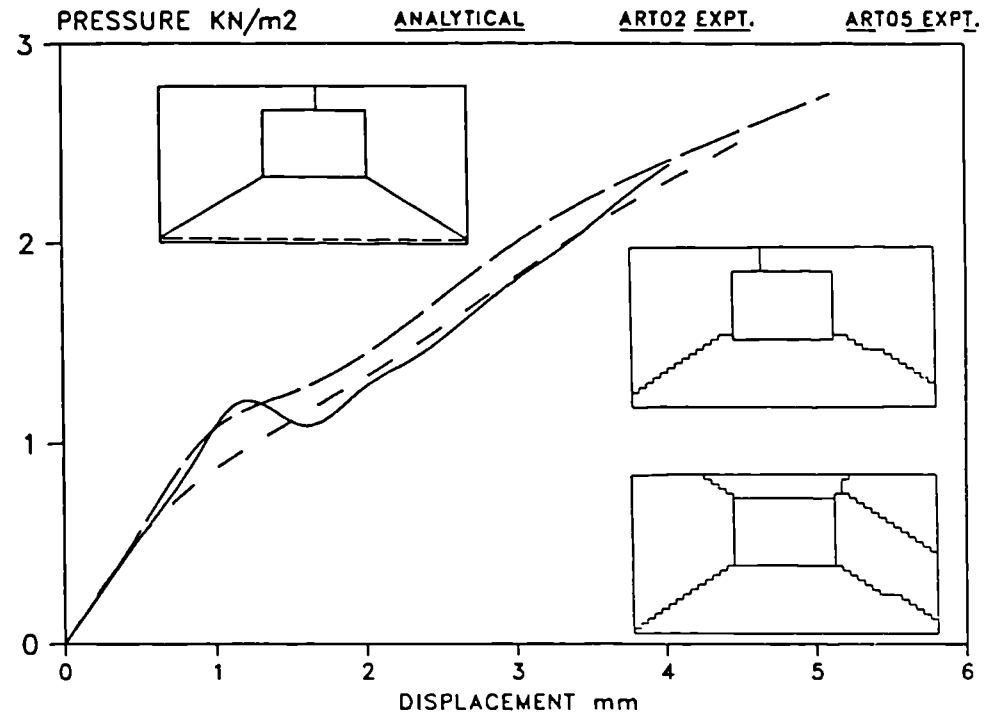

Figure 3.13 Wall ART03 Load-Displacement Relationship.

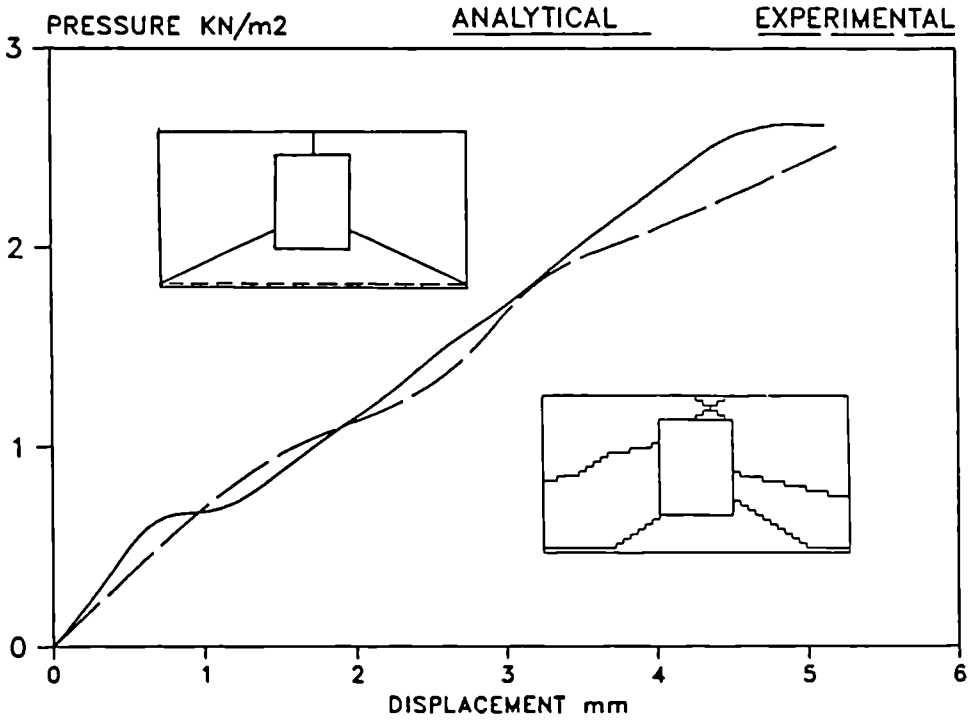

Figure 3.14 Wall ART04 Load-Displacement Relationship.

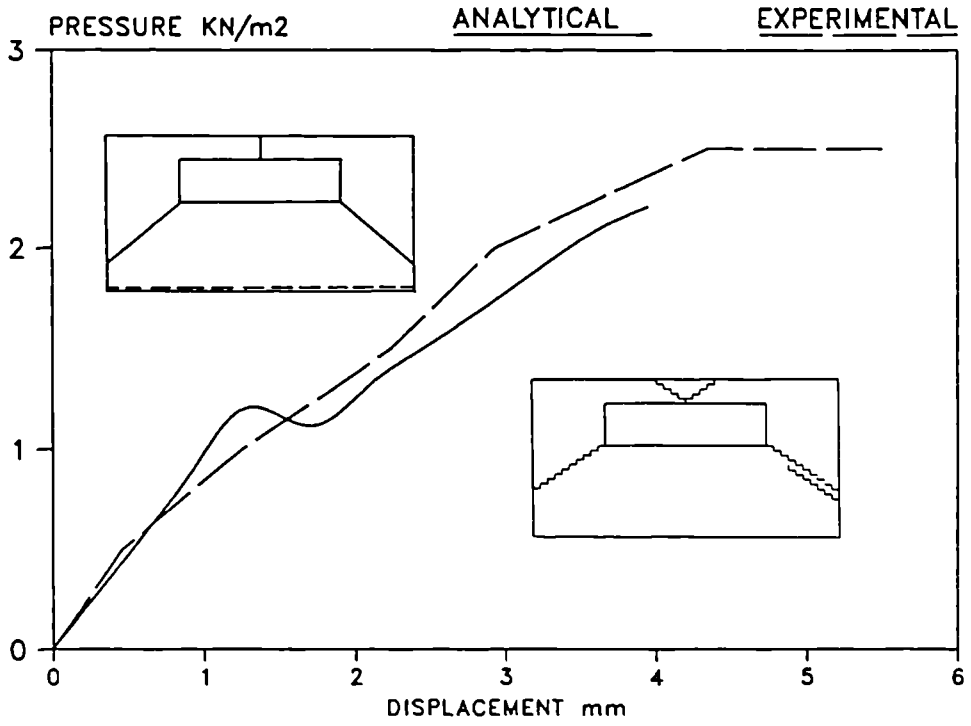

Figure 3.15 Wall ART06 Load-Displacement Relationship.

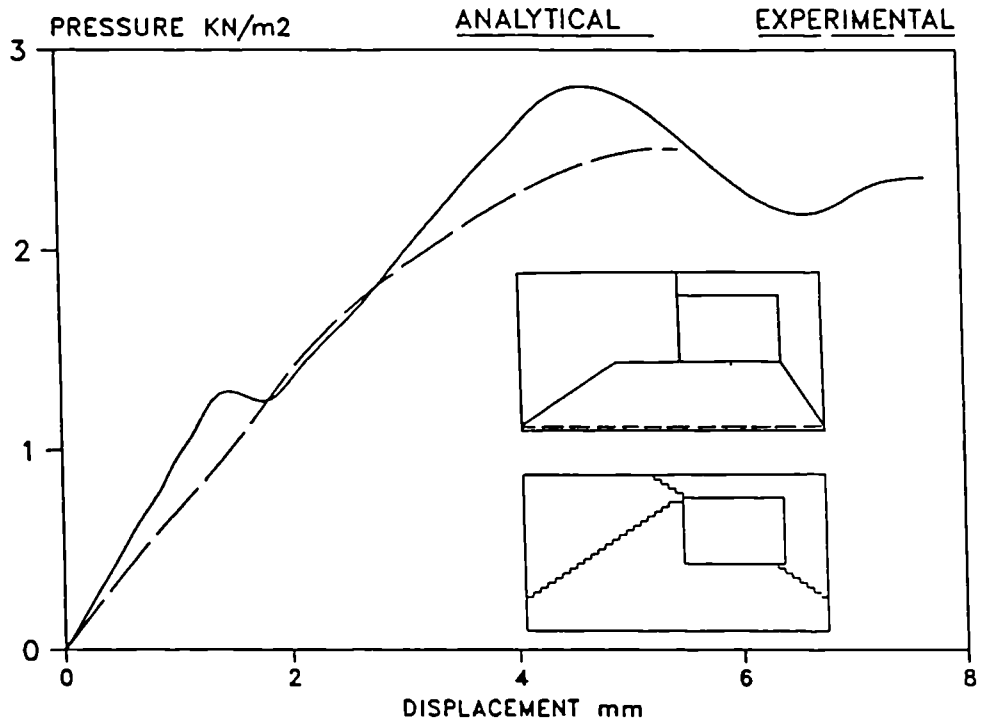

4.0 LABORATORY TESTS

4.1 Introduction

Analysis of the results from the initial theoretical studies highlighted areas where further investigations were required. Experimental and theoretical research have therefore been carried out to investigate the following parameters which may influence the behaviour and failure pattern of laterally loaded masonry panels:

(a) size and position of openings,

(b) support conditions and abutment stiffness,

(c) precompression and arching action,

(d) panel thickness and cavity construction.

The laboratory programme involved the testing of 18 full scale panels, these were single and cavity construction with various restraint conditions to investigate the effects mentioned above. Taking into consideration the number of factors known to influence the flexural strength of a masonry panels, it was decided to vary one such factor from test to test in order to quantify the influence of the factor. Three series of test programmes comprising three types of masonry units have been conducted. All panels were tested to failure using a computer controlled air bag loading system. The load-displacement relationship, and the initial crack and failure patterns of the panels were obtained. A series of supporting tests of wallette and bond wrench specimens were also carried out to assist in establishing the numerical constitutive model for the masonry.

4.2 Materials

4.2.1 Introduction

Three types of units were used in the tests, facing bricks, concrete blocks and class A engineering bricks remaining from early tests described in section (3.2.2). Although the engineering bricks delivered in 1985, were from the same production batch, tests were carried out to detect any changes in the material properties after six years of storage.

The masonry units used were:

(a) Accrington 65mm Class A 3-hole engineering bricks as used in the earlier test,

(b) Westbrick 65mm class B sand texture facing 10-hole perforated,

(c) 7 N/mm^2 dense concrete blocks.

All masonry units were sampled in random in accordance with clause 9 of BS3921: 1985 [96] and tested for dimensional in accordance with Appendix A of BS3921 [96].

The compressive strength tests were carried out in accordance with Appendix D of BS3921 [96].

The water absorption and initial rate of suction tests were carried out using the methods described in Appendix E and Appendix H of BS3921 [96]. The bricks were tested on the bed face only.

4.2.2 Class A Engineering Bricks

The total water absorption and the initial rate of suction of the bricks were found to be very similar to the results obtained from the early tests [1]. Hence the brick properties were considered to be consistent with the test results produced earlier [1].

A summary of the brick properties are listed in Tables 4.1 and 4.2, and details of the test results are shown in Appendix A.1.

4.2.3 Class B Facing Bricks

26 packs, 12480 bricks were delivered. The bricks were brittle with a rough texture. Random samples of bricks were taken for testing. They complied with the requirements of BS3921 [96], having a work size of 215mm x 102.5mm x 65mm. The mean compressive strength of the bricks tested on bed was 38.2 N/mm^2. The mean total water absorption was 9.0% of the dry mass. The mean initial rate of suction of the samples tested on the bed face was found to be 1.56 $kg/m^2/min$ compared with that of oven dried samples of 1.87 $kg/m^2/min$. After docking, the mean initial rate of suction of the bricks was reduced to 0.49 $kg/m^2/min$. The adjustment of the initial rate of suction by docking the bricks is desirable for higher and more consistent flexural strengths of the resulting panels. The bricks were docked before laying for all panels.

A summary of the brick properties are listed in Tables 4.1 and 4.2, and details of the test results are shown in Appendix A.2.

4.2.4 Dense Concrete Blocks

12 packs, 1800 blocks, all from one production batch were delivered. They were found to comply with the requirements of BS3921 [96], with a work size 440mm x 100mm x 215mm. The mean compressive strength tested was 12 N/mm^2, Table 4.2. Details of the test results are given in Appendix A.3.

4.2.5 Mortar

The mortar used in the construction of the panels built with the class A engineering was a designation (ii) mortar. The other panels built with the facing bricks and concrete blocks were set in a designation (iii) mortar. The two mixes were chosen because they were more representative of that to be used in common practice with the relevant masonry units.

Each mortar was batched immediately prior to mixing. A pan type mixer was used and the mixing time was 4 minutes for each batch. By using a constant source of supply of materials throughout the test program and carefully batching the ingredients by weight, the mortar properties were kept as consistent as possible. It was found that in general, a consistent mortar, in terms of workability, could be achieved as a matter of routine by adjusting the water quantity. The mortar consistency test was carried out using the Dropping ball apparatus described in BS4551: 1980 [97]. A consistency of approximately 10mm was used for the 1:1/2:4 1/2 designation (ii) mortar and approximately 14mm for the 1:1:6 designation (iii) mortar.

The mortar was used before any initial setting and was discarded 1.5 hours after mixing. Two hand-tamped 100mm mortar cube specimens were taken from each batch of mortar. The cubes were stored in air for the first 24 hours before they were removed from the mould and cured in water at 20°C for 13 days. The cubes were weighted in air and in water to determine the mortar relative density. They were then loaded at a rate of 0.1 $N/mm^2/sec$ to determine the compressive strength of the mortar.

A summary of the test results is listed in Table 4.3. Details are included in Appendix B.

4.2.6 Cement

Fresh supplies of fresh Ordinary Portland Cement to BS12 were used for the construction of each panel.

4.2.7 Lime

The hydrated lime powder used in the mortar mix conformed to the requirements of BS890 [98].

4.2.8 Sand

Two deliveries of medium grade natural building sand were supplied by a local quarry for the tests. The sand was graded in accordance with the requirements of BS812: part 3: 1985 [99], with tests being carried out using both dry and wet sieving methods. The result were compared to the requirements of a zone 2 sand, and type S and G sands to BS1200 [95], Appendix C.

The sand was found to be generally well graded and complied with the requirements of BS1200 [95]. It contained a high proportion of medium graded material which produced relatively good working qualities in the mortar. The fine contained was considered to be relatively high with a fineness modulus of 3.58 compared with the BCRA 'reference' sand of a value of 1.24. Results given by West et. al. have indicated that mortars containing sand with a high fineness modulus generally gave higher masonry flexural strengths.

The relative density of the sand was found to be 2.631 determined using the density bottle method described in BS812: part 2: 1975 [100].

Details of the test results are included in Appendix C.

4.2.9 Water

Tap water was added to the mortar to produce a suitable workability for bricklaying

requirements.

4.2.10 Frame for Opening

Window and door frames, constructed of planed 50mm square softwood jointed at the corners, were built in as the panels were constructed. The frames were braced and a sheet of 18mm chipboard was used to fill the opening. The window frames were located on top of the brickwork at the sill level set flush with the rear of the brickwork which was built tight to the frame. No fixings between frame and brickwork were used. In this way, only shear force is allowed to be transmitted from the frames to the panels by friction at the contacts between the frames and the brickwork. However, the rigidity of the chipboard infilled frames may enable some in-plane compressive forces to be transmitted.

4.3 Panel Configurations

4.3.1 Series 1, SB01-SB08 and CB01-CB02

This series consisted of eight single leaf and two cavity panels with two panel sizes and three types of restraint conditions. All panels were constructed using perforated class B facing bricks, set in 1:1:6 designation (iii) mortar. In order to improve the consistency of the unit moisture contents and hence the consistency and flexural strength of the resulting panels, the bricks were docked before laying.

Four basic types of openings were considered as representative of window and door openings. The opening sizes and dimensions used in the tests were chosen to be representative of those used in practice. The panel configurations are shown in Figure 4.1. An opening area of 10% of the panel area was used in SB03 and SB07, this being the maximum size of opening that BS5628 [8] permits designers to ignore in design. Opening sizes of 16.5%, SB02, 12.0%, SB08, and 6%, SB09, were also tested.

Three solid single skin panels, SB01, SB03 and SB05 were also tested to act as reference panels.

Each panel was built in stretcher bond between two stiff abutments. All panels except SB03, SB04 and SB09 were 5600mm long and 2475mm high with the vertical edges simply supported and the top edge left free. Panels SB06 and SB07 were each 2900mm long and 2475mm high with both the vertical and the top edges simply supported. The base of all panels, except SB05, was fully restrained. A bituminous d.p.c was introduced in the first bed joint of panel SB05. Construction details of all the edge restraints are shown in Chapter 5. Panel SB09 was 2475mm high and of length 5600mm supported at either end by two nominal 1000mm returns.

Two panels of cavity construction with a cavity width of 50mm, CB01 and CB02, were also tested. The panel configurations were similar to that of SB01 and SB02, so that a direct comparison could be made between the single leaf and the cavity panels. The leaves of the two cavity walls were tied together by stainless steel flat fish tail wall ties with a nominal cross section of 20mm x 3mm. The ties spacing was 900mm horizontally and 450mm vertically.

4.3.2 Series 2, DC01-DC02

This series contained three single leaf panels of each constructed using dense concrete blocks set in 1:1:16 designation (iii) mortar. The panel configurations and opening sizes and positions were similar to that of SB01 and SB02. The bituminous d.p.c introduced in panel DC02*B* was laid dry in the first bed joint and no mortar was used to bind the d.p.c to the masonry. This configuration allowed the effect of self weight on the flexural strength of panel to be studied more closely. The panel configurations are shown in Figure 4.2.

4.3.3 Series 3, HW01-HW04 and W01

This series was designed to investigate the effect of support stiffness on the lateral behaviour of masonry panels. All five panels were constructed using perforated class A engineering bricks set in 1:1/2:4 1/2 designation (ii) mortar. The panel configurations are shown in Figure 4.3. The four half size panels, 2700mm long 2475mm high, were fully restrained at the base, simply supported on one vertical edge with the other vertical edge left unsupported. The top edge was supported by a flexible abutment constructed of a universal beam section with the support edge faced with a 10mm inner diameter rubber hydraulic bolster. The universal beam spanned 5635mm between the two vertical abutments in panels HW01 and HW02, an intermediate support was provided for panels HW03 and HW04 by connecting the mid-span of the universal beam to the reaction frame by cleat bolts, Figure 4.3. The details of the simply supported edge and the fixed base are given in section (4.6.2).

Shear failure at a d.p.c can greatly reduce the lateral load capacity of masonry panels. A panel of 5600mm long by 2475mm high, W01, was constructed to investigate the effect of this shear failure. The wall was built on a sand bedding to represent the worse possible bed joint in an actual building. The two vertical sides were simply supported and the top edge was left free. A small opening 340mm x 235mm was introduced in the centre of the panel.

4.3.4 Construction Process

As discussed earlier, many factors are known to influence the flexural strength of masonry during the construction and curing of the masonry. A strict regime was implemented throughout the test to minimise the influence of construction and curing variability from panel to panel.

Bulk delivery of masonry units and sand, of sufficient quantity for the construction of an adequate number of panels and control specimens were arranged, so that the raw materials used in each of the panels and the control specimens in each series were comparable. All masonry units were stored outside the laboratory, and were therefore subjected to the natural environment. The sand was stored in closed covered concrete bunkers. The material properties were determined from random samples selected from the bulk delivery.

Sufficient masonry units and sand from the stockpile for a panel were brought into the laboratory a day before the construction to minimise the variation in their moisture content. Class B facing bricks were docked prior to use.

All the panels and the control specimens were constructed using the same technique by the same sub-contract bricklayer. The front face of each wall was given a 'fair face' where the joints were struck flush and rubbed over with a piece of scrim. The joints at the back face were simply struck flush. Each full size single leaf brickwork panel took three working days to complete and the cavity wall took five working days. Both the full size blockwork panel and the half size brickwork panel, took one and a half days to construct. After completion, all panels and specimens were cured in the laboratory atmosphere without covering at a laboratory temperature of 15-20°C. No other curing regime was carried out.

Each panel was tested at an age of 14 days counting from the second day of construction in order that a reasonable number of panels could be tested in the available time.

Other miscellaneous post-construction details are given elsewhere [1].

4.4 Wallette Test

BS5628: part 1 Appendix A3 [8] specifies a method to determine the flexural strength of masonry in the two orthogonal directions by the use of wallettes.

The aims of the experiment were to establish flexural strengths and orthogonal ratio representative of the full size panels. The wallettes were constructed and cured in the same manner as the panels. The wallettes had the joints struck flush on the back face and tooled on the front face. Due to the lack of laboratory space, wallettes constructed of class B facing

bricks and concrete blocks were constructed at a nearby unheated warehouse where the temperature was observed to have varied from 4°C to 12°C during the time of curing. All the specimens were tested, with the tooled joints on the tension face, at an age of 14 days, the same age as the panels.

4.5 BRENCH (Bond Wrench) Test

The bond wrench method was also used to determine the flexural strength of masonry across the bed joint.

The aim of the experiment was to investigate the effect of axial pre-compression on the flexural bond strength of single joint specimens. The two courses specimens, Figure 4.4, were built in stretcher bond with the first course built into a steel channel. The perpend joints at the top course were left unfilled. The construction and curing regimes were similar to that of the panels. Three series of specimens were built with one series left unloaded. The other two series had each specimen loaded with 9 kg or 4.0 kN/m^2 and 28 kg or 12.5 kN/m^2 of dead weights respectively. Each specimen was loaded with dead weights of 9 kg immediately after building, and was subsequently loaded with additional 9 kg of dead weights every 1.5 hours, the same rate as they would be loaded in actual construction.

The dead weights were removed immediately prior to testing. All the specimens were tested with the tooled joints on the tension face at an age of 14 days, the same age as the panels.

4.6 Test Equipment

4.6.1 Test Rig

The test rig was designed to be free standing with abutments on either side, Figures 4.5 and 4.6. The abutments were designed to minimise twisting under load. They were each constructed of two 432 x 102mm rolled steel channel sections, cross braced by 8mm thick triangular steel plates to form a 432 x 500mm column and welded to a 20mm thick steel base plate bolted into position onto the laboratory strong floor. A 10mm thick steel capping plate was welded to the top of the column to provide torsional restraint.

A reaction frame constructed of rectangular hollow sections was held in position behind the wall panels by cleats, bolted to the abutments, Figure 4.6. The system was designed such that the load on the abutment from the wall was balanced by the load transmitted by the reaction frame.

The complete test rig contained two pairs of columns positioned back to back with the reaction frame sandwiched in between, Figure 4.6. The arrangement allowed two panels to be constructed and tested alternately, and this in turn provided the test capacity of two rigs but without occupying the space of two separate rigs.

4.6.2 Peripheral Restraint

The test facility was intended to allow the vertical edges of the test panels to be restrained

in any of the four support conditions, free, simple, fixed, arching. However, it was considered initially that the most realistic model was provided by a simple support condition for the vertical edges. The detail of the support is similar to that used by Tapp [11].

The simple support on the vertical edge consisted of a 70 x 70 x 10mm steel angle bolted to the face of the abutment, Figure 4.6. A rounded steel plate was welded to the angle to produce a near knife edge contact at the support. The support edge was faced with an 8mm thick flat steel plate bedded on the face of the masonry panel so that contact was spread across the face of the panel and not concentrated at high spots. To ensure that in-plane displacement of the panel was allowed to occur without restraint, slip was allowed between the rounded plate and the flat plate and a 10mm gap was left between the ends of the panel and the abutments.

The top edge of a panel can either be left unsupported or simply supported. The top support was made up of a 330 x 102mm R.S.C. section spanning between the two columns. The steel channel section was welded with web stiffeners at frequent interval to enhance the torsional restraint capacity of the section. The arrangement of the simple support was similar to that of the vertical support.

A 'fixed' support was provided at the base because of the practical difficulties of providing a simple support. The base support consisted of a 178 x 76mm rolled steel channel bolted to the laboratory strong floor into which the first course of the panel was built. The rotational and lateral restraint was achieved by filling the gaps between the masonry and the channel sides with mortar.

4.6.3 Instrumentation

The instrumentation system employed to measure panel deflections was similar to that used by Tapp [1]. A set of four LVDTs were mounted on a rigid travelling beam which was made of a 3.5m length of aluminium channel section. The beam was light enough to be handled easily and was sufficiently rigid so as not to bend during usage. When taking the deflection reading, the beam was traversed across the face of the panel, with a number of stations being located at a regular intervals along the traverse onto which the beam sat. At each station a reading was taken from each of the LVDTs. By using this method, the number of readings could simply be increased by increasing the number of stations or by putting extra LVDTs on the beam.

The traversing system was made of a steel travelling rail (bar) bolted to the laboratory floor, Figure 4.7a. The lower stops were provided by drilling the travelling steel bar with a 10mm diameter hole. This system allow for any number of 'stops' to be made easily.

The top stops consisted of 10mm studs fixed to a steel tube running horizontally across the top of the test rig, Figure 4.7b. The tube was supported on an independent frame, Figure 4.5.

Details of the LVDT beam, traversing and data logging systems, are give by Tapp [1].

Tests using the system by taking repeated readings have shown that an accuracy of 0.2mm could be achieved.

4.6.4 Deflection Monitoring System

The system was based on a microprocessor controlled data collection system using a Hewlett Packard desk-top computer, a Biodata Microlink III interface unit and a signal conditioning unit. The system was configured to collect data from the LVDT's used to measure the panel deflections. Tapp [1] gives details.

4.6.5 Loading System

The loading system was computer controlled. The lateral load was generated by admitting compressed air into polythene bags sandwiched between the rear face of the panels and the steel reaction frame, Figure 4.6. Each bag was 2.475m high by 1.4m wide, and was placed directly against the rear of the test panel, and against sheets of 12mm thick plywood bearing onto the steel reaction frame. Timber beams were used to stiffen the plywood. A full scale 5.6m length panel would be loaded by four air bags.

A uniformly distributed load was applied incrementally using a computer system to control a set of valves which regulated the air flow from a compressor unit. The air pressure in each air bag was monitored using an electronic pressure gauge. A set of four pressure gauges would be required for the load measurement of a full size panel. The pressure of each air bag could be regulated individually to ensure the pressure was uniformly distributed on the whole of the panel.

4.6.6 Testing Procedure

At the start of the test the panel deflection LVDTs were calibrated using a micrometer. A 'zero' reference deflection reading was then taken from all the gauge positions. The deflection readings were again taken for each load increment. Some time was allowed at each load interval for the panel under test to distribute the pressure before any readings were recorded.

On the occurrence of the initial cracks, the panel would deflect steeply and this caused the volume between the rear face of the panel and the reaction frame of the rig to increase. This increase in the air bag volume would result in a corresponding decrease of air pressure. The drop in pressure was particularly pronounced in the central area of the panel. Air bags were then re-pressurised to the pre-cracking point before deflections measurement were taken. This re-pressurisation was necessary to synchronise the pressure in the air bags. In some panels, the load required to produce the initial cracks was never established. In other cases, the panel continued to carry an additional load until further cracking occurred with a prominent reduction in flexural stiffness. At this point, failure was said to occur as the maximum flexural capacity of the panel had been reached and the flexural strength was greatly reduced by the extensive cracking. More air being introduced into the air bags would only result in a huge increase in the panel deflection without any increase in the applied load. For safety reasons, the test was terminated before complete collapse of the panel occurred. A typical panels under test is shown in Figure 4.8.

4.6.7 Wallette Apparatus

The test equipment used were constructed to meet the requirements of the standard, BS5628 Appendix A3 Section 1 [8].

All wallettes were tested in an upright vertical attitude set on a deformable water filled hydraulic bolster, in order to obviate any friction restraint. The loading edges were also faced with the same type of hydraulic bolsters, so that contact was spread across the face of the wallette and not concentrated at high spots. In addition to the irregularities in the wallette being accommodated by the hydraulic bolsters, the rig was fully articulated with each loading and reaction arm being able to take up their alignment.

The outer bearings were set at approximately 50mm from the edge of the wallettes and the spacing of the inner bearings was 0.6 times the span of the spacing of the outer bearings. The actual values used are given in Table 4.4.

Due to the limitation of laboratory space, the test rig was designed to be portable so that it could be placed anywhere inside or outside the laboratory. The wallettes were then lifted into position in the rig by using a forklift.

A manually operated hydraulic jet system was used to operated the loading arms each of which, were connected to a hydraulic jet attached to a common hydraulic ram supply. The failure load was measured using an electrical oil pressure gauge, and the loading rate was approximately 2.5 kN/min.

4.6.8 BRENCH (Bond Wrench) Apparatus

The BRENCH [101] is a Building Research Establishment (BRE) development of the bond wrench [102], an in-situ tool for testing the bond of masonry units to mortar.

A basic bond wrench, Figure 4.9, is simply a long lever which is clamped to a brick or concrete block at one end. The other end is free. An increasing weight is gradually applied at the free end until the masonry unit is rotated free from the mortar joint. The load and the associated moment at which this occurs is a measure of the strength of the masonry.

The BRENCH is a portable bond wrench which needs no ancillary equipment. It consists of a lever about 800mm long which weights about 9 kg. At one end are jaws, which can be adjusted to fit the commoner thickness of masonry, 90mm to 215mm blockwork or brickwork. At the other end is a crossbar handle, mounted on a load cell. Load is applied manually by putting weight smoothly without jerks on to the crossbar handle.

The bond wrench and the BRENCH have different lever arms; this means that there is a slight difference in the ratio between the compressive load and the bending moment. Laboratory tests by BRE have shown that this has no significant effect.

Table 4.1 Brick Properties

Type of Masonry	Condition of Specimens	Number of Test Specimens	Total water Absorption % of Dry Mass	Initial Rate of Suction kg/m²/min
Class B Fac. Bricks	Oven Dried Undocked Docked	5 5 5	9.01(0.04) - -	1.88(0.11) 1.56(0.05) 0.45(0.36)
Class A	Oven Dried	10	3.70(0.29)	0.27(0.44)

Note: ( ) coefficient of variation

Table 4.2 Unit Compressive Strengths

Type of Units	Number of Test Specimens	Compressive Strength	
		Mean N/mm²	C.V.
Class A Eng. Bricks	20	130.90	0.16
Class B Fac. Bricks	10	38.20	0.18
Dense Con. Blocks	5	12.00	0.11

Table 4.3 Mortar Cube Properties

Panel Ref.	Mortar Mix	Density kg/m³		Compressive Strength N/mm²	
		Mean for panel	C.V (%)	Mean for panel	C.V (%)
W01	(ii)	2072	0.8	18.5	9.9
HW01 & HW02	(ii)	2020	1.4	25.5	5.6
HW03 & HW04	(ii)	1999	1.2	26.5	10.7
SB01	(iii)	2113	0.4	11.5	11.9
SB02	(iii)	2107	0.5	10.5	4.0
SB03	(iii)	2100	0.8	13.5	3.5
SB04	(iii)	2115	0.4	12.5	3.0
SB05	(iii)	2095	1.0	10.5	7.6
SB06	(iii)	2095	0.6	13.0	4.4
SB07	(iii)	2095	0.6	13.5	6.7
SB09	(iii)	2100	0.5	12.5	13.0
CB02	(iii)	2095	0.5	11.0	11.2
DC01	(iii)	2095	1.3	12.5	5.2
DC02	(iii)	2100	1.0	14.0	5.9
DC02	(iii)	2100	0.4	14.0	3.5

Table 4.4 Wallette Dimensions

Type of Masonry	Horizontal Wallettes				Vertical Wallettes			
	Face dimensions		Support span mm	Loading span mm	Face dimensions		Support span mm	Loading span mm
	Unit lengths	Courses			Unit lengths	Courses		
Bricks	4	4 or 6	800	480	2	10	650	390
Blocks	2.5	4	1040	625	2	5	1020	610

Figure 4.1 Panel Configurations - Series 1

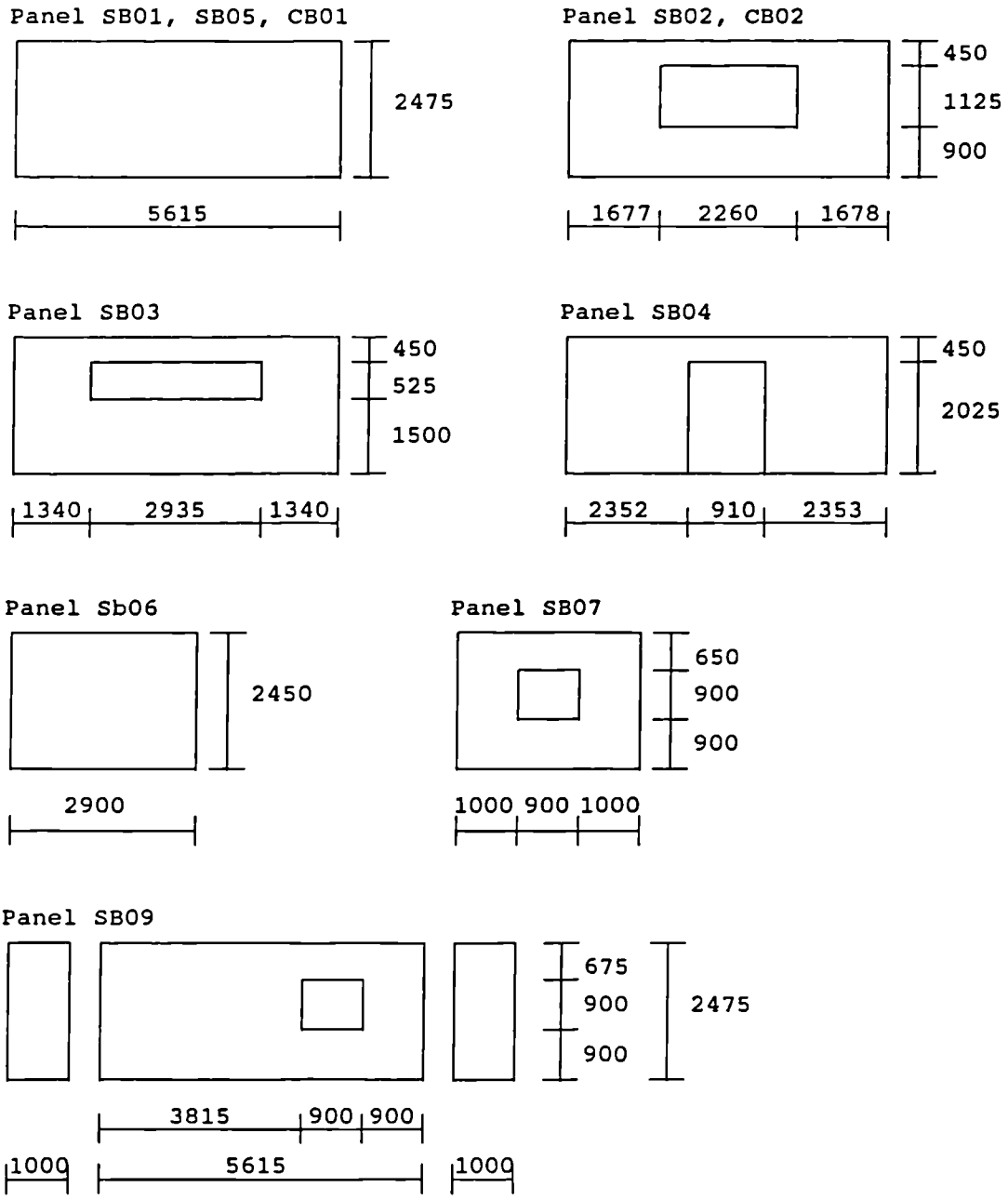

Figure 4.2 Panel Configurations - Series 2

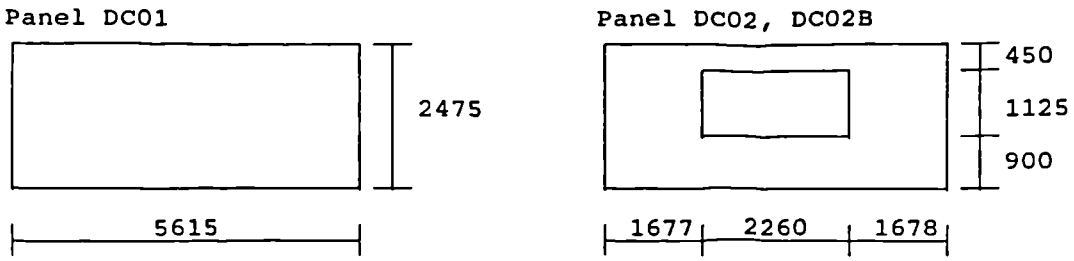

Figure 4.3 Panel Configurations - Series 3

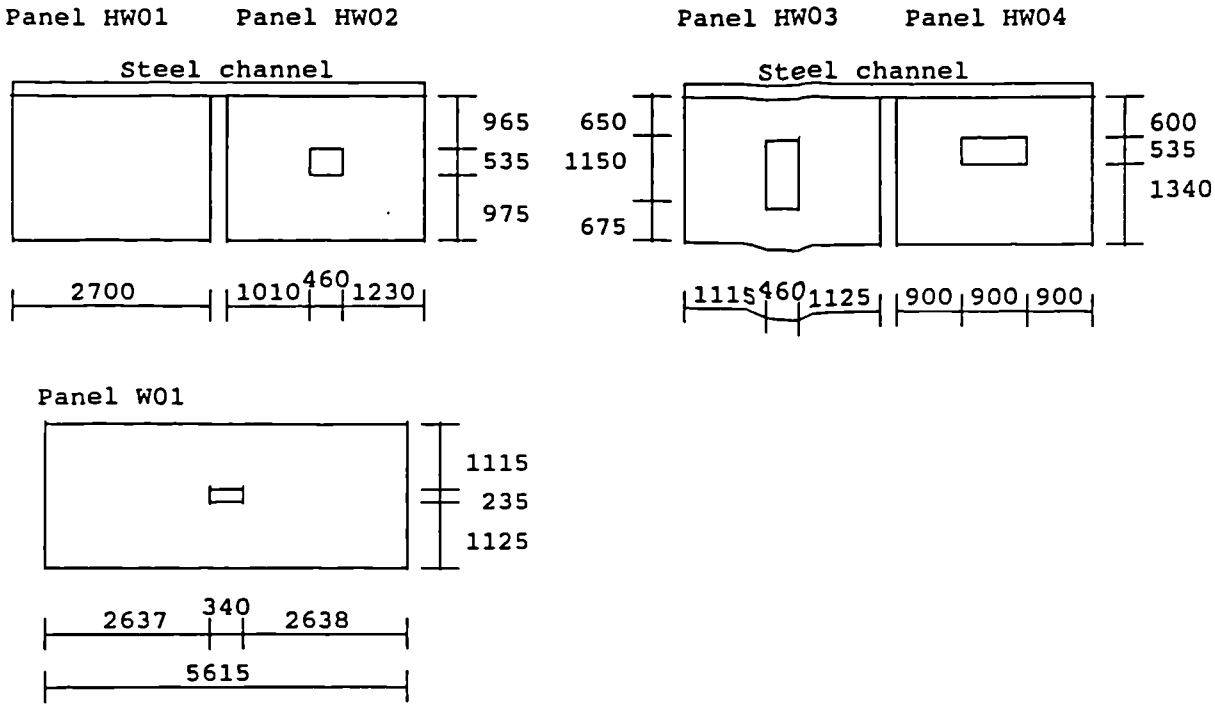

Fig re 4.4 Bond Wrench Specimens.

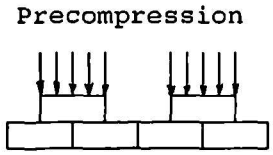

Figure 4.5 Test Rig and LVDT Beam.

Figure 4.6 Abutment and Vertical Edge Support.

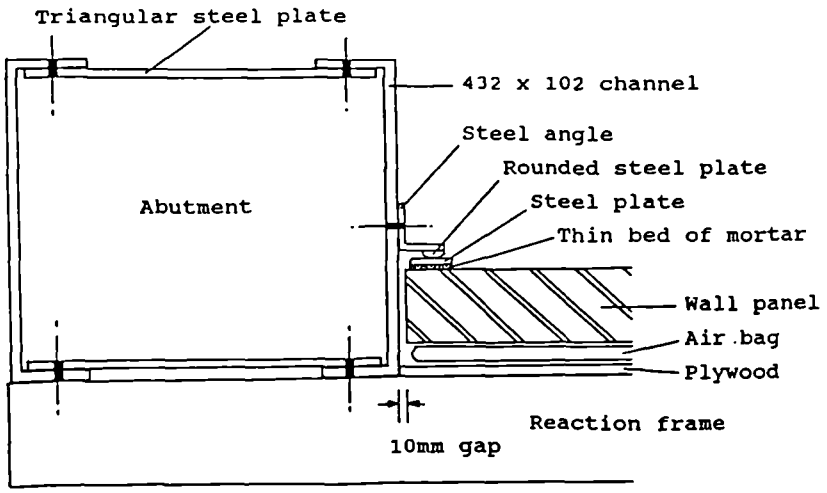

Figure 4.7 Detail of Top and Bottom Stops for LVDT Beam.

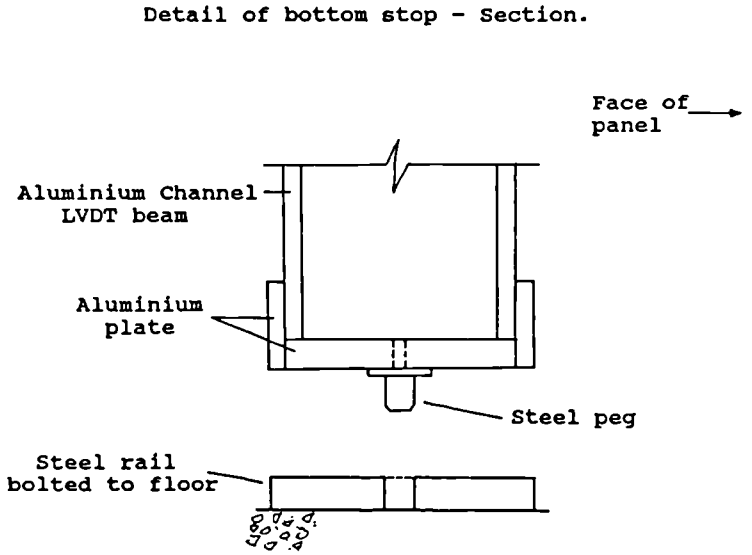

(a) Bottom Stop

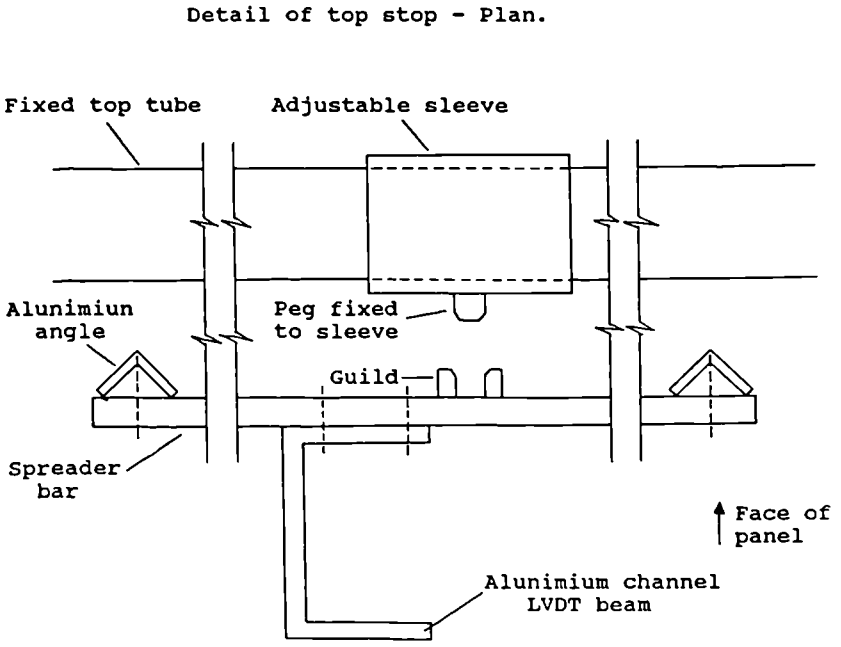

(a) Top Stop

Figure 4.8 Panel SB02 under Test.

Figure 4.9 The Bond Wrench - Shown in Position before a Test and after Bond Failure

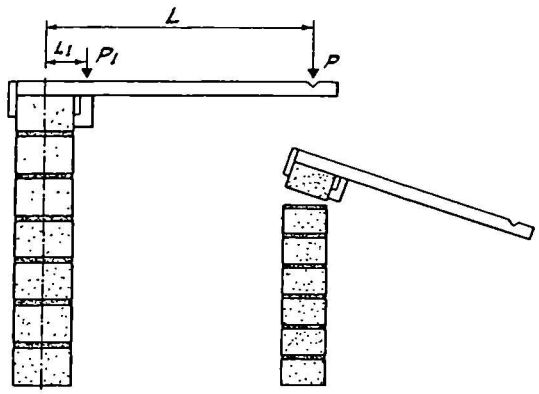

5.0 EXPERIMENTAL AND ANALYTICAL RESULTS

5.1 Introduction

The accuracy of any method of analysis is largely dependent upon the values assigned to the material properties in the calculations as discussed in section (1.3.1). It is therefore vitally important to investigate the effect of material parameters before assessing the experimental and analytical results of the full size panels tested.

5.2 Flexural Strengths of Wallette

The method given in BS5628 [8] for the determination of the flexural strength of masonry parallel to the bed joint is a four point test on a two bricks wide wallette. In the case of a vertical brickwork wallette, five of the nine bed joints are subjected to a constant bending moment. Wallettes of this form invariably fail at a bed joint and thus the test actually determines the strength of the weakest of the five joints. It could be expected that an increase in the number of joints would increase the probability of a weaker joint being found and, for a series of tests, give a decrease in the mean flexural strength of the specimens compared to that for the five joints tests. Similarly, decreasing the number of joints would increase the mean flexural strength.

Although the strength of the specimen is also influenced by the number of perpend joints in the span, no programme of tests has been recorded to assess the effect of the perpends on the bed joint strength. However, it has been suggested [103] that a two and a half bricks

wide wallette should be more representative of a full scale wall than the usual two bricks wide wallette.

In the stronger horizontal spanning wallette, the failure mode will one of the following:

(a) failure in a straight line through the perpend joints and units,

(b) failure in the bed and perpend joints only, with the units remaining intact,

(c) a combination of failure in the units, bed joints and perpend joints.

The mode of failure depends upon the relative flexural strength of the individual units and the mortar, and the bond between the mortar and the units. This type of wallette almost invariably fails through at least one perpend joint and failure is thought to be initiated in a perpend joint in either the top or bottom course. This suggests that the flexural strength across the perpend joints is less than that of the units. The results of the uneven distribution of strength across the height of the wallette would cause some torsional effects. It has been suggested [103] that the torsional effects could be reduced by increasing the number of courses. A reduction in the ratio of the load span to the support span could reduce the number of prospective failure planes and give a better representation of the distribution of strengths.

A computer based statistical analysis was carried out to investigate the effect of the specimen format on the flexural strength of wallettes and to determine a more representative bed joint strength. In considering the flexural strength of a vertical wallette it is possible to treat it as a number of discrete elements equal to the number of joints in the specimen, each with a

strength based on an assumed distribution. The individual element within the wallette is considered as a single joint, two bricks in length, 440mm, this also takes into account the presence of perpend joints in the span. A similar method of analysis but with the elements each one brick wide has been presented by Lawrence [104].

Because of the constant bending moment applied to the joints, the only variable considered is the random distribution of joint strengths. A Monte-Carlo simulation was carried out based on the assumption of a Normal distribution for the joint strengths. The steps taken in the analysis are as follows:

a. for the assumed distribution, a mean and coefficient of variation for the joint strengths were adopted,
b. different joint strengths were then assigned randomly to each of the joints in the span,
c. the weakest joint in the span was then identified.

The above procedure was repeated 10000 times and the mean and coefficient of variation were obtained for the wallette strength. The theoretical wallette coefficient of variation was compared with the experimental result and the simulation was repeated with various coefficient of variations for the joint strengths until reasonable agreement was obtained. The mean wallette strength was then scaled to that in the test and hence the mean joint strength was obtained.

The same analysis was applied to horizontal wallettes assuming failure through an equal

number of perpend joints and units. The height of the wallette, four or six courses, was considered as one discrete unit to give a representation of a smeared strength of the units and mortar.

Similarly, the weakest-link hypothesis can be easily applied by using order statistics. For a Normal Distribution of joint strengths the mean and variance of the weakest joint in the span selected at random from this distribution can be easily determined. Tables of order statistics are given by Mosteller and Rourke [105].

$$Mean\ (weakest\ of\ five) = \mu - 1.16\sigma \qquad \ldots(5.1a)$$

$$S.D.\ (weakest\ of\ five) = 0.669\sigma \qquad \ldots(5.1b)$$

$$Mean\ (weakest\ of\ three) = \mu - 0.84\sigma \qquad \ldots(5.2a)$$

$$S.D.\ (weakest\ of\ three) = 0.750\sigma \qquad \ldots(5.2b)$$

$$Mean\ (weakest\ of\ two) = \mu - 0.56\sigma \qquad \ldots(5.3a)$$

$$S.D.\ (weakest\ of\ two) = 0.826\sigma \qquad \ldots(5.3b)$$

where μ and σ are the mean and standard deviation of the distribution of joint strength.

5.3 Experimental and Analytical Wallette Results

All wallettes were constructed and tested to the requirements of BS5628 [8]. Only the results of tests where failure was within the load span were accepted. The nominal thickness of the units was used in the calculation of flexural strength. A summary of the experimental wallette strengths and the analytical results are given in Tables 5.1 and 5.2. Details of the test results are given in Appendix D.

5.3.1 Class B Facing Bricks

A total of 45 standard wallettes were tested and the results are summarised in Tables 5.1 and 5.2.

To investigate the effect of docking on the flexural strength of the wallettes, undocked specimens of each wallette type were also tested. The mean vertical flexural strength of the undocked specimens was 0.474 N/mm^2 with a coefficient of variation of 0.388 compared with the docked specimens of 0.740 N/mm^2 and a coefficient of variation of 0.162. It can be seen that docking of the bricks, which had a high initial rate of suction, improved the mean bed joint strength and reduced the variability. Little improvement of the flexural strength in the horizontal wallettes was observed with a mean flexural strength of 1.700 N/mm^2 compared with that of the undocked specimens of 1.670 N/mm^2. However, the inconsistent bonding caused by the dry bricks was evident from the high coefficient of variation of 0.291. Due to the large variation encountered in the horizontal wallette test

results, ten additional wallettes, each six courses high, were constructed to attempt to reduce the torsional effects [103] and the risk of damage caused by handling. An increase in the mean flexural strength to 2.090 N/mm^2 was observed. The coefficient of variation was also reduced from 0.166 to 0.088. All the docked specimens failed in a straight line through perpend joints and units.

For the bed joint flexural strength, the prediction from the Monte Carlo simulation for a coefficient of variation of 0.200 with the weakest of five joints gave a ratio of mean wallette to mean joint strength of 0.770. The same simulation was applied to the horizontal wallette for a constant moment zone of three joints. A coefficient of variation of 0.100 was used and a mean wallette to mean joint strength ratio of 0.917 was obtained. The predicted joint strengths in the vertical and horizontal directions were found to be 0.965 N/mm^2 and 2.280 N/mm^2.

5.3.2 Dense Concrete Blocks

The mean vertical and horizontal wallette strengths obtained were 1.367 N/mm^2 and 1.676 N/mm^2. Relatively low coefficients of variation of 0.131 and 0.048 were observed for the vertical and horizontal specimens respectively. The predicted joint strengths were found to be 1.578 N/mm^2 and 1.731 N/mm^2 in the two directions.

5.3.3 Class A Engineering Bricks

Due to the unavailability of laboratory space, only six specimens for each wallette type were built. The mean wallette strength in the weak direction was found to be 0.770 N/mm^2 with a coefficient of variation of 0.172, Table 5.1. A very high mean flexural strength of 4.12 N/mm^2 with a coefficient of variation of 0.070 were found in the other orthogonal direction, Table 5.2. Due to the high flexural strength of the units with a mean of 14.20 N/mm^2, the failure was caused by joints failure alone with all the units remaining intact. No additional specimens were constructed because of the reasonably low coefficients of variation obtained.

The predicted horizontal joint strength were found to be 1.000 N/mm^2. The vertical joint strength was treated as the same as the horizontal wallette strength. The assumption was thought to be reasonable due to the mode of failure which was caused by joints failure alone.

5.4 BRENCH (Bond Wrench) Test Results

Only specimens made with the class B facing bricks were tested and a summary of the results is given in Table 5.3. The nominal thickness of the units was used in the calculation of flexural strength.

As can be seen from Table 5.3 the mean flexural strength of the specimens increased with increasing precompression. The mean flexural strength of the uncompressed specimens obtained was 0.936 N/mm^2 compared with that of the pre-loaded specimens of 1.042 N/mm^2

and 1.082 N/mm^2 respectively. The coefficient of variation was improved from 0.202 to 0.166. Thus the presence of pre-compression during the initial setting period and the subsequent curing of masonry improved the bonding at the unit/mortar interface and reduced the variability of strengths.

The mean bond wrench strength was found to be in the order of 1.35 times the mean wallette strength. This was in agreement with the joint strength predictions using the weakest link hypothesis, Table 5.1.

Also listed on Table 5.3 is the predicted mean bond wrench strength evaluated from specimens subjected to an axial precompression of 22.5 kN/m^2, equivalent to an axial load from 16 courses of brickwork. The prediction was based on a linear extrapolation from the experimental results, Figure 5.1. The coefficient of variation was calculated to be 0.14.

In order to make the bond wrench results comparable to the two bricks wide joint strength, the equivalent joint strength was deduced from the bond wrench strength based on the averaging hypothesis. This suggests the strength of each pair of adjacent joints will be averaged to account for plastic behaviour and/or strength sharing.

The average hypothesis can be applied by using the well known properties of samples from a Normal Distribution:

$$\textit{Estimation of sample mean} = \mu \qquad \ldots(5.4a)$$

$$\textit{Estimation of sample S.D.} = \frac{\sigma}{\sqrt{n}} \qquad \ldots(5.4b)$$

where μ and σ are the mean and standard deviation of the distribution of joint strength, and n is the number of units in the sample.

5.5 Comparison of Experimental and Analytical Panels Results

The biaxial stress failure criterion adopted in the finite element analysis is independent from the effect of elastic modulus, and therefore typical values of elastic modulus were assigned to each the materials used. The initial elastic modulus was assumed to be 9 kN/m^2 for dense concrete blocks, 12 kN/m^2 for class B facing bricks and 16 kN/m^2 for class A Engineering bricks. The Poison's ratio for all materials were taken as 0.2. The flexural strengths were taken as those listed in Tables 5.1 and 5.2. The self-weight of the masonry was taken into account. Typical finite element mesh patterns adopted for the panels analysed are shown in Appendix E. It can be seen from Table 5.4 that the finite element predictions using the strengths from the wallette test underestimated the lateral capacity of all of the panels. The predictions using the mean joint strengths obtained from the statistical analysis or using equations 5.1 to 5.3 were however closer to the experimental results. The modes of failure were all predicted with, generally, very good correlation, Figures 5.2 to 5.17. When the stiffness of the window frame and the chipboard infill were taken into account, an increase of up to 19% in the panel strengths was predicted. This suggests that the frame and the

chipboard contributed to the stiffness and strength of the panel. The low coefficient of variation obtained between the analytical and the experimental results indicated that the material variability often associated with masonry might have little influence on the flexural strength of full size panels.

As expected, the yield line method overestimated the failure strength of all the panels tested, except for panel W01 because of the different boundary conditions taken for yield line analysis. However, the failure modes of all panels, except panels DC01 and W01, were correctly predicted.

When the analytical and the experimental load-displacement relationships are compared, it can be seen that, Figures 5.2 to 5.17, the analytical results follow the loading curves up to and above the cracking loads. The analysis predicted a sudden decrease in the stiffness after cracking occurred at the fixed base whereas a very gradual change in stiffness was observed for all the panels tested. This behaviour may be partially explained by a change in the mortar properties at the unit/mortar interface due to precompression. In addition to the effect of self-weight, the presence of precompression at the initial setting period was found to result in better bonding at the unit/mortar interface, Table 5.3. The strength of the unit/mortar interface would increase with respect to the applied precompression as indicted in Table 5.3. Thus, the cracking load towards to bottom of the panel would be higher than that at the top. Therefore, it is possible that the analysis may provide a slightly conservative estimation of the panel capacity when the joint strength results obtained from uncompressed specimens were used. It is also suggested that the formation of the horizontal cracks at the early stage are evenly distributed at the lower part of the panel due to this precompression effect.

Another consideration is that the actual stress-strain relationship of masonry is not perfectly elastic brittle, especially for bending normal to the bed joint. A falling branch in the stress-strain relationship may have resulted in a smoother panel load-displacement relationship.

For panels with the top or one vertical end free, the load-displacement relationships were measured half way along the free edge of the panels unless indicated otherwise. The deflection profile of all panels are given in Appendix F.

5.5.1 Panel SB01

The deflected shape of the panel given in Appendix F.1 shows that slight movement on the right edge restraint occurred as the panel settled against the vertical support during loading. It is practically impossible for the bricklayer to produce a perfect gap free edge support. However, the movement was small and it is suggested that it did not effect the overall behaviour of the panel. As can be from Figure 5.2, the deflections increased linearly with increasing load until visible cracking occurred at a load of 2.7 kN/m^2. It would be expect that in this and the subsequent tests that horizontal cracking would occur at or near the base at a relatively low load. However, this cracking was not visible as the face on which it occurred was the loaded face. The panel was able to carry an increase in load up to 2.8 kN/m^2 at which extensive cracking occurred which divided the panel into three. For safety reasons, the test was concluded at this point. The failure pattern, Figure 5.2, which was asymmetric comprised a vertical crack toward the top right of the panel and two diagonal cracks joining the vertical crack to the bottom corners of the panel.

5.5.2 Panel SB02

Behaviour, similar to that in the solid panel SB01, was observed during the initial phase of the test, Figure 5.3. A vertical crack above the opening was observed to occur at a lateral pressure of 2.0 kN/m^2 and the deflections increased abruptly. Failure occurred at a load of 2.3 kN/m^2. The failure mode comprised diagonal cracks from each of the lower corners of the opening to the bottom corners of the panel and a vertical crack above the opening.

5.5.3 Panel SB03

The panel was observed to behave in a similar manner to panel SB02. The failure mode also consisted of a vertical crack forming in the masonry above the opening and diagonal cracks extending from the lower corners of the opening to the bottom corners of the panel. All the cracks were observed to occur at a load of 2.3 kN/m^2, Figure 5.4.

5.5.4 Panel SB04

An opening of door height which extended almost the full height of the panel was incorporated. A vertical crack splitting the panel into two was first observed at a lateral load of 1.8 kN/m^2. The panel continued to carry load until failure occurred at a load of 2.2 kN/m^2, Figure 5.5. The failure pattern comprised the initial vertical crack and two additional diagonal cracks from approximately the mid-height of the opening to the bottom corners of

the panel.

5.5.5 Panel SB05

A solid panel, SB05, with a bituminous d.p.c. built into the first bed joint was also tested. The load-deflection behaviour was nearly identical to that of panel SB01, Figure 5.2, which suggests that the flexural strength of the course with the bituminous d.p.c is similar to the bed joints. Initial cracking developed at a load of 2.7 kN/m^2 at which stage the load dropped to 2.55 kN/m^2. The failure pattern although more symmetric, was similar to that of panel SB01 with two vertical cracks forming in the top half of the panel and two diagonal cracks joining the vertical cracks to the bottom corners of the panel. A horizontal crack was also observed, this joined the intersections of the vertical and diagonal cracks.

5.5.6 Panel SB06

The solid panel was rotationally restrained at the base and simply supported on the other three sides as shown in Figure 5.6. Section (4.6.2) gives restraint details.

The deflected shape of the panel given in Appendix F.6 shows that movement occurred on the right edge support during loading. It is considered that the movement was caused by settlement alone, as a large displacement at the top right support of the panel was observed at the initial loading stage. Irregularity of the steel bearing plate at the support could also

have given rise to settlement. The settlement, however, appeared to have no effect on the flexural behaviour of the panel apart from a slight increase in the panel deflections.

The load-displacement relationship at the centre of the panel was essentially linear until cracking developed. A horizontal crack separating the panel into two was observed to occurred at approximately the 2/3 height of the panel at a load of 4.5 kN/m^2. This converted the panel from four sides supported, two way bending, into two panels with three sides supported. The panel continued to carry load with a reduction in stiffness until failure occurred at a load of 7.5 kN/m^2. The failure mode of the bottom half of the panel was similar to that of panels SB01 and SB05. The failure pattern consisted of two vertical cracks joined by two diagonal cracks to the bottom corners of the panel. A horizontal crack also occurred between the two vertical cracks. The failure pattern of the upper half consisted of three vertical cracks only. It was considered that a fan type failure might have occurred at the top corners of the panel. It is suggested that a slight movement at the top restraint edge due to settlement may have effected the failure pattern.

5.5.7 Panel SB07

The behaviour was similar to that of the solid panel SB06 but a reduction in the lateral stiffness and resistance was observed. A horizontal crack splitting the panel into two halves was noted at a lateral load of 3.5 kN/m^2, Figure 5.7. Similar to panel SB06, the panel continued to carry load with a reduction in stiffness until failure arose at a load of 5.5 kN/m^2. The failure modes of the top and bottom halves, Figure 5.7, were similar to that of

the solid panel SB06, Figure 5.6. Similarly, the settlement observed at the right edge support appeared to have no effect on the panel lateral load capacity.

5.5.8 Panel SB09

The behaviour of the panel with two 1.0m returns at each end was observed to be very similar to panels SB01 and SB05. The load-displacement relationship is shown on Figure 5.8. Failure occurred at a load of 2.4 kN/m^2 at which a vertical crack above the opening was first developed before further cracking occurred. The failure pattern is essentially identical to that of SB01 and SB05. Shear failure was also observed to occur at the base of the two returns.

Also plotted on Figure 5.8 are the analytical load-displacement relationships of the panel assuming the vertical edges were rotationally restrained and simply supported. The analyses assuming returns and rotationally restraint at each end both yielded identical results suggesting the two support conditions were identical. It was believed that the size of the panel and the presence of the opening prevented any substantial in-plane arching to be generated.

5.5.9 Panel CB01

A solid cavity panel identical to the single leaf panel SB01 was tested. Similar to panel SB01, the cavity panel initially deflected linearly with respect to load, Figure 5.9.

Non-linearity in the load-displacement was first observed to develop at a load of 2.0 kN/m^2. This was likely to be caused by the initial cracking at the fixed base. The panel stiffness continued to reduce as the load increased before failure occurred at a load of 5.8 kN/m^2. The panel was observed to be more ductile than the single leaf panel after cracking. The failure mode was identical to that of panels SB01 and SB05.

As the inner leaf was not visible, it was believed that the inplane restraint provided by the brick ties caused the outer leaf to fail before the inner leaf. The neutral axis then shifted toward the inner leaf as the panel continued to deflect before failure occurred in the inner leaf. This may explain the ductile behaviour observed at the failure load of 5.8 kN/m^2.

5.5.10 Panel CB02

As with the solid panel CB01, the panel deflected linearly with respect to load until at a load of 1.8 kN/m^2 where non-linearity occurred, Figure 5.10. The panel was also observed to be more ductile than the single skin panel SB02, with a distinct non-linearity in the load-displacement relationship. A vertical crack above the opening was first observed at a lateral load of 3.6 kN/m^2 and the deflection of the panel increased abruptly. Failure occurred at a load of 3.8 kN/m^2. The failure mode was identical to that of the single skin panel, SB02.

The failure pressure of the cavity panel was only 1.6 times the failure pressure of the single leaf panel SB02 of 2.4 kN/m^2. This can be explained by the lack of chipboard infilled to the window frame at the outer leaf. The reduction in the inplane stiffness would result in a lower

lateral resistance of the panel, Table 5.4. As the nominal inplane restraint provided by the wall ties was greatly reduced by the presence of the opening, it is likely that the panel would act as two separate single leaf panels. The outer leaf, having the lower lateral capacity, would invariably fail prior to the inner leaf. Due to the brittle nature of masonry, the lateral strength of the cracked panel would decrease abruptly, and this would result a huge increase in the applied pressure on the inner leaf in order to preserve equilibrium. It was suggested that the inner leaf would fail following the failure of the outer leaf without an increase in the total applied load. This would result in a lateral wall strength lower than the sum of the individual leaf strengths. The difference in the load capacity of an elastic-plastic and elastic-brittle material was demonstrated earlier in section (3.1.4).

5.5.11 Panel DC01

As can be seen from Figure 5.11, the load-displacement relationship of the blockwork panel is very similar to the brickwork panel. The deflections increased linearly with the applied load until initial cracking occurred. A slight change in gradient in the load-displacement relationship was observed at a load of 1.6 kN/m^2. Failure occurred at a load of 2.6 kN/m^2 when extensive cracking formed. The failure pattern comprised two short vertical cracks at the top part of the panel and diagonal cracks joining the vertical cracks to the bottom corner of the panel. The failure pattern was similar to the analytical failure mode that is two diagonals cracks stretching from the free edge to the bottoms corners of the panel. The panel also behaved in a 'ductile' manner at failure, due to in-plane arching and friction.

5.5.12 Panel DC02

The load-displacement relationship at the top centre of the panel is shown on Figure 5.12. It was considered that cracking at the fixed base occurred at a load of 1.2 kN/m^2, when the initial non-linearity in the load-displacement relationship was first observed. A vertical crack above the opening formed at a load of 1.6 kN/m^2. Failure occurred at a load of 1.8 kN/m^2 when horizontal cracks generated from each of the lower corners of the opening to the vertical supports together with diagonal cracks from the same point to the bottom of the panel. The diagonal cracks did not propagate as far as the bottom corners. It is suggested that the horizontal cracks might have separated the panel into two halves with the top half forming from the cill level upward. The failure load of the two halves would be greatly effected by the shear resistance across the horizontal cracks.

5.5.13 Panel DC02B

A panel similar to panel DC02B but with a d.p.c laid dry in the first joint was also tested. The initial behaviour of the panel was slightly less rigid otherwise similar to that of panel DC02 as shown in Figure 5.12. However, the linearity of the load-displacement relationship was maintained until failure occurred at a load of 1.5 kN/m^2. No slip at the d.p.c. level was observed. The failure pattern was less symmetrical but otherwise similar to that of panel DC02.

In order to demonstrate the effect of self-weight on the base restraint and the behaviour of

the panel, the panel was analysed assuming a simple support at the base. It can be seen from Figure 5.12 that analysed panel yielded a more flexible loading curve than the experimental results. The predicted failure strength was however very close to the experimental value.

5.5.14 Panel W01

It would be reasonable to anticipate that a wall panel, which was built on a sand bed, would initially act as a three sided simply supported panel until shear failure occurred at the sand bed. The lateral strength of the panel would be dependent upon the frictional shear strength of the sand bed, the flexural strength of the masonry and the aspect ratio of the panel.

The deflection profile of the panel, Appendix F.18, and Figure 5.13 have clearly indicated a linear load-displacement relationship for loading up to 1.6 kN/m^2. Shear failure at the sand bed occurred at a load of 1.6 kN/m^2 and the deflections of the panel increased abruptly. At a lateral load of 2.2 kN/m^2 the first cracks became visible with horizontal cracks from each side of the opening to the vertical supports. Failure occurred shortly after at a load of 2.3 kN/m^2. More than 10mm deflection at the base of the panel was observed. The failure pattern was asymmetric and consisted of a combination of diagonal cracks and the initial horizontal cracks. As the opening was considered to be too small to have any effect on the behaviour of the panel, it was considered that the irregularity in the crack pattern was caused by uneven shearing at the sand bed.

The panel was analysed with the base simply supported initially. Shear failure was introduced

at a lateral load of 1.6 kN/m^2. The analytical results were virtually identical to that of the experimental. In order to clarify the behaviour of the panel, analytical loading curves assuming the base simply supported and unsupported were also plotted on Figure 5.13. It is clearly indicated that the behaviour of the panel is between that of the two idealised support conditions.

5.5.15 Panel HW01

The load-displacement relationship at the mid height of the free edge of the panel is plotted on Figure 5.14. It can be seen that a linear relationship was maintained up to a loading of 2.4 kN/m^2 at which point it was considered that rotation at the fixed base occurred. The flexible top support and the deformable hydraulic bolster were considered to greatly reduce the flexural stiffness and the flexural strength of the panel as indicated on the same Figure by reanalysing the panel assuming full rigidity at the top support. At a lateral load of 3.15 kN/m^2, the panel was separated into two halves by horizontal cracks which extended the full width of the panel. Diagonal cracks were observed at the bottom corner of the panels as the panel deflected abruptly. Further cracking occurred at a lateral pressure of 3.7 kN/m^2 with horizontal and diagonal cracks forming at the top of the panel. The panel appeared to have separated into three parts, top, middle and bottom. At this stage, failure was considered to occur. The top right corner of the panel was observed to have deflected more than 20mm and the maximum deflection at the free edge of the panel was measured to be more than 35mm.

5.5.16 Panel HW02

Similar to panel HW01, the panel deflected linearly with respect to load until cracking occurred, Figure 5.15. Horizontal cracks which separated the panel into two halves developed at a lateral load of 2.4 kN/m^2. A diagonal crack running from the opening lower corner to the bottom right corner of the panel was observed at a load of 2.6 kN/m^2. At this stage, the panel stiffness was greatly reduced with sheer deflections, Figure 5.15. However, the panel continued to carry further load until failure occurred at a load of 2.8 kN/m^2. The failure pattern contained a further extension of diagonal cracks to the left of the opening and a horizontal crack above the opening.

The analytical loading curve assuming full rigidity at the top support plotted on Figure 5.15 indicated that the presence of small openings in panels with flexible supports reduced the failure load more than in those with rigid supports.

5.5.17 Panel HW03

It can be seen from Figure 5.16 that the panel was much more rigid than the other two panels HW01 and HW02, as an intermediate restraint was provided at the top support. However, initial cracking was observed to occur at a lower load of 1.0 kN/m^2 at which the panel was divided into two sub-panels by horizontal cracks. After a sudden reduction in the flexural stiffness due to the initial cracking, the panel regained rigidity with a linear load-displacement profile. The lower sub-panel failed at lateral load 3.6 kN/m^2 and failure of the

upper half of the panel followed shortly at a load of 3.7 kN/m^2. The failure pattern included the initial horizontal cracks and two diagonal cracks running from the top and bottom left of the opening corners to the top and bottom of the supported vertical edge.

5.5.18 Panel HW04

Similar to panel HW03, the panel divided into two sub-panels by horizontal cracks at a lateral load of 0.7 kN/m^2. The top half formed from the sill level upward, Figure 5.17. The panel continued to carry load with regained stiffness until failure arose. A horizontal crack to the top right of opening developed at a load of 3.1 kN/m^2. Subsequent failure at the lower half of the panel occurred at a load of 3.3 kN/m^2. The failure mode was essentially identical to that of panel HW02 with diagonal cracks forming at the lower half of the panel.

5.6 Monte-Carlo Simulation

The Monte-Carlo Simulation approach [106] is well established as a method of dealing with random variability and has been successfully applied to simple problems of brittle masonry behaviour [104].

A laterally loaded masonry panel can be analysed by establishing a grid of points over the surface of the panel, sub-divided into domains by the finite element method. Random horizontal and vertical flexural strengths are assigned to each gauss point in the various

domains by sampling a distribution function with a mean and a coefficient of variation. A Normal Distribution was used, based on the joint strengths results obtained in section (5.3).

For the analysis the sub-division into finite elements is based on the unit size of which the joint strengths are based. That is, there are approximately the same number of elements in the model as there are joint units in the wall. This is to give the correct number of contributory elements for dealing with the random strength variation from point to point and for representing the number of the joint units in the wall.

Experimenting with various number samples in the Monte-Carlo simulation has shown that 100 cycles of analysis gives very close approximation within a few percentage points of consistency, Table 5.5. All the results of the wall panels considered were derived from runs of 100 cycles, Table 5.6. The mean joint strengths and the associated coefficients of variation were taken from Tables 5.1 and 5.2.

Also listed on Table 5.6 are the predictions using the predicted equivalent joint strength evaluated from the bond wrench specimens subjected to an axial precompression of 22.5 kN/m^2, Table 5.3 .

It is clear from Table 5.6 that in nearly all cases the analysis provided a slightly conservative estimation of the panel capacity when using the joint strengths obtained from the wallette specimens as previously visualised in section (5.5). The predictions using the bond wrench strength obtained from precompressed specimens were however much closer to the experimental values. The low coefficients of variation obtained from the Monte-Carlo

simulation were also in very good agreement with the coefficient of variation found between the analytical and the experimental results as shown in Table 5.4. This confirmed that the finite element analysis provided accurate and consistent predictions for the flexural strength of masonry panels, and that the variability of the wall strengths caused by the effect of material variability is small as previously suggested in section (5.5).

Table 5.1 Vertical Wallette and Joint Strengths

Type of Masonry	Condition of Specimens	Number of Test Specimens	Number of Valid Specimens	Vertical Flexural Strength N/mm²		
				Experimental	Analytical	
				Wallette	Joint	Wallette
Class B Fac. Bricks	Undocked Docked	5 10	4 7	0.474(0.388) 0.740(0.162)	0.792(0.346) 0.965(0.200)	0.474(0.385) 0.740(0.172)
Class A Eng. Bricks	Undocked	6	6	0.770(0.172)	1.000(0.200)	0.770(0.172)
Dense Conc. Blocks	Undocked	10	9	1.367(0.131)	1.578(0.153)	0.367(0.131)

Note: ( ) coefficient of variation

Table 5.2 Horizontal Wallette and Joint Strength

Type of Masonry	Condition of Specimens	Number of Test Specimens	Number of Valid Specimens	Horizontal Flexural Strength N/mm²		
				Experimental	Analytical	
				Wallette	Joint	Wallette
Class B Fac. Bricks	Undocked Docked Docked*	5 15 10	4 13 9	1.670(0.291) 1.700(0.166) 2.090(0.088)	2.214(0.293) 2.017(0.187) 2.280(0.100)	1.670(0.291) 1.700(0.166) 2.090(0.082)
Class A Eng. Bricks	Undocked	6	6	4.120(0.07)	4.120(0.000)	4.120(0.000)
Dense Conc. Blocks	Undocked	10	8	1.676(0.048)	1.731(0.056)	1.676(0.048)

Note: * six courses high specimens
( ) coefficient of variation

Table 5.3 Bond Wrench Strength

Type of Masonry	Condition of Specimens	Pre-Comp. Stress kN/m²	Number of Test Specimens	Number of Valid Specimens	Bond Wrench N/mm²	Equivalent Joint Strength N/mm²
Class B Fac. Bricks	Docked	0.0 4.0 12.5 22.5	12 12 10 -	12 11 10 -	0.936(0.202) 1.042(0.188) 1.082(0.166) 1.130(0.140)*	0.936(0.142) 1.042(0.133) 1.082(0.117) 1.130(0.100)*

Note: ( ) coefficient of variation
* predicted value

Table 5.4 Experimental and Analytical Failure Load

Panel No.	Expt. Failure Pressure kN/m²	Y. Line / Expt.	FEA Prediction / Expt. Failure Load			
			exc. Window Frame		inc. Window Frame	
			(a)	(b)	(a)	(b)
SB01	2.80	1.13	0.88	0.98	0.88	0.98
SB02	2.40	1.08	0.76	0.84	0.90	1.00
SB03	2.30	1.06	0.69	0.84	0.83	0.97
SB04	2.20	1.17	0.82	0.95	0.88	1.03
SB05	2.70	1.17	0.91	1.02	0.91	1.02
SB06	7.50	1.16	0.90	0.98	0.90	0.98
SB07	5.50	1.27	0.94	0.97	1.05	1.06
SB09	2.40	1.32	0.87	1.00	0.94	1.03
CB01	5.80	1.22	0.87	0.97	0.87	0.97
CB02	3.80	1.53	0.89	0.98	0.91	1.01
DC01	2.65	1.18	0.90	0.97	0.90	0.97
DC02	1.75	1.26	0.81	0.95	0.97	1.02
DC02B	1.50	1.27	0.78	0.83	0.92	0.96
HW01	3.70	1.77	0.98	0.98	-	-
HW02	2.80	1.97	0.91	1.00	-	-
HW03	3.30	1.58	0.89	0.97	-	-
HW04	3.70	1.35	1.08	1.12	-	-
W01	2.30	0.80	1.00	1.00	1.00	1.00
	Mean =	1.29	0.88	0.96	0.92	1.00
	C.V. =	0.21	0.09	0.07	0.06	0.03

(a) predictions using wallette strengths
(b) predictions using joint strengths

Table 5.5 Performance of Monte-Carlo Simulation

Panel NO.	Monte-Carlo Simulation kN/m²		
	Number of Iterations		
	10	100	1000
SB01	2.31(0.031)	2.27(0.029)	2.27(0.031)
SB02	2.21(0.027)	2.23(0.026)	2.24(0.029)

Note: ( ) coefficient of variation

Table 5.6 Panel Lateral Strength Predictions Using Monte-Carlo Simulation

Panel No.	Expt. Failure Pressure kN/m^2	Monte-Carlo Simulation	
		Joint Strength	Bond Wrench
SB01	2.80	2.27(0.029)	2.46(0.028)
SB02	2.40	2.04(0.027)	2.23(0.026)
SB03	2.30	2.02(0.028)	2.21(0.023)
SB04	2.20	1.90(0.025)	2.22(0.019)
SB05	2.70	2.27(0.029)	2.46(0.028)
SB06	7.50	6.95(0.035)	7.21(0.019)
SB07	5.50	5.60(0.032)	5.80(0.017)
SB09	2.40	2.16(0.060)	2.54(0.035)
CB01	5.80	5.10(0.025)	5.50(0.018)
CB02	3.80	3.61(0.027)	3.81(0.021)
DC01	2.65	2.23(0.019)	-
DC02	1.75	1.69(0.035)	-
DC02B	1.50	1.37(0.016)	-

Note: ( ) coefficient of variation

Figure 5.1 Bed Joint Strength Vs Vertical Precompression.

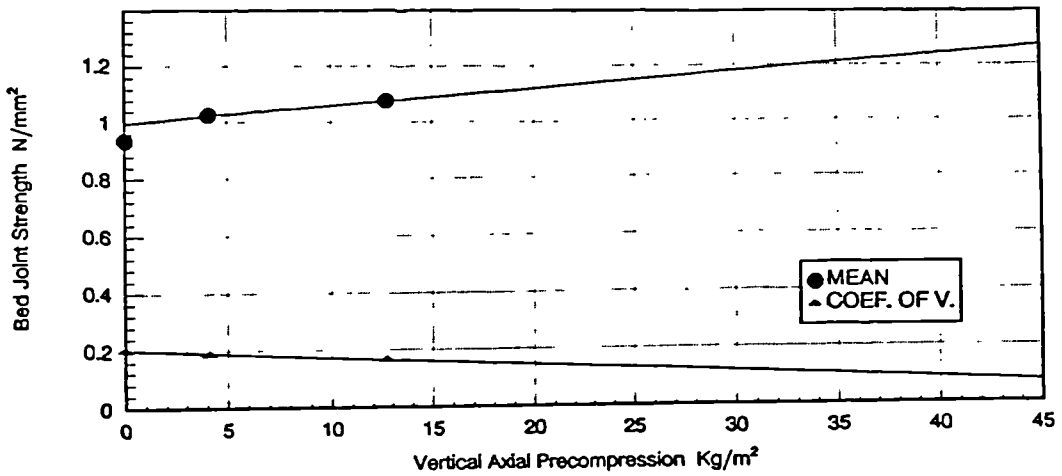

Figure 5.2 Wall SB01 and SB05 Load-Displacement Relationship.

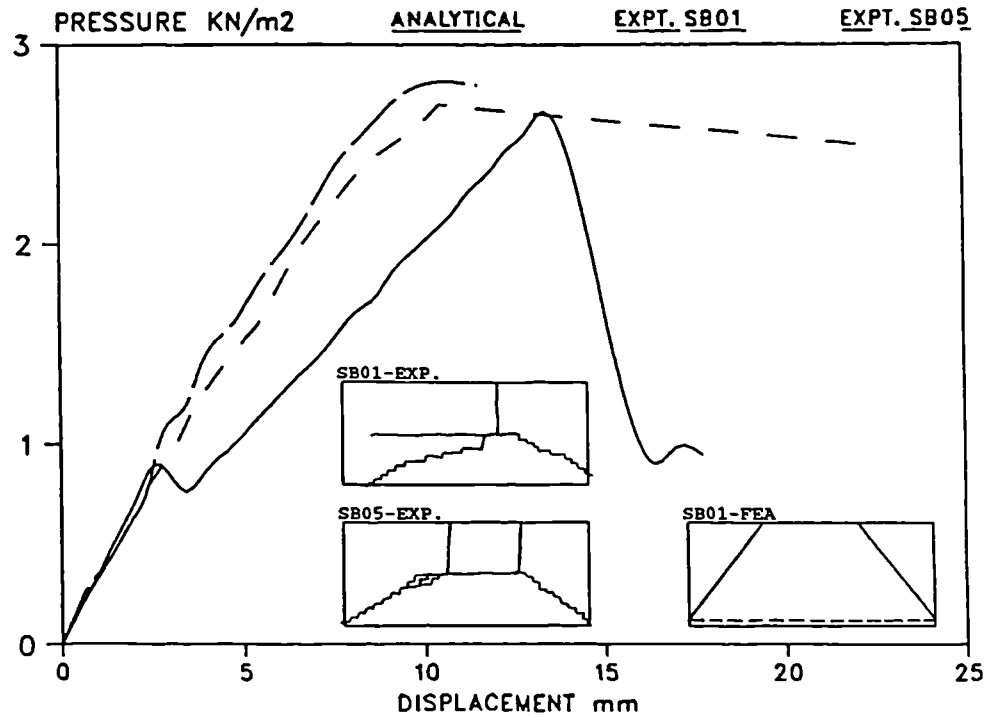

Figure 5.3 Wall SB02 Load-Displacement Relationship.

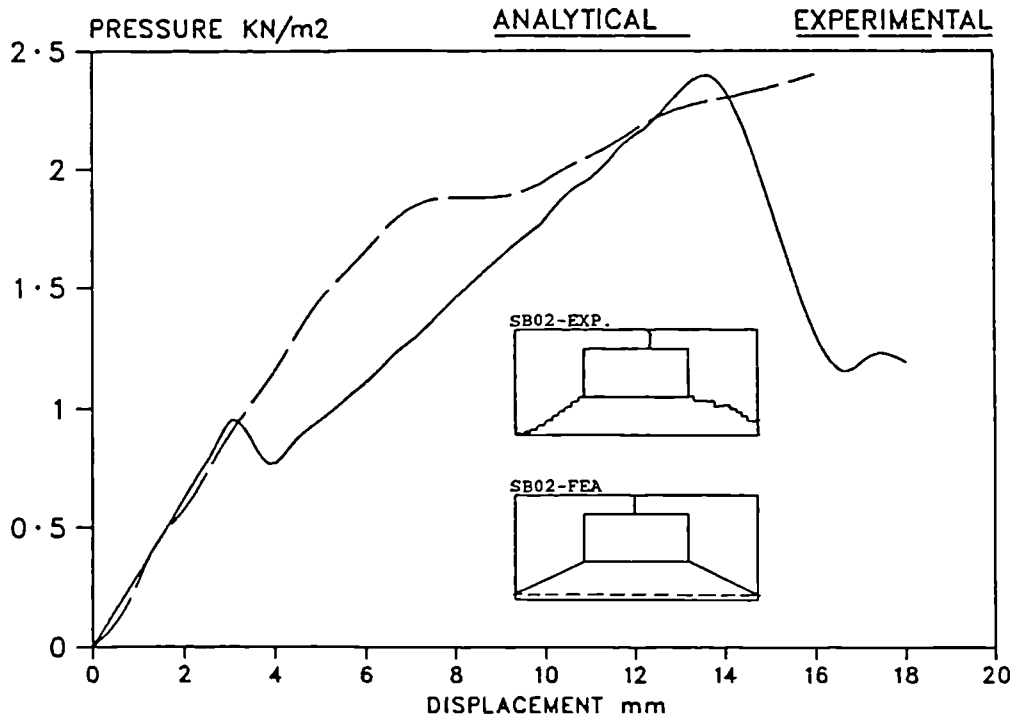

Figure 5.4 Wall SB03 Load-Displacement Relationship.

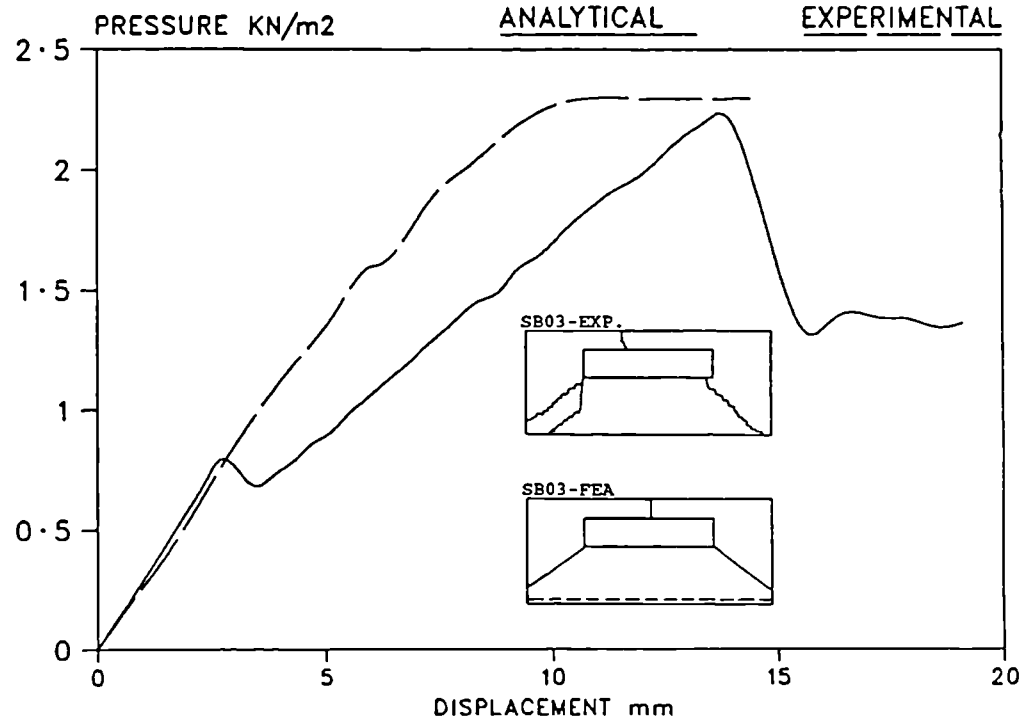

Figure 5.5 Wall SB04 Load-Displacement Relationship.

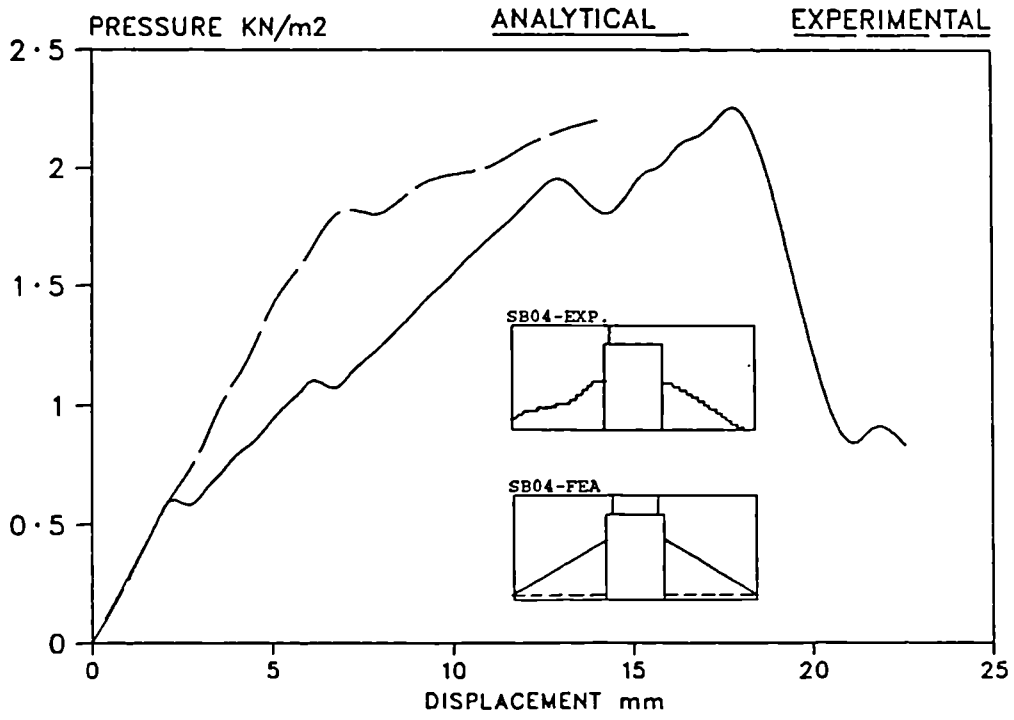

Figure 5.6 Wall Sb06 Load-Displacement Relationship.

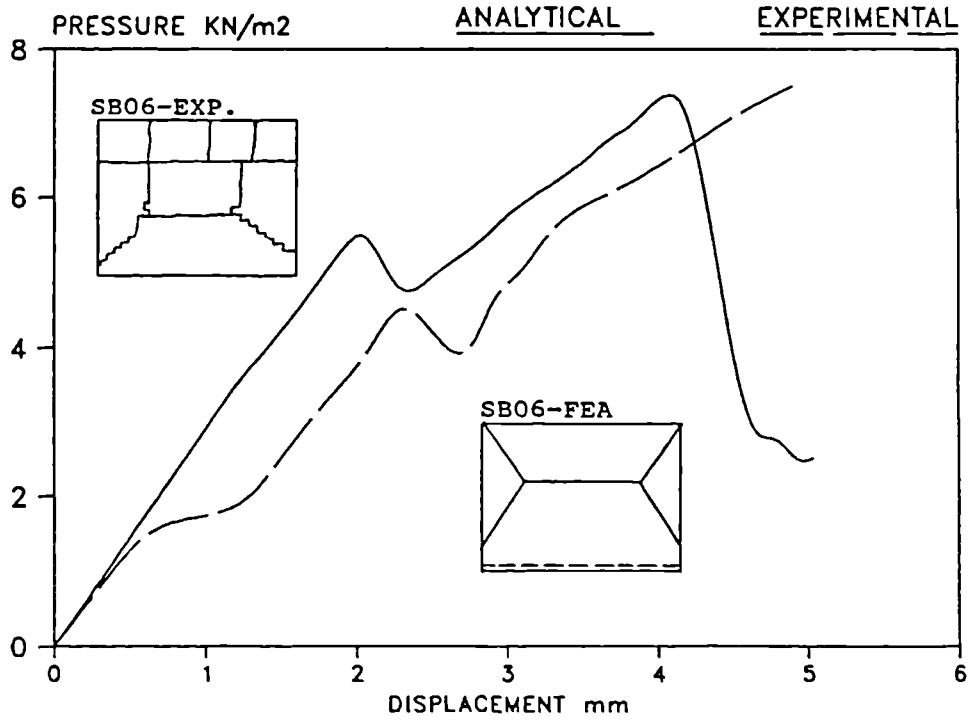

Figure 5.7 Wall SB07 Load-Displacement Relationship.

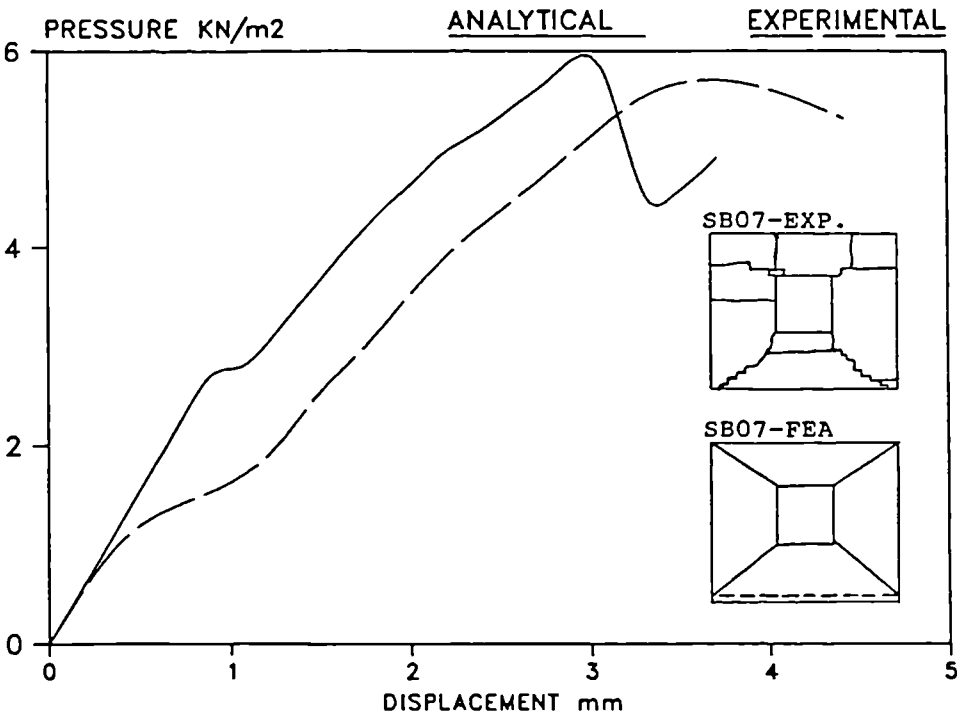

Figure 5.8 Wall SB09 Load-Displacement Relationship.

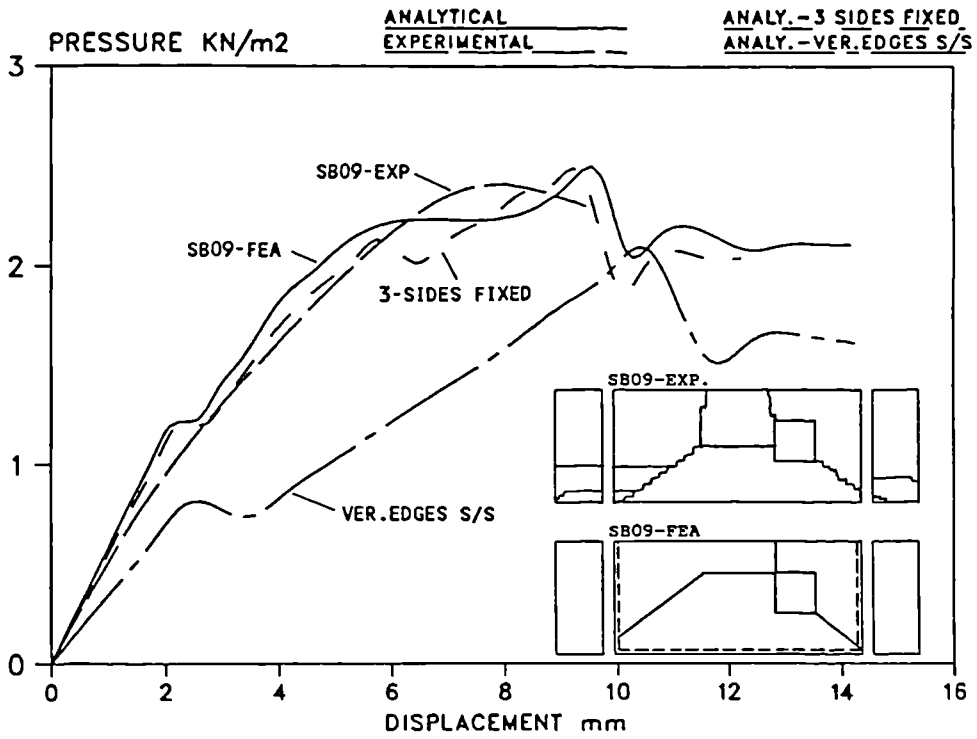

Figure 5.9 Wall CB01 Load-Displacement Relationship.

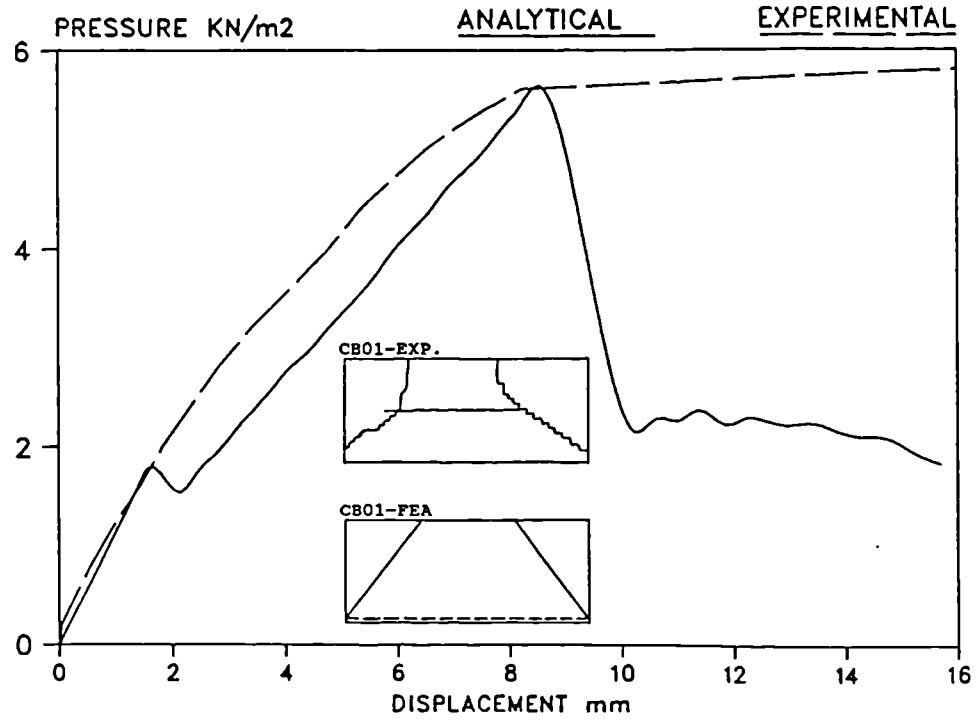

Figure 5.10 Wall CB02 Load-Displacement Relationship.

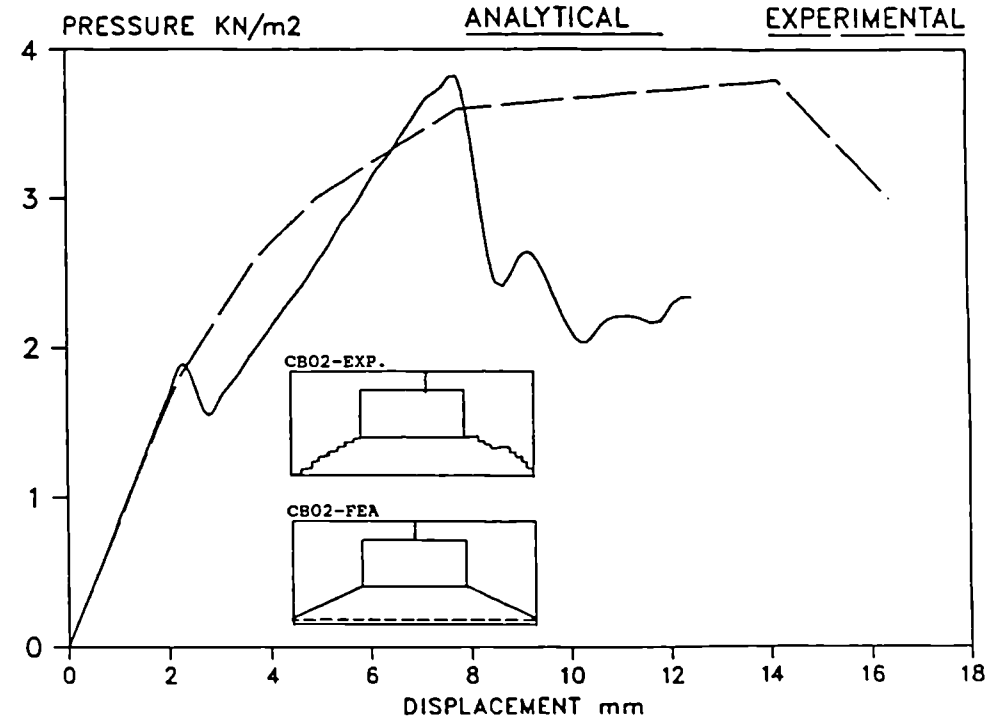

Figure 5.11 Wall DC01 Load-Displacement Relationship.

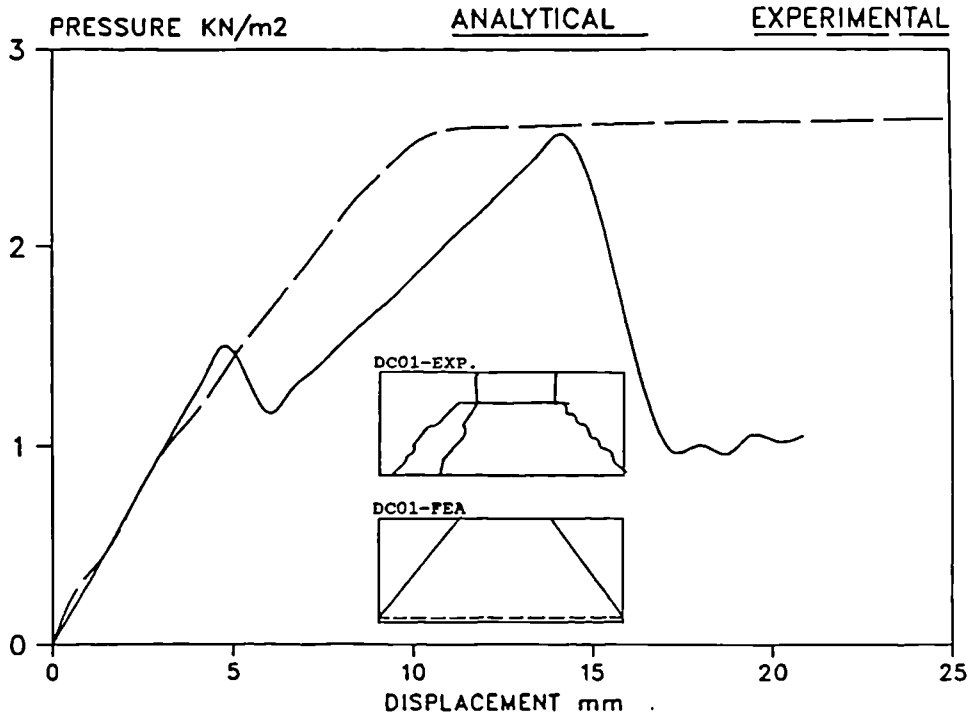

Figure 5.12 Wall DC02 and DC02B Load-Displacement Relationship.

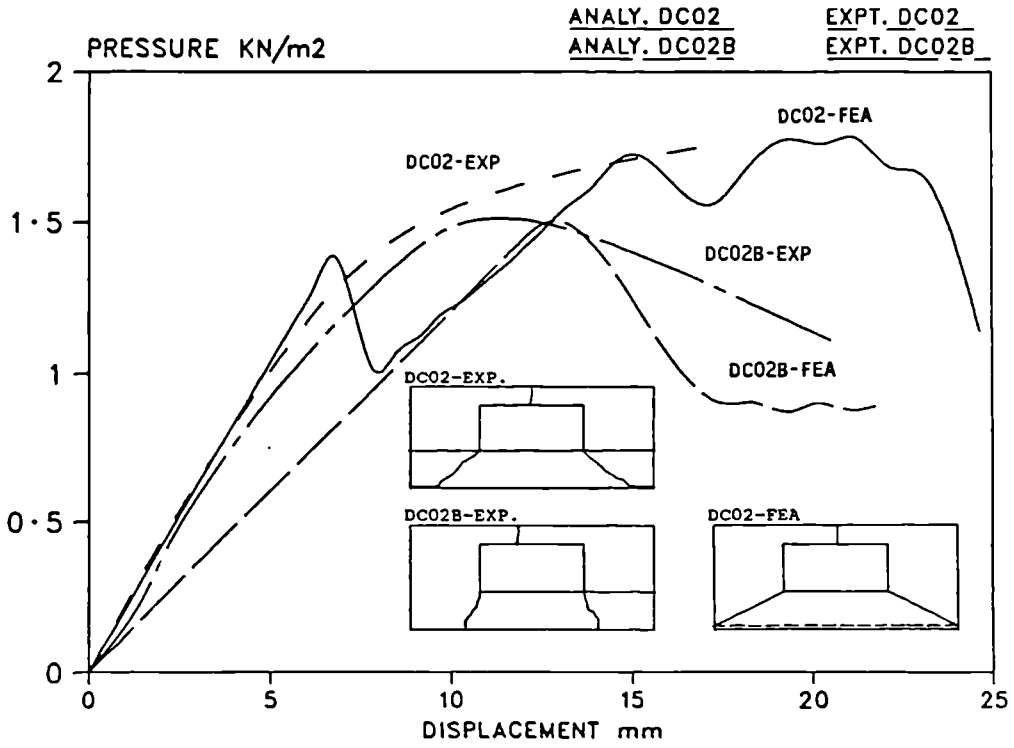

Figure 5.13 Wall W01 Load-Displacement Relationship.

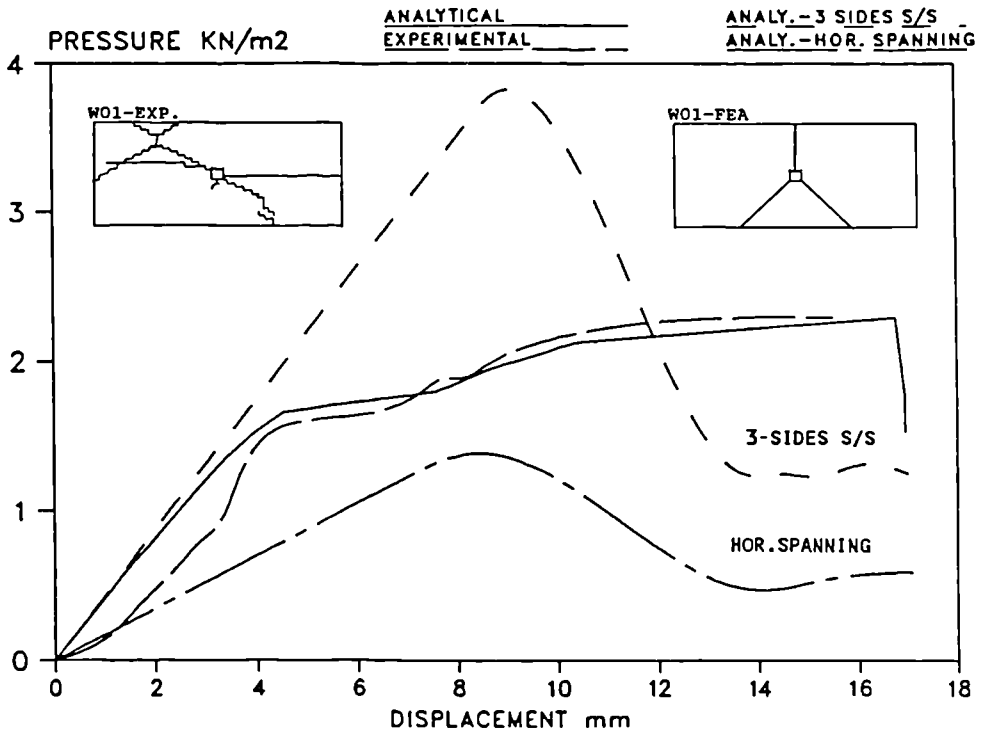

Figure 5.14 Wall HW01 Load-Displacement Relationship.

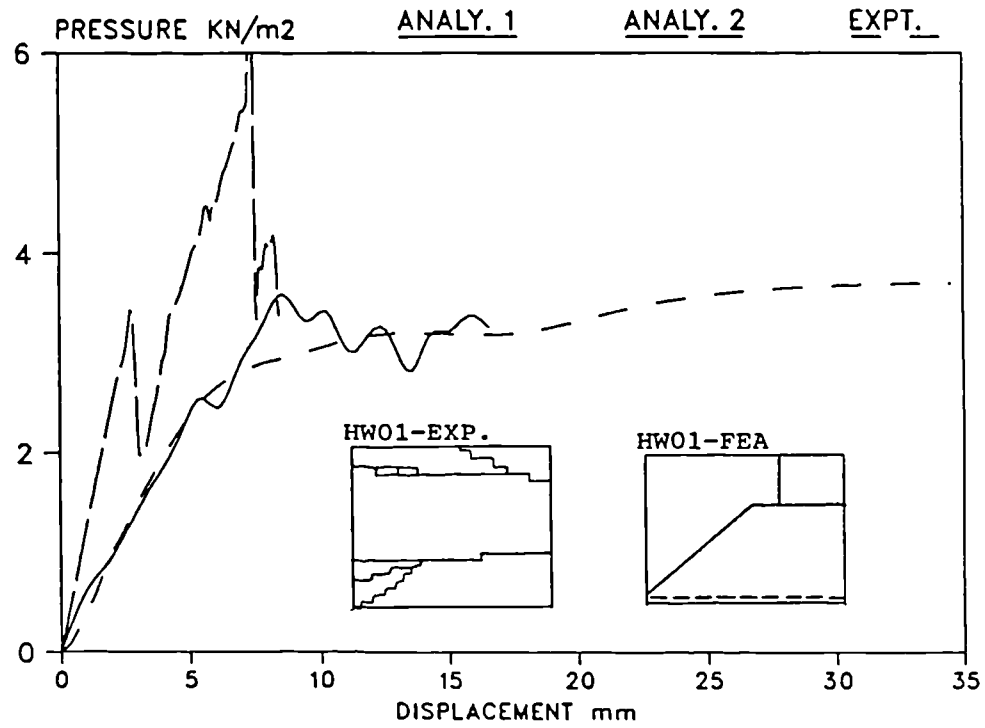

Figure 5.15 Wall HW02 Load-Displacement Relationship.

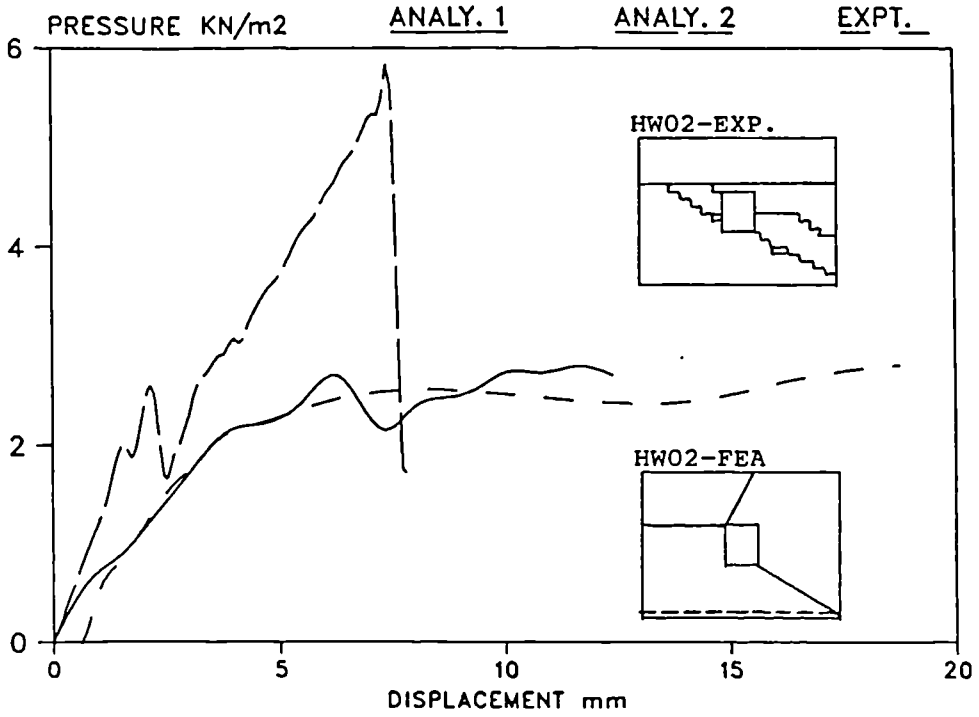

Figure 5.16 Wall HW03 Load-Displacement Relationship.

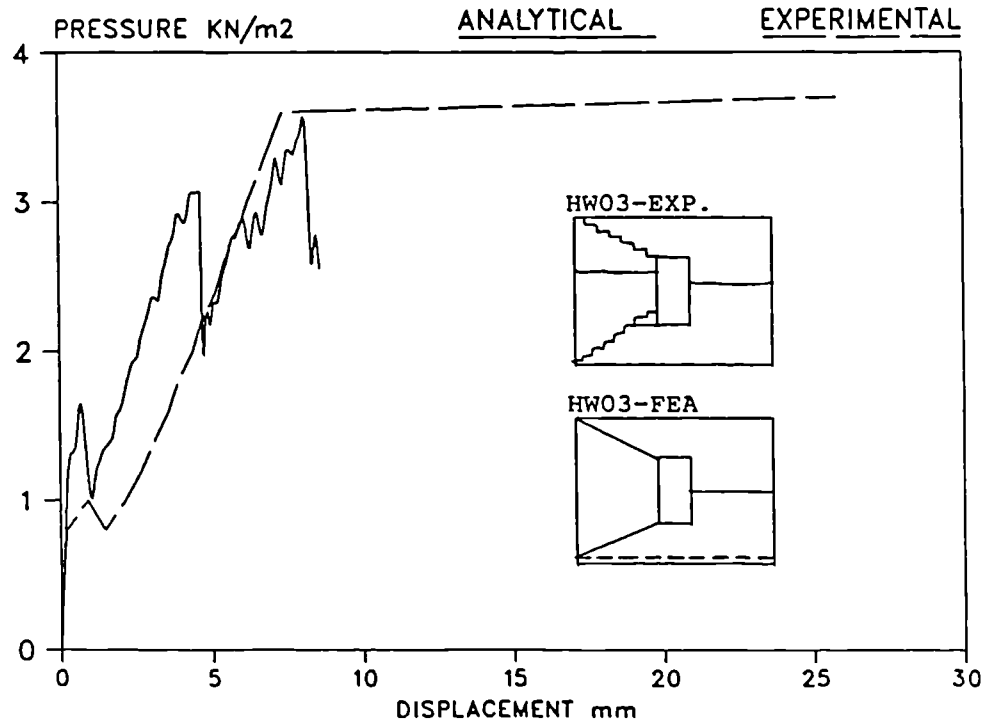

Figure 5.17 Wall HW04 Load-Displacement Relationship.

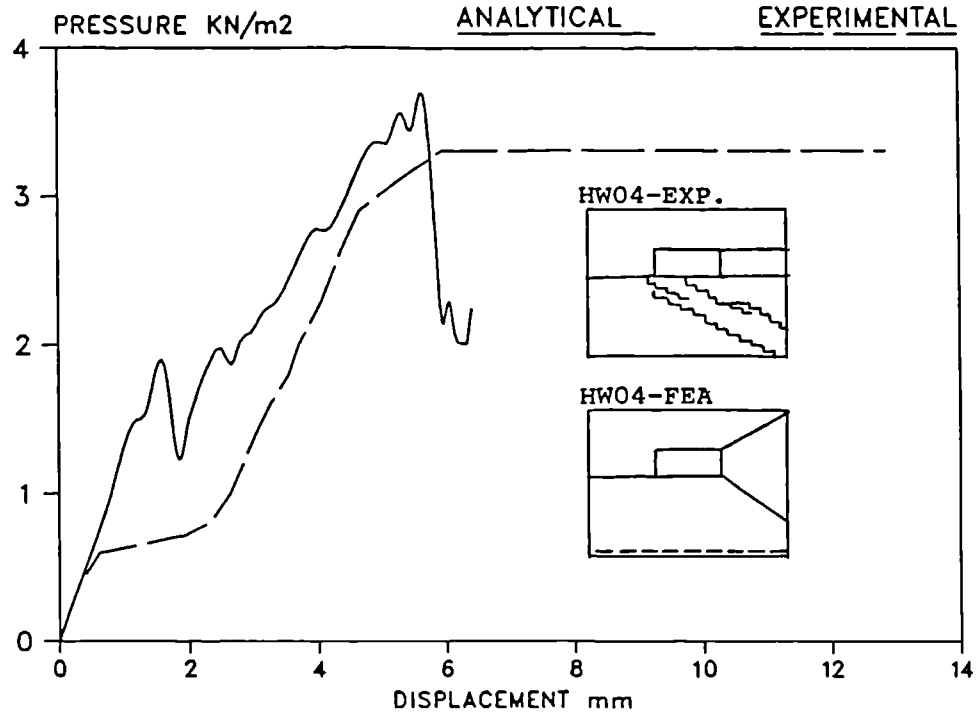

6.0 PARAMETRIC SURVEY

6.1 Introduction

Parametric studies using the finite element analysis have been carried out to investigate the following effects on the flexural strength of masonry panels:-

(a) Aspect ratios

(b) Orthogonal ratios

(c) Edge support conditions

(d) Opening sizes and positions

In order to qualify and quantify the influence of the factors, only one factor was varied at a time. A similar parametric survey with the conventional yield line design method was previously carried out by May [107].

Comparison between the results obtained with the finite element analysis and that with the yield line method was also made.

Before evaluating the outcome of the parametric survey, it is essential to first discuss the normally accepted differences between yield line theory proposed by other researchers and the finite element analysis developed in this report. Consideration is given to upper and lower bound solutions.

6.2 Limit Analysis

When considering a rigid-perfectly plastic material, the conditions required to establish an upper or lower bound solution for the collapse load are considered essentially as follows:

(a) Upper bound solution - which either overestimates, or gives the correct value of the collapse load. It is based on the following:-

1. A valid collapse mechanism must be found which satisfies the kinematic boundary conditions.
2. The work equation must be satisfied.
3. The criteria of plastic flow must be obeyed.

(b) Lower bound solution - which either underestimates, or gives the correct value of the collapse load. It is based on the following:-

4. Equilibrium must be satisfied throughout the structure.
5. The yield criterion must not be violated.

From these rules it can be shown that, in the limit, the finite element analysis is closer to a lower bound solution.

When applying yield line theory to Johansen's equilibrium method the stress state is specified only along the yield lines and not everywhere in the slab, as required by item 4. Prager's findings therefore explained why nodal force theory [108] could not say which kind of mode would give the lowest possible collapse load and indicate no circumstances was it a lower

bound lower. It was pointed out [109] that nodal forces theory had an important role to play in the derivation of upper bound solutions.

It is suggested that yield line theory, which ever technique is used, should be regarded as an upper bound solution. It should be noted that by employing simplified stress fields and satisfying items 4 and 5, Hillerborg [110] produced a relatively simplified method which supposedly provides solutions that underestimate the collapse load. In fact, it has been suggested [111] that, because of the simplifications which have been introduced, yield line analysis with simple yield pattern is likely to be a closer assessment of the true failure load than a lower bound solution.

It is normally expected, in all circumstances, that the yield line analysis should produce a higher collapse load than a lower bound solution. At low values of orthogonal ratio, the finite element analysis predicted higher collapse loads than the yield line method, as described in section (6.5). The reasons for this are unclear. A possible explanation, in part, is that the membrane action generated in the panel is not considered in the yield line method. More work, in this area of study, is required to look into the fundamental theories of the yield line method and the finite element analysis.

6.3 A Note on Yield Line Theory

The yield criterion that has already been established for reinforced concrete, namely Johansen's "stepped" yield criterion derives the yield moment

$$m_n = m_1 \cos^2\phi + m_2 \sin^2\phi$$

where m_1 and m_2 are moment of resistance per unit length in the x and y axis, and ϕ is the angle from m_1 to the yield line.

However, left in the above form, the yield criterion does not completely satisfy the limit analysis and is not really based on a valid kinematic system once the corresponding twisting is evaluated by considering individual steps [109].

There are many points of divergence between the criterion of idealised limit analysis and the stepped criterion. The present trend is for yield line theory to drift away from the rigorous mathematical standpoint dictated by limit analysis. It has been suggested [111] that, until yield-line theory and limit analysis employ the same criterion of yield, they must be considered in isolation.

6.4 Effect of Aspect Ratios

The analyses performed for panels supported on all four sides, with aspect ratios ranging from 0.43 to 4.24, yielded the results given in Table 6.1 and shown in Figure 6.1. These results show two distinct regions of behaviour. For aspect ratios up to 0.43, all cracks were developed at failure to form a crack pattern (I), Figure 6.1. This was characterised by a central vertical crack and diagonal cracks originating from the panel corners and meeting at this vertical crack. For aspect ratios larger than 0.43, the behaviour was characterised by an initial horizontal crack extending virtually the whole panel length and diagonal cracks meeting at this horizontal crack to complete the failure pattern (II), Figure 6.1.

Wall panels supported on three sides with the top edge free were also analysed for the same range of aspect ratios. The results are given in Table 6.2 and Figure 6.2. According to the analyses all of the crack patterns developed instantaneously at failure. The results also showed two distinct crack patterns. For aspect ratios up to 1.43, the predicted crack patterns were composed of two diagonal cracks forming from the panel corners and meeting at a central vertical crack. This extended to the free edge, failure mode (I), Figure 6.2. However, for aspect ratios larger than 1.43, only diagonal cracks formed, which extended up to the free edge, failure mode (II), Figure 6.2.

The panel capacities calculated by the yield line method are given in Table 6.3 and their comparison with the finite element predictions are shown in Figures 6.3 and 6.4. When compared to the finite element model predictions, the yield line method overestimated the panel capacity for panels supported on all four sides by 2% to 60%. For panels supported

on three sides with the top edge free, the yield line predictions were in reasonably good agreement with the model predictions for L/H ratios greater 1.43, Figure 6.3.

Table 6.4 contains the predicted results, using the moment coefficients given in BS5628 [8], and shows comparison with the finite element model predictions, Figures 6.3 and 6.4. The BS5628 moment coefficients provided similar collapse loads to those for the yield line method, except for aspect ratios over 1.43 where the moment coefficients produced considerably lower failure loads for panels supported on three and four sides. This agreement was expected because the moment of coefficients were based on yield line analysis, with some modifications based on available experimental data [8].

6.5 Effect of Orthogonal Ratios

A total of 9 cases of panels constructed of calcium silicate brickwork and AAC blockwork with various orthogonal ratios were considered. Three types of edge support conditions with three different aspect ratios were examined in this comprehensive study. The results are given in Table 6.5 and shown in Figures in 6.5 to 6.8.

Parametric study of calcium silicate brick and AAC blockwork

Orthogonal ratios

(i) Calcium silicate brickwork

Failure moment normal to bed joints	1.500 kNm
F_{kx} normal to bed joints	0.900 N/mm^2

F_{ky} parallel to bed joints case	(a)	0.300 N/mm^2	μ = 0.333
	(b)	0.240 N/mm^2	μ = 0.267
	(c)	0.150 N/mm^2	μ = 0.167
	(d)	0.050 N/mm^2	μ = 0.056

(ii) AAC blockwork

Failure moment normal to bed joints		0.667 kNm	
F_{kx} normal to bed joints		0.400 N/mm^2	
F_{ky} parallel to bed joints case	(a)	0.250 N/mm^2	μ = 0.625
	(b)	0.200 N/mm^2	μ = 0.500
	(c)	0.125 N/mm^2	μ = 0.3125
	(d)	0.025 N/mm^2	μ = 0.0625

It can be seen from Figures 6.6 to 6.8 that the relationship between the yield line method and the finite element analysis is erratic. In most cases, particularly at high orthogonal ratios the yield line method provided higher predictions than the finite element analysis, whereas at low orthogonal ratios the yield line method provided unconservative predictions.

For some cases, the results obtained by the yield line method and using the BS5628 coefficients were reasonably accurate. However this does not change the fact that this method is not rationally justified for use in masonry.

When comparing the mode of failure with decreasing values of orthogonal ratio, the results obtained from the finite element analysis were generally in good agreement with that of the yield line method. In other cases different failure modes were predicted. For example considering a square panel with an orthogonal ratio of 0.33. The yield line method predicted a failure mode 'b', Figure 6.5. However the finite element analysis, based on isotropic plate theory, predicted an initial crack to occur in the weaker horizontal direction. This converted

the panel from a two way bending four side supported to a one way bending three side supported load carrying mechanism. Hence, failure mode 'a' was predicted, Figure 6.5. It was evident from case number 1, 2, 4 and 5, Table 6.5 and Figures 6.6 and 6.7 that the flexural strength of panels supported on all four sides were identical to the case of panels which were twice the height and supported on three sides with the top edge free. The finite element analyses showed a transition cracking behaviour in addition to the two distinct crack patterns detected in each of the support conditions.

6.6 Effect of Opening Sizes and Positions

The accuracy of any methods of analysis to predict the flexural strength of masonry panels with openings may be best clarified by evaluating the normalised flexural strength of the panels by using the flexural strength of solid panels.

This study comprised a total of 8 cases of various opening sizes and positions. Three types of edge support conditions and two values of orthogonal ratios were considered, Figure 6.9.

It can be seen from Table 6.6 that there was no consistent relationship between the flexural strength of masonry panels with opening sizes and positions. The effect of the opening varied with edge support conditions and orthogonal ratios. For masonry panels with opening sizes up to 25% of the panel area, it was generally established that the normalised flexural strength of a panel was directly proportional to the square of the net area divided by the gross area of the panel, Equation (6.1), Figure 6.10.

$$Normalised\ Flexural\ Strength = \frac{W}{W_s} = \left(\frac{A_n}{A_g}\right)^2 \qquad \ldots(6.1)$$

Where W is the failure load of the panel with openings

W_s is the failure load of solid panel

A_g is the gross area of panel

A_n is the net area of panel = gross area - opening area

Although the yield line predictions proved to be slightly unconservative, in comparison with the finite element model predictions, it was apparent that reasonably good correlations were obtained when comparisons were made using normalised flexural strengths. The actual predicted failure loads were however dependent on the flexural strength of the reference solid panels. The failure loads provided by the yield line method in this case were undoubtedly higher than that predicted by the finite element model, since the flexural strength of the solid panels were overestimated by the yield line method.

6.7 Discussion

From the above investigation, it is suggested that further experimental and theoretical works are required to justify the finite element predictions for panels with low orthogonal ratio, less than 0.2. However, it is unlikely that masonry with such low values of orthogonal ratio, will occur in practice. For masonry panels with orthogonal ratios between 0.2 and 1.0, the finite element analysis provided a relatively close correlation with the experimental results, as

shown in Chapter 5 and Table 6.7. The experimental and analytical results listed in Table 6.7 and shown in Figure 6.11 were normalised using the flexural strength of the solid panels. It is clear that the finite element model predictions using the wallette strengths and that using the joint strengths were similar.

The results obtained using the yield line method were also in reasonable agreement with the experimental results, Table 6.7, although it was found to overestimate the flexural strength of all panels. It was not possible to obtain a direct comparison because the strength of the window frames were excluded in the yield line analysis. The predictions given by Equation (6.1), in terms of normalised strength, were in closer agreement with the experimental results, than those given by the yield line method. The equation is semi-empirical and does not account for the positions of openings. Yield line method can be used, in terms of normalised flexural strength, especially for the design of panels with off-centre openings.

Table 6.1 FEA Model Predictions for Walls Simply Supported on All Four Sides, μ=0.33.

Wall	L x H m	Predicted capacities Ratio L/H	Crack Pattern	kN/m² Initial Crack	kN/m² Failure
a	1.2 x 2.8	0.43	I	5.15	5.15
b	1.6 x 2.8	0.57		2.80	4.43
c	2.0 x 2.8	0.71		1.85	2.38
d	2.4 x 2.8	0.86		1.32	2.10
e	2.8 x 2.8	1.00		1.19	1.93
f	3.6 x 2.8	1.29		0.62	1.34
g	4.0 x 2.8	1.43		0.56	1.20
h	5.2 x 2.8	1.86		0.43	0.90
i	6.0 x 2.8	2.14	II	0.43	0.79
j	8.0 x 2.8	2.86		0.38	0.62
k	9.6 x 2.8	3.43		0.38	0.38
l	10.0 x 2.8	3.57		0.38	0.38
m	11.2 x 2.8	4.00		0.37	0.37
n	12.0 x 2.8	4.29		0.37	0.37

Table 6.2 FEA Model Predictions for Walls Simply Supported on Three Sides with the Top Edge Free, μ=0.33.

Wall	L x H m	Predicted capacities Ratio L/H	Crack Patter	kN/m² Initial Crack	kN/m² Failure
a	1.2 x 2.8	0.43		-	5.11
b	1.6 x 2.8	0.57		-	2.96
c	2.0 x 2.8	0.71		-	1.95
d	2.4 x 2.8	0.86	I	-	1.43
e	2.8 x 2.8	1.00		-	1.16
f	3.6 x 2.8	1.29		-	0.85
g	4.0 x 2.8	1.43		-	0.74
h	5.2 x 2.8	1.86		-	0.57
i	6.0 x 2.8	2.14		-	0.47
j	8.0 x 2.8	2.86		-	0.31
k	9.6 x 2.8	3.43	II	-	0.25
l	10.0 x 2.8	3.57		-	0.24
m	11.2 x 2.8	4.00		-	0.21
n	12.0 x 2.8	4.29		-	0.19

Table 6.3 Wall Capacities Predicted using the Yield Line Design Method and Their Comparison to Finite Element Model Predictions, μ=0.33.

Wall	Aspect Ratio	Wall Supported on All Four Sides		Wall Supported on Three Sides with the Top Edge Free	
		Y.L.	Y.L. / FEA	Y.L.	Y.L. / FEA
	L/H	kN/m^2		kN/m^2	
a	0.43	7.39	1.43	6.41	1.25
b	0.57	4.56	1.03	3.78	1.28
c	0.71	3.21	1.35	2.54	1.30
d	0.86	2.44	1.16	1.85	1.29
e	1.00	1.96	1.02	1.42	1.22
f	1.29	1.42	1.06	0.95	1.12
g	1.43	1.25	1.04	0.80	1.08
h	1.86	0.95	1.06	0.55	0.96
i	2.14	0.84	1.06	0.46	0.98
j	2.86	0.68	1.10	0.31	1.00
X	*3.43*	*0.62*	*1.63*	*0.24*	*0.96*
l	3.57	0.60	1.58	0.23	0.96
m	4.00	0.57	1.54	0.20	0.95
n	4.29	0.56	1.51	0.18	0.95

Table 6.4 Wall Capacities Predicted using the British Code Coefficients and Their Comparison to Finite Element Model Predictions, μ=0.33.

Wall	Aspect Ratio	Wall Supported on All Four Sides		Wall Supported on Three Sides with the Top Edge Free	
		BS5628	BS5628 / FEA	BS5628	BS5628 / FEA
	L/H	kN/m^2		kN/m^2	
a	0.43	5.55	1.08	5.55	1.09
b	0.57	4.48	1.01	3.77	1.27
c	0.71	3.17	1.33	2.54	1.30
d	0.86	2.36	1.14	1.86	1.29
e	1.00	1.96	1.02	1.42	1.22
f	1.29	1.42	0.99	0.95	1.12
g	1.43	1.16	0.96	0.84	1.08
h	1.86	0.88	0.98	0.55	0.96
i	2.14	0.77	0.97	0.45	0.97
j	2.86	0.61	0.99	0.31	0.98
K	3.43	0.58	1.53	0.24	0.94
l	3.57	0.54	1.43	0.22	0.92
m	4.00	0.43	1.16	0.17	0.81
n	4.29	0.37	1.00	0.15	0.79

Table 6.5 Parametric Study for Calcium Silicate Brick and AAC Blockwork

CASE 1 Aspect ratio L/H = 2.0 L = 5.6 m H = 2.8 m
Simply supported along all edges

Material	μ	x	Mode of Failure	Yield Line kN/m²	Code kN/m²	Mode of Failure	FEA Model kN/m²
	1.00	0.326	a	2.660	2.705	a	2.025
Calc. sil.	0.333	0.463	a	1.339	1.329	a	1.352
Calc. sil.	0.267	0.490	a	1.194		a	1.283
Calc. sil.	0.167	0.451	b	1.030		a	1.183
Calc. sil.	0.056	0.246	b	0.655		a1	1.070
AAC	1.00	0.326	a	1.187	1.187	a	0.900
AAC	0.625	0.383	a	0.869	0.854	a	0.731
AAC	0.50	0.411	a	0.757	0.764	a	0.675
AAC	0.3125	0.472	a	0.573	0.562	a	0.592
AAC	0.0625	0.326	b	0.302		a1	0.479

CASE 2 Aspect ratio L/H = 2.0 L = 5.6 m H = 2.8 m
Free along top, simply supported remaining three sides

Material	μ	x	Mode of Failure	Yield Line kN/m²	Code kN/m²	Mode of Failure	FEA Model kN/m²
	1.00	0.360	c	1.148	1.063	c	0.874
Calc. sil.	0.333	0.718	d	0.733	0.735	c	0.758
Calc. sil.	0.267	0.670	d	0.691		c1	0.714
Calc. sil.	0.167	0.564	d	0.613		c1	0.626
Calc. sil.	0.056	0.271	d	0.502		c1	0.620
AAC	1.00	0.360	c	0.514	0.514	c	0.388
AAC	0.625	0.880	d	0.441	0.403	c	0.356
AAC	0.50	0.823	d	0.381	0.381	c1	0.355
AAC	0.3125	0.705	d	0.321	0.321	c1	0.330
AAC	0.0625	0.375	d	0.227		c1	0.280

CASE 3 Aspect ratio L/H = 2.0 L = 5.6 m H = 2.8 m
Free along one side, simply supported along remaining three edges

Material	μ	x	Mode of Failure	Yield Line kN/m²	Code kN/m²	Mode of Failure	FEA Model kN/m²
	1.00	0.375	e	2.040	2.079	e	1.592
Calc. sil.	0.333	0.553	e	0.829	0.823	e	0.694
Calc. sil.	0.267	0.476	e	0.714		e	0.628
Calc. sil.	0.167	0.345	e	0.517		e	0.561
Calc. sil.	0.056	0.111	f	0.246		e	0.460
AAC	1.00	0.375	e	0.929	0.929	e	0.717
AAC	0.625	0.917	e	0.612	0.610	e	0.450
AAC	0.50	0.765	e	0.512	0.508	e	0.385
AAC	0.3125	0.531	e	0.356	0.356	e	0.302
AAC	0.0625	0.177	f	0.119		e	0.209

CASE 4 Aspect ratio L/H = 1.0 L = 5.6 m H = 5.6 m
Simply supported along all edges

Material	μ	x	Mode of Failure	Yield Line kN/m²	Code kN/m²	Mode of Failure	FEA Model kN/m²
	1.00	0.500	b	1.148	1.139	a	0.895
Calc. sil.	0.333	0.359	b	0.733	0.725	a1	0.756
Calc. sil.	0.267	0.335	b	0.691		a1	0.710
Calc. sil.	0.167	0.282	b	0.613		a1	0.652
Calc. sil.	0.056	0.136	b	0.502		a1	0.620
AAC	1.00	0.500	b	0.512	0.512	a	0.393
AAC	0.625	0.440	b	0.413	0.410	a	0.354
AAC	0.50	0.411	b	0.377	0.373	a1	0.354
AAC	0.3125	0.352	b	0.321	0.317	a1	0.327
AAC	0.0625	0.187	b	0.227		a1	0.280

CASE 5 Aspect ratio L/H = 1.0 L = 5.6 m H = 5.6 m
Free along top, simply supported remaining three sides

Material	μ	x	Mode of Failure	Yield Line kN/m²	Code kN/m²	Mode of Failure	FEA Model kN/m²
	1.00	0.651	d	0.674	0.674	d	0.473
Calc. sil.	0.333	0.422	d	0.533	0.531	d	0.436
Calc. sil.	0.267	0.387	d	0.516		d	0.420
Calc. sil.	0.167	0.317	d	0.484		d	0.420
Calc. sil.	0.056	0.143	d	0.438		d	0.420
AAC	1.00	0.651	d	0.300		d	0.209
AAC	0.625	0.546	d	0.267	0.269	d	0.199
AAC	0.50	0.500	d	0.255	0.256	d	0.199
AAC	0.3125	0.412	d	0.235	0.233	d	0.193
AAC	0.0625	0.201	d	0.197		d	0.190

CASE 6 Aspect ratio L/H = 1.0 L = 5.6 m H = 5.6 m
Free along one side, simply supported along remaining three edges

Material	μ	x	Mode of Failure	Yield Line kN/m²	Code kN/m²	Mode of Failure	FEA Model kN/m²
	1.00	0.451	e	0.677	0.674	e	0.488
Calc. sil.	0.333	0.213	f	0.319	0.319	e	0.314
Calc. sil.	0.267	0.186	f	0.279		e	0.297
Calc. sil.	0.167	0.138	f	0.207		e1	0.280
Calc. sil.	0.056	0.050	f	0.106		f	0.248
AAC	1.00	0.451	e	0.301	0.301	e	0.218
AAC	0.625	0.326	e	0.217	0.126	e	0.174
AAC	0.50	0.283	e	0.187	0.188	e	0.159
AAC	0.3125	0.205	f	0.137	0.136	e	0.138
AAC	0.0625	0.075	f	0.050		e1	0.115

CASE 7 Aspect ratio $L/H = 0.5$ L = 5.6 m H = 11.2 m
Simply supported along all edges

Material	μ	x	Mode of Failure	Yield Line kN/m²	Code kN/m²	Mode of Failure	FEA Model kN/m²
	1.00	0.326	b	0.677	0.663	b	0.488
Calc. sil.	0.333	0.211	b	0.532	0.525	b	0.444
Calc. sil.	0.267	0.194	b	0.516		b	0.420
Calc. sil.	0.167	0.158	b	0.484		b	0.420
Calc. sil.	0.056	0.071	b	0.438		b	0.420
AAC	1.00	0.326	b	0.301		b	0.219
AAC	0.625	0.273	b	0.267	0.262	b	0.199
AAC	0.50	0.250	b	0.255	0.250	b	0.199
AAC	0.3125	0.206	b	0.234	0.231	b	0.196
AAC	0.0625	0.101	b	0.197		b	0.190

CASE 8 Aspect ratio $L/H = 0.5$ L = 5.6 m H = 11.2 m
Free along top, simply supported remaining three sides

Material	μ	x	Mode of Failure	Yield Line kN/m²	Code kN/m²	Mode of Failure	FEA Model kN/m²
	1.00	0.375	d	0.510	0.509	d	0.403
Calc. sil.	0.333	0.229	d	0.451	0.456	d	0.385
Calc. sil.	0.267	0.209	d	0.444		d	0.380
Calc. sil.	0.167	0.168	d	0.430		d	0.380
Calc. sil.	0.056	0.073	d	0.410		d	0.380
AAC	1.00	0.375	d	0.227		d	0.179
AAC	0.625	0.305	d	0.213	0.215	d	0.179
AAC	0.50	0.276	d	0.209	0.210	d	0.179
AAC	0.3125	0.223	d	0.200	0.201	d	0.170
AAC	0.0625	0.104	d	0.183		d	0.170

CASE 9 Aspect ratio $L/H = 0.5$ L = 5.6 m H = 11.2 m
Free along one side, simply supported along remaining three edges

Material	μ	x	Mode of Failure	Yield Line kN/m²	Code kN/m²	Mode of Failure	FEA Model kN/m²
	1.00	0.360	f	0.264	0.264	f	0.225
Calc. sil.	0.333	0.237	f	0.133	0.132	f	0.160
Calc. sil.	0.267	0.219	f	0.117		f	0.147
Calc. sil.	0.167	0.180	f	0.090		f	0.125
Calc. sil.	0.056	0.082	f	0.049		f	0.102
AAC	1.00	0.360	f	0.117		f	0.099
AAC	0.625	0.305	f	0.087	0.087	f	0.091
AAC	0.50	0.280	f	0.076	0.076	f	0.084
AAC	0.3125	0.232	f	0.057	0.057	f	0.069
AAC	0.0625	0.115	f	0.023		f	0.046

Note: (1) Code values extrapolated.

Table 6.6 Analytical Lateral Load Capacity of Panels with Openings

Case No.	Support Condition	Ortho. Ratio μ	Normalised Flexural strength		
			Yield Line	FEA	$(A_n/A_g)^2$
1	a	1.00	0.616	0.557	0.563
		0.33	0.572	0.586	0.563
	b	1.00	0.644	0.595	0.563
		0.33	0.561	0.509	0.563
	c	1.00	0.566	0.520	0.563
		0.33	0.565	0.540	0.563
2	a	1.00	0.690	0.667	0.563
		0.33	0.912	0.734	0.563
	b	1.00	0.681	0.642	0.563
		0.33	0.708	0.472	0.563
3	a	1.00	0.692	0.554	0.563
		0.33	0.728	0.633	0.563
	b	1.00	0.894	0.711	0.563
		0.22	0.767	0.586	0.563
4	a	1.00	0.928	0.742	0.879
		0.33	0.877	0.637	0.879
	b	1.00	0.823	0.776	0.879
		0.33	0.966	0.725	0.879
5	c	1.00	0.703	0.545	0.563
		0.33	0.596	0.564	0.563
6	c	1.00	0.835	0.836	-
		0.33	0.728	0.709	-
7	b	1.00	0.380	0.472	0.563
		0.33	0.527	0.557	0.563
8	b	1.00	0.491	0.647	-
		0.33	0.668	0.617	-

Note: (a) Simply support all edges
(b) Top free simply supported other three sides
(c) One side free simply supported other three sides
A_g Gross area of panel
A_n Net area of panel = Gross area - opening area

Table 6.7 Comparison of Experimental and Analytical Panel Failure Load in terms of Normalised Flexural Strength against Solid Panels

Panel No.	Expt. Failure Pressure	Y. Line	FEA model Prediction				$(A_n/A_g)^2$
			exc. Window Frame		inc. Window Frame		
			(a)	(b)	(a)	(b)	
SB01	1.00	1.00	1.00	1.00	1.00	1.00	1.00
SB02	0.86	0.82	0.74	0.74	0.87	0.87	0.67
SB03	0.82	0.77	0.65	0.70	0.78	0.82	0.79
SB04	0.79	0.82	0.73	0.76	0.78	0.82	0.75
SB05	0.96	1.00	1.00	1.00	1.00	1.00	1.00
SB06	1.00	1.00	1.00	1.00	1.00	1.00	1.00
SB07	0.73	0.80	0.77	0.67	0.85	0.73	0.78
SB09	0.86	0.85	0.84	0.83	0.91	0.90	0.89
CB01	1.00	1.00	1.00	1.00	1.00	1.00	1.00
CB02	0.66	0.82	0.67	0.66	0.69	0.68	0.67
DC01	1.00	1.00	1.00	1.00	1.00	1.00	1.00
DC02	0.66	0.70	0.59	0.67	0.71	0.72	0.67
DC02B	0.57	0.61	0.49	0.50	0.58	0.58	-

(a) predictions using wallette strengths
(b) predictions using joint strengths

Figure 6.1 FEA Model Predicted Behaviour of Walls Supported on All Four Sides, H = 2.8 m.

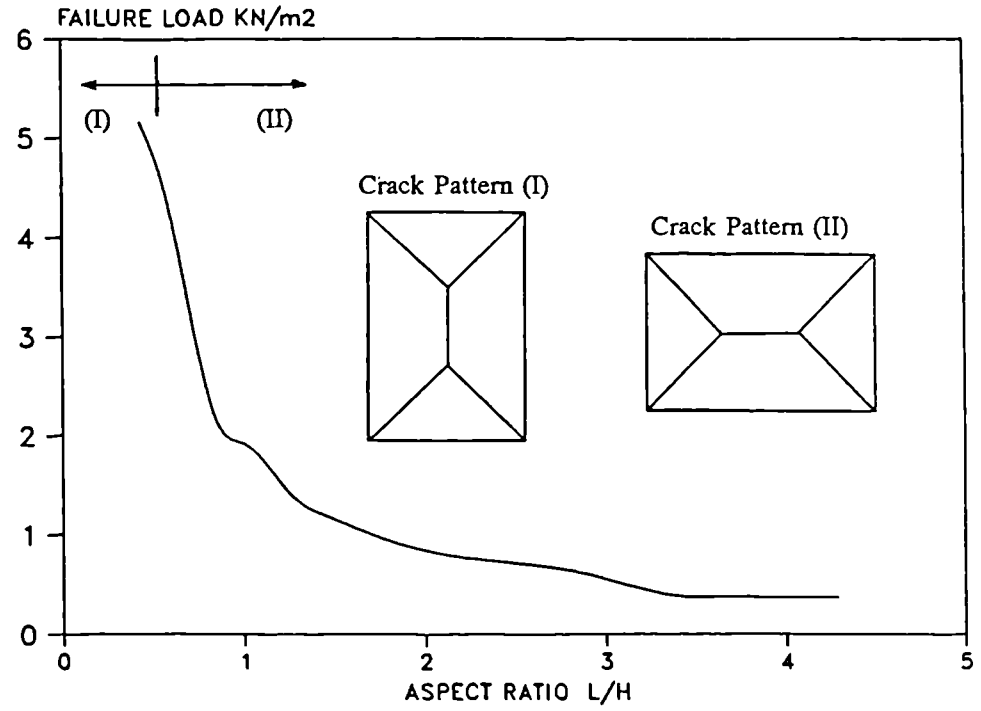

Figure 6.2 FEA Model Predicted Behaviour of Walls Supported on Three Sides with the Top Edge Free, H = 2.8 m.

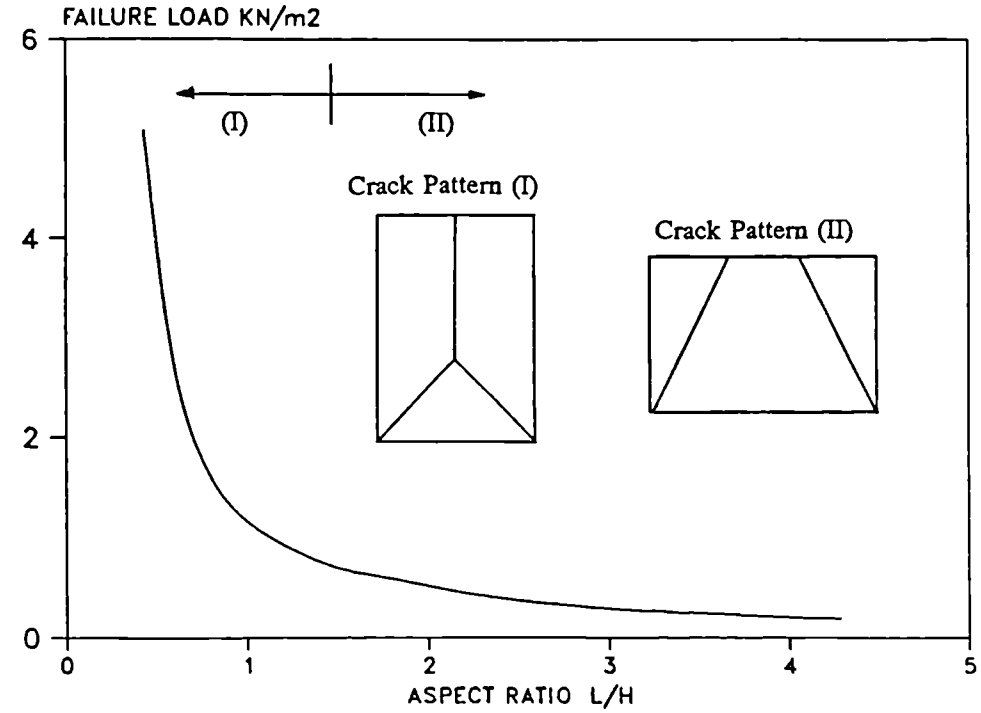

Figure 6.3 Panel Failure Capacity Prediction using Available Design Methods, Three Sides Simply supported and the Top Edge Free.

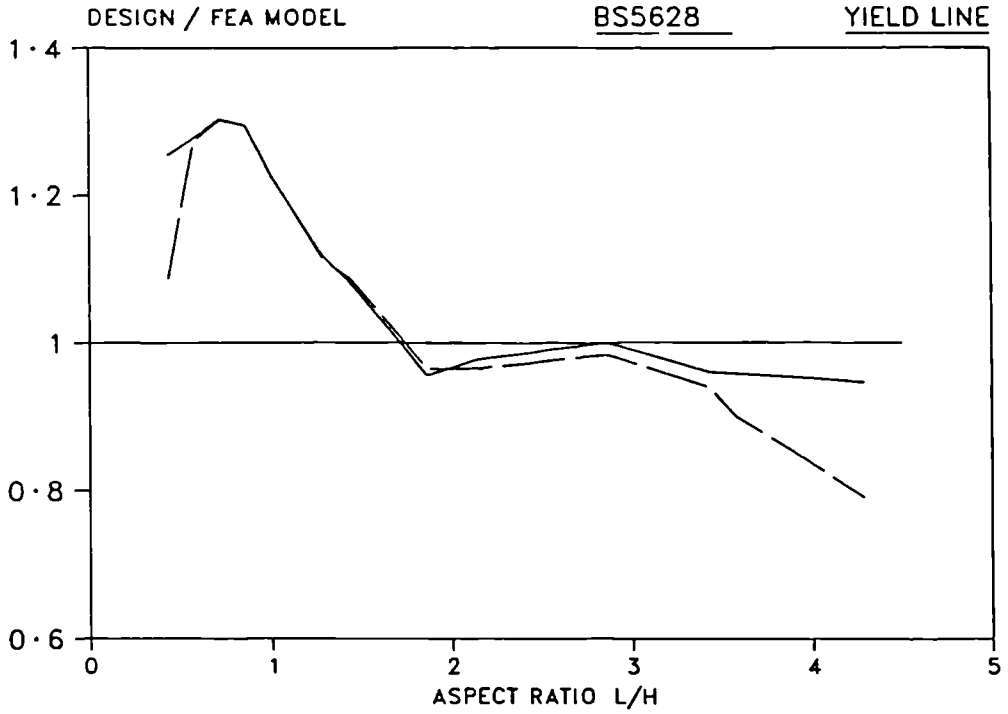

Figure 6.4 Panel Failure Capacity Prediction using Available Design Methods, All Four Edges Simply supported.

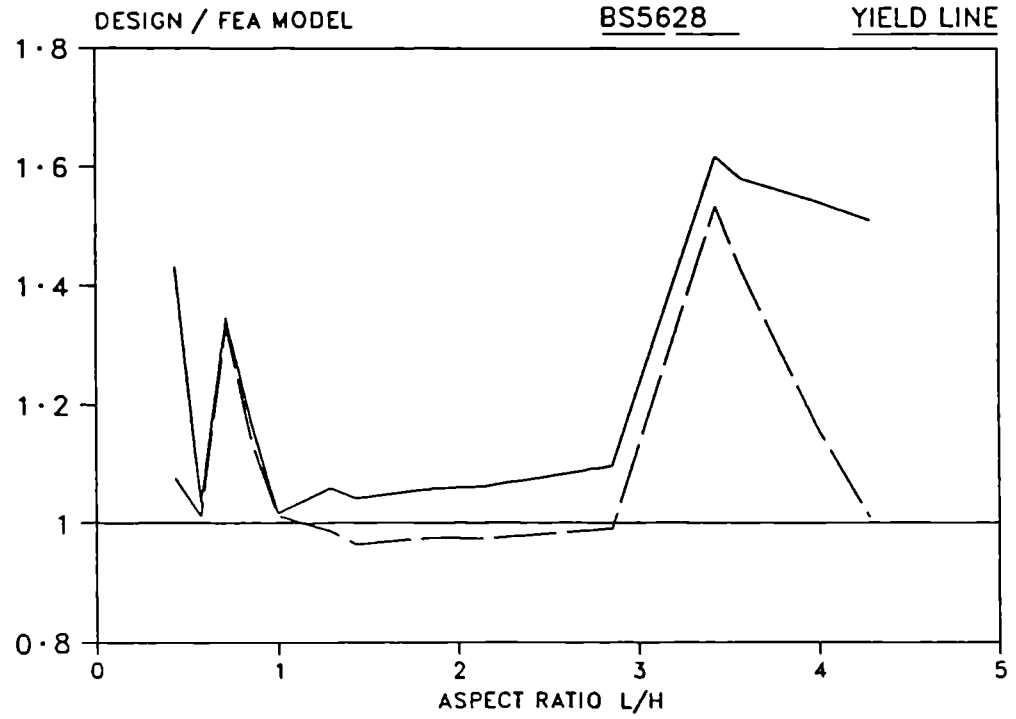

Figure 6.5 Failure Modes

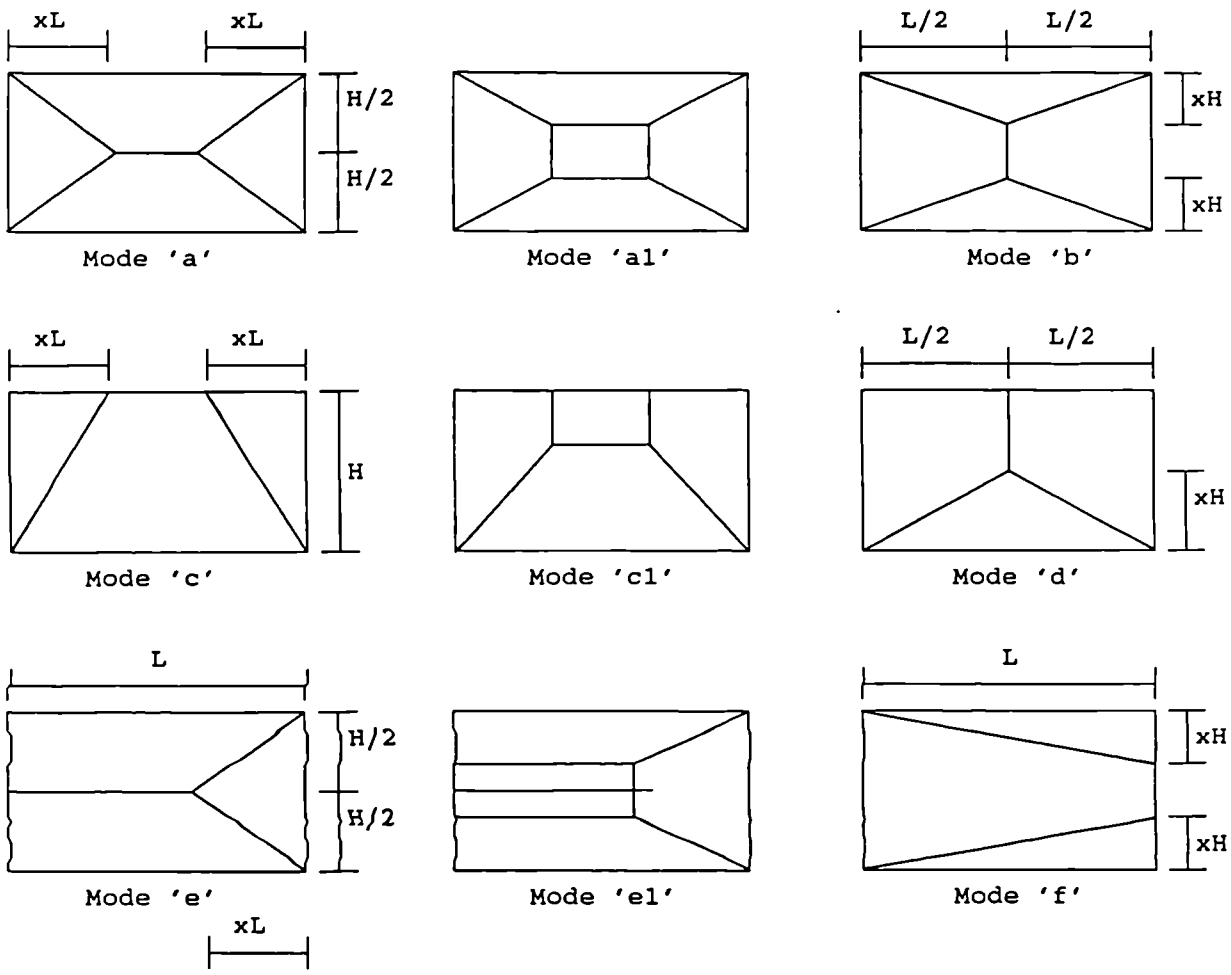

Figure 6.6 Comparison of Yield Line Prediction with the FEA Model, Three Sides Simply supported and the Top Edge Free.

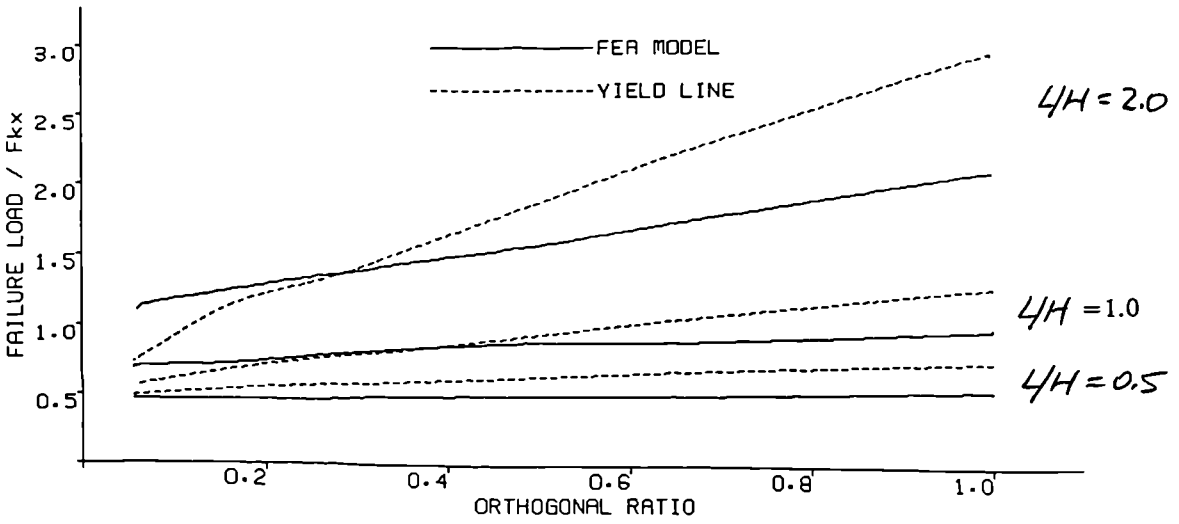

Figure 6.7 Comparison of Yield Line Prediction with the FEA Model, All Four Edges Simply supported.

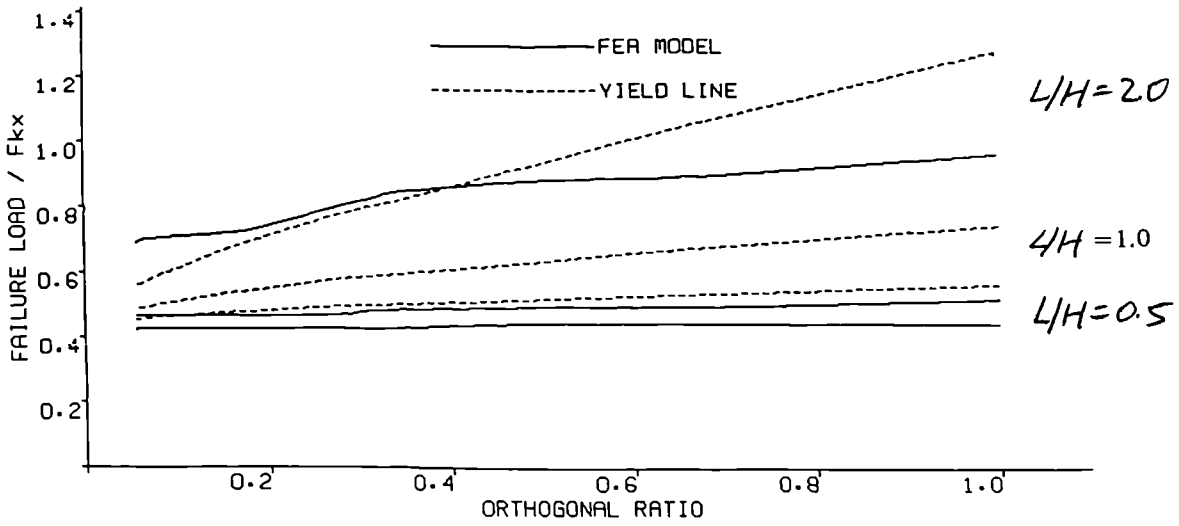

Figure 6.8 Comparison of Yield Line Prediction with the FEA Model, Three Sides Simply supported and One Side Edge Free.

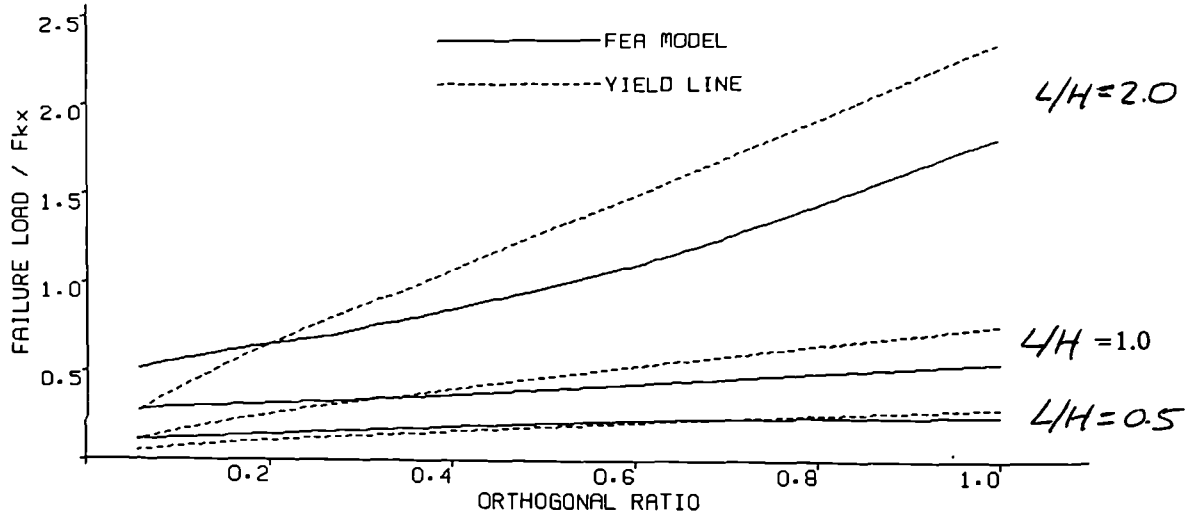

Figure 6.9 Parametric Survey for the Lateral Load Capacity of Panels with Openings

Case 1 - Single central opening

It was assumed that the loading on the opening was distributed at 45° and then taken as uniformly distributed load along the edge of the opening.

Panel dimensions = 5.6m x 2.8m
Opening dimensions = 2.8m x 1.4m

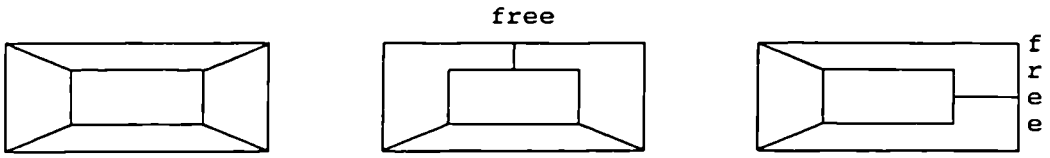

Mode 'a' Mode 'b' Mode 'c'

Case 2 - Single opening centrally positioned along top edge

Loading from opening - method as case 1 used

Panel dimensions = 5.6m x 2.8m
Opening dimensions = 2.8m x 1.4m

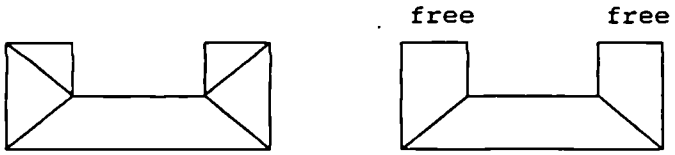

Mode 'a' Mode 'b'

Case 3 - Large corner opening

Loading from opening - method as case 1 used

Panel dimensions = 5.6m x 2.8m
Opening dimensions = 2.8m x 1.4m

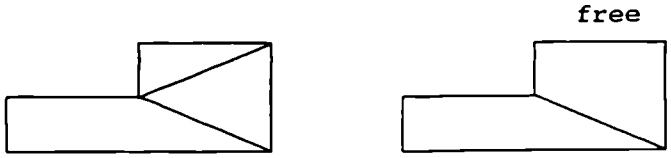

Mode 'a' Mode 'b'

Case 4 - Small corner opening

Loading from opening - method as case 1 used

Panel dimensions = 5.6m x 2.8m
Opening dimensions = 1.4m x 0.7m

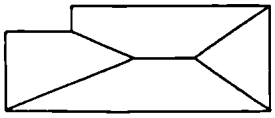

Mode 'a'

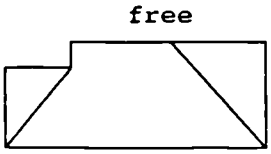

Mode 'b'

Case 5 - Side opening

Half loading from glazing taken as line loading along edge of masonry.

Panel dimensions = 5.6m x 2.8m
Opening dimensions = 1.4m x 2.8m

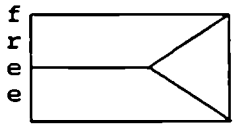

Case 6 - C shaped wall

Same as Case 5 but no opening therefore no loading from glazing.

Panel dimensions = 4.2m x 2.8m

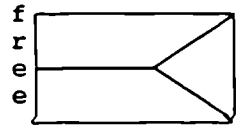

Case 7 - Top opening

Loading from opening equally divided by top support and along bottom of opening on wall.

Panel dimensions = 5.6m x 2.8m
Opening dimensions = 5.6m x 0.7m

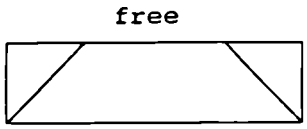

Case 8 - U shaped wall

As Case 7 but no opening.

Panel dimensions = 5.6m x 2.1

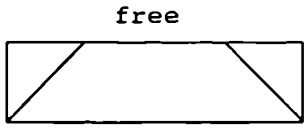

Figure 6.10 Failure Load Predictions for Panels with Openings

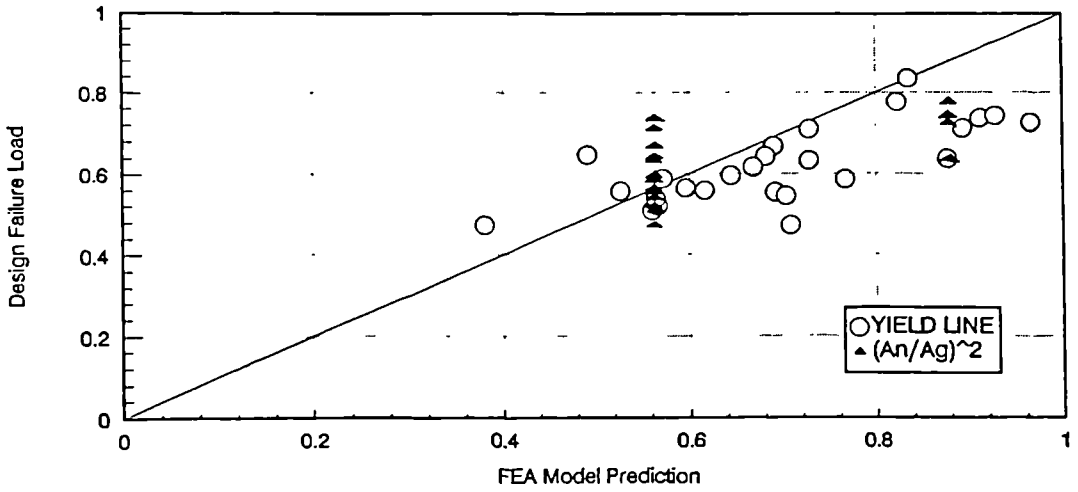

Figure 6.11 Analytical Failure Load Vs Experimental Failure Load, Panels with Openings

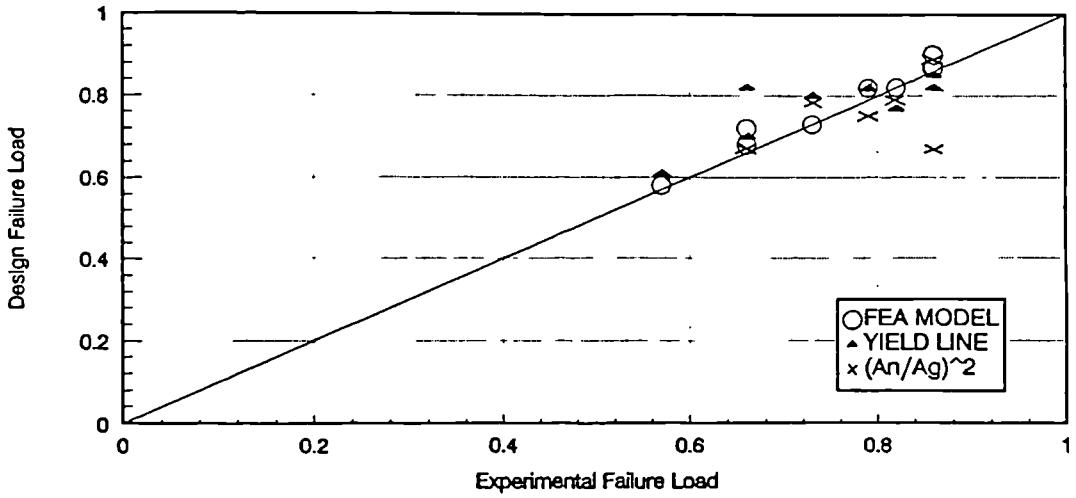

7.0 CONCLUSIONS AND PROPOSALS FOR FUTURE RESEARCH

7.1 Conclusions

Based on the experimental and the theoretical investigations carried out in the present studies, the following conclusions were made;

1. Docking of bricks with high initial rate of suction was found to significantly increase the flexural strength and the consistency of the resulting brickwork.
2. Where the horizontal flexural strength was determined by brick strength, a higher and more consistent horizontal flexural wallette strength was observed by increasing the number of courses in the wallettes from four to six.
3. The measured Brench (Bond Wrench) strength was 1.33 times the wallette strength.
4. The presence of precompression during the initial setting and the subsequent curing period of the brickwork, improved the bonding at the unit/mortar interface and resulted in higher bed joint strengths.
5. A Monte-Carlo analysis was successfully used to account for the effect of specimen format to determine a more representative bed joint strength. Estimation of single joint strength was obtained by the analysis and by using order statistics.
6. A non-linear finite element analysis was successfully applied to study and predict the flexural strength of masonry panels.
7. The prediction from the finite element analysis when using the mean joint strength obtained was in good agreement with the experimental results.

8. The wallette strengths were found to provide a conservative representation of the true strength of masonry.

9. A rational analysis of the lateral behaviour of masonry panels was obtained by using the finite element method in conjunction with the variation of flexural strength and the Monte-Carlo simulation. The results of this analysis were in good agreement with the experimental results when bed joint strength obtained from precompressed specimens was used.

10. The effect of material variability on the variation of wall strength was found to be small for masonry panels with three or more edges supported . A 10% to 20% material variation resulted in only 3% to 4% variation of flexural strength in the resulting panels.

11. The variation of wall strength caused by material variability was found to be marginally higher in solid panels than that of panels with openings.

12. The flexural strength of brickwork incorporating the selected d.p.c. appeared to be similar to that of the brickwork with no d.p.c. However, more work is required to determine the flexural strength of brickwork with a d.p.c.

13. The experimental results of the flexural strength of panels with two 1.0 m returns at each end were comparable to the results obtained analytically in which it was assumed both ends were rotationally restrained.

14. A flexible support greatly reduced the flexural stiffness and strength of masonry panels and the effect was more significant for panels with openings.

15. The flexural strength of panels supported on all sides was similar to the case of panels of double the height with three sides supported and the top edge free.

16. The failure strength of cavity panels with two nominal identical leaves was found to be equal to the sum of the strengths of the individual leaves. In the case of panels with a window frame built into one leaf, the strength of the cavity panels was approximately twice the strength of the weaker leaf.

17. For panels with openings, the window frame and the chipboard infill was found to increase the flexural strength of the panels by up to 19%.

18. Openings of area less than 10% of the panel area was found to reduce the flexural strength of the panel by up to 25%.

19. In general, the flexural strength of panels with openings was found to be directly proportional to the square of the net area divided by the gross area of the panels.

20. For panels with three sides simply supported and the top edge free, the yield line method provided very similar predictions to that of the finite element analysis for range of H/L ratios between 0.23 and 0.66 and with orthogonal strength ratios between 0.15 and 0.4.

21. The yield line approach, which forms the basis of BS5628, tended to overestimate the flexural strength of masonry panels as H/L increased, especially for panels with fixed edges. However, it provided reasonably good predictions for panels with openings in terms of normalised flexural strength. This indicated that there was a basis for using yield line method for the design of masonry panels with openings even though there was no justification for the use of such a theory in the analysis of masonry.

7.2 Proposals for Future Research

As discussed, in Chapter 2, non-linear structural analysis, using the finite element method, can be satisfactorily applied to a variety of structural materials. However, unless the fundamental properties of the materials are known, the accuracy of any method of analysis may be in doubt.

The ideal way of modelling the composite behaviour of masonry panel requires data on the individual elements of brick and mortar in conjunction with the failure criteria for brick, mortar, and the interface in a three dimensions system. In this respect, the constitutive models of the individual material properties need to be defined accurately by experimental and theoretical investigations.

In relation to lateral loaded masonry walls, more work is required to firstly establish:-

1. A stress-strain relationship of masonry prior to failure.
2. A cracking and failure criterion representing the cracking and ultimate strength of masonry under lateral loading.
3. The effect of precompression on the cracking and failure criterion.
4. A post failure stress-strain relationship to account for any change of behaviour.
5. A crack model to define direction and propagation of cracks.

REFERENCES

1. TAPP, A. "An investigate of laterally loaded fenestrated masonry panels". M.Phil Transfer Report, Department of Civil and Structure Engineering, Polytechnic South West, Plymouth, 1985.

2. WEST, H.W.H., HODGKINSON, H.R., HASELTINE, B.A. and DE VEKEY, R.C. "Research results on brickwork and aggregate blockwork since 1977". The Structural Engineer, Vol. 64A, No. 11, Nov. 1986.

3. LOVEGROVE, R. and DE VEKEY, R.C. "The effect of specimen format on the flexural strength of wallettes". Pro. British Masonry Society, NO. 1, pp. 7-9, Nov 1986.

4. LAWRENCE, S.J. "Flexural strength of brickwork normal to and parallel to the bed joints". J. Australia Ceramic Society, Vol. 11, No. 1, May 1975.

5. British Standards Inst. "Code of Practice for Structural used of Masonry". CP 111, London, 1948.

6. British Standards Inst. "Code of practice for structural used of masonry". CP 111, London, 1964.

7. British Standards Inst. "Code of practice for structural used of masonry, part 1". CP 111; Part 1, London, 1970.

8. British Standards Inst. "British standard code of practice for the use of masonry, Part 1. Structural use of unreinforced masonry". BS5628; Part 1, London, 1978.

9. BAKER, L.R., GAIRNS, D.A., LAWRENCE, S.J. and SCRIVENER, J.C. "Flexural behaviour of masonry panels - a State of the Art". Proc. 7th IBMAC, Melbourne, *Australia, pp. 27 -55, Feb. 1985.*

10. MAY, I.M. and MA, S.Y.A. "Design of masonry panels under lateral load". Proc. Brit. Mas. Soc., 1st Int. Mas. Conf., pp. 118-120, Dec. 1986.

11. British Standards Inst. "British standard code of practice for structural used of masonry, part 3. Materials and components, design and workmanship". BS5628; Part 3, London, 1985.

12. "Design guide for laterally loaded masonry walls". Directorate of Civil Engineering Services, Department of Environment, Property Services Agency, 1986.

13. TELLETT, J "Pocket-type reinforced brickwork retaining walls", Ph.D. Thesis, University of Bradford, April, 1984.

14. TAPP, A. and SOUTHCOMBE, C. "An investigation of laterally loaded brickwork panels with openings". Technical Report, Polytechnic South West, Plymouth, 1988.

15. BAKER, L.R. "The lateral strength of brickwork - an overview". Proc. Brit. Ceram. Soc., P27, Dec. 1978.

16. BAKER, L.R. and FRANKEN, G.L. "Variability aspects of the flexural strength of brickwork". Proc. 4th IBMAC, Brugge, April 1976.

17. ANDERSON, C. " Test on transverse laterally loaded walls". South Bank Polytechnic, Jan. 1985.

18. CAJDERT, A. "A Lateral Loaded Masonry Walls". Division of Concrete Structures, Publication 50:5, Chalmers University of Technology, 1980.

19. WEST, H.W.H., HODGKINSON, H.R. and HASELTINE, B.A. "The resistance of brickwork to lateral loading, part 1; Experimental methods and results of tests on small specimens and full sized walls". The Structural Engineer, Vol. 55, page 411, Oct. 1977.

20. LAWRENCE, S.J. "Full-scale tests of brickwork panels under simulated wind load". Proc. 5th IBMAC, Washington, 1979.

21. WEST, H.W.H. "The flexural strength of clay masonry determined from wallette specimens". Proc. 4th IBMAC, Brugge, paper, April 1976.

22. WEST, H.W.H. "The flexural strength of clay masonry". Proc. British Masonry, paper 4.a.6., Nov. 1986.

23. KAMPH, H. "Factors affecting bond of mortar to brick". Proc. Am. Soc. Test. Mortar. Symposium on Masonry Testing, P127, 1963.

24. PALMER, L.A. and PARSONS, D.A. "A study of the properties of mortars and bricks and their relation to bond". U.S. Dept. of Commerce Bureau of Standards. Res. Paper. RP 683, Bur. J. Stand. Res. v12, May 1934.

25. DE VEKEY, R.C. and WEST, H.W.H. "The Flexural Strength of Concrete Blockwork". Magazine of Concrete Research, Vol. 32, No. 113, Dec 1980, PP. 206-218.

26. ALAN, H. and YORKDALE, P.E. " Structure research and investigation for the development of a rational engineering design standard for hollow brick masonry". Proc. British Masonry Conference, Paper 4.d.4, Nov. 1986.

27. GAIRNS,D., FRIED, A. and ANDERSON, C. "Determination of the flexural resistance of masonry - A study comparing experimental and theoretical techniques". Technical Report, South Bank Polytechnic, Structural Research Unit,

1986.

28. GAIRNS, D., ANDERSON, C. and FRIED, A. "Preparation and curing of masonry specimens for structural testing". Masonry Int. Journal of British Masonry Society, page 25, spring, 1987.

29. WEST, H.W.H., HODGKINSON, H.R. and GOODWIN, J.F. " The resistance to lateral loads of walls built of calcium silicate bricks". Proc. 5th IBMAC, Washington, pp. 302 -313, 1979.

30. EDGELL, G.J. "Factors Affecting the Flexural Strength of Brick Masonry". Masonry International, Vol. 1, No. 1, PP. 16-24, 1987.

31. WEST, H.W.H. "The Influence of Time Docking and Draining on the Properties of Bricks and Brickwork Specimens". Proc. 6th IBMAC, Rome, PP, 283-289, May 1982.

32. GAIRNS, D.A. and SCRIVENER, J.C. "The effect of masonry unit characteristics on panel lateral capacity". Proc. 8th IBMAC, Dublin, pp. 230-239, Sept. 1988

33. GRIMM, C.T. and TUCKER, R.L. "Flexural strength of masonry prisms versus wall panels". Journal of Structural Engineer, Vol. 111, No. 9, Page 2021, Sept. 1985.

34. ANDERSON, C. "Lateral strength from full sized tests related to the flexural properties of masonry". Masonry Int., Vol. 1, No. 2, pp. 51-55, 1987.

35. FRIED, A., ANDERSON, C. and SMITH, D. "Predicting the transverse lateral strength of masonry walls", Proc. 8th IBMAC, Dublin, pp. 1171-1183, Sept. 1988.

36. LAWRENCE, S.J. "The Flexural Behaviour of Brickwork". Proc. of the North American Masonry Conference, University of Colorado, Boulder, Colorado, August 1978.

37. KNOTSSON, H.H. "Carrying capacity of masonry". Proc. 8th IBMAC, Dublin, PP. 350-361, Sept. 1988.

38. GAIRNS, D.A. and SCRIVENER, J.C. "Lateral load capacity of concrete masonry panels, part 1; Flexural properties of concrete masonry". Masonry Int., pp. 23-32, Nov. 1984.

39. BAKER, L.R. "Some factors affecting the bond strength of brickwork". Proc. 5th IBMAC, Washington D.C., PP. 84-89, 1979.

40. POLYAKOV, S.V. "Masonry in frame buildings". Gosundarst-vennoe izdatel'stvo Literatury po stroitel'stvu: arkhitekture. Moscow, 1956.

41. HAMID, M.H., YAGI, O.I. and AWAD, M.E. "Mortar from indigenous materials". Masonry Int. No. 7, P25, March 1986.

42. MATTHYS, J.H. "Brick masonry flexural bond strength using conventional masonry mortars". 5th Canadian Masonry Symposium, PP. 745-756, June 1989.

43. MATTHYS, J.H. "Flexural strengths of portland cement lime and masonry unit mortar". 5th Canadian Masonry Symposium, pp. 284-291, June 1989.

44. WEST, H.W.H., EVERILL, J.B. and BEECH, D.G. "Testing of bricks and blocks for loadbearing brickwork". Trans. Xth Int. Ceramic Congress, Gothenburg, Swedish Institute for Silicate Research, p559, 1966.

45. EDGAR, J. "The binding between mortar and brick". Proc. 8th IBMAC, Dublin, pp. 182-193, Sept. 1988.

46. GHOSH, S.K. "Flexural bond strength of masonry". 5th Can. Mas. Symp., pp. 735-744, University of British Columbia, Vancouver, June 1989.

47. LAWRENCE, S.J. and CAO, H.T. "Microstructure of the interface between brick and mortar". Proc. 8th IBMAC, Dublin, pp. 194-203, Sept 1988.

48. SCHUBERT, I.P. "The influence of mortar on the strength of masonry". Proc. 8th IBMAC, Dublin, pp. 162-173, Sept. 1988.

49. ANDERSON, C. and HELD, L.C. "The effect of sand grading on mortar properties and the tensile bond of brickwork". Proc. 4th IBMAC, pp. 1-6, 1976.

50. MATTHYS, J.H. and GRIMM, C.T. "Flexural strength of non-reinforced brick masonry". Proc. 5th IBMAC, Washington, P114, 1979.

51. ARORA, S.K. and HODGKINSON, H.R. "Durability of brickwork change in flexural strength with time". Proc. 4th IBMAC, PP. 10-12, 1976.

52. HODGKINSON, H.R., HASELTINE, B.A. and WEST, H.W.H. "Insitu test on 10-year old building". Proc. Brit. Ceram. Soc., P177, 1982.

53. ISBERNER, A.W. "Properties of masonry cement mortars - Designing engineering and construction with masonry products". Gulf publicising company, Houston Texas, 1969.

54. ANDERSON, C. "Some observation on masonry wallette testing". Int. J. Mas. Constr., vol. 2, pp. 140-154, 1982.

55. SCRIVENER, J.C. and GAIRNS, D.A. "Curing and the modulus of rupture of concrete masonry". Masonry Int. No. 7, P8, 1986.

56. JAMES, J.A. "Investigation of the effect of workmanship and curing conditions on the strength of brickwork". Proc. 3rd IBMAC, Essex, P192, 1973.

57. MARQUIS, E.L. and BORCHELT, G. "Bond strength comparison of laboratory and field tests". Proc. 4th Can. Mas. Symp. Federation, P94, 1986.

58. GARRITY, S.W. and PHIPPS, M.E."A Study of the effect of vertical prestress on the horizontal flexural strength on clay brickwork". Proc. of the 4th North American Masonry Conference, University of California, Los Angeles, California, August 1987.

59. MORTON, J. and HENDRY, A.W. "A Theoretical Investigation of the Lateral Strength of Brick Walls with Precompression". Pro. British Ceramic Society, Vol. 21, April 1973, PP. 181-194.

60. PAYNE, D.C. and BROOKS, D.S. "The Flexural Stiffness of Brickwork Panels Subjected to Vertical and Lateral Loads". Proc. 6th IBMAC, Rome, May 1982.

61. ANDERSON, C. "Lateral tests on cavity walls for the Property Services Agency, phases 1 - 6". Technical report, South Bank Polytechnic, Sept. 1986.

62. MOORE, J.F.A., HASELTINE, B.A. and HODGKINSON, H.R. "Edge restraint provided by continuity of panel walls". Proc. 5th IBMAC, Washington, PP. 478-481, 1979.

63. ANDERSON, C. "Arching action in transverse laterally loaded masonry wall panels". Structure Engineer, Vol. 62B(1), P12-23, 1984.

64. BAKER, L.R. "Precracking behaviour of laterally loaded brickwork panels with in plane restraints". Proc. Brit. Ceram. Soc., P129, Dec. 1978.

65. COLVILE, J. and RAMSEUR, R. "The interaction of masonry wall panels and a steel frame". Proc. North American Mas. Conf., Paper 15, Aug. 1978.

66. HODGKINSON, H.R., HASELTINE, B.A. and WEST, H.W.H. "Preliminary tests on the effect of arching in laterally loaded walls". Paper 4.a.5, Proc. Brit. Mas. Soc., Nov. 1986.

67. MCDOWEL, E.L., MCKEE, K.E. and SEVIN "Arching theory of masonry walls". Journal of Structural Div. Proc. A.S.C.E. Paper 915, ST2, 1956.

68. HUMMEL, A. "Research on mortar for free standing chimneys". Commentary on research of T.H. Aachen IfB, 1952-53.

69. ROYEN, N. "Design of masonry walls accounting for friction and bond". Hafet 9, Byggmactaren, Stockholm, 1936.

70. RYDER, G.H. "Strength of materials". MacMillan Press, London, 1969.

71. BAKER, L.R. "Failure criterion for brickwork in biaxial bending". Proc. 5th IBMAC, Washington, pp. 71-78, 1979.

72. BAKER, L.R., PADHYE, P.Y. and SCHULZE, P.H. "Torsional resistance from friction between overlapping masonry units". Int. Joun. of Mas. Const. Vol 1, No 2, 1980.

73. GARRITR, S.W. and PHIPPS, M.E. "An experimental study of the influence of vertical prestress on the horizontal flexural strength of clay brickwork" Proc. 8th IBMAC, Dublin, pp. 642-652, Sept. 1988.

74. BAKER, L.R. "The failure criterion of brickwork in vertical flexure". Proc. Brit. Ceram. Soc., pp. 203-216, Dec. 1978.

75. SAMARASINGHE, W., PAGE, A. W. and HENDRY A. W. "A finite element model for the inplane behaviour of brickwork" Proc. Inst. Civ. Engrs. Part 2, vol 73, March 1983".

76. BAKER, L.R. "A principal stress failure criterion for brickwork in biaxial bending". Proc. 5th IBMAC, Washington, 1979.

77. MAY, I.M. and MA, S.Y.A. "A complete biaxial stress failure criterion for brick masonry". Proc. Brit. Mas. Soc., 1st Int. Mas. Conf., pp. 115-117, Dec. 1986.

78. LAWRENCE, S.J. and CAO, H.T. "Cracking of non-loadbearing masonry under lateral forces". Proc. 8th IBMAC, Dublin, pp. 1184-1194, Sept. 1988.

79. TIMOSHENKO, S.P. and FRIEGET, W. "Theory of Plates and Shells". 2nd edition, Mc Graw-Hill Book, New York, 1959.

80. SINHA, B.P. "A simplified ultimate load analysis of laterally loaded model orthotropic brickwork panels of low tensile strength". The Structure Engineer, Vol. 4, pp. 81-84, Dec. 1978.

81. BAKER, L.R. "Lateral loading of masonry panels". Structure design of masonry, Cement and Concrete Association of Australia, Sydney, Feb. 1980.

82. ESSAWY, A.S., DRYSDALE, R.G. and MIRZA, F.A. " Non linear microscopic finite element model for masonry walls". Proc. of New Analysis Techniques for Structural Masonry, ASCE Structures Congress' 85". pp. 19-45, Chicago, Illinois, Sept. 1985.

83. BAKER, L.R. "An elastic stress theory for brickwork panels in flexure". 6th IBMAC, Rome, May 1982.

84. SEWARD, D.W. "A developed elastic analysis of lightly loaded brickwork with lateral loading". Int. J. of Aus. Constr., Vol. 2, No. 3, 1982.

85. HENRY, A.W. "The lateral strength of unreinforced Brickwork". The Structure Engineer, Vol. 51, No. 2, pp. 422-433, Feb. 1973.

86. BRINKER, R. "Yieldline theory and material properties of lateral loaded masonry panels". Masonry. Int. No. 1, April 1984.

87. LOVEGROVE, R. "A discussion of 'yieldlines' in unreinforced masonry". The Structural Engineer, Vol. 66, No. 22, 15 Nov. 1988.

88. LOVEGROVE, R. "Correspondence - A discussion of 'yieldlines' in unreinforced masonry". The Structural Engineer, Vol. 67, No. 8, 18 April 1989.

89. CHONG, V.L. ,MAY, I.M and SOUTHCOMBE, C. "A non-linear finite element program for the analysis of unreinforced masonry structure". Technical Report, Polytechnic South West, Sept. 1990.

90. PAGE, A.W. "A non-linear analysis of the composite action of masonry wall on beams". Proc. Instn. Civil Eng. Part 2, vol. 67 March 1979.

91. PAGE, A.W. "The biaxial compressive strength of brick masonry". Proc. Inst. Civ. Engrs., Part 2, 893-906, Sept. 1981.

92. MOFFATT, K.R. and LIM, P.T.K. "Finite element analysis of composite box girder bridges having complete or incomplete interaction". Proc. Inst. Civil Eng. Part 2, Vol. 61, pp. 1-22, March 1976.

93. CRISFIELD. M.A. "A fast incremental/iteration solution procedure that handles 'Snap-Through'". Computing of Structures, vol. 13, pp. 55-62. 1981.

94. COPE, R.J. and CLARK, L.A. "Concrete slab analysis and design". Elsevier Applied Science Publishers, London and New York, 1984.

95. British Standards Inst. "Building sand from natural sources". BS 1199 and 1200, London, 1976.

96. British Standards Inst. "British standard specification for clay bricks". BS 3921, London, 1985.

97. British Standards Inst. "Methods of testing mortars, screeds plasters". BS 4551, London, 1980.

98. British Standards Inst. "British standard specification for building lime". BS 890, London, 1972.

99. British Standards Inst. "Methods for determination of particle size distribution". BS 812; Part 3, 1985, London, 1985.

100. British Standards Inst. "Methods for determination of physical properties". BS 812; Part 2, 1975, London, 1975.

101. BRE Digest. "Testing bond strength of masonry". Concise reviews of building technology, Digest 360, April 1991.

102. SAA Masonry Code AS 3700-1988 Masonry in buildings, Appendix A7, Flexural strength by bond wrench. Standards Association of Australia. Sydney N.S.W. 1988.

103. ANDERSON, C. "Some observation on masonry wallette testing". Int. Jour. Mas. Constr., Vol. 2, pp. 140-154, 1982.

104. LAWRENCE, S.J. "Behaviour of brick masonry walls under lateral loading". Ph.D. Thesis, School of Civil Engineering, University of New South Wales, Nov 1983.

105. MOSTELLER, F. and ROURKE, R.E.K. "Sturdy statistics, nonparametrics and order statistics, Appendix 7". Addison-Weslley, Reading, Massachusetts, 1973.

106. RUBINSTEIN, R.Y. "Simulation and the Monte-Carlo method". John Wiley, 1981.

107. MAY, I.M. "Desk top study into the lateral strength of walls with openings and the sensitivity of the BS 5628 design method". Department of Civil Engineering, University of Bradford, April 1989.

108. PRAGER, W. and HODGE, P.G. " Theory of perfectly plastic solids". Wiley.

109. WOOD, R.H., "Plastic and Elastic Design of Slabs and Plates". London, Thames & Hudson, 1961.

110. Hillerborg, A. "A plastic theory the design of reinforced concrete slabs". Prel. Publications, 6th Congr. Int. Ass. Bri. Struct. Eng., Stockholm, 1960.

111. JONES, L.L. AND WOOD, R.H., "Yield-Line Analysis of Slabs". London, Thames & Hudson, Chatto & Windus, 1967.

112. LAWRENCE, S.J and LU, J.P. " An Investigation of laterally loaded masonry walls with openings". Computer Methods in Structure Masonry, Eds. Middleton, J. and Pander, G.N, Books and journals Int. Ldt., pp. 39-48, April 1991.

APPENDIX A - BRICK PROPERTIES

A.1 CLASS A ENGINEERING BRICKS

BRICK DIMENSIONS

TESTING METHOD: IN ACCORDANCE WITH BS3921, 1985, APPENDIX A
BRICK TYPE: ACCRINGTON 65mm CLASS A PERFORATED

WORK SIZE	OVERALL MEASUREMENT OF 24 BRICKS		
	LIMITS		MEASURED
	MAXIMUM	MINIMUM	
(mm)	(mm)	(mm)	(mm)
215.0	5235	5085	5105
102.5	2505	2415	2455
65.0	1605	1515	1555

BRICK TOTAL WATER ABSORPTION

TESTING METHOD: IN ACCORDANCE WITH BS3921: 1985, APPENDIX E
BRICK TYPE: ACCRINGTON 65mm CLASS A PERFORATED
SAMPLE CONDITION: OVEN DRIED

BRICK NUMBER	DRY MASS (g)	WET MASS (g)	WATER ABSOTPTION (% OF DYR MASS)
1	2982	3037	1.84
2	2939	3063	4.22
3	2950	3055	3.56
4	2938	3041	3.51
5	2952	3038	2.91
6	2938	3102	5.56
7	2940	3092	5.12
8	2961	3044	2.78
9	2964	3076	3.79
10	2942	3051	3.70
		MEAN	3.70
		STANDART DEVIATION	1.09

BRICK INITIAL RATE OF SUCTION

TESTTING METHOD: IN ACCORDANCE WITH BS3921: 1985, APPENDIX H
BRICK TYPE: ACCRINGTON 65mm CLASS A PERFORATED
SAMPLE CONDITION: OVEN DRIED

BRICK NUMBER	DRY MASS (g)	WET MASS (g)	INITIAL RATE OF SUCTION ($Kg/m^2/min$)
1	2945	2950	0.23
2	2932	2937	0.23
3	2936	2945	0.41
4	2944	2949	0.23
5	2929	2932	0.14
6	2955	2966	0.50
7	2939	2947	0.36
8	2931	2935	0.18
9	2956	2961	0.23
10	2943	2947	0.18
		MEAN	0.27
		STANDART DEVIATION	0.12

A.2 CLASS B WESTBRICK

BRICK DIMENSIONS

TESTING METHOD: IN ACCORDANCE WITH BS3921, 1985, APPENDIX A
BRICK TYPE: WESTBRICK 65mm CLASS B FACING 10 HOLES PEFORATED

WORK SIZE	OVERALL MEASUREMENT OF 24 BRICKS		
	LIMITS		MEASURED
	MAXIMUM	MINIMUM	
(mm)	(mm)	(mm)	(mm)
215.0	5235	5085	5180
102.5	2505	2415	2445
65 .0	1605	1515	1580

BRICK TOTAL WATER ABSORPTION

TESTING METHOD: IN ACCORDANCE WITH BS3921: 1985, APPENDIX E
BRICK TYPE: WESTBRICK 65mm CLASS B FACING 10 HOLES PEFORATED
SAMPLE CONDITION: OVEN DRIED

BRICK NUMBER	DRY MASS (g)	WET MASS (g)	WATER ABSOTPTION (% OF DYR MASS)
1	2307.2	2507.2	8.67
2	2284.6	2496.0	9.25
3	2266.3	2479.8	9.42
4	2290.5	2485.6	8.52
5	2260.0	2468.2	9.21
		MEAN	9.01
		STANDART DEVIATION	0.39

BRICK INITIAL RATE OF SUCTION

TESTTING METHOD: IN ACCORDANCE WITH BS3921: 1985, APPENDIX H
BRICK TYPE: WESTBRICK 65mm CLASS B FACING 10 HOLES PEFORATED
SAMPLE CONDITION: OVEN DRIED

BRICK NUMBER	DRY MASS (g)	WET MASS (g)	INITIAL RATE OF SUCTION ($Kg/m^2/min$)
1	2253.3	2294.8	1.91
2	2281.7	2321.0	1.81
3	2310.5	2345.6	1.62
4	2291.3	2331.0	1.83
5	2281.0	2328.9	2.21
		MEAN	1.88
		STANDART DEVIATION	0.21

BRICK INITIAL RATE OF SUCTION

TESTTING METHOD: IN ACCORDANCE WITH BS3921: 1985, APPENDIX H
BRICK TYPE: WESTBRICK 65mm CLASS B FACING 10 HOLES PEFORATED
SAMPLE CONDITION: UNDOCKED

BRICK NUMBER	DRY MASS (g)	WET MASS (g)	INITIAL RATE OF SUCTION ($Kg/m^2/min$)
1	2274.7	2308.0	1.53
2	2255.1	2291.5	1.68
3	2292.7	2327.7	1.61
4	2273.0	2306.5	1.54
5	2297.8	2329.4	1.46
		MEAN	1.56
		STANDART DEVIATION	0.08

BRICK INITIAL RATE OF SUCTION

TESTTING METHOD: IN ACCORDANCE WITH BS3921: 1985, APPENDIX H
BRICK TYPE: WESTBRICK 65mm CLASS B FACING 10 HOLES PEFORATED
SAMPLE CONDITION: DOCKED

BRICK NUMBER	DRY MASS (g)	MASS DOCKED (g)	WET MASS (g)	INITIAL RATE OF SUCTION ($Kg/m^2/min$)
1	2297.1	2328.1	2335.8	0.35
2	2292.7	2323.0	2330.4	0.34
3	2250.2	2286.4	2301.4	0.69
4	2299.3	2336.4	2349.3	0.59
5	2280.6	2317.2	2327.2	0.29
			MEAN	0.45
			STANDART DEVIATION	0.16

APPENDIX B

MORTAR CUBE PROPERTIES

Panel ref.	Mortar Mix	Mortar batch No.	Density (Kg/m^3) Mean of 2 Cubes	Density (Kg/m^3) Mean for panel	Density (Kg/m^3) C.V (%)	Compressive Strength (N/mm^2) Mean of 2 Cubes	Compressive Strength (N/mm^2) Mean for panel	Compressive Strength (N/mm^2) C.V (%)
W01	(ii)	1	2068	2072	0.8	15.5	18.5	9.9
		2	2093			19.0		
		3	2080			17.0		
		4	2082			16.5		
		5	2090			19.5		
		6	2050			19.0		
		7	2086			18.0		
		8	2085			21.5		
		9	2050			19.0		
		10	2060			20.5		
HW01 & HW02	(ii)	1	2011	2020	1.4	25.0	25.5	5.6
		2	2036			26.5		
		3	2005			25.0		
		4	2082			28.0		
		5	2026			24.5		
		6	1996			24.5		
		7	1980			25.0		
		8	2000			24.5		
		9	2039			27.0		
		10	2030			24.0		
HW03 & HW04	(ii)	1	1960	1999	1.2	23.0	26.5	10.7
		2	1990			28.0		
		3	2055			31.0		
		4	1995			31.0		
		5	1985			23.0		
		6	2005			27.5		
		7	2010			25.0		
		8	2000			25.0		
		9	1995			27.5		
		10	1995			26.0		
SB01	(iii)	1	2115	2113	0.4	11.0	11.5	11.9
		2	2120			15.0		
		3	2110			10.5		
		4	2125			12.0		
		5	2105			11.0		
		6	2105			12.0		
		7	2125			11.0		
		8	2115			11.5		
		9	2100			10.5		

Panel ref.	Mortar Mix	Mortar batch No.	Density (Kg/m^3) Mean of 2 Cubes	Density (Kg/m^3) Mean for panel	Density (Kg/m^3) C.V (%)	Compressive Strength (N/mm^2) Mean of 2 Cubes	Compressive Strength (N/mm^2) Mean for panel	Compressive Strength (N/mm^2) C.V (%)
SB02	(iii)	1	2110	2107	0.5	10.5	10.5	4.0
		2	2110			11.0		
		3	2100			10.5		
		4	2105			10.0		
		5	2100			11.0		
		6	2120			10.5		
		7	2090			10.0		
		8	2120			11.0		
SB03	(iii)	1	2110	2100	0.8	13.5	13.5	3.5
		2	2080			13.5		
		3	2120			13.0		
		4	2110			14.0		
		5	2100			14.0		
		6	2070			14.0		
		7	2090			14.5		
		8	2100			14.0		
		9	2120			14.5		
SB04	(iii)	1	2110	2115	0.4	12.5	12.5	3.0
		2	2120			13.0		
		3	2120			12.0		
		4	2100			12.5		
		5	2120			12.5		
		6	2120			12.0		
SB05	(iii)	1	2105	2095	1.0	11.5	10.5	7.6
		2	2110			11.5		
		3	2105			11.0		
		4	2105			10.5		
		5	2110			10.5		
		6	2040			11.0		
		7	2100			10.5		
		8	2100			10.5		
		9	2080			9.5		
		10	2090			9.0		
SB06	(iii)	1	2080	2095	0.6	12.5	13.0	4.4
		2	2100			13.5		
		3	2090			13.5		
		4	2110			12.5		
SB07	(iii)	1	2105	2095	0.6	13.5	13.5	6.7
		2	2075			13.5		
		3	2095			12.0		
		4	2110			13.5		
		5	2100			14.5		

Panel ref.	Mortar Mix	Mortar batch No.	Density (Kg/m³) Mean of 2 Cubes	Density (Kg/m³) Mean for panel	Density (Kg/m³) C.V (%)	Compressive Strength (N/mm²) Mean of 2 Cubes	Compressive Strength (N/mm²) Mean for panel	Compressive Strength (N/mm²) C.V (%)
SB09	(iii)	1	2100	2100	0.5	12.5	12.0	13.0
		2	2115			10.5		
		3	2110			11.0		
		4	2120			10.5		
		5	2080			11.5		
		6	2095			14.0		
		7	2100			14.5		
		8	2110			10.5		
		9	2110			12.0		
		10	2100			11.5		
		11	2085			13.5		
		12	2095			14.5		
		13	2110			10.5		
CB02	(iii)	1	2090	2095	0.5	10.0	11.0	11.2
		2	2110			11.0		
		3	2100			12.5		
		4	2120			12.0		
		5	2100			12.0		
		6	2100			12.0		
		7	2090			10.5		
		8	2080			10.5		
		9	2100			10.5		
		10	2100			12.0		
		11	2080			8.5		
		12	2090			9.0		
		13	2090			10.0		
		14	2090			11.5		
DC01	(iii)	1	2110	2095	1.3	12.5	12.5	5.2
		2	2120			12.0		
		3	2100			12.0		
		4	2050			13.0		
		5	2090			13.5		
DC02	(iii)	1	2090	2100	1.0	15.5	14.0	5.9
		2	2120			14.0		
		3	*2070*			*14.5*		
		4	2120			13.5		
		5	2110			13.5		
DC02B	(iii)	1	2100	2100	0.4	14.0	14.0	3.5
		2	2110			13.5		
		3	2105			13.5		
		4	2090			14.5		

APPENDIX C - SAND PROPERTIES

PARTICLE SIZE DISTRIBUTION

SIEVING METHOD: DRY SIEVING TO BS8122: PART 103: 1985
DESCRIPTION OF MATERIAL: MEDIUM GRADE NATURAL BUILDING SAND, ZIG-ZAG QUARY, NEWTON ABBORT.
TOTAL MASS OF DRY SAMPLE: 1008.5 g

BS TEST SIEVE (mm)	MASS RETAINED (g)	PERCENTAGE RETAINED (%)	PERCENTAGE PASSING (%)
5.00	0.0	0.00	100.00
2.36	26.5	2.63	97.37
1.18	232.8	23.08	74.29
0.60	312.6	30.99	43.30
0.30	242.3	24.03	19.27
0.15	123.8	12.28	6.99
TRAY	70.5	6.99	0.00
TOTAL	1008.5	100.00	

PARTICLE SIZE DISTRIBUTION

SIEVING METHOD: WASHIING AND SIEVING TO BS812: PART 103: 1985
DESCRIPTION OF MATERIAL: MEDIUM GRADE NATURAL BUILDING SAND, ZIG-ZAG QUARY, NEWTON ABBORT.
TOTAL MASS OF DRY SAMPLE: 336.7 g

BS TEST SIEVE (mm)	MASS RETAINED (g)	PERCENTAGE PASSING (%)	PERCENTAGE PASSING (%)	CUMULATIVE PERCENTAGE RETAINED (%)
5.00	0.0	0.00	100.00	0.00
2.36	9.6	2.85	97.15	2.85
1.18	79.3	23.55	73.60	26.40
0.60	106.7	31.69	41.91	58.09
0.30	79.4	23.58	18.33	81.67
0.15	35.6	10.57	7.76	92.24
0.075	14.2	4.22	3.54	96.46
TRAY	11.9	3.54	0.00	
TOTAL		336.70	100.00	357.71

$$FINENESS\ MODULUS = \frac{357.71}{100} = 3.58$$

RELATIVE DENSITY

TEST METHOD: DENSITY BOTTLE METHOD TO BS812: PART 2: 1975
DESCRIPTION OF MATERIAL: MEDIUM GRADE NATURAL BUILDING SAND, ZIG-ZAG QUARY, NEWTON ABBORT.
DILATOMETRIC LIQUID: DISTILLED WATER
SAMPLE CONDITION: OVEN DRIED

DENSITY BOTTLE NUMBER		1	2	3
(A) MASS OF STOPPER AND BOTTLE	(g)	45.1	44.0	43.6
(B) MASS OF STOPPER, BOTTLE AND SAND	(g)	88.2	103.1	93.0
(C) MASS OF STOPPER, BOTTLE, SAND AND WATER	(g)	170.3	179.2	172.4
(D) MASS OF STOPPER, BOTTLE AND WATER	(g)	143.6	142.5	141.8
RELATIVE DENSITY OF SAND		2.628	2.638	2.628
MEAN			2.631	

RELATIVE DENSITY

TEST METHOD: DENSITY BOTTLE METHOD TO BS812: PART 2: 1975
DESCRIPTION OF MATERIAL: MEDIUM GRADE NATURAL BUILDING SAND, ZIG-ZAG QUARY, NEWTON ABBORT.
DILATOMETRIC LIQUID: DISTILLED WATER
SAMPLE CONDITION: SURFACE SATURATED

DENSITY BOTTLE NUMBER		1	2	3
(A) MASS OF STOPPER AND BOTTLE	(g)	45.1	44.0	43.6
(B) MASS OF STOPPER, BOTTLE AND SAND	(g)	82.8	90.8	91.6
(C) MASS OF STOPPER, BOTTLE, SAND AND WATER	(g)	166.9	171.4	171.5
(D) MASS OF STOPPER, BOTTLE AND WATER	(g)	143.4	142.3	141.6
RELATIVE DENSITY OF SAND		2.618	2.615	2.623
MEAN			2.619	

APPENDIX D - WALLETTE FLEXURAL STRENGTH

D.1 CLASS B WESTBRICK

(a) HORIZONTAL FLEXURE

(i) UNDOCK SPECIMENS - 10 COURSES HIGH BY 2 BRICKS WIDE

SPECIMEN NO.	WALLETTE STRENGTH KN/mm^2
1	0.739
2	0.429
3	-
4	0.421
5	0.310
MEAN	0.474
S.D.	0.184
C.V.	0.388

(ii) DOCK SPECIMENS - 10 COURSES HIGH BY 2 BRICKS WIDE

SPECIMEN NO.	WALLETTE STRENGTH KN/mm^2
1	0.763
2	0.668
3	-
4	0.684
5	0.684
6	0.692
7	-
8	1.002
9	0.690
10	-
MEAN	0.740
S.D.	0.120
C.V.	0.162

(b) VERTICAL FLEXURE

(i) UNDOCK SPECIMENS - 4 COURSES HIGH BY 4 BRICKS WIDE

SPECIMEN NO.	WALLETTE STRENGTH KN/mm^2
1	-
2	2.115
3	1.895
4	1.684
5	0.989
MEAN	1.671
S.D.	0.487
C.V.	0.291

(ii) DOCK SPECIMENS - 4 COURSES HIGH BY 4 BRICKS WIDE

SPECIMEN NO.	WALLETTE STRENGTH KN/mm²
1	-
2	1.712
3	1.602
4	1.162
5	1.791
6	-
7	1.906
8	2.026
9	1.535
10	1.597
11	1.228
12	1.986
13	2.006
14	1.638
15	1.946
MEAN	1.703
S.D.	0.282
C.V.	0.166

(iii) VERTICAL FLEXURE

DOCK SPECIMENS - 6 COURSES HIGH BY 4 BRICKS WIDE

SPECIMEN NO.	WALLETTE STRENGTH KN/mm²
1	1.987
2	2.182
3	1.959
4	2.084
5	-
6	2.084
7	1.791
8	2.252
9	2.434
10	2.043
MEAN	2.091
S.D.	0.185
C.V.	0.088

D.2 DENCE CONCRETE BLOCK

(a) HORIZONTAL FLEXURE

UNDOCK SPECIMENS - 5 COURSES HIGH BY 1.5 BLOCKS WIDE

SPECIMEN NO.	WALLETTE STRENGTH KN/mm^2
1	1.420
2	1.161
3	1.340
4	1.572
5	1.331
6	1.492
7	1.135
8	1.510
9	-
10	1.536
MEAN	1.367
S.D.	0.179
C.V.	0.131

(b) VERTICAL FLEXURE

UNDOCK SPECIMENS - 4 COURSES HIGH BY 2.5 BLOCKS WIDE

SPECIMEN NO.	WALLETTE STRENGTH KN/mm^2
1	1.671
2	1.725
3	1.691
4	1.798
5	-
6	-
7	1.624
8	1.550
9	1.738
10	1.610
MEAN	1.676
S.D.	0.080
C.V.	0.048

D.3 CLASS A ENGINEERING BRICKS

(a) HORIZONTAL FLEXURE

UNDOCK SPECIMENS - 10 COURSES BY 2 BRICKS WIDE

SPECIMEN NO.	WALLETTE STRENGTH KN/mm^2
1	0.910
2	0.756
3	0.837
4	0.881
5	0.585
6	0.642
MEAN	0.770
S.D.	0.132
C.V.	0.172

(b) VERTICAL FLEXURE

UNDOCK SPECIMENS - 4 COURSES HIGH BY 4 BRICKS WICE

SPECIMEN NO.	WALLETTE STRENGTH KN/mm^2
1	4.515
2	4.307
3	3.994
4	4.116
5	5.054
6	3.664
MEAN	4.120
S.D.	0.288
C.V.	0.070

APPENDIX E - TYPICAL FINITE ELEMENT MESH PATTERNS

E.1 Series 1 and 2

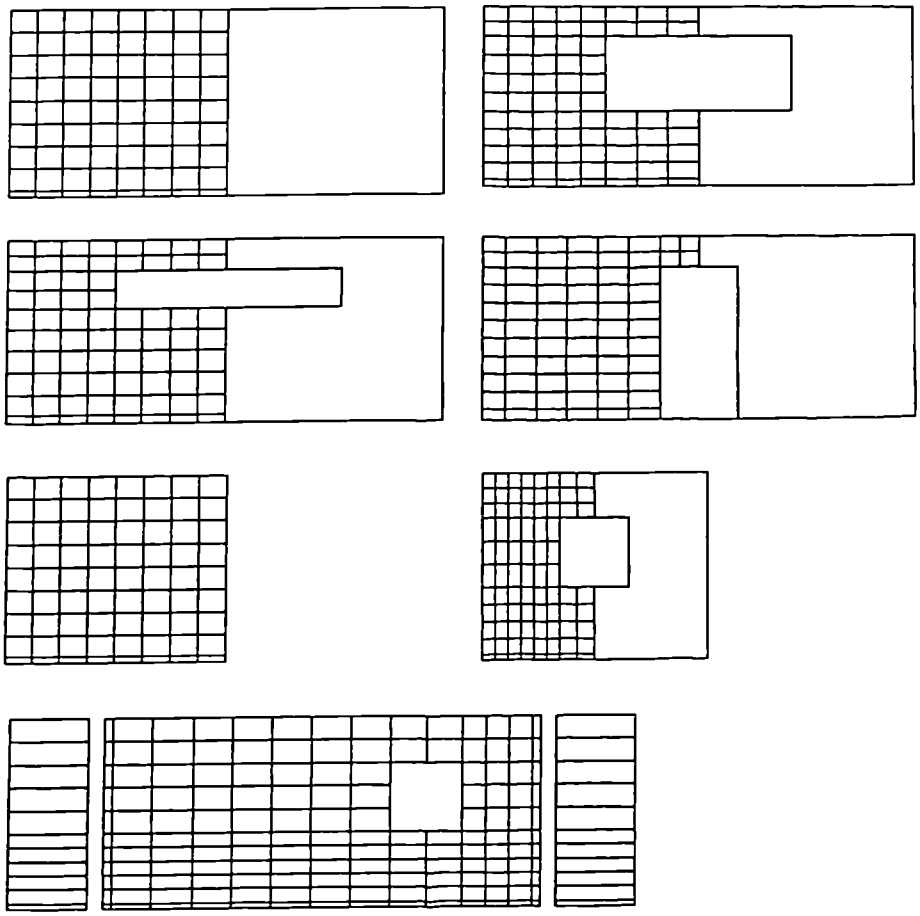

E.2 Series 3

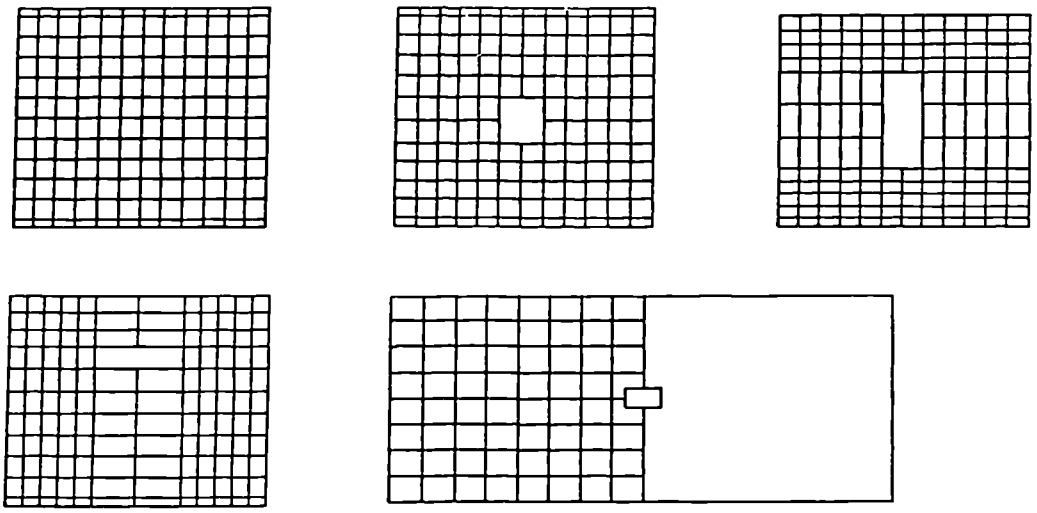

APPENDIX F - PANEL DEFLECTION PROFILE

All Dimensions in mm

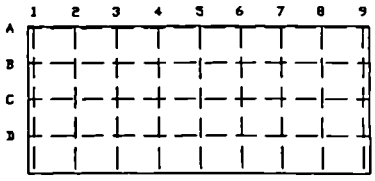

F.1 *WALL SB01*

0.2 KN/m²

*	1	2	3	4	5	6	7	8	9
A *	-0.04	0.04	0.44	0.46	0.48	0.78	0.67	1.40	0.23
B *	-0.25	-0.02	0.54	0.53	0.28	0.84	0.80	1.15	0.19
C *	-0.37	-0.33	0.43	0.20	0.03	0.55	0.37	0.62	0.06
D *	-0.47	-0.55	0.27	0.08	0.29	0.21	0.39	0.11	0.13

0.4 KN/m²

*	1	2	3	4	5	6	7	8	9
A *	0.18	0.41	0.94	0.93	1.23	1.39	1.00	1.75	0.28
B *	0.18	0.38	1.11	0.99	1.17	1.49	0.97	1.39	0.14
C *	0.01	0.03	0.72	0.48	0.60	1.00	0.36	0.76	0.10
D *	-0.08	-0.20	0.58	0.33	0.43	0.67	0.19	0.15	0.15

0.6 KN/m²

*	1	2	3	4	5	6	7	8	9
A *	0.39	0.83	1.47	1.58	1.87	1.75	1.51	2.28	0.63
B *	0.48	0.83	1.69	1.45	1.95	1.77	1.45	1.76	0.66
C *	0.32	0.42	1.13	0.82	1.15	0.99	0.65	1.05	0.23
D *	0.24	0.23	0.80	0.27	0.74	0.57	0.25	0.32	0.10

0.8KN/m²

*	1	2	3	4	5	6	7	8	9
A *	0.31	0.90	1.74	2.01	2.42	2.16	1.97	2.31	0.64
B *	0.28	0.78	1.84	1.87	2.26	2.06	1.99	1.86	0.53
C *	0.05	0.07	1.08	0.85	1.20	1.20	1.02	0.99	0.22
D *	-0.02	-0.36	0.74	0.31	0.72	0.41	0.79	0.37	0.10

1.0 KN/m²

*	1	2	3	4	5	6	7	8	9
A *	0.28	1.24	2.06	2.56	2.70	2.76	2.34	2.63	0.59
B *	0.14	1.28	2.04	2.35	2.45	2.67	2.26	1.15	0.31
C *	-0.13	0.56	1.12	1.13	1.31	1.50	1.04	1.18	0.01
D *	-0.32	0.13	0.65	0.43	0.57	0.59	0.57	0.38	0.17

1.2 KN/m²

*	1	2	3	4	5	6	7	8	9
A *	0.37	1.81	2.61	3.09	3.48	3.48	2.91	3.06	1.05
B *	0.25	1.96	2.71	2.96	3.37	3.52	2.82	2.62	1.38
C *	-0.04	1.23	1.67	1.56	1.89	2.13	1.54	1.57	0.77
D *	-0.36	0.68	1.09	0.71	1.06	1.21	1.00	0.72	0.48

1.4 KN/m²

*	1	2	3	4	5	6	7	8	9
A *	0.42	1.65	3.21	3.77	3.89	4.09	3.33	3.34	1.04
B *	0.24	1.52	3.37	3.74	3.50	4.07	3.24	2.91	0.87
C *	-0.02	0.57	2.16	2.20	1.83	2.49	1.80	1.73	0.47
D *	-0.31	0.08	1.45	1.39	0.75	1.40	1.18	0.82	0.19

1.6 KN/m²

*	1	2	3	4	5	6	7	8	9
A *	0.64	2.00	3.60	4.26	4.72	4.64	3.75	3.75	1.08
B *	0.66	1.94	3.69	3.85	4.31	4.61	3.51	3.31	0.85
C *	0.30	0.81	2.18	1.99	2.48	2.70	1.76	2.18	0.42
D *	0.09	0.09	1.41	0.89	1.07	1.36	0.85	1.03	0.12

1.8 KN/m²

*	1	2	3	4	5	6	7	8	9
A *	0.81	2.41	4.15	5.19	5.42	5.46	4.50	4.33	1.48
B *	0.96	2.45	4.30	5.03	5.15	5.41	4.32	3.95	1.28
C *	0.55	1.18	2.61	2.95	2.85	3.19	2.24	2.45	0.73
D *	0.28	0.34	1.62	1.74	1.41	1.62	1.14	1.42	0.48

2.0 KN/m²

*	1	2	3	4	5	6	7	8	9
A *	0.52	2.79	4.73	5.62	6.26	5.90	5.00	4.45	1.47
B *	0.43	2.83	4.93	5.54	6.08	5.72	4.83	3.82	1.15
C *	0.06	1.42	3.08	2.97	3.56	3.34	2.74	2.19	0.68
D *	0.36	0.87	2.52	2.40	2.50	2.10	3.82	4.05	8.65

2.2 KN/m²

*	1	2	3	4	5	6	7	8	9
A *	0.73	3.15	5.31	6.44	6.96	6.73	5.55	4.87	1.58
B *	0.47	3.21	5.14	6.24	6.62	6.50	5.21	4.20	1.11
C *	0.00	1.89	3.16	3.82	3.91	3.90	2.99	2.52	0.65
D *	0.46	1.49	2.17	2.49	2.43	2.58	1.89	1.52	1.83

2.4 KN/m²

*	1	2	3	4	5	6	7	8	9
A *	0.92	3.25	5.94	7.16	7.62	7.40	6.17	5.32	1.54
B *	0.80	3.11	5.96	6.85	7.12	7.08	5.76	4.65	0.90
C *	0.42	1.61	3.81	4.14	4.06	4.21	3.26	2.83	0.45
D *	0.35	0.60	2.50	2.39	2.61	2.27	4.13	4.28	0.51

2.6 KN/m²

*	1	2	3	4	5	6	7	8	9
A *	0.93	3.93	6.54	7.96	8.63	8.36	6.92	5.68	1.87
B *	0.71	3.89	6.48	7.46	8.21	8.04	6.59	4.82	1.18
C *	0.22	2.24	4.08	4.34	4.86	4.82	3.92	2.82	0.66
D *	0.03	1.25	2.63	2.24	2.66	2.47	2.42	1.48	0.44

2.7 KN/m²

*	1	2	3	4	5	6	7	8	9
A	0.75	3.85	6.78	8.25	9.14	8.83	7.27	6.05	2.03
B	0.37	3.64	6.60	7.80	8.73	8.46	6.80	5.20	1.38
C	-0.05	1.91	4.05	4.51	5.20	5.11	3.88	3.24	0.93
D	-0.21	0.73	2.51	2.27	3.19	2.64	2.12	1.84	0.91

2.8 KN/m²

*	1	2	3	4	5	6	7	8	9
A	0.87	4.64	7.93	10.09	11.53	12.04	9.03	6.79	1.85
B	0.62	5.07	8.56	10.61	11.94	12.74	9.22	6.39	1.23
C	0.24	3.56	6.16	7.68	8.41	9.01	6.37	4.48	0.95
D	-0.22	1.91	3.70	4.09	4.52	4.75	3.63	2.93	1.58

F.2 *WALL SB02*

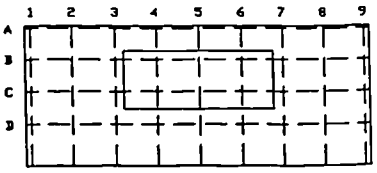

0.1 KN/m²

*	1	2	3	4	5	6	7	8	9
A *	0.16	0.22	0.25	0.30	0.44	0.46	0.38	0.48	0.21
B *	0.38	0.28	0.26	*.**	*.**	*.**	0.36	0.46	0.11
C *	0.21	0.09	0.04	*.**	*.**	*.**	0.21	0.33	0.02
D *	0.21	0.06	0.03	0.09	0.13	0.07	0.13	0.15	-0.19

0.2 KN/m²

*	1	2	3	4	5	6	7	8	9
A *	0.09	0.16	0.44	0.55	0.81	0.72	0.65	0.50	0.33
B *	0.10	0.32	0.41	*.**	*.**	*.**	0.56	0.44	0.05
C *	0.08	0.14	0.19	*.**	*.**	*.**	0.33	0.30	0.04
D *	0.09	0.01	0.06	0.19	0.24	0.22	0.20	0.10	-0.24

0.4 KN/m²

*	1	2	3	4	5	6	7	8	9
A *	0.10	0.58	0.94	1.18	1.28	1.33	1.09	0.68	0.46
B *	0.15	0.50	1.03	*.**	*.**	*.**	0.94	0.71	0.31
C *	0.01	0.33	0.52	*.**	*.**	*.**	0.55	0.38	0.16
D *	0.04	0.14	0.27	0.40	0.42	0.38	0.27	0.19	-0.11

0.6 KN/m²

*	1	2	3	4	5	6	7	8	9
A *	0.15	0.77	1.39	1.80	2.09	1.93	1.54	0.97	0.36
B *	0.25	0.79	1.43	*.**	*.**	*.**	1.48	1.00	0.19
C *	0.14	0.46	0.82	*.**	*.**	*.**	0.90	0.58	0.03
D *	0.18	0.21	0.43	0.63	0.65	0.59	0.49	0.29	-0.28

0.8 KN/m²

*	1	2	3	4	5	6	7	8	9
A *	0.05	0.95	1.79	2.32	2.71	2.49	1.95	1.29	0.53
B *	0.18	0.89	1.83	*.**	*.**	*.**	1.85	1.25	0.35
C *	0.03	0.61	0.95	*.**	*.**	*.**	1.10	0.76	0.01
D *	0.08	0.30	0.54	0.75	0.82	0.75	0.60	0.42	-0.15

1.0 KN/m²

*	1	2	3	4	5	6	7	8	9
A *	0.15	1.13	2.23	2.87	3.40	3.12	2.37	1.49	0.52
B *	0.24	1.89	2.42	*.**	*.**	*.**	2.35	1.57	0.40
C *	0.13	0.72	1.34	*.**	*.**	*.**	1.34	0.87	0.25
D *	0.17	0.35	0.75	0.95	1.02	0.92	0.73	0.50	-0.06

1.2 KN/m²

*	1	2	3	4	5	6	7	8	9
A *	0.12	1.55	2.81	3.72	4.15	3.78	2.94	1.73	0.53
B *	0.16	1.32	2.66	*.**	*.**	*.**	2.82	1.71	0.30
C *	0.19	1.05	1.69	*.**	*.**	*.**	1.73	1.08	0.12
D *	0.20	0.56	0.92	1.24	1.26	1.08	0.89	0.58	-0.27

1.4 KN/m²

*	1	2	3	4	5	6	7	8	9
A *	0.17	0.73	3.31	4.34	4.81	4.42	3.51	2.10	0.54
B *	0.36	1.76	3.47	*.**	*.**	*.**	3.30	2.09	0.34
C *	0.27	1.19	2.05	*.**	*.**	*.**	2.02	1.28	0.22
D *	0.24	0.65	1.13	1.45	1.50	1.38	1.13	0.72	-0.16

1.6 KN/m²

*	1	2	3	4	5	6	7	8	9
A *	0.20	2.01	3.83	5.16	5.74	5.26	3.98	2.43	0.60
B *	0.41	1.99	3.99	*.**	*.**	*.**	3.73	2.49	0.52
C *	0.36	1.30	2.26	*.**	*.**	*.**	2.30	1.49	0.36
D *	0.32	0.73	1.32	1.74	1.79	1.59	1.28	0.88	0.03

1.8 KN/m²

*	1	2	3	4	5	6	7	8	9
A *	0.16	2.30	4.37	5.90	6.70	6.03	4.40	2.77	0.72
B *	0.44	2.49	4.80	*.**	*.**	*.**	4.33	2.67	0.59
C *	0.31	1.62	2.73	*.**	*.**	*.**	2.58	1.60	0.33
D *	0.34	0.90	1.59	2.01	2.06	1.92	1.46	0.92	-0.09

2.0 KN/m²

*	1	2	3	4	5	6	7	8	9
A *	0.24	3.09	5.67	8.16	10.43	9.91	6.58	3.67	0.90
B *	0.55	3.44	6.49	*.**	*.**	*.**	6.70	3.93	0.85
C *	0.39	2.16	3.64	*.**	*.**	*.**	3.87	2.25	0.36
D *	0.42	1.30	2.22	2.80	2.95	2.81	2.25	1.36	0.06

2.1 KN/m²

*	1	2	3	4	5	6	7	8	9
A *	0.19	3.14	6.02	8.88	11.48	10.79	7.13	3.98	0.76
B *	0.74	3.88	7.04	*.**	*.**	*.**	7.34	4.46	1.07
C *	0.33	2.34	3.96	*.**	*.**	*.**	4.19	2.49	0.36
D *	0.43	1.42	2.41	3.06	3.23	3.08	2.44	1.51	0.04

2.2 KN/m²

*	1	2	3	4	5	6	7	8	9
A *	0.32	3.37	6.50	9.53	12.33	11.62	7.55	4.16	0.88
B *	0.98	4.02	7.71	*.**	*.**	*.**	7.97	4.82	1.23
C *	0.55	2.57	4.40	*.**	*.**	*.**	4.57	2.73	0.51
D *	0.66	1.47	2.70	3.26	3.52	3.26	2.64	1.59	0.53

2.3 KN/m²

*	1	2	3	4	5	6	7	8	9
A *	0.13	3.76	7.28	10.83	14.09	13.40	8.75	4.80	0.96
B *	0.81	4.67	8.74	*.**	*.**	*.**	9.40	5.57	1.46
C *	0.48	3.98	5.24	*.**	*.**	*.**	5.50	3.19	0.61
D *	0.51	1.94	3.42	3.99	4.13	3.89	3.20	1.83	0.10

F.3 *WALL SB03*

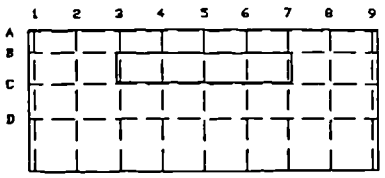

0.4 KN/m²

*	1	2	3	4	5	6	7	8	9
A	0.07	0.65	0.98	1.26	1.50	1.42	1.28	1.01	0.60
B	0.33	0.95	1.13	1.43	1.73	1.54	1.46	1.11	0.58
C	0.16	0.47	0.65	0.70	0.90	0.73	0.85	0.64	0.33
D	*.**	1.92	1.59	1.35	1.80	2.01	1.56	0.97	0.23

0.8 KN/m²

*	1	2	3	4	5	6	7	8	9
A	0.14	1.04	1.62	2.21	2.82	2.33	2.24	1.73	1.05
B	0.58	1.58	2.13	2.70	3.38	2.77	2.62	2.09	1.25
C	0.31	0.75	1.08	1.22	1.68	1.23	1.51	1.13	0.56
D	*.**	1.98	1.49	0.96	2.34	2.14	2.18	2.02	0.33

1.2 KN/m²

*	1	2	3	4	5	6	7	8	9
A	0.20	1.73	2.93	3.87	4.34	4.06	3.29	2.41	1.13
B	0.87	2.41	3.61	4.52	5.07	4.70	3.82	2.83	1.38
C	0.38	1.34	2.01	2.47	2.54	2.37	2.27	1.62	0.60
D	*.**	2.36	1.78	1.43	1.50	1.37	1.22	0.96	0.34

1.6 KN/m²

*	1	2	3	4	5	6	7	8	9
A	0.43	2.44	4.03	5.40	6.05	5.56	4.50	3.08	0.89
B	1.13	3.27	4.71	6.36	7.01	6.31	5.06	3.55	1.07
C	0.61	1.99	2.94	3.48	3.64	3.34	3.12	2.15	0.58
D	*.**	2.88	3.62	3.42	4.18	4.21	5.96	4.58	0.44

2.0 KN/m²

*	1	2	3	4	5	6	7	8	9
A	0.43	3.02	5.32	7.07	8.05	7.43	5.85	3.85	1.54
B	1.22	3.98	6.41	8.20	9.36	8.55	6.69	4.52	1.91
C	0.61	2.39	3.98	4.40	4.80	4.56	4.17	2.79	0.97
D	*.**	3.10	2.40	2.60	2.98	2.86	2.62	1.92	0.66

2.2 KN/m²

*	1	2	3	4	5	6	7	8	9
A	0.47	3.43	5.99	8.13	9.34	8.62	6.61	4.19	1.60
B	1.52	4.65	7.33	9.62	10.85	9.89	7.63	5.00	2.09
C	0.74	2.86	4.49	5.24	5.63	5.41	4.84	3.16	1.10
D	*.**	2.34	4.02	4.10	3.47	3.32	2.99	2.15	0.76

2.3 KN/m²

*	1	2	3	4	5	6	7	8	9
A	0.53	3.91	7.08	10.23	10.90	9.49	7.19	4.55	1.53
B	1.23	4.89	8.18	11.68	12.60	10.88	8.10	5.14	1.65
C	0.82	3.33	5.17	5.93	6.36	5.97	5.60	3.64	1.10
D	*.**	2.03	3.10	3.61	3.91	3.63	3.40	2.37	0.68

2.3 KN/m²

*	1	2	3	4	5	6	7	8	9
A *	0.54	4.15	7.77	11.38	11.70	10.21	7.63	4.69	1.48
B *	1.52	5.30	9.11	13.00	13.59	11.88	8.77	5.53	1.80
C *	0.76	3.35	5.63	6.37	6.61	6.43	6.00	3.75	0.98
D *	*.**	2.70	3.87	4.98	4.85	4.98	4.67	3.86	0.75

2.35 KN/m²

*	1	2	3	4	5	6	7	8	9
A *	12.14	14.43	15.20	14.82	14.44	14.62	14.97	14.49	12.21
B *	12.70	17.32	16.66	21.64	23.57	19.02	21.07	17.95	14.66
C *	4.82	7.88	10.32	9.42	10.50	11.03	8.74	7.93	4.84
D *	*.**	11.41	10.93	12.27	11.61	11.70	9.97	11.33	6.67

F.4 *WALL SB04*

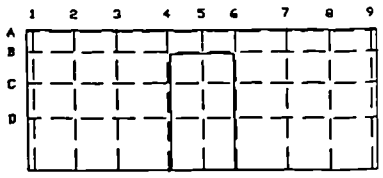

0.2 KN/m²

*	1	2	3	4	5	6	7	8	9
A *	0.34	0.70	0.65	0.66	0.76	0.89	0.64	0.49	0.37
B *	0.38	0.56	0.59	0.63	0.76	0.96	0.66	0.44	0.34
C *	0.15	0.52	0.36	0.53	*.**	0.67	0.49	0.25	0.20
D *	0.13	0.30	0.21	0.24	*.**	0.52	0.33	0.14	0.12

0.4 KN/m²

*	1	2	3	4	5	6	7	8	9
A *	0.73	0.97	1.20	1.29	1.43	1.49	1.00	0.83	0.56
B *	0.71	0.98	1.14	1.22	1.40	1.53	0.97	0.71	0.39
C *	0.29	0.72	0.75	0.94	*.**	0.99	0.85	0.48	0.22
D *	0.34	0.42	0.45	0.52	*.**	0.79	0.44	0.28	0.06

0.6 KN/m²

*	1	2	3	4	5	6	7	8	9
A *	0.72	1.35	1.68	1.92	2.11	2.11	1.65	1.14	0.64
B *	0.66	1.36	1.58	1.88	2.11	2.15	1.60	1.02	0.46
C *	0.23	0.84	1.05	1.28	*.**	1.41	1.15	0.70	0.40
D *	0.27	0.60	0.59	0.79	*.**	0.93	0.67	0.41	0.18

0.8 KN/m²

*	1	2	3	4	5	6	7	8	9
A *	0.93	1.71	2.23	2.64	2.95	2.86	2.14	1.42	0.78
B *	0.88	1.52	2.11	2.65	3.01	2.90	2.11	1.30	0.60
C *	0.58	1.13	1.48	1.92	*.**	1.92	1.56	0.78	0.40
D *	0.43	0.64	0.89	1.14	*.**	1.36	0.95	0.43	0.22

1.0 KN/m²

*	1	2	3	4	5	6	7	8	9
A *	0.73	1.94	2.67	3.37	3.55	3.46	2.66	1.79	0.89
B *	0.66	1.93	2.65	3.42	3.64	3.58	2.60	1.61	0.67
C *	0.27	1.41	1.78	2.37	*.**	2.37	1.93	1.10	0.44
D *	0.31	0.88	1.02	1.49	*.**	1.65	1.17	0.65	0.26

1.2 KN/m²

*	1	2	3	4	5	6	7	8	9
A *	0.87	2.30	3.08	4.01	4.35	4.00	3.23	1.93	0.83
B *	0.87	2.22	3.02	4.08	4.50	4.23	3.24	1.87	0.67
C *	0.47	1.53	1.96	2.85	*.**	2.84	2.14	1.21	0.43
D *	0.40	0.96	1.16	1.75	*.**	1.85	1.43	0.78	0.22

1.4 KN/m²

*	1	2	3	4	5	6	7	8	9
A *	0.86	2.49	3.61	4.73	4.94	4.93	3.72	2.42	1.03
B *	0.82	2.47	3.58	4.90	5.11	5.13	3.74	2.30	0.84
C *	0.52	1.79	2.40	3.33	*.**	3.48	2.49	1.50	0.57
D *	0.38	1.13	1.53	2.15	*.**	2.33	1.60	0.96	0.35

1.6 KN/m²

*	1	2	3	4	5	6	7	8	9
A *	0.89	2.97	4.39	5.26	5.85	5.34	4.24	2.21	1.17
B *	0.76	2.73	4.41	5.53	6.11	5.56	4.27	2.21	0.95
C *	0.27	2.00	3.00	3.71	*.**	3.66	0.97	1.48	0.59
D *	0.46	1.20	1.92	2.44	*.**	2.38	1.84	1.00	0.37

1.75 KN/m²

*	1	2	3	4	5	6	7	8	9
A *	1.17	3.53	5.53	7.74	7.74	6.93	4.00	2.97	1.06
B *	1.05	3.57	5.64	8.20	8.13	7.31	4.26	2.92	0.90
C *	0.78	2.49	3.87	5.61	*.**	5.00	3.01	1.90	0.55
D *	0.52	1.67	2.46	3.66	*.**	3.30	1.77	1.21	0.33

1.8 KN/m²

*	1	2	3	4	5	6	7	8	9
A *	1.13	3.84	5.71	8.21	7.89	7.13	5.23	3.24	1.17
B *	1.12	3.84	5.91	8.80	8.34	7.58	5.36	3.21	0.98
C *	0.87	2.67	4.11	6.08	*.**	5.23	3.71	2.15	0.65
D *	0.61	1.85	2.67	4.03	*.**	3.55	2.50	1.40	0.40

1.9 KN/m²

*	1	2	3	4	5	6	7	8	9
A *	1.14	3.48	6.11	8.86	8.85	7.76	5.57	3.44	1.09
B *	1.28	3.68	6.49	9.70	9.50	8.37	5.82	3.50	1.03
C *	1.00	2.70	4.70	6.92	*.**	5.81	4.01	2.32	0.64
D *	0.68	1.83	3.04	4.58	*.**	4.07	2.74	1.54	0.42

2.0 KN/m²

*	1	2	3	4	5	6	7	8	9
A *	1.08	4.33	6.86	10.01	9.77	8.67	6.14	3.62	1.20
B *	1.19	4.61	7.42	10.96	10.54	9.38	6.46	3.69	1.04
C *	1.01	3.55	5.44	7.95	*.**	6.56	4.50	2.56	0.68
D *	0.69	2.42	3.66	5.33	*.**	4.51	3.14	1.77	0.46

2.1 KN/m²

*	1	2	3	4	5	6	7	8	9
A *	0.81	4.51	7.61	11.04	10.76	9.45	6.52	4.02	1.31
B *	1.00	4.84	8.22	12.16	11.66	10.24	6.94	4.13	1.13
C *	1.00	3.60	6.07	8.99	*.**	7.22	4.96	2.85	0.77
D *	0.65	2.40	4.15	6.04	*.**	4.99	3.43	2.01	0.53

F.5 *WALL SB05*

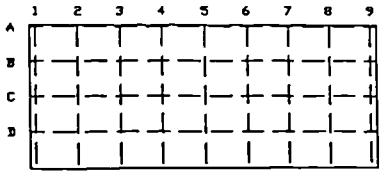

0.2 KN/m²

*	1	2	3	4	5	6	7	8	9
A *	0.21	0.18	0.18	0.51	0.54	0.49	0.33	0.26	0.02
B *	0.34	0.14	0.01	0.49	0.50	0.43	0.35	0.15	-0.03
C *	0.35	-0.03	-0.28	0.23	0.19	0.25	0.31	-0.00	-0.02
D *	0.47	-0.06	-0.52	0.03	0.05	0.05	0.06	-0.14	-0.13

0.4 KN/m²

*	1	2	3	4	5	6	7	8	9
A *	0.32	0.53	0.75	1.07	1.25	0.66	0.98	0.62	0.42
B *	0.50	0.61	0.63	1.04	1.21	0.65	1.06	0.57	0.39
C *	0.24	0.32	0.11	0.54	0.62	0.29	0.66	0.23	0.22
D *	0.25	0.25	-0.23	0.23	0.32	0.13	0.55	0.05	0.19

0.6 KN/m²

*	1	2	3	4	5	6	7	8	9
A *	0.43	0.91	1.16	1.75	1.89	1.58	1.32	1.00	0.27
B *	0.49	0.93	1.09	1.83	0.90	1.55	1.20	0.91	0.11
C *	0.25	0.59	0.45	1.21	1.13	0.79	0.89	0.52	0.13
D *	0.25	0.34	0.09	0.72	0.39	0.39	0.40	0.16	0.11

0.8 KN/m²

*	1	2	3	4	5	6	7	8	9
A *	0.64	1.08	1.64	2.42	2.43	2.17	1.81	1.29	0.47
B *	0.79	0.90	1.41	2.41	2.23	1.93	1.67	1.13	0.29
C *	0.69	0.44	0.75	1.64	1.31	1.16	1.13	0.69	0.20
D *	0.74	0.04	0.19	1.16	0.72	0.53	0.55	0.31	0.04

1.0 KN/m²

*	1	2	3	4	5	6	7	8	9
A *	0.59	1.33	2.33	2.76	3.19	2.84	2.28	1.51	0.36
B *	0.66	1.16	2.19	2.86	3.01	2.66	2.13	1.38	0.18
C *	0.39	0.61	1.35	1.93	1.90	1.60	1.32	0.79	0.01
D *	0.38	0.08	0.71	1.38	1.15	0.88	0.68	0.44	-0.16

1.2 KN/m²

*	1	2	3	4	5	6	7	8	9
A *	0.72	1.89	2.90	3.49	3.72	3.36	3.01	1.92	0.56
B *	0.84	1.81	2.77	3.25	3.42	3.11	2.96	1.81	0.41
C *	0.67	1.36	1.81	1.99	2.055	1.86	2.09	1.19	0.33
D *	0.79	0.92	1.06	1.19	1.17	1.06	1.49	0.69	0.19

1.4 KN/m²

*	1	2	3	4	5	6	7	8	9
A *	0.80	2.25	3.18	4.28	4.49	4.00	3.47	2.33	0.68
B *	0.91	2.17	2.94	4.09	4.12	3.73	3.18	2.19	0.48
C *	0.62	1.46	1.79	2.64	2.60	2.36	2.13	1.57	0.39
D *	0.62	0.99	0.97	1.64	1.49	1.39	1.24	1.10	0.24

1.6 N/m^2

*	1	2	3	4	5	6	7	8	9
A *	0.82	2.56	3.87	4.77	5.04	4.66	3.81	2.55	0.76
B *	1.01	2.58	3.80	4.50	4.64	4.37	3.59	2.38	0.60
C *	0.75	1.85	2.47	2.75	2.79	2.62	2.27	1.62	0.53
D *	0.80	1.39	1.60	1.48	1.49	1.47	1.37	0.98	0.42

1.8 N/m^2

*	1	2	3	4	5	6	7	8	9
A *	0.79	2.79	4.30	5.47	5.76	5.26	4.45	2.88	0.71
B *	0.99	2.78	4.08	5.19	5.34	4.86	4.23	2.82	0.51
C *	0.75	1.86	2.47	3.15	3.21	2.98	2.82	1.84	0.45
D *	0.82	1.30	1.29	1.80	1.73	1.56	1.73	1.09	0.23

2.0 KN/m^2

*	1	2	3	4	5	6	7	8	9
A *	0.64	3.13	4.79	5.95	6.65	5.97	5.10	3.05	0.80
B *	0.63	3.07	4.44	5.53	6.27	5.54	4.92	2.82	0.68
C *	0.40	2.13	2.65	3.48	3.98	3.38	3.37	1.84	0.68
D *	0.35	1.47	1.36	1.94	2.45	1.89	2.21	1.04	0.51

2.2 KN/m^2

*	1	2	3	4	5	6	7	8	9
A *	0.97	3.19	5.41	6.76	7.50	6.74	5.60	3.37	0.64
B *	1.17	2.90	4.99	6.26	7.02	6.22	5.31	3.14	0.40
C *	0.92	1.78	2.99	3.77	4.42	3.82	3.50	2.04	0.43
D *	1.04	0.96	1.58	2.03	2.64	2.03	2.19	1.19	0.25

2.4 KN/m^2

*	1	2	3	4	5	6	7	8	9
A *	0.91	3.48	6.11	7.77	8.42	7.74	6.44	3.81	0.69
B *	0.98	3.22	5.66	7.22	7.74	7.14	6.14	3.55	0.39
C *	0.76	2.01	3.36	4.51	4.85	4.48	4.20	2.28	0.50
D *	0.91	1.06	1.62	2.46	2.78	2.40	2.73	1.26	0.19

2.6 KN/m^2

*	1	2	3	4	5	6	7	8	9
A *	1.08	4.27	7.22	8.99	9.96	9.08	7.48	4.36	0.43
B *	1.19	4.02	6.83	8.38	9.30	8.53	7.04	4.07	0.19
C *	0.95	2.63	4.35	5.19	6.05	5.47	4.69	2.67	0.56
D *	1.09	1.53	2.40	2.82	3.69	3.25	2.95	1.50	0.54

2.7 KN/m^2

*	1	2	3	4	5	6	7	8	9
A *	1.31	8.14	14.69	19.94	22.50	22.23	17.23	9.32	1.03
b *	1.53	8.93	16.21	21.46	23.84	23.82	18.80	10.36	0.99
C *	1.17	7.53	13.89	17.93	19.39	19.25	16.88	9.21	1.27
D *	1.09	6.68	8.85	9.12	9.99	9.98	9.70	8.42	1.57

F.6 *WALL SB06*

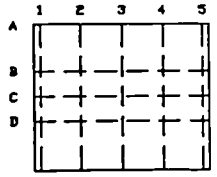

1.0 KN/m²

*	1	2	3	4	5
A *	-0.39	0.18	0.22	0.48	0.68
B *	-0.06	0.05	0.38	0.55	0.66
C *	-0.08	0.05	0.30	0.31	0.44
D *					

1.5 KN/m²

*	1	2	3	4	5
A *	-0.32	0.06	0.47	0.98	1.59
B *	0.06	0.28	0.62	0.95	1.36
C *	0.00	0.24	0.49	0.83	1.17
D *					

2.0 KN/m²

*	1	2	3	4	5
A *	0.01	0.55	1.08	1.66	2.14
B *	0.46	0.85	1.29	1.69	2.07
C *	0.64	0.96	1.25	1.60	1.87
D *					

2.5 KN/m²

*	1	2	3	4	5
A *	0.01	0.58	1.24	1.79	2.25
B *	0.48	0.91	1.50	1.87	2.17
C *	0.71	1.01	1.45	1.81	1.94
D *					

3.5 KN/m²

*	1	2	3	4	5
A *	0.17	1.01	1.70	2.01	2.28
B *	0.77	1.43	2.04	2.19	2.26
C *	1.01	1.62	2.05	2.08	2.15
D *					

4.0 KN/m²

*	1	2	3	4	5
A *	0.35	1.14	1.86	2.41	2.38
B *	0.86	1.56	2.09	2.52	2.32
C *	1.13	1.60	2.05	2.46	2.17
D *					

4.0 KN/m²

*	1	2	3	4	5
A *	1.19	2.47	3.25	3.59	3.19
B *	1.12	2.16	2.79	2.91	2.51
C *	1.13	1.86	2.27	2.31	2.16
D *					

4.5 KN/m²

*	1	2	3	4	5
A *	1.28	2.75	3.51	3.77	3.29
B *	1.16	2.36	2.88	3.00	2.52
C *	1.13	1.98	2.38	2.29	2.03
D *					

5.0 KN/m²

*	1	2	3	4	5
A *	1.42	2.95	3.77	4.00	3.60
B *	1.28	2.49	3.09	3.19	2.74
C *	1.37	1.98	2.53	2.56	2.33
D *					

5.5 KN/m²

*	1	2	3	4	5
A *	1.66	3.12	4.12	4.24	3.64
B *	1.45	2.59	3.28	3.32	2.73
C *	1.30	2.34	2.65	2.54	2.29
D *					

6.0 KN/m²

*	1	2	3	4	5
A *	1.80	3.59	4.55	4.64	3.67
B *	1.47	2.92	3.63	3.60	2.78
C *	1.40	2.60	3.01	2.91	2.33
D *					

6.5 KN/m²

*	1	2	3	4	5
A *	1.95	4.16	5.10	5.10	3.64
B *	1.51	3.36	4.07	3.95	2.75
C *	1.50	2.73	3.29	3.10	2.22
D *					

7.0 KN/m²

*	1	2	3	4	5
A *	2.01	4.42	5.61	5.58	3.94
B *	1.61	3.60	4.44	4.32	2.95
C *	1.46	2.97	3.58	3.62	2.63
D *					

F.7 *WALL SB07*

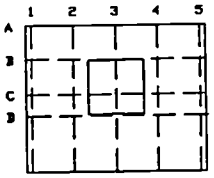

1.0 KN/m²

*	1	2	3	4	5
A *	0.01	0.05	0.07	0.42	0.68
B *	0.23	0.51	*.**	0.80	0.71
C *	0.21	0.22	0.38	0.53	0.61
D *					

1.5 KN/m²

*	1	2	3	4	5
A *	0.04	0.07	0.52	0.94	1.45
B *	0.44	0.81	*.**	1.33	1.25
C *	0.60	0.70	0.86	0.89	0.93
D *					

2.0 KN/m²

*	1	2	3	4	5
A *	0.21	0.03	1.06	1.31	1.67
B *	0.96	1.26	*.**	1.69	1.66
C *	0.86	0.96	1.26	1.12	1.14
D *					

2.5 KN/m²

*	1	2	3	4	5
A *	0.45	0.47	1.15	1.72	1.84
B *	1.26	1.67	*.**	2.02	1.77
C *	1.31	1.43	1.48	1.41	1.17
D *					

3.0 KN/m²

*	1	2	3	4	5
A *	0.42	0.73	1.70	1.96	2.12
B *	1.30	2.08	*.**	1.99	1.75
C *	1.37	1.67	1.75	1.43	1.17
D *					

3.5 KN/m²

*	1	2	3	4	5
A *	0.70	1.48	2.39	3.00	2.86
B *	1.49	2.43	*.**	2.47	1.95
C *	1.41	2.05	1.99	1.80	1.40
D *					

4.0 KN/m²

*	1	2	3	4	5
A *	0.85	1.69	2.88	3.30	3.03
B *	1.76	2.74	*.**	2.47	1.87
C *	1.40	2.08	2.26	1.74	1.25
D *					

4.5 KN/m²

*	1	2	3	4	5
A *	0.67	2.07	3.71	4.58	3.58
B *	1.57	3.02	*.**	2.98	2.03
C *	1.50	2.41	2.60	2.10	1.40
D *					

5.0 KN/m²

*	1	2	3	4	5
A *	0.69	2.39	4.24	5.12	3.84
B *	1.53	3.39	*.**	3.32	1.91
C *	1.47	2.67	2.93	2.31	1.38
D *					

5.5 KN/m²

*	1	2	3	4	5
A *	3.15	6.21	8.19	8.73	5.86
B *	2.23	4.83	*.**	4.91	2.30
C *	1.79	3.88	4.42	3.47	1.57
D *					

1.8 kN/m²

*	1	2	3	4	5
A *	5.47	21.24	25.32	23.97	7.46
B *	3.16	16.47	*.**	16.69	3.12
C *	2.51	15.46	19.70	14.96	1.77
D *					

F.8 *WALL SB09*

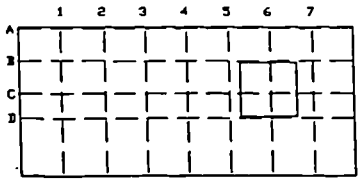

0.5 KN/m²

*	1	2	3	4	5	6	7
A *	0.34	0.58	0.63	0.99	0.95	0.76	0.35
B *	0.24	0.47	0.52	0.84	0.92	0.71	0.27
C *	0.11	0.29	0.32	0.63	0.56	*.**	0.24
D *	0.16	0.25	0.26	0.28	0.35	0.26	0.16

1.0 KN/m²

*	1	2	3	4	5	6	7
A *	0.87	1.54	1.90	2.13	2.06	1.66	0.77
B *	0.77	1.41	1.73	1.99	1.97	1.66	0.64
C *	0.47	0.83	0.94	1.10	1.11	*.**	0.44
D *	0.47	0.63	0.71	0.82	0.82	0.83	0.30

1.5 KN/m²

*	1	2	3	4	5	6	7
A *	1.55	2.67	3.41	3.60	3.50	2.77	1.61
B *	1.55	2.54	3.12	3.28	3.30	2.71	1.40
C *	0.94	1.51	1.91	1.93	1.95	*.**	0.99
D *	0.79	1.22	1.65	1.45	1.47	1.33	0.78

2.0 KN/m²

*	1	2	3	4	5	6	7
A *	2.29	3.95	5.04	5.49	5.33	4.15	2.10
B *	2.16	3.72	4.58	5.03	4.90	4.01	1.98
C *	1.32	2.26	2.75	3.00	3.00	*.**	1.41
D *	1.04	1.81	2.26	2.30	2.38	2.08	1.25

2.4 KN/m²

*	1	2	3	4	5	6	7
A *	3.76	6.32	8.34	9.45	10.13	7.86	4.78
B *	3.64	6.04	7.84	8.86	9.78	7.98	4.59
C *	2.38	4.01	5.40	6.07	6.65	*.**	3.43
D *	2.12	3.42	4.51	4.70	5.10	4.77	3.22

F.9 *WALL CB01*

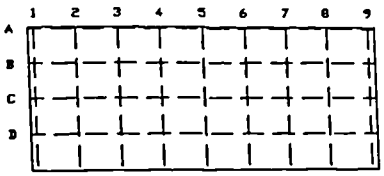

0.8 KN/m²

*	1	2	3	4	5	6	7	8	9
A *	0.12	0.15	0.51	0.82	0.55	0.50	0.51	0.21	0.10
B *	0.34	0.24	0.51	0.67	0.42	0.38	0.41	0.15	0.10
C *	0.37	0.07	0.35	0.45	0.28	0.43	0.35	0.16	0.08
D *	0.05	0.01	0.14	0.27	0.11	0.17	0.16	0.11	0.02

1.2 KN/m²

*	1	2	3	4	5	6	7	8	9
A *	0.14	0.42	0.70	1.19	0.96	0.85	0.70	0.29	0.20
B *	0.40	0.46	0.62	0.87	0.68	0.58	0.53	0.23	0.25
C *	0.23	0.12	0.50	0.62	0.51	0.59	0.44	0.29	0.15
D *	0.09	0.02	0.22	0.32	0.26	0.20	0.14	0.12	0.09

1.6 KN/m²

*	1	2	3	4	5	6	7	8	9
A *	0.08	0.51	1.22	1.58	1.43	1.20	1.00	0.37	0.14
B *	0.31	0.54	1.06	1.15	1.08	0.86	0.68	0.28	0.15
C *	0.28	0.14	0.90	0.92	0.87	0.80	0.67	0.36	0.11
D *	0.01	0.03	0.34	0.44	0.39	0.33	0.24	0.20	0.06

2.0 KN/m²

*	1	2	3	4	5	6	7	8	9
A *	0.08	0.80	1.52	1.96	1.83	1.35	1.35	0.59	0.21
B *	0.33	0.82	1.33	1.38	1.29	0.91	0.97	0.44	0.20
C *	0.34	0.36	0.87	1.02	0.99	0.82	0.85	0.41	0.08
D *	0.02	0.11	0.45	0.59	0.50	0.39	0.42	0.22	0.00

2.4 KN/m²

*	1	2	3	4	5	6	7	8	9
A *	0.09	0.94	1.83	1.82	2.32	2.04	1.73	0.82	0.19
B *	0.34	1.02	1.54	1.31	1.66	1.44	1.23	0.60	0.16
C *	0.36	0.57	1.07	1.11	1.35	1.20	1.14	0.65	0.10
D *	0.05	0.27	0.51	0.68	0.68	0.63	0.52	0.32	0.03

2.8 KN/m²

*	1	2	3	4	5	6	7	8	9
A *	0.09	1.16	1.96	2.97	2.82	2.51	2.01	0.94	0.05
B *	0.27	1.10	1.68	2.13	2.00	1.72	1.38	0.64	0.13
C *	0.27	0.51	1.23	1.72	1.60	1.45	1.19	0.62	0.73
D *	0.06	0.24	0.65	0.88	0.85	0.73	0.58	0.34	0.05

3.2 KN/m²

*	1	2	3	4	5	6	7	8	9
A *	0.09	1.37	2.63	3.47	3.40	2.99	2.46	1.20	0.37
B *	0.26	1.30	2.19	2.44	2.40	2.05	1.76	0.85	0.26
C *	0.26	0.65	1.47	1.91	2.01	1.71	1.52	0.86	0.02
D *	0.13	0.34	0.78	1.06	0.99	0.90	0.80	0.50	0.03

3.6 KN/m²

*	1	2	3	4	5	6	7	8	9
A *	0.26	1.73	3.14	4.07	4.11	3.69	2.86	1.27	0.44
B *	0.32	1.49	2.51	2.86	2.92	2.61	2.03	0.98	0.37
C *	0.43	0.86	1.86	2.28	2.46	2.31	1.74	0.94	0.08
D *	0.00	0.39	0.94	1.23	1.26	1.19	0.96	0.52	0.01

4.0 KN/m²

*	1	2	3	4	5	6	7	8	9
A *	0.30	1.99	3.73	4.68	4.78	4.23	3.18	1.61	0.50
B *	0.35	1.77	2.93	3.27	3.39	2.98	2.25	1.12	0.43
C *	0.44	1.00	2.34	2.64	2.85	2.53	2.13	1.13	0.07
D *	0.04	0.55	1.19	1.45	1.49	1.32	1.05	0.57	0.05

4.4 KN/m²

*	1	2	3	4	5	6	7	8	9
A *	0.30	2.36	4.22	5.33	5.35	4.62	3.80	1.63	0.45
B *	0.25	2.01	3.28	3.74	3.74	3.17	2.68	1.14	0.31
C *	0.20	1.20	2.56	3.10	3.09	2.66	2.32	1.24	0.02
D *	0.03	0.68	1.32	1.73	1.63	1.39	2.11	0.68	0.07

4.8 KN/m²

*	1	2	3	4	5	6	7	8	9
A *	0.34	2.48	4.71	6.02	6.14	5.54	4.37	2.06	0.47
B *	0.22	2.07	3.62	4.21	4.32	3.82	3.09	1.47	0.38
C *	0.29	1.19	2.77	3.45	3.57	3.28	2.78	1.46	0.12
D *	0.03	0.65	1.42	1.86	1.92	1.66	1.40	0.82	0.08

5.2 KN/m²

*	1	2	3	4	5	6	7	8	9
A *	0.49	3.18	5.59	6.97	7.04	6.37	5.07	2.54	0.49
B *	0.29	2.59	4.30	4.94	4.94	4.44	3.59	1.85	0.39
C *	0.43	0.74	3.41	4.06	4.10	3.84	3.19	1.76	0.10
D *	0.02	0.81	1.81	2.18	2.18	2.05	1.63	0.97	0.16

5.6 KN/m²

*	1	2	3	4	5	6	7	8	9
A *	0.54	3.78	6.28	8.04	8.22	7.55	5.89	2.92	0.47
B *	0.26	3.05	4.73	5.66	5.77	5.28	4.20	2.11	0.33
C *	0.37	2.08	3.56	4.71	4.82	4.48	3.63	2.02	0.14
D *	0.05	1.08	1.97	3.04	2.51	2.37	1.89	1.10	0.26

F.10 *WALL CB02*

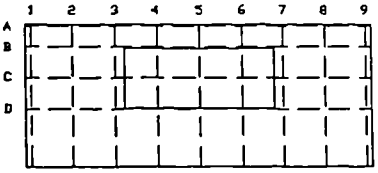

0.2 KN/m²

*	1	2	3	4	5	6	7	8	9
A *	0.18	0.01	0.12	0.12	0.23	0.07	0.15	0.12	0.02
B *	0.15	0.06	0.09	0.04	0.16	0.09	0.08	0.06	0.04
C *	0.06	0.18	0.03	*.**	*.**	*.**	0.05	0.02	0.08
D *	0.05	0.03	0.01	0.02	0.07	0.02	0.02	0.04	0.08

0.4 KN/m²

*	1	2	3	4	5	6	7	8	9
A *	0.22	0.14	0.36	0.15	0.25	0.24	0.24	0.09	0.01
B *	0.20	0.17	0.39	0.13	0.25	0.24	0.11	0.05	0.08
C *	0.06	0.00	0.29	*.**	*.**	*.**	0.16	0.05	0.06
D *	0.07	0.04	0.11	0.01	0.01	0.05	0.02	0.08	0.10

0.8 KN/m²

*	1	2	3	4	5	6	7	8	9
A *	0.33	0.47	0.73	0.63	0.97	0.52	0.63	0.13	0.04
B *	0.21	0.46	0.74	0.57	0.95	0.51	0.49	0.18	0.01
C *	0.15	0.16	0.45	*.**	*.**	*.**	0.45	0.14	0.02
D *	0.10	0.13	0.24	0.20	0.34	0.19	0.20	0.04	0.01

1.1 KN/m²

*	1	2	3	4	5	6	7	8	9
A *	0.44	0.64	1.06	1.10	1.32	1.13	0.83	0.18	0.12
B *	0.26	0.53	0.99	0.98	1.30	1.08	0.65	0.18	0.04
C *	0.02	0.15	0.62	*.**	*.**	*.**	0.47	0.11	0.08
D *	0.08	0.17	0.33	0.35	0.53	0.41	0.28	0.05	0.04

1.4 KN/m²

*	1	2	3	4	5	6	7	8	9
A *	0.38	0.66	1.32	1.38	1.70	0.98	0.84	0.20	0.01
B *	0.26	0.64	1.26	1.34	1.67	1.01	0.74	0.21	0.08
C *	0.03	0.19	0.74	*.**	*.**	*.**	0.59	0.15	0.06
D *	0.06	0.18	0.43	0.48	0.61	0.40	0.32	0.03	0.12

1.8 KN/m²

*	1	2	3	4	5	6	7	8	9
A *	0.41	0.84	1.88	2.08	2.21	1.89	1.45	0.52	0.14
B *	0.40	0.89	1.92	2.08	2.27	1.86	1.25	0.55	0.16
C *	0.00	0.37	1.22	*.**	*.**	*.**	1.04	0.44	0.28
D *	0.09	0.31	0.74	0.78	0.88	0.72	0.58	0.22	0.20

2.2 KN/m²

*	1	2	3	4	5	6	7	8	9
A *	0.54	1.29	2.35	2.64	2.97	2.55	1.74	0.61	0.04
B *	0.39	1.26	2.34	2.70	3.00	2.53	1.58	0.62	0.13
C *	0.12	0.65	1.50	*.**	*.**	*.**	1.28	0.50	0.08
D *	0.08	0.47	0.96	1.04	1.20	1.05	0.77	0.35	0.11

2.6 KN/m²

*	1	2	3	4	5	6	7	8	9
A *	0.60	1.46	2.71	3.35	3.73	3.18	2.16	0.98	0.00
B *	0.48	1.45	2.80	3.38	3.81	3.16	1.93	1.00	0.01
C *	0.16	0.83	1.85	*.**	*.**	*.**	1.60	0.80	0.04
D *	0.12	0.52	1.14	1.34	1.48	1.31	0.85	0.47	0.01

3.0 KN/m²

*	1	2	3	4	5	6	7	8	9
A *	0.68	1.86	3.06	4.26	4.96	4.15	2.99	1.17	0.06
B *	0.57	1.91	3.17	4.41	5.05	5.16	2.74	1.18	0.00
C *	0.20	1.06	2.11	*.**	*.**	*.**	2.21	0.95	0.04
D *	0.32	0.83	1.40	1.79	1.93	1.72	1.36	1.62	0.01

3.3 KN/m²

*	1	2	3	4	5	6	7	8	9
A *	0.63	2.09	3.98	5.04	6.37	5.40	3.76	1.65	0.07
B *	0.50	2.15	4.08	5.14	6.43	5.38	3.45	1.62	0.06
C *	0.01	1.18	2.68	*.**	*.**	*.**	2.79	1.35	0.04
D *	0.09	0.85	1.78	2.15	2.53	2.22	1.85	0.92	0.09

3.6 KN/m²

*	1	2	3	4	5	6	7	8	9
A *	0.81	2.64	4.23	6.30	7.65	6.16	4.24	1.99	0.09
B *	0.57	2.73	4.35	6.42	7.78	6.23	3.99	1.97	0.10
C *	0.10	1.63	3.04	*.**	*.**	*.**	3.40	1.76	0.05
D *	0.18	1.20	2.15	2.86	3.03	2.90	2.49	1.28	0.04

3.8 KN/m²

*	1	2	3	4	5	6	7	8	9
A *	0.76	4.51	8.21	10.80	14.20	12.25	8.32	3.99	0.22
B *	0.61	4.90	8.73	11.30	14.28	12.12	7.92	3.96	0.20
C *	0.13	3.47	6.93	*.**	*.**	*.**	7.35	3.75	0.36
D *	0.18	3.04	6.05	6.83	7.36	7.05	6.46	3.40	0.40

3.0 KN/m²

*	1	2	3	4	5	6	7	8	9
A *	1.01	5.16	9.29	13.14	16.42	14.41	9.33	4.61	0.26
B *	0.75	5.75	9.96	13.59	16.47	14.21	8.96	4.62	0.33
C *	0.41	0.45	4.12	8.07	*.**	*.**	*.**	8.49	0.36
D *	0.22	3.59	7.16	8.36	8.60	8.45	7.67	4.08	0.45

F.11 *WALL DC01*

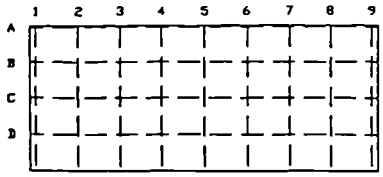

0.2 KN/m²

*	1	2	3	4	5	6	7	8	9
A	0.30	1.15	0.95	1.26	1.00	0.85	0.92	0.43	0.30
B	0.23	0.99	0.84	1.15	0.91	0.75	0.86	0.41	0.27
C	0.17	0.68	0.52	0.72	0.57	0.51	0.53	0.29	0.17
D	0.13	0.40	0.29	0.33	0.33	0.29	0.34	0.24	0.14

0.4 KN/m²

*	1	2	3	4	5	6	7	8	9
A	0.63	1.21	0.97	1.48	1.18	1.21	1.19	0.95	0.88
B	0.49	0.82	0.95	1.33	1.09	1.03	0.12	0.84	0.78
C	0.24	0.43	0.66	0.78	0.64	0.64	0.65	0.51	0.49
D	0.14	0.26	0.43	0.37	0.38	0.34	0.40	0.33	0.27

0.6 KN/m²

*	1	2	3	4	5	6	7	8	9
A	0.78	1.39	1.75	1.93	1.94	1.68	1.83	1.41	1.04
B	0.63	1.22	1.58	1.72	0.76	1.48	1.65	1.22	0.83
C	0.31	0.73	0.98	1.02	1.04	0.90	0.98	0.75	0.54
D	0.18	0.43	0.59	0.54	0.57	0.44	0.54	0.44	0.28

0.7 KN/m²

*	1	2	3	4	5	6	7	8	9
A	0.76	1.95	2.02	1.99	2.33	1.93	2.01	1.10	0.84
B	0.50	1.72	1.76	1.72	2.02	1.66	1.79	1.92	0.66
C	0.27	1.18	1.10	1.09	1.33	1.07	1.12	0.58	0.48
D	0.17	0.68	0.61	0.65	0.71	0.60	0.51	0.35	0.28

1.0 KN/m²

*	1	2	3	4	5	6	7	8	9
A	0.60	2.42	2.48	3.59	3.24	2.98	2.70	1.66	1.25
B	0.35	2.17	2.31	3.26	2.94	2.67	2.42	1.44	0.98
C	0.22	1.45	1.52	1.99	1.81	1.67	1.49	0.96	0.69
D	0.16	0.89	0.95	1.02	0.99	0.91	0.88	0.62	0.43

1.2 KN/m²

*	1	2	3	4	5	6	7	8	9
A	0.96	2.57	3.07	4.24	4.16	3.83	3.22	2.31	1.34
B	0.61	2.19	2.78	3.77	3.74	3.35	2.92	2.04	1.04
C	0.32	1.38	1.80	2.29	2.24	2.04	1.73	1.29	0.77
D	0.16	0.76	1.07	1.19	1.19	1.02	0.92	0.78	0.44

1.3 KN/m²

*	1	2	3	4	5	6	7	8	9
A	1.18	2.95	3.46	4.57	4.54	4.25	3.66	2.58	1.31
B	0.82	2.40	3.11	4.03	4.03	3.78	3.26	2.28	1.00
C	0.45	1.51	1.57	2.46	2.45	2.28	2.09	1.45	0.78
D	0.24	0.77	1.10	1.20	1.33	1.22	1.11	0.88	0.41

1.5 KN/m²

*	1	2	3	4	5	6	7	8	9
A *	1.26	3.21	4.28	5.48	5.27	4.75	4.31	2.90	1.39
B *	0.87	2.66	3.82	4.87	4.76	4.25	3.85	2.64	1.14
C *	0.45	1.72	2.43	2.98	3.01	2.59	2.36	1.68	0.84
D *	0.26	0.87	1.37	1.59	1.63	1.29	1.36	1.02	0.50

1.6 KN/m²

*	1	2	3	4	5	6	7	8	9
A *	1.29	3.53	4.66	5.51	5.70	5.42	4.58	2.92	1.32
B *	0.83	3.08	4.12	4.87	5.10	4.85	4.12	2.64	1.02
C *	0.38	2.00	2.53	3.02	3.13	2.99	2.50	1.66	0.69
D *	0.21	1.18	1.50	1.56	1.71	1.61	1.41	1.02	0.47

1.8 KN/m²

*	1	2	3	4	5	6	7	8	9
A *	1.37	3.88	5.21	6.09	6.58	5.56	4.92	2.86	1.24
B *	0.96	3.32	4.65	5.42	5.86	4.98	4.52	2.59	1.03
C *	0.57	2.09	2.88	3.24	3.60	3.14	2.83	1.74	0.76
D *	0.24	1.19	1.65	1.57	1.96	1.84	1.62	1.10	0.49

2.0 KN/m²

*	1	2	3	4	5	6	7	8	9
A *	1.37	4.30	5.99	7.40	7.44	6.68	5.60	3.83	1.35
B *	0.91	3.77	5.42	6.50	6.71	6.03	5.12	3.53	1.10
C *	0.52	2.58	3.38	4.07	4.06	3.71	3.17	2.22	0.82
D *	0.23	1.43	1.97	2.16	2.25	2.13	1.84	1.34	0.56

2.2 KN/m²

*	1	2	3	4	5	6	7	8	9
A *	1.43	4.61	6.31	8.28	8.24	7.18	6.08	4.01	1.36
B *	1.01	3.92	5.74	7.44	7.48	6.49	5.56	3.66	1.18
C *	0.46	2.43	3.56	4.49	4.56	4.09	3.32	2.34	1.08
D *	0.27	1.21	2.07	2.48	2.60	2.40	2.00	1.47	0.65

2.4 KN/m²

*	1	2	3	4	5	6	7	8	9
A *	1.47	4.67	7.57	9.25	9.30	8.68	7.09	4.43	1.49
B *	1.01	3.92	6.89	8.41	8.48	7.87	6.51	4.13	1.29
C *	0.64	2.10	4.37	5.14	5.18	4.92	4.00	2.69	1.14
D *	0.29	0.80	2.53	2.90	2.95	2.75	2.31	1.66	0.76

2.5 KN/m²

*	1	2	3	4	5	6	7	8	9
A *	1.48	5.43	7.85	9.88	9.88	8.89	7.57	4.39	1.36
B *	1.05	4.87	7.26	9.08	9.05	8.07	6.94	4.07	1.21
C *	0.50	3.10	4.63	5.50	5.60	5.08	4.27	2.60	0.95
D *	0.36	1.84	2.71	3.16	3.15	2.90	2.42	1.53	0.64

2.6 KN/m²

*	1	2	3	4	5	6	7	8	9
A	1.43	5.78	9.17	11.98	11.76	10.46	7.71	4.79	1.35
B	1.08	5.05	8.58	11.46	10.90	9.58	7.21	4.59	1.30
C	0.52	3.02	5.54	6.81	6.69	6.01	4.43	2.98	1.03
D	0.31	1.46	3.23	3.75	3.66	3.27	2.65	1.85	0.76

2.65 KN/m²

*	1	2	3	4	5	6	7	8	9
A	2.09	11.03	18.37	25.54	24.79	24.06	20.72	11.34	1.51
B	2.00	11.79	19.55	27.10	26.16	25.33	22.81	13.22	2.24
C	0.90	9.37	15.89	17.34	16.79	16.25	15.63	12.07	2.40
D	0.43	7.68	8.93	10.42	10.18	10.28	12.48	11.31	2.65

F.12 *WALL DC02*

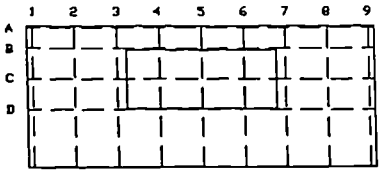

0.4 KN/m²

*	1	2	3	4	5	6	7	8	9
A *	0.70	1.11	1.52	1.61	1.83	1.67	1.37	0.87	0.62
B *	0.72	1.06	1.46	1.65	1.99	1.78	1.32	0.81	0.58
C *	0.33	0.65	1.03	*.**	*.**	*.**	0.92	0.51	0.42
D *	0.31	0.38	0.64	0.55	0.53	0.80	0.63	0.42	0.27

0.8 KN/m²

*	1	2	3	4	5	6	7	8	9
A *	1.18	2.01	2.92	3.33	3.88	3.49	2.82	1.84	0.96
B *	1.10	2.00	2.89	3.62	4.38	3.75	2.98	2.00	0.99
C *	0.55	1.14	1.95	*.**	*.**	*.**	2.01	1.34	0.67
D *	0.47	0.69	1.26	1.21	1.14	1.46	1.32	0.87	0.40

1.2 KN/m²

*	1	2	3	4	5	6	7	8	9
A *	1.49	2.99	4.63	5.80	6.19	5.56	4.28	2.58	1.05
B *	1.49	3.05	4.77	6.32	6.85	5.95	4.57	2.85	1.01
C *	0.85	1.86	3.28	*.**	*.**	*.**	3.04	1.98	0.65
D *	0.56	1.11	2.13	2.42	2.08	2.25	2.02	1.28	0.41

1.6 KN/m²

*	1	2	3	4	5	6	7	8	9
A *	1.55	4.11	6.70	9.06	11.25	9.98	6.99	4.17	1.29
B *	1.53	4.35	7.20	10.06	12.48	10.81	7.60	4.50	1.15
C *	0.72	2.72	4.79	*.**	*.**	*.**	5.07	3.17	0.72
D *	0.48	1.69	3.10	3.78	3.66	4.06	3.50	2.16	0.51

1.75 KN/m²

*	1	2	3	4	5	6	7	8	9
A *	1.91	5.82	9.63	13.50	16.99	14.88	10.28	5.91	1.78
B *	2.13	6.34	10.50	15.10	18.95	16.43	11.32	6.39	1.52
C *	1.14	4.28	7.62	*.**	*.**	*.**	8.14	4.66	0.97
D *	0.60	2.90	5.79	7.15	7.06	6.44	6.43	3.31	0.46

F.13 *WALL DC02B*

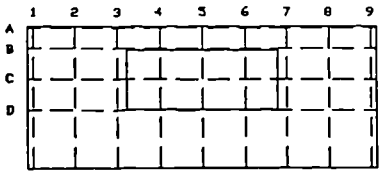

0.4 KN/m²

*	1	2	3	4	5	6	7	8	9
A *	0.66	1.14	1.54	1.93	2.12	1.79	1.74	1.17	0.55
B *	0.80	1.31	1.80	2.12	2.31	2.06	1.87	1.44	0.85
C *	0.40	0.82	1.04	*.**	*.**	*.**	1.31	0.98	0.39
D *	0.08	1.77	0.56	0.93	1.44	0.76	0.80	0.67	0.28

0.8 KN/m²

*	1	2	3	4	5	6	7	8	9
A *	1.01	2.16	3.07	3.86	4.25	3.67	3.27	2.04	0.93
B *	0.90	2.14	3.14	3.97	4.35	3.79	3.29	2.11	1.02
C *	0.44	1.49	2.09	*.**	*.**	*.**	2.47	1.59	0.71
D *	0.06	0.87	1.24	1.389	1.57	1.60	1.51	1.05	0.41

1.2 KN/m²

*	1	2	3	4	5	6	7	8	9
A *	1.38	3.35	4.91	6.41	7.07	6.10	5.06	3.23	1.27
B *	1.37	3.43	4.99	6.58	7.26	6.32	5.05	3.32	1.49
C *	0.74	2.38	3.40	*.**	*.**	*.**	3.84	2.55	1.13
D *	0.08	1.31	2.18	3.23	3.17	2.80	2.44	1.66	0.72

1.4 KN/m²

*	1	2	3	4	5	6	7	8	9
A *	1.77	3.92	5.84	7.88	8.87	7.50	6.08	3.59	1.41
B *	1.65	3.85	5.79	7.99	9.05	7.74	6.11	3.72	1.73
C *	1.07	2.82	4.19	*.**	*.**	*.**	4.73	2.82	1.35
D *	0.27	1.62	2.84	3.68	3.92	3.43	3.04	1.83	0.89

1.5 KN/m²

*	1	2	3	4	5	6	7	8	9
A *	1.78	4.94	7.97	11.06	12.44	9.75	7.38	4.45	1.43
B *	1.61	4.83	7.90	11.01	12.76	9.90	7.36	4.66	1.63
C *	0.93	3.58	5.80	*.**	*.**	*.**	5.77	3.75	1.32
D *	0.08	2.01	4.11	5.06	6.06	4.75	4.02	2.63	1.14

1.0 KN/m²

*	1	2	3	4	5	6	7	8	9
A *	1.89	7.52	13.06	18.50	20.49	15.39	10.97	6.08	1.48
B *	2.18	8.05	13.84	19.06	21.58	16.23	11.47	6.70	1.84
C *	1.47	6.65	11.75	*.**	*.**	*.**	10.26	6.00	1.83
D *	0.10	3.69	8.56	10.42	10.13	10.15	8.98	5.39	1.81

F.14 *WALL HW01*

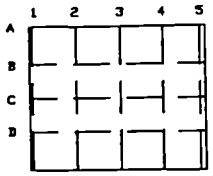

0.1 KN/m²

*	1	2	3	4	5
A *	*.**	*.**	*.**	*.**	*.**
B *	0.43	0.26	0.34	0.71	0.40
C *	0.28	0.14	0.20	0.65	0.23
D *	0.12	0.10	0.04	0.22	0.15

0.4 KN/m²

*	1	2	3	4	5
A *	*.**	*.**	*.**	*.**	*.**
B *	0.90	0.66	0.80	1.18	0.97
C *	0.63	0.39	0.31	0.98	0.45
D *	0.22	0.01	0.19	0.49	0.25

0.6 KN/m²

*	1	2	3	4	5
A *	*.**	*.**	*.**	*.**	*.**
B *	0.81	0.83	1.15	1.24	1.39
C *	0.38	0.31	0.58	0.70	0.81
D *	0.21	0.11	0.28	0.43	0.50

0.8 KN/m²

*	1	2	3	4	5
A *	*.**	*.**	*.**	*.**	*.**
B *	0.86	1.06	1.29	1.62	1.64
C *	0.41	0.46	0.62	1.05	1.06
D *	0.14	0.26	0.38	0.51	0.57

1.2 KN/m²

*	1	2	3	4	5
A *	*.**	*.**	*.**	*.**	*.**
B *	0.85	1.31	1.86	2.19	2.40
C *	0.37	0.58	1.00	1.44	1.59
D *	0.10	0.13	0.63	0.86	0.96

1.6 KN/m²

*	1	2	3	4	5
A *	*.**	*.**	*.**	*.**	*.**
B *	1.20	1.77	2.42	2.95	3.20
C *	0.74	0.95	1.42	2.03	2.21
D *	0.27	0.33	0.80	1.05	1.20

2.0 KN/m²

*	1	2	3	4	5
A *	*.**	*.**	*.**	*.**	*.**
B *	1.28	1.98	2.93	3.53	4.08
C *	0.71	1.16	1.86	2.51	2.96
D *	0.36	0.51	1.00	1.40	1.67

2.4 KN/m²

*	1	2	3	4	5
A	*.**	*.**	*.**	*.**	*.**
B	1.32	2.33	3.47	4.44	5.06
C	0.79	1.41	2.25	3.23	3.70
D	0.37	0.75	1.21	1.84	2.15

2.8 KN/m²

*	1	2	3	4	5
A	*.**	*.**	*.**	*.**	*.**
B	1.38	2.62	4.76	5.92	6.85
C	0.86	1.79	3.58	4.71	5.33
D	0.64	1.27	2.41	3.05	3.27

3.0 KN/m²

*	1	2	3	4	5
A	*.**	*.**	*.**	*.**	*.**
B	1.50	3.12	5.91	7.65	9.22
C	1.08	2.47	4.76	6.52	7.92
D	0.89	2.12	3.62	4.59	5.24

3.15 KN/m²

*	1	2	3	4	5
A	*.**	*.**	*.**	*.**	*.**
B	1.53	4.24	7.10	9.48	11.26
C	1.13	3.47	6.08	8.48	10.11
D	0.93	3.05	4.95	6.11	6.89

3.2 KN/m²

*	1	2	3	4	5
A	*.**	*.**	*.**	*.**	*.**
B	0.88	5.67	10.47	14.60	17.80
C	1.73	5.95	10.79	15.14	18.40
D	2.11	6.24	10.03	12.20	13.86

3.4 KN/m²

*	1	2	3	4	5
A	*.**	*.**	*.**	*.**	*.**
B	0.47	6.52	12.28	17.31	21.23
C	1.89	7.41	13.32	18.72	22.92
D	2.47	8.07	12.84	15.50	17.53

3.7 KN/m²

*	1	2	3	4	5
A	*.**	*.**	*.**	*.**	*.**
B	1.57	11.26	20.67	28.76	34.50
C	2.42	11.22	20.53	29.37	36.73
D	2.70	11.09	19.11	23.55	26.98

F.15 *WALL HW02*

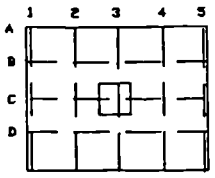

0.1 KN/m²

*	1	2	3	4	5
A	*.**	*.**	*.**	*.**	*.**
B	0.72	0.66	0.65	0.85	0.54
c	0.49	0.40	*.**	0.57	0.43
D	0.26	0.18	0.24	0.29	0.12

0.4 KN/m²

*	1	2	3	4	5
A	*.**	*.**	*.**	*.**	*.**
B	0.90	0.95	0.83	0.79	0.44
C	0.68	0.65	*.**	0.59	0.44
D	0.40	0.26	0.29	0.20	0.11

0.8 KN/m²

*	1	2	3	4	5
A	*.**	*.**	*.**	*.**	*.**
B	1.41	1.36	1.13	0.68	0.56
C	1.02	1.02	*.**	0.59	0.66
D	0.50	0.47	0.45	0.39	0.37

1.2 KN/m²

*	1	2	3	4	5
A	*.**	*.**	*.**	*.**	*.**
B	2.03	1.92	1.41	1.31	0.72
C	1.43	1.43	*.**	1.08	0.68
D	0.68	0.65	0.53	0.47	0.36

1.6 KN/m²

*	1	2	3	4	5
A	*.**	*.**	*.**	*.**	*.**
B	2.66	2.35	1.22	1.44	0.76
C	1.89	1.82	*.**	1.13	0.77
D	0.94	0.82	0.59	0.54	0.37

1.8 KN/m²

*	1	2	3	4	5
A	*.**	*.**	*.**	*.**	*.**
B	3.14	2.63	2.10	1.46	0.69
C	2.32	2.02	*.**	1.20	0.81
D	1.15	1.02	0.83	0.57	0.41

2.2 KN/m²

*	1	2	3	4	5
A	*.**	*.**	*.**	*.**	*.**
B	3.50	3.12	2.31	1.70	0.62
C	2.62	2.31	*.*	1.38	0.75
D	1.32	1.15	0.92	0.61	0.41

2.15 KN/m²

*	1	2	3	4	5
A *	*.**	*.**	*.**	*.**	*.**
B *	4.39	3.83	2.83	1.93	0.98
C *	3.37	2.99	*.**	1.81	1.22
D *	1.59	1.35	1.16	0.84	0.62

2.4 KN/m²

*	1	2	3	4	5
A *	*.**	*.**	*.**	*.**	*.**
B *	5.77	4.66	3.58	2.43	1.12
C *	4.45	3.80	*.**	2.36	1.39
D *	2.12	1.82	1.53	1.11	0.73

2.6 KN/m²

*	1	2	3	4	5
A *	*.**	*.**	*.**	*.**	*.**
B *	7.37	6.13	4.18	3.13	1.15
C *	5.71	5.03	*.**	3.15	1.59
D *	2.78	2.43	1.98	1.71	0.95

2.55 KN/m²

*	1	2	3	4	5
A *	*.**	*.**	*.**	*.**	*.**
B *	9.78	8.09	6.00	3.80	1.17
C *	7.74	7.10	*.**	3.87	1.64
D *	3.57	3.27	2.99	2.55	1.31

2.45 KN/m²

*	1	2	3	4	5
A *	*.**	*.**	*.**	*.**	*.**
B *	14.96	12.11	8.60	4.96	1.13
C *	11.83	11.39	*.**	5.43	1.83
D *	5.53	5.19	4.86	4.16	1.74

2.6 KN/m²

*	1	2	3	4	5
A *	*.**	*.**	*.**	*.**	*.**
B *	15.86	12.71	9.07	5.27	1.23
C *	12.57	12.00	*.**	5.84	2.12
D *	5.83	5.49	5.17	4.45	1.86

2.8 KN/m²

*	1	2	3	4	5
A *	*.**	*.**	*.**	*.**	*.**
B *	18.77	15.24	10.90	5.97	0.92
C *	16.31	16.38	*.**	8.31	3.39
D *	7.68	7.67	6.94	5.92	2.15

F.16 *WALL HW03*

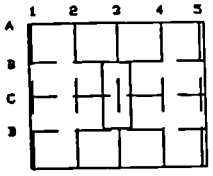

0.2 KN/m²

	1	2	3	4	5
A	*.**	*.**	0.00	*.**	0.00
B	-0.34	-0.14	-0.22	0.07	-0.34
C	-0.16	0.06	*.**	0.18	-0.30
D	-0.10	0.06	*.**	0.15	-0.19

0.4 KN/m²

	1	2	3	4	5
A	*.**	*.**	0.02	*.**	0.03
B	-0.23	-0.22	-0.10	0.08	0.01
C	-0.05	-0.05	*.**	0.18	-0.08
D	-0.01	0.14	*.**	0.14	-0.10

0.6 KN/m²

	1	2	3	4	5
A	*.**	*.**	0.19	*.**	0.10
B	-0.24	-0.13	-0.12	0.23	0.13
C	0.03	0.07	*.**	0.42	0.10
D	0.01	0.03	*.**	0.25	-0.04

0.8 KN/m²

	1	2	3	4	5
A	*.**	*.**	0.32	*.**	0.19
B	-0.09	0.05	0.05	0.29	0.21
C	0.12	0.25	*.**	0.41	0.17
D	0.11	0.09	*.**	0.33	0.02

1.0 KN/m²

	1	2	3	4	5
A	*.**	*.**	0.43	*.**	0.27
B	-0.01	0.30	0.38	0.56	0.57
C	0.35	0.69	*.**	0.99	0.90
D	0.25	0.39	*.**	0.49	0.33

0.8 KN/m²

	1	2	3	4	5
A	*.**	*.**	0.30	*.**	0.22
B	0.45	0.63	0.60	1.02	0.88
C	1.05	1.18	*.**	1.78	1.46
D	0.50	0.54	*.**	0.81	0.55

1.0 KN/m²

	1	2	3	4	5
A	*.**	*.**	0.38	*.**	0.23
B	0.87	1.17	1.06	1.26	1.10
C	1.62	1.91	*.**	2.35	2.12
D	0.68	0.92	*.**	1.00	0.80

1.2 KN/m²

*	1	2	3	4	5
A	*.**	*.**	0.47	*.**	0.27
B	1.14	1.32	1.48	1.69	1.43
C	1.92	2.19	*.**	3.02	2.67
D	0.82	1.05	*.**	1.38	1.04

1.4 KN/m²

*	1	2	3	4	5
A	*.**	*.**	0.60	*.**	0.35
B	1.20	0.87	1.55	1.94	1.57
C	2.17	1.60	*.**	3.58	3.10
D	0.90	0.37	*.**	1.59	1.23

1.6 KN/m²

*	1	2	3	4	5
A	*.**	*.**	0.72	*.**	0.42
B	1.37	1.65	1.80	2.10	1.99
C	2.35	2.67	*.**	3.84	3.57
D	0.98	1.16	*.**	1.71	1.42

1.8 KN/m²

*	1	2	3	4	5
A	*.**	*.**	0.87	*.**	0.50
B	1.45	1.88	2.02	2.40	2.18
C	2.48	2.97	*.**	4.25	3.90
D	1.01	1.32	*.**	1.87	1.54

2.0 KN/m²

*	1	2	3	4	5
A	*.**	*.**	0.97	*,**	0.59
B	1.66	1.29	2.34	2.59	2.46
C	2.69	2.09	*.**	4.58	4.39
D	1.09	0.31	*.**	2.02	1.80

2.2 KN/m²

*	1	2	3	4	5
A	*.**	*.**	1.15	*.**	0.66
B	1.59	2.07	2.36	2.70	2.55
C	2.67	3.35	*.**	4.85	4.68
D	1.09	1.47	*.**	2.12	1.89

2.4 KN/m²

*	1	2	3	4	5
A	*.**	*.**	1.26	*.**	0.75
B	1.66	2.20	2.17	3.01	2.89
C	2.81	3.47	*.**	5.40	5.17
D	1.07	1.52	*.**	2.33	2.10

2.6 KN/m²

*	1	2	3	4	5
A	*.**	*.**	1.37	*.**	0.84
B	1.91	2.24	2.86	3.18	2.90
C	3.01	3.51	*.**	5.76	5.45
D	1.12	1.21	*.**	2.44	2.20

2.8 KN/m²

*	1	2	3	4	5
A	*.**	*.**	1.49	*.**	0.91
B	1.91	4.43	2.85	3.28	3.27
C	3.18	3.85	*.**	6.00	5.91
D	1.15	1.53	*.**	2.55	2.38

3.0 KN/m²

*	1	2	3	4	5
A	*.**	*.**	1.55	*.**	0.96
B	1.85	2.63	3.09	3.54	3.46
C	3.21	4.15	*.**	6.39	6.23
D	1.14	1.72	*.**	2.72	2.54

3.2 KN/m²

*	1	2	3	4	5
A	*.**	*.**	1.62	*.**	1.05
B	1.88	2.85	3.32	3.73	3.78
C	3.25	4.44	*.**	6.75	6.63
D	1.18	1.88	*.**	2.81	2.72

3.4 KN/m²

*	1	2	3	4	5
A	*.**	*.**	1.65	*.**	1.09
B	1.87	2.85	3.58	4.00	3.92
C	3.28	4.43	*.**	7.13	7.01
D	1.16	1.94	*.**	3.01	2.90

3.6 KN/m²

*	1	2	3	4	5
A	*.**	*.**	1.65	*.**	1.09
B	2.89	11.01	13.22	14.01	14.19
C	4.12	13.25	*.**	25.84	25.83
D	1.63	8.74	*.**	10.76	10.70

F.17 *WALL HW04*

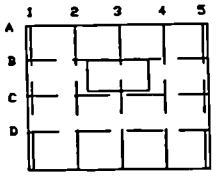

0.2 KN/m²

	1	2	3	4	5
A	0.00	*.**	0.00	*.**	*.**
B	0.28	0.19	*.**	0.27	0.08
C	0.15	0.24	0.36	0.25	0.08
D	0.05	0.10	0.15	0.09	0.04

0.4 KN/m²

	1	2	3	4	5
A	0.10	*.**	0.15	*.**	*.**
B	0.43	0.30	*.**	0.09	0.04
C	0.32	0.36	0.45	0.13	0.17
D	0.14	0.17	0.13	0.04	0.11

0.6 KN/m²

	1	2	3	4	5
A	0.19	*.**	0.27	*.**	*.**
B	0.56	0.49	*.**	0.53	0.29
C	0.62	0.63	0.58	0.67	0.42
D	0.31	0.29	0.30	0.27	0.11

0.7 KN/m²

	1	2	3	4	5
A	0.14	*.**	0.17	*.**	*.**
B	1.22	1.03	*.**	1.13	0.99
C	1.95	1.92	1.85	1.94	1.85
D	0.82	0.85	0.81	0.76	0.73

0.8 KN/m²

	1	2	3	4	5
A	0.16	*.**	0.255	*.**	*.**
B	1.40	1.32	*.**	1.30	1.13
C	2.32	2.38	2.34	2.32	2.19
D	0.97	1.03	1.04	0.94	0.91

1.0 KN/m²

	1	2	3	4	5
A	0.23	*.**	0.41	*.**	*.**
B	1.52	1.39	*.**	1.43	1.22
C	2.64	2.67	2.82	2.51	2.32
D	1.13	1.18	1.27	1.03	0.94

1.4 KN/m²

	1	2	3	4	5
A	0.34	*.**	0.56	*.**	*.**
B	1.86	1.82	*.**	1.60	1.23
C	3.03	3.17	3.08	2.83	2.47
D	1.27	1.35	1.30	1.17	1.00

1.6 KN/m²

	1	2	3	4	5
A	0.43	*.**	0.67	*.**	*.**
B	2.07	1.76	*.**	1.74	0.95
C	3.26	3.15	3.30	3.00	2.09
D	1.41	1.30	1.44	1.22	0.62

1.8 KN/m²

	1	2	3	4	5
A	0.51	*.**	0.79	*.**	*.**
B	2.18	1.98	*.**	1.76	1.39
C	3.55	3.48	3.54	3.10	2.70
D	1.49	1.51	1.48	1.29	1.08

2.0 KN/m²

	1	2	3	4	5
A	0.57	*.**	0.88	*.**	*.**
B	2.30	1.69	*.**	1.84	1.31
C	3.71	3.06	3.60	3.15	2.63
D	1.60	0.99	1.56	1.32	1.07

2.3 KN/m²

	1	2	3	4	5
A	0.62	*.**	1.00	*.**	*.**
B	2.50	2.30	*.**	2.02	1.52
C	4.06	4.02	3.89	3.48	2.88
D	1.76	1.71	1.70	1.46	1.20

2.6 KN/m²

	1	2	3	4	5
A	0.62	*.**	1.07	*.**	*.**
B	2.62	2.33	*.**	1.94	1.13
C	4.33	4.18	4.13	3.47	2.64
D	1.85	1.82	1.77	1.43	1.06

2.9 KN/m²

	1	2	3	4	5
A	0.61	*.**	1.13	*.**	*.**
B	2.83	2.63	*.**	2.16	1.28
C	4.65	4.58	4.35	3.76	2.73
D	1.97	1.91	1.89	1.59	1.09

3.1 KN/m²

	1	2	3	4	5
A	0.54	*.**	1.04	*.**	*.**
B	3.05	2.86	*.**	2.33	1.76
C	5.25	5.09	4.89	3.79	2.85
D	2.24	2.16	2.06	1.61	1.18

3.2 KN/m²

*	1	2	3	4	5
A	0.54	*.**	1.025	*.**	*.**
B	3.19	2.92	*.**	2.80	1.76
C	5.58	5.32	5.03	4.10	2.87
D	2.39	2.22	2.13	1.74	1.22

3.3 KN/m²

*	1	2	3	4	5
A	0.45	*.**	1.00	*.**	*.**
B	3.41	3.20	*.**	3.16	2.29
C	5.93	5.73	5056	4.48	3019
D	2.49	2.34	2.32	1.93	1.57

3.3 KN/m²

*	1	2	3	4	5
A	0.05	*.**	0.79	*.**	*.**
B	7.15	7.02	*.**	6.52	3.40
C	12.86	12.58	11.90	8.04	3.81
D	5.38	5.22	4.90	4.29	3.51

F.18 *WALL W01*

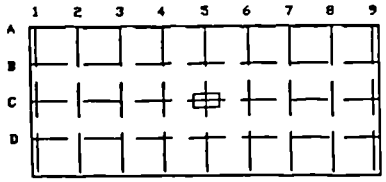

0.2 KN/m²

*	1	2	3	4	5	6	7	8	9
A *	0.75	0.82	0.81	1.01	1.19	1.43	1.13	1.13	1.21
B *	0.73	0.54	0.66	0.83	0.97	1.13	0.68	0.77	0.83
C *	0.42	0.43	0.54	0.52	*.**	1.00	0.42	0.47	0.72
D *	0.20	0.10	0.16	0.35	0.33	0.40	0.14	0.14	0.23
E *	*.**	*.**	*.**	*.**	0.02	*.**	*.**	*.**	*.**

0.4 KN/m²

*	1	2	3	4	5	6	7	8	9
A *	1.03	1.16	1.81	1.38	1.52	2.06	1.64	1.29	1.55
B *	0.82	0.75	1.09	1.35	1.19	1.64	1.19	0.92	1.81
C *	0.47	0.60	0.73	0.85	*.**	1.41	0.82	0.50	0.94
D *	0.15	0.21	0.18	0.48	0.43	0.62	0.19	0.21	0.39
E *	*.**	*.**	*.**	*.**	0.04	*.**	*.**	*.**	*.**

0.6 KN/m²

*	1	2	3	4	5	6	7	8	9
A *	1.05	1.34	0.70	1.90	1.84	2.36	1.99	1.93	1.72
B *	1.00	0.96	1.34	1.49	1.50	1.95	1.34	1.45	1.27
C *	0.59	0.76	0.88	1.00	*.**	1.52	0.95	0.96	0.93
D *	0.33	0.28	0.28	0.54	0.62	0.64	0.20	0.38	0.44
E *	*.**	*.**	*.**	*.**	0.05	*.**	*.**	*.**	*.**

0.8 KN/m²

*	1	2	3	4	5	6	7	8	9
A *	0.91	1.52	2.03	2.29	2.55	2.91	2.45	2.20	1.94
B *	0.81	1.08	1.58	1.86	1.91	2.28	1.79	1.56	1.34
C *	0.34	0.97	1.03	1.29	*.**	1.87	1.29	1.08	1.08
D *	0.03	0.36	0.34	0.66	0.63	0.76	0.25	0.43	0.39
E *	*.**	*.**	*.**	*.**	0.07	*.**	*.**	*.**	*.**

1.0 KN/m²

*	1	2	3	4	5	6	7	8	9
A *	1.28	1.77	2.34	2.75	2.81	3.40	2.85	2.55	2.15
B *	1.26	1.37	1.84	2.12	2.21	2.72	2.11	1.89	1.55
C *	0.82	0.97	1.24	1.44	*.**	2.26	1.50	1.33	1.30
D *	0.28	0.33	0.32	0.57	0.88	1.02	0.37	0.51	0.44
E *	*.**	*.**	*.**	*.**	0.09	*.**	*.**	*.**	*.**

1.2 KN/m²

*	1	2	3	4	5	6	7	8	9
A *	1.24	2.27	2.80	2.76	3.62	3.88	3.19	2.65	2.20
B *	1.06	1.69	2.22	2.20	2.77	3.00	2.35	1.96	1.56
C *	0.52	1.30	1.63	1.65	*.**	2.45	1.69	1.30	1.14
D *	0.25	0.46	0.62	0.80	0.90	1.04	0.48	0.56	0.44
E *	*.**	*.**	*.**	*.**	0.11	*.**	*.**	*.**	*.**

1.4 KN/m²

*	1	2	3	4	5	6	7	8	9
A *	1.44	2.43	3.19	3.38	3.92	3.62	3.67	3.17	2.52
B *	1.46	1.86	2.59	2.68	3.09	2.86	2.68	2.29	1.78
C *	1.08	1.57	1.98	2.05	*.**	2.14	1.98	1.69	1.44
D *	0.63	0.65	0.83	0.98	1.15	0.89	0.67	0.66	0.58
E *	*.**	*.**	*.**	*.**	0.14	*.**	*.**	*.**	*.**

1.6 KN/m²

*	1	2	3	4	5	6	7	8	9
A *	1.61	2.70	3.59	4.12	4.32	4.81	4.02	3.40	2.72
B *	1.57	2.12	2.89	3.28	3.33	3.77	2.97	2.48	1.86
C *	1.15	1.78	2.09	2.45	*.**	3.06	2.19	1.77	1.50
D *	0.47	0.77	0.89	1.04	1.14	1.36	0.72	0.76	0.51
E *	*.**	*.**	*.**	*.**	0.19	*.**	*.**	*.**	*.**

1.7 KN/m²

*	1	2	3	4	5	6	7	8	9
A *	1.73	3.38	5.11	5.92	6.67	5.89	5.51	4.16	2.68
B *	2.28	3.33	4.97	5.77	6.02	5.53	4.97	3.75	2.36
C *	2.17	3.17	4.60	5.51	*.**	5.66	5.07	3.77	2.73
D *	0.75	1.27	2.20	3.16	3.57	3.28	2.70	1.85	1.05
E *	*.**	*.**	*.**	*.**	2.21	*.**	*.**	*.**	*.**

1.8 KN/m²

*	1	2	3	4	5	6	7	8	9
A *	1.82	3.75	5.72	6.68	7.26	7.26	5.97	4.46	2.69
B *	2.37	3.69	5.59	6.36	6.75	6.67	5.40	4.03	2.39
C *	2.38	3.69	5.36	6.37	*.**	7.03	5.77	4.41	2.95
D *	0.69	1.53	2.71	3.61	4.14	4.06	3.02	2.11	1.22
E *	*.**	*.**	*.**	*.**	2.67	*.**	*.**	*.**	*.**

1.9 KN/m²

*	1	2	3	4	5	6	7	8	9
A *	1.45	3.98	6.07	7.06	7.77	7.86	6.46	4.72	2.39
B *	2.05	4.05	6.04	6.84	7.37	7.28	6.04	4.41	2.28
C *	1.90	3.95	5.75	6.80	*.**	7.92	6.61	4.98	2.96
D *	0.30	1.63	3.03	3.94	4.49	4.59	3.71	2.48	1.14
E *	*.**	*.**	*.**	*.**	3.20	*.**	*.**	*.**	*.**

1.9 KN/m²

*	1	2	3	4	5	6	7	8	9
A *	1.49	4.11	6.15	6.74	8.09	7.97	6.45	4.47	2.61
B *	1.98	4.19	6.10	6.63	7.58	7.41	5.98	4.22	2.44
C *	1.83	4.16	5.74	6.83	*.**	8.06	6.51	4.72	3.04
D *	0.19	1.79	3.176	4.09	4.75	4.75	3.58	2.48	1.19
E *	*.**	*.**	*.**	*.**	3.29	*.**	*.**	*.**	*.**

2.0 KN/m²

*	1	2	3	4	5	6	7	8	9
A *	1.73	4.21	6.53	8.02	8.65	8.43	6.93	4.92	2.58
B *	2.44	4.33	6.42	7.93	8.24	7.93	6.50	4.66	2.59
C *	2.42	4.29	6.14	7.88	*.**	8.68	7.17	5.30	3.34
D *	0.59	1.82	3.16	4.73	5.21	5.25	3.95	2.73	1.40
E *	*.**	*.**	*.**	*.**	3.83	*.**	*.**	*.**	*.**

2.1 KN/m²

*	1	2	3	4	5	6	7	8	9
A *	1.66	4.44	7.09	8.84	9.30	9.26	7.06	5.15	2.63
B *	2.31	4.55	7.04	8.49	8.89	8.71	6.64	4.88	2.67
C *	2.18	4.68	6.77	8.58	*.**	9.62	7.48	5.65	3.47
D *	0.19	2.16	3.71	5.25	5.88	5.87	4.24	2.99	1.46
E *	*.**	*.**	*.**	*.**	4.40	*.**	*.**	*.**	*.**

2.2 KN/m²

*	1	2	3	4	5	6	7	8	9
A *	1.63	4.96	7.72	9.88	10.51	10.11	8.09	5.59	2.81
B *	2.38	5.30	7.81	9.56	10.01	9.59	7.71	5.42	2.85
C *	2.21	5.29	7.60	9.70	*.**	10.66	8.65	6.26	3.70
D *	0.24	2.69	4.27	6.04	6.67	6.68	5.05	3.35	1.55
E *	*.**	*.**	*.**	*.**	5.19	*.**	*.**	*.**	*.**

2.3 KN/m²

*	1	2	3	4	5	6	7	8	9
A *	1.78	8.21	14.34	16.87	15.52	13.48	9.95	6.37	2.45
B *	2.74	8.471	14.27	15.95	14.64	12.75	9.51	6.24	2.71
C *	3.35	9.08	11.99	14.61	*.**	14.47	10.82	7.17	3.45
D *	2.06	4.34	6.51	8.44	9.48	9.88	7.52	4.62	1.84
E *	*.**	*.**	*.**	*.**	10.32	*.**	*.**	*.**	*.**